THE USE OF THE *THY-1-YFP-H* TRANSGENIC MOUSE STRAIN IN STUDIES OF PERIPHERAL NERVE INJURY

By

Adam John Harding

Academic Unit of Oral and Maxillofacial Medicine and Surgery,

School of Clinical Dentistry,

Claremont Crescent,

Sheffield, S10 2TA

A thesis submitted to the Faculty of Medicine, Dentistry and Health of the University of Sheffield for the degree of Doctor of Philosophy

June 2014

SUMMARY

The aim of these studies was to utilise the *thy-1-YFP-H* transgenic mouse strain to investigate the effects of exogenous agents and the use of nerve conduits on peripheral nerve repair, while developing analysis methods to quantify nerve regeneration in this strain. Using a *thy-1-YFP-H* mouse common fibular nerve repair model, two potential nerve regeneration enhancing agents [mannose-6-phosphate and EC23] and four conduit designs were assessed.

The outcomes of the experiments were measured by analysing whole mount images of the repaired nerves and comparing: axon numbers across the repairs, the proportion of unique axons reaching set distances within the repairs, and the disruption of axons as they entered the repairs. Of the two potential nerve regeneration enhancing agents [administered by pre-soaking the graft tissue and injections into the surrounding tissue] mannose-6-phosphate was shown to significantly reduce the disruption of axons entering the graft, which tied in with results of previous studies on mannose-6-phosphate. EC23 did not appear to have any significant effect upon nerve regeneration, displaying similar results to vehicle treated grafts. Within the conduit studies, both micro-stereolithography produced hollow conduit designs proved successful at enabling regeneration across a short nerve defect - with quantitative results similar to graft repairs - however, axon organisation within those repairs was greatly reduced. The other two conduit designs [aligned fibre filled and hollow nylon-12] were less successful, with limited regeneration occurring across the nerve defect.

Through the results of these studies the usefulness of the *thy-1-YFP-H* transgenic mouse strain in assessing nerve regeneration has been further established. The ability to trace the fate of individual axons through repairs reveals much information that was previously not possible or very difficult to obtain. In addition, the ability to obtain results in only 2-3 weeks makes this model ideal for obtaining useful data quickly for pilot studies.

ACKNOWLEDGEMENTS

Many, many people - both professionally and personally - deserve to be acknowledged for their contributions which have enabled this thesis to come into being. Listing each person and their contribution individually would result in this thesis requiring a separate acknowledgements volume; so for those of you who don't get a specific mention here, I apologise and thank you for your contribution.

Amongst my colleagues I have to thank my primary supervisor, Professor Fiona Boissonade, whose style of supervising perfectly suited my own working style and greatly enhanced my PhD experience. I would also like to thank my second supervisor, Dr. Claire Christmas, for taking time out of her own busy schedule to train me in many of the techniques I have used throughout my PhD. Much of the work presented within this thesis would not have been possible without the assistance of my collaborators, Professor John Haycock, Dr. Frederik Claeyssens and Professor Neil Hopkinson, and the members of their research groups who worked with me. Specifically, Dr. Kiran Pawar and Christopher Pateman for their work on the artificial nerve guides discussed in chapter 5 of this thesis, and Wendy Birtwistle for her work on the artificial nerve guides discussed in chapter 6. Ultimately, it would be remiss of me to forget the vital role played by those who have funded my research to date, namely the School of Clinical Dentistry, Renovo plc and the MRC.

Over the past few years numerous significant events have taken place in my life - many stemming from my decision to undertake a PhD, which was greatly influenced by the support and encouragement of my final year undergraduate project supervisor at the University of Aston, Dr. Eustace Johnson, without whom I would certainly be doing something markedly different.

Those who have had the greatest influence on this thesis are probably those who understand its contents the least - my friends and family. To my friends, I'm afraid I will have

to give you a collective thank you - but you know who you are and I'm sure you've each contributed to a word or two.

Obviously I couldn't have done this without my parents, Ian and Patricia, who have always helped and encouraged me to be the best I can be. My younger sister, Rebecca, deserves a mention for continually forcing me to attempt to prove I'm the smart one in the family and my Aunt, Cortina Willock, claims that her giving me my first screwdriver and plug has led directly to this. The influence of my grandfather, Joseph Ryan, in nurturing my eternal curiosity by encouraging me to always ask questions, and always responding to those questions with an answer - even if those answers may not have always been the whole truth! - is a huge part of who I am today.

Finally my wife, Emma, should be commended for putting up with my seemingly perpetual life as a student. Her decision to move one hundred miles north to be with me, away from friends and family, was a hard one for her to make but I could not have achieved this without her presence in my life.

PUBLICATIONS AND PRESENTATIONS

The following papers [awaiting publication] have been prepared from work detailed within this thesis:

A. Harding, C. Christmas, M. Ferguson, A. Loescher, P. Robinson and F. Boissonade. 2014. **Mannose-6-Phosphate Facilitates Early Peripheral Nerve Regeneration in *thy-1-YFP-H* Mice**. Neuroscience 279: 23-32.

A. Harding, C. Pateman, S. Rimmer, F. Boissonade, F. Claeyssens and J. Haycock. 2014. **Photocurable Polymeric Nerve Guides for Peripheral Nerve Repair.** [Submitted to Biomaterials]

The following communications have been presented at meetings of scientific societies:

A. Harding, C. Pateman, C. Christmas, A. Loescher, P. Robinson, F. Claeyssens, J. Haycock and F. Boissonade. **The use of Aligned Electrospun Fibre Filled Conduits for Repair of the Common Fibular Nerve in *thy-1-YFP-H* Mice**. Poster presentation at the Regener8 annual meeting; Leeds, UK. September 2014.

C. Pateman, **A. Harding**, R. Plenderleith, S. Rimmer, F. Boissonade, F. Claeyssens and J. Haycock. **3D Micro-Printing of Nerve Guides for Peripheral Nerve Repair**. Poster presentation at the TCES annual meeting; Newcastle, UK. July 2014.

C. Pateman, **A. Harding**, R. Plenderleith, F. Boissonade, S. Rimmer, J. Haycock and F. Claeyssens. **Nerve Guides from Photocurable Polymers for Peripheral Nerve Repair**. Pateman et al. Poster Presentation at the TERMIS-EU annual meeting; Genova, Italy. June 2014.

A. Harding, C. Pateman, C. Christmas, A. Loescher, P. Robinson, F. Claeyssens, J. Haycock and F. Boissonade. **A Comparison Between Poly-caprolactone Based Nerve**

Guide Conduits and Graft Repair of the Common Fibular Nerve in *thy-1-YFP-H* Mice. Poster presentation at the Regener8 annual meeting; Leeds, UK. October 2013.

A. Harding, C. Pateman, C. Christmas, M. Ferguson, A. Loescher, P. Robinson, F. Claeyssens, J. Haycock and F. Boissonade. **The Use of *thy-1-YFP-H* Mice in Analysing Peripheral Nerve Regeneration.** Oral presentation at the BSODR annual meeting; Bath UK. September 2013.

C. Pateman, R. Plenderleith, M. Daud, **A. Harding**, C. Christmas, F. Boissonade, S. Rimmer, F. Claeyssens and J. Haycock. **3D Micro-Printing of Nerve Guides for Peripheral Nerve Repair.** Poster presentation at the TCES annual meeting; Cardiff, UK. July 2013.

C. Pateman, R. Plenderleith, M. Daud, **A. Harding**, C. Christmas, F. Boissonade, S. Rimmer, F. Claeyssens and J. Haycock. **Photocurable Polymeric Nerve Guides For Peripheral Nerve Repair.** Poster presentation at the TERMIS-EU annual meeting; Istanbul, Turkey. June 2013.

A. Harding, C. Pateman, C. Christmas, A. Loescher, P. Robinson, F. Claeyssens, J. Haycock and F. Boissonade. **A Comparison Between Polyethylene-glycol Based Nerve Guide Conduits and Graft Repair of the Common Fibular Nerve in *thy-1-YFP-H* Mice**. Poster presentation at the Regener8 annual meeting; Newcastle, UK. September 2012.

A. Harding, C. Christmas, M. Ferguson, A. Loescher, P. Robinson and F. Boissonade. **The Effects of Mannose-6-Phosphate on Nerve Regeneration in *thy-1-Yfp-H* Mice**. Poster presentation at the 14th World Congress on Pain; Milan, Italy. August 2012.

A. Harding, C. Christmas, M. Ferguson, A. Loescher and F. Boissonade. **Visual Analysis of Axonal Regeneration in *thy-1-YFP-H* Mice**. Poster presentation at the BSODR annual meeting; Sheffield, UK. September 2011.

TABLE OF CONTENTS

LIST OF FIGURES

LIST OF TABLES

1.0 INTRODUCTION

The body of work presented within this thesis utilises a transgenic mouse strain - *thy-1-YFP-H* - to develop a range of analysis methods for assessing nerve regeneration in a peripheral nerve repair model. These methods were used to assess the regeneration of injured peripheral nerves following a variety of interventions carried out using the *thy-1-YFP-H* peripheral nerve repair model.

Prior to discussing results of the studies carried out I will provide a general overview of the current state of knowledge on peripheral nerve injuries and their repair.

1.1 CAUSES AND IMPACT OF NERVE INJURIES

Injuries to the peripheral nerves are commonplace throughout the world, with a reported 300,000 cases annually in Europe alone (Ciardelli and Chiono, 2006). These range from minor compression injuries and simple transections, through to injuries associated with severe lacerations or avulsion fractures.

Of the vast number of potential causes of peripheral nerve injury [PNI] motor vehicle accidents account for a large percentage among the general population [43.9%]; more than three-quarters of non-iatrogenic civilian PNIs can be accounted for when combining the number of injuries caused by motor vehicle accidents with those caused by falls and laceration/penetration injuries [77.8%] (Kouyoumdjian, 2006). One particular injury associated with motor vehicle accidents is to the brachial plexus, which consists of a series of major nerve trunks originating from the C5 to T1 spinal nerves that come together near the shoulder joint (Orebaugh and Williams, 2009). It is estimated that around 1.2% of multiple-trauma patients suffer an injury to the brachial plexus and of those patients the causative factor is stated as motor vehicle accident in 21-29% of cases and motorcycle accident in 22-27% (Midha, 1997, Dubuisson and Kline, 2002).

Bone fractures and dislocations are another important cause of PNIs, with the median and radial nerves in the arms appearing particularly susceptible. Galbraith and McCulloch (1979) reported an incidence of 1.4% [over a seven year period] of nerve injuries associated with fractures and dislocations of the elbow. A more recent study by Senes et al. (2009) reported that 42.9% of PNIs resulting from upper limb trauma were as a result of bone fractures - 84.4% of those involved either median or ulnar nerves.

Both upper and lower extremities appear to suffer a higher level of nerve injuries than the torso, perhaps in part as a result of the higher range of flexibility and movement required by the limbs. In a military setting it has been estimated that 30% of combat injuries to the extremities include PNIs (Roganovic and Petkovic, 2004). Schulz et al. (2012) reported that, over a recent three year period, 5.8% of neurological surgical procedures carried out at an Afghanistan field hospital were for PNIs. In the past, this high incidence of PNIs sustained by military personnel in wars has proven to be an important factor in driving forward the understanding of PNIs and methods to repair them (Seddon, 1943).

The surgical setting is another area where a significant number of nerve injuries occur. In a study by Kretschmer et al. (2001) it was reported that, over a nine-year period at one nerve centre, 4.5% of all operations to repair PNIs were iatrogenic in origin, with the largest proportion as a result of orthopaedic surgeries. Location plays an important role in iatrogenic injuries for certain nerves: for example, those in the mandibular branch of the trigeminal nerve are at relatively high risk of becoming damaged during extraction of the lower third molars due to their close proximity to the roots of those teeth (Holland and Robinson, 1998, Fried et al., 2001). In addition, procedures involving general anaesthesia can result in indirect nerve injuries, often in the upper extremities and possibly as a result of a patient's position during the procedure (Kroll et al., 1990, Cheney et al., 1999, Welch et al., 2009).

Aside from the impact upon the patient there is the potential for litigation against the surgeon and medical institution, a previous study reported that from 2500 medical liability cases, 217

[8.7%] were for iatrogenic PNIs (Mullervahl, 1984). Two closed claims analyses by Kroll et al. (1990) and Cheney et al. (1999) which looked at anaesthesia related nerve injuries reported 15% - 16% of claims in the American Society of Anesthesiologists Closed Claims Project Database were for nerve injuries related to anesthesia. The median compensation payments related to these claims were $18,000 (Kroll et al., 1990) and $35,600 (Cheney et al., 1999), though in both studies the median payments for nerve injury claims were significantly lower than non-nerve injury claims.

Although the impact of peripheral nerve injuries will naturally vary between cases - based on severity, permanence and location - most injuries will have a major effect on the quality of life of a patient. Declines in both physical and psychological quality of life, along with increased indications of clinical depression, have been shown in studies assessing the impact of upper extremity nerve injuries (Bailey et al., 2009). Moreover, the level of post-traumatic stress following traumatic injuries to the arms and hands, which often result in PNIs, has been quoted as being equivalent to that experienced by survivors of a high mortality shipwreck (Ruijs et al., 2005). Damage to nerves supplying the mouth and lips can be extremely traumatic, as symptoms often include problems with speech and taste (Hillerup, 2007).

The poor prognosis for recovery of function in many nerve injuries is likely an important factor in the increase of depression and decrease in quality of life perceived by patients. Despite many important breakthroughs and discoveries, and the ability of peripheral nerves to regenerate following injury, full functional recovery following surgical intervention is still unpredictable and never complete (Robinson et al., 2000). The morphology of individual nerves and the complex anatomy of peripheral nerves as a whole is a key factor in this failure of complete regeneration.

1.2 THE INTACT PERIPHERAL NERVE

The peripheral nervous system [PNS] is a complex network of nerves consisting of 12-pairs of cranial nerves and 31-pairs of spinal nerves, each made up of many thousands of individual nerve cells connecting a wide variety of end organs with the central nervous system [CNS] (Fernandez et al., 1996, Zochodne, 2008).

Information flows to and from the CNS via individual sensory and motor nerve cell axons. These axons can be either myelinated or unmyelinated: myelinated axons are individually enveloped by the myelin sheath from a series of Schwann cells running along the length of the axon. Each individual Schwann cell myelinates a separate section of the axon - these myelinated sections are termed internodes as they separate areas of bare axon called nodes of Ranvier (Vizoso and Young, 1948, Lascelle and Thomas, 1966). The length of these internodes is an important factor in nerve function, with faster conductance achieved in axons with longer internodes (Wu et al., 2012). The length of the internodes of nerves increase linearly in relation to the diameter of the nerve, with larger diameter nerves possessing internodes of longer length (Boycott, 1903, Vizoso and Young, 1948, Cragg and Thomas, 1964, Lascelle and Thomas, 1966). Once an axon is myelinated the number of internodes it has remains constant, with the only change being the increase in length of the internodes to accommodate a juvenile animal's transition to adult (Vizoso and Young, 1948, Vizoso, 1950).

Unmyelinated axons are not, as the name suggests, completely devoid of Schwann cell myelination - the axons are grouped together within myelin from a single Schwann cell at each internode, forming a Remak bundle (Geuna et al., 2009, Kaplan et al., 2009). A large proportion of axons in the mammalian PNS are unmyelinated, with myelination generally occurring in larger diameter [1.5µm and above] axons (Matthews, 1968). In the dorsal and ventral spinal roots the percentages of unmyelinated axons are 75% and 30% respectively (Geuna et al., 2009).

Within a peripheral nerve the neuronal axons are bound together by connective tissue sheaths. The endoneurium surrounds the axons of individual nerve cells, the perineurium surrounds bundles of endoneurial tubes [known as fascicles], and the epineurium is the outer layer of nerve tissue responsible for much of the protection required by the nerve [fig. 1.1](Geuna et al., 2009).

The endoneurium consists mainly of type I and III collagen along with endoneurial fluid, blood vessels and a variety of cells [mainly Schwann and endothelial cells]. It functions to protect the fascicles from blunt trauma and each fascicle within a nerve is surrounded by the perineurium (Zochodne, 2008, Geuna et al., 2009)[fig. 1.1].

The perineurium is a dense, strong sheath that is made up of layers of collagen and epithelium-like cells, with these layers arranged in an alternating pattern. Towards the outer edge of the perineurium the alternating collagen/cell layers give way to fibrous tissue which merges with the epineurium (Geuna et al., 2009)[fig. 1.1].

The epineurium [which is also known as the epineural sheath] is the outer layer of a nerve and contains blood and lymph vessels and cells, such as resident macrophages, fibroblasts, and mast cells. It is mostly made up of type I collagen with some elastic fibres and it's structure, along with its limited connection to other local tissues, allows the nerve to slide into different positions and extend [to a limited extent] during movement (Zochodne, 2008)[fig. 1.1].

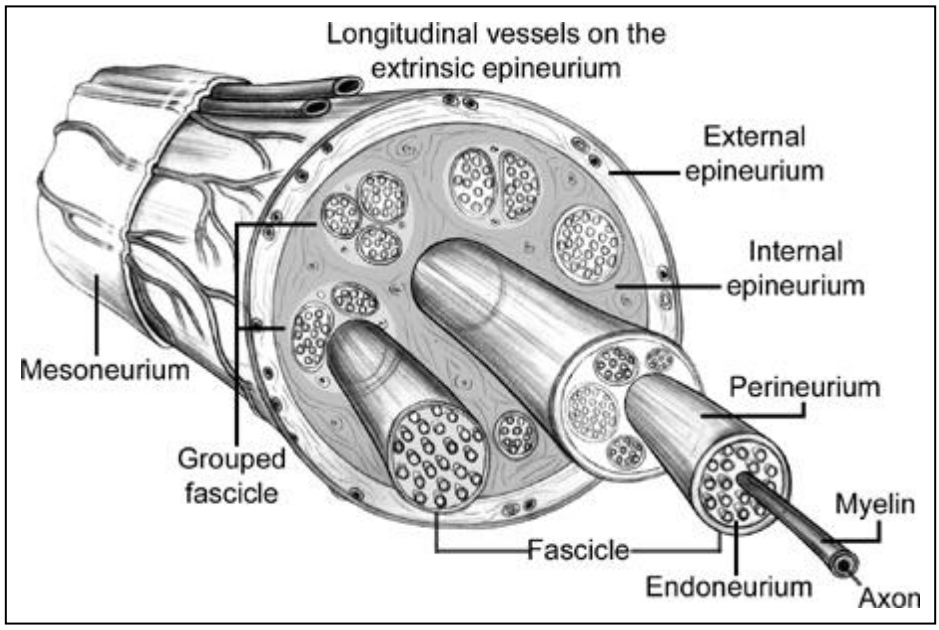

Figure 1.1: Diagram showing the general structure of a peripheral nerve trunk (Weber and Dellon, 2004) Used with permission from Lippincott Williams and Wilkinson, http://www.lww.com/Product/9780781728744.

1.3. CLASSIFICATION OF PERIPHERAL NERVE INJURIES

1.3.1 Seddon's Classification.

The first published attempt at classifying nerve injuries was made by H. J. Seddon and published in 1943. At that time the terms used in situations where nerve damaged had occurred tended to describe 'how' the injury had occurred [e.g. compression, contusion etc.] rather than describing the actual injury suffered by the nerve (Seddon, 1943). Seddon defined three types, or grades, of nerve injury; neurotmesis, axonotmesis and neurapraxia - the terms used were suggested by Professor Henry Cohen (Seddon, 1943).

Neurapraxia is the mildest nerve injury type in Seddon's classification and, unlike axonotmesis and neurotmesis, no Wallerian degeneration occurs following the injury. It is often caused by blunt trauma or compression and is essentially a temporary block in axonal conductance. Recovery from the associated, often incomplete impairment is rapid and complete (Seddon, 1943).

In Seddon's classification the next level of nerve injury is termed axonotmesis; this type of injury occurs when individual axons become disrupted to the extent that Wallerian degeneration takes place. With axonotmesis the supporting structures remain relatively intact which allows the damaged nerve to recover, spontaneously, to a good level of functionality (Seddon, 1943).

The term used for the most severe level of nerve injury in Seddon's classification is neurotmesis; this type of injury involves the complete transection of all essential structures in the nerve and has the poorest prognosis for recovery. The main difficulty for the regenerating nerve fibres is that the supporting structures, that in the case of axonotmesis would serve to guide them to where they should be, have also been damaged (Seddon, 1943). The retraction of the nerve stumps following neurotmesis is another major factor in the ability of the nerve to regenerate successfully, as without surgical repair the nerve fibres would need to bridge a potentially significant gap.

1.3.2 Sunderland's Classification.

Expanding the concepts proposed by Seddon in 1943, S. Sunderland proposed a method of classification which involved five degrees of nerve injury [fig. 1.2]. Sunderland's classification is comparable with Seddon's, with a 1st degree injury equivalent to neurapraxia, 2nd, 3rd & 4th degree injuries roughly equivalent to varying severities of axonotmesis and 5th degree injuries roughly equivalent to neurotmesis (Sunderland, 1951).

In 1st degree nerve injuries [fig. 1.2a], as in neuropraxia, a blunt trauma or compression of the nerve results in a conduction block; this block can result in paralysis due to loss of nerve motor function, and also sensory impairment. Both motor and proprioceptor function [the ability to know the position of one's limbs/body] are affected more than the sensations of touch and pain, with the latter sensations regained earlier during recovery (Sunderland, 1978). Unlike the more severe degrees of injury, where axon conductance is lost distal to the lesion, in 1st degree injuries distal nerve fibres are still excitable – although not across the lesion area (Fowler et al., 1972, Sunderland, 1978). Recovery from 1st degree injury is spontaneous; sensory function is first to return followed by motor function. Recovery of motor function in this type of nerve injury, unlike nerve injuries where the axon is transected, does not have a sequential recovery order related to the distance that the innervated muscle is from the lesion and muscles will either recover function simultaneously or in a random order over the course of a few days (Sunderland, 1978). In experimental studies relationships between the length of time of compression and recovery [longer compression time resulting in longer recovery time] and also between the length of compressed nerve and recovery [a longer section of nerve compressed resulting in longer recovery] have been established (Fowler et al., 1972, Rudge et al., 1974, Sunderland, 1978), although clinical observations often differ. Occasionally the instigation of recovery is delayed until exploratory surgery and neurolysis is performed, in those cases that are not simply coincidental this is due to continued pressure from fibrous tissue in the local area that is relieved during the surgical procedure (Sunderland, 1978).

In 2nd degree nerve injury [fig. 1.2b] the continuity of the axon is compromised, either by the distal portion becoming detached or axonal mechanisms becoming disrupted to the extent that the distal portion fails to survive (Sunderland, 1978). Other than the damage to the axon, the nerve is relatively damage free; with the endoneurium surrounding each axon remaining continuous. Wallerian degeneration occurs due to the loss of axon continuity and the axon, along with its myelin sheath, is broken down - this results in the target organ becoming denervated (Sunderland, 1978). As the nerve must regenerate axons in order to reinnervate its target, the recovery time is longer than in 1st degree injury and muscles supplied by the nerve demonstrate signs of atrophy. Overall recovery of the nerve is good due to affected axons being constrained to their original endoneurial tube, which guides them along their original pathway to their target synapse - in some exceptional cases some minor traces of nerve defect remain due to the loss of axons (Sunderland, 1978). There are influencing factors that determine the length of time between the injury occurring and full recovery of function, such as the level of injury [how far the axons need to re-grow], rate of axon growth and how long the affected tissues are denervated. Reinnervation occurs in a systematic fashion, with the target organs closest to the lesion recovering prior to ones further away (Sunderland, 1978).

In 3rd degree injury [fig. 1.2c] there is intra-fascicular damage which results, in addition to the axon severance seen in 2nd degree injury, in the loss of endoneurial continuity within fascicles. The loss of endoneurial continuity is an important factor in the additional recovery time and poorer functional recovery of 3rd degree injury when compared to 2nd degree injury (Sunderland, 1978). As axons are no longer constrained to their original endoneurial tube there is a significant chance that they may enter the wrong endoneurial tube distal to the lesion or fail to reach a distal endoneurial tube at all. An additional obstacle for axons to overcome is the fibrosis that forms within the fascicle due to the intra-fascicle damage suffered [haemorrhage, oedema, ischemia]. This fibrosis causes the rate of regeneration of axons to slow and can also block and divert axons away from their intended path

(Sunderland, 1978). As the regenerating axons may enter the wrong distal endoneurial tubes or become delayed by fibrosis, the subsequent re-innervation usually occurs in a much less systematic manner than in 2nd degree injuries and in addition is much less complete due to an increase in neurone death in addition to axon misguidance (Sunderland, 1978). Differences in the level of impact of 3rd degree injuries can occur as a result of the affected fascicles composition; with injuries to fascicles containing axons wholly responsible for motor function resulting in localised paralysis but mixed axon fascicle injuries often resulting in more wide spread parethisis and sensory impairment (Sunderland, 1978).

With 4th degree nerve injury [fig. 1.2d] the continuity of the perineurium is affected in addition to the epineurium, resulting in axons being able to enter the intra-fascicular space with the potential to form painful neuromas. An increase in fibrosis formation, neuronal cell death and difficulty in axons reaching the correct epineurial tube result in very poor, if any, true functional recovery without surgical intervention (Sunderland, 1978).

Corresponding to Seddon's neurotmesis, 5th degree nerve injury [fig. 1.2e] involves the complete disruption of the nerve, to the extent that the portion of nerve distal to the lesion site is no longer physically connected to the portion proximal of the lesion. This exacerbates the problems observed in 4th degree nerve injury as, in addition to navigating across the gap formed when the nerve is transected, there is also considerable scar tissue formation in the area surrounding the lesion site (Sunderland, 1978) and potential for infection in cases where the injury is caused by an external object piercing the skin. The severity of this degree of injury often leads to significant neurone death and, with many of the axons of remaining neurons unable to navigate successfully to the distal stump, functional recovery is negligible. Additional features of 5th degree nerve injury that add to the difficulty of regeneration are that the distal end often shrinks in diameter following transection leading to a difference in the cross-sectional area between nerve ends, and the pattern of fascicles is affected during the injury event - especially if, rather than a straight forward clean cut, some of the nerve tissue is destroyed or removed (Sunderland, 1978).

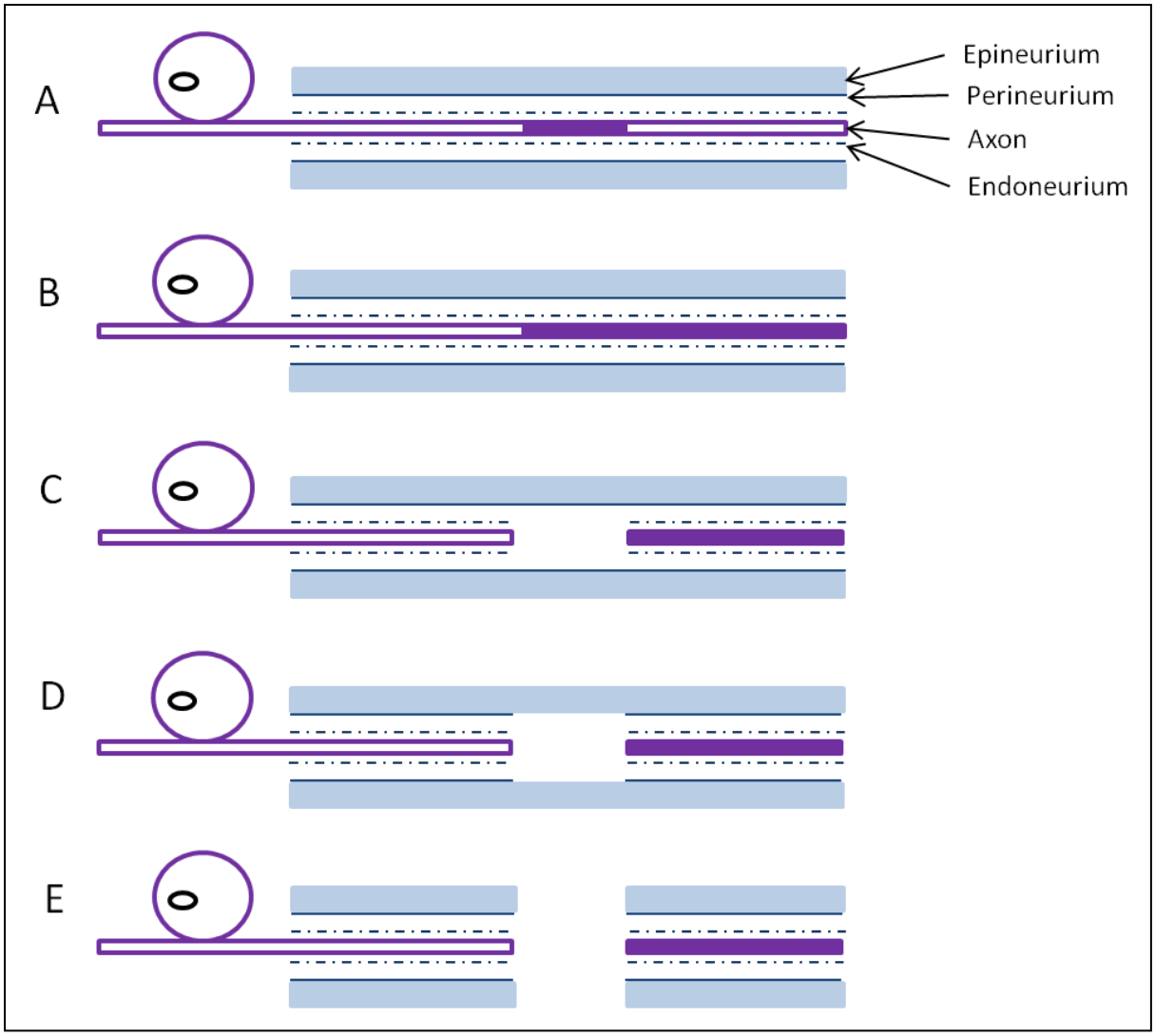

Figure 1.2: Simple diagrammatical representation of nerve injuries in Sunderland's classification system. A) 1st degree injury - transient conductance block. B) 2nd degree injury - severance of axon. C) 3rd degree injury - severance of axon and endoneurial sheath. D) 4th degree injury - severance of axon, endoneurial sheath and perineurium. E) 5th degree injury - complete severance of nerve.

1.4. EVENTS IN THE PERIPHERAL NERVE FOLLOWING INJURY

In nerve injuries where the continuation of axons is interrupted, Wallerian degeneration is instigated within hours, along with numerous other changes around both the injury site and the cell bodies of neurons affected. Within the first few hours of transection the axons reseal their ends in order to prevent the continued loss of axoplasm and Schwann cells change from their seemingly dormant state to a more active state and undergo hypertrophy of the cytoplasm (Lubinska, 1982, Zochodne, 2008)

In the first twenty-four hours following injury a number of important events take place: calcium dependant axonal degeneration, down regulation of myelin synthesis and retraction of cytoplasm from the myelin sheath by Schwann cells, and the loss of nerve action potentials (Brueck, 1997). The calcium dependant degeneration of axons occurs due to an influx of calcium into the nerve environment which modulates the activity of local enzymes involved in the degeneration of enzymes. Calpain is one enzyme whose activation appears critical in triggering axon degeneration (Schlaepfer and Hasler, 1979, George et al., 1995), and is necessary in order to clear the distal section of the nerve for the regenerating axons to travel through. This degeneration has been shown to be a pre-requisite of sensory nerve regeneration (Bisby and Chen, 1990), although some experiments involving motor neurons did not display the same inhibitory effects (Lunn et al., 1989). In a study by Sørensen et al. (2001) axonal outgrowth only occurred in sections of nerve that had been cleared of myelin and axonal sprouts did not enter areas containing intact myelin debris. Some early studies identified this apparent passive degeneration process as the solitary mechanism of direct axonal degeneration with the cessation of the supply of proteins from the cell body also an indirect factor (Schlaepfer and Hasler, 1979). The discovery of the role of various cytokines, chemokines, growth factors and adhesion molecules, along with studies on C57BL/*Wld*$^{S-}$ mutant mice [which have axons resistant to Wallerian degeneration] demonstrated the multi-mechanistic and active process nature of Wallerian degeneration following injury (Coleman and Perry, 2002, Martini et al., 2008).

The breakdown and clearance of myelin is another key event in Wallerian degeneration with Schwann cells playing a key role in the process. Shortly after injury Schwann cells proliferate rapidly and change to a more active phenotype that, instead of maintaining myelination of the axon, is geared towards the breakdown and phagocytosis of myelin (Clemence et al., 1989). How Schwann cells become activated is not fully understood, however, the binding of endogenous molecules [such as mRNA] derived from damaged nerves to toll-like receptors [TLRs] expressed on the surface of Schwann cells is implicated (Karanth et al., 2006, Lee et al., 2006). Once activated Schwann cells begin expressing monocyte chemotactic protein-1 [MCP-1], which in turn is linked to the expression of members of the phospholipase A_2 [PLA_2] family of enzymes (Martini et al., 2008). Two forms of PLA_2 have been identified as being present in the very early stages following nerve injury; group IIA $sPLA_2$ [a secreted form] and group IVA $cPLA_2$ [a cytosolic form] and their expression correlates with the rate of Wallerian degeneration (De et al., 2003). PLA_2s hydrolyse membrane phospholipids and when hydrolysed phosphotidylcholine - found in high quantities in myelin membranes - becomes lysophosphotidylcholine [LPC]: a potent myelinolytic agent [fig. 3] (Hall and Gregson, 1971, Martini et al., 2008) which can initiate signs of demyelination in 30 minutes when injected into peripheral nerves (Hall and Gregson, 1971).

Although local Schwann cells are capable of a certain amount of myelin degradation and clearance, perhaps enough to clear myelin from small myelinated fibres (Stoll et al., 1989), the presence of macrophages recruited to the area by Schwann cell signalling enables further degradation and clearance along with the triggering of rapid Schwann cell proliferation (Clemence et al., 1989, Kubota et al., 1998, Liu et al., 2000).

Despite the ability of Schwann cells to degrade myelin and also proliferate to some extent [in part through assistance of the local macrophage population] (Fernandezvalle et al., 1995) and actively participate in Wallerian degeneration (Shen et al., 2000), it is recruited hematogenous macrophages that enable the rapid degredation and clearance of myelin (Beuche and Friede, 1984). Beuche and Friede (1984) demonstrated the importance of

hematogenous macrophages in Wallerian degeneration in an experiment where sections of pre-degenerated peripheral nerves of mice were implanted within the peritoneal cavity within diffusion chambers with pore sizes that either excluded macrophages or did not exclude macrophages. The results of the experiment showed that when macrophages were excluded, limited myelin degradation occurred over a long course of time but the nerves where macrophages were not excluded underwent a breakdown of myelin much closer to normal Wallerian degeneration. Numerous molecules are linked with hematogenous macrophage recruitment following nerve injury, though the exact recruitment process is complex, it relies of many different systems and is not fully understood (Martini et al., 2008). Monocyte chemoattractant protein-1 [MCP-1] and macrophages inflammatory protein-1α [MIP-1α] are known to be important in macrophage recruitment as their inhibition by function blocking antibodies has been shown to reduce macrophage numbers in an injured nerve by 78% (Perrin et al., 2005). Also linked to macrophage recruitment into nerve tissue are tumour necrosis factor-α (TNF-α), interleukin-1α [IL-1α] and interleukin-1β [IL-1β], which are expressed by Schwann cells and whose deficiency is notable in delayed Wallerian degeneration in certain mutant strains of mice (Shamash et al., 2002).

Once recruited to the site of nerve injury hematogenous macrophages contribute to the expression of PLA_2 and resultant LPC production, which is capable of activating the complement element of the immune system (Hack et al., 1997). The activation of complement results in the opsonization of myelin with C3 protein, which enables myelin to be phagocytosed at an increased rate due to the increased efficiency of phagocytosis of cells and cellular material following opsonization (Kemp and Turner, 1986). As a matter of fact, macrophage phagocytosis of myelin is highly dependent on myelin becoming opsonized as blocking complement receptor 3, which is one of two phagocytosis mediating receptors found on macrophages, halts myelin phagocytosis but blocking of the other, non-complement dependant, Fc receptor does not (Brueck, 1997).

Around 10-20 days after the initiation of Wallerian degeneration the local Schwann cells and endoneurial tubes form guidance tubes known as bands of Büngner which provide both physical and neurotrophic guidance for regenerating axons and increase the potential for re-innervation of target organs/tissues (Sunderland, 1978).

The central ends of damaged axons usually begin sprouting from the first node of Ranvier proximal to the site of injury, though some may begin sprouting from the second node of Ranvier (Friede and Bischhausen, 1980). Although it is primarily the injured axons that sprout, collateral sprouting from nearby uninjured axons can also take place (Zochodne, 2008).

The leading edge of the regenerating axon is formed into a structure called the growth cone, which has a key role in the navigation and continued growth of the axon. The growth cone structure is often compared to a hand - a central 'palm' area contains the terminal ends of microtubules and axoplasm from which the web-like lamellipodia emerge and actin filaments from the lamellipodia help to form the finger-like extensions called filopodia (Zochodne, 2008).

The area of the growth cone consisting of lamellipodia and filopodia is motile and responsible for exploration of the local area, responding to various signals that guide the regenerating axon towards its target; the filamentous actin [f-actin] that makes up this portion of the growth cone is in a state of constant retrograde flow [movement towards the central region of the growth cone, powered by myosin connected to a non-moving sub-membranous matrix] which is counteracted by what is called f-actin treadmilling [where f-actin subunits are moved towards the edge of the filopodia] and it is the balance between these two movements that allow filopodia to extend, retract or remain stationary (Mitchison and Kirschner, 1988, Lowery and Van Vactor, 2009). The rate of retrograde flow is continuous so in order for filopodia to extend or retract the rate of f-actin subunit transportation to the end of the filopodia needs to increase or decrease respectively - this is dependent on the

availability of f-actin subunits and also the accessibility of the distal f-actin end (Mitchison and Kirschner, 1988). Forward movement of the growth cone [rather than just filopodia extension] occurs when filopodia bind to adhesion molecules that fix the f-actin in position; now the myosin will effectively 'pull' the growth cone forwards, resulting in the extension of the axon behind it - this mechanism is often likened to placing a car in gear (Mitchison and Kirschner, 1988).

Axon regeneration following 2nd degree nerve injury, where the axons remain confined to their original endoneurial tubes, is considered a simpler process than axon regeneration following a more severe injury where the endoneurial tubes are breached. However, the actual method of axon regeneration remains the same in either case - figures 1.3 & 1.4 show the differences in regeneration between these injuries.

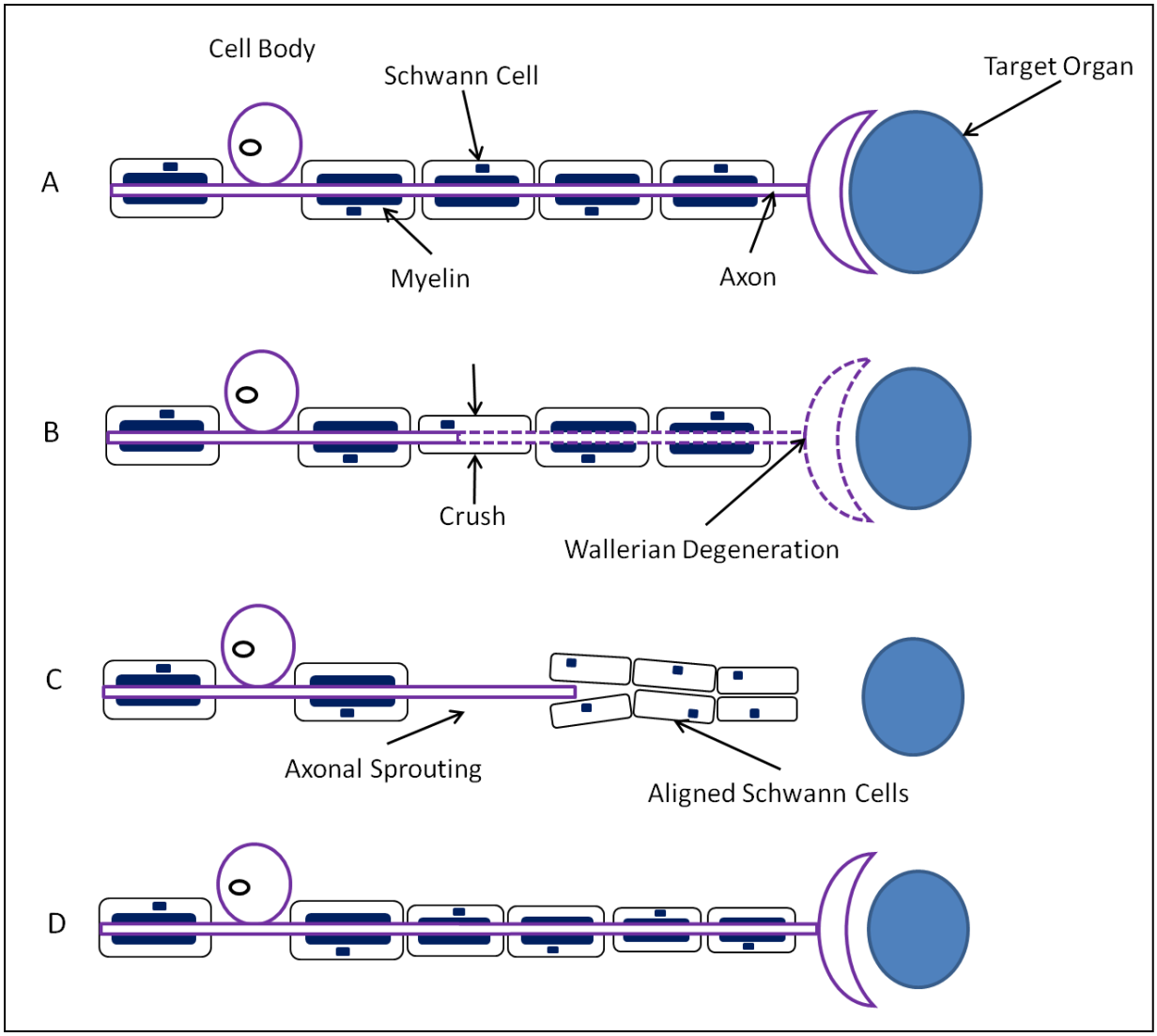

Figure 1.3: Axon regeneration following a crush injury resulting in a 2nd degree nerve injury. A) Uninjured nerve. B) Crush injury to the nerve. C) Axon sprouting and regenerating along original endoneurial tube. D) Successful regeneration. (Holland and Robinson, 1998).

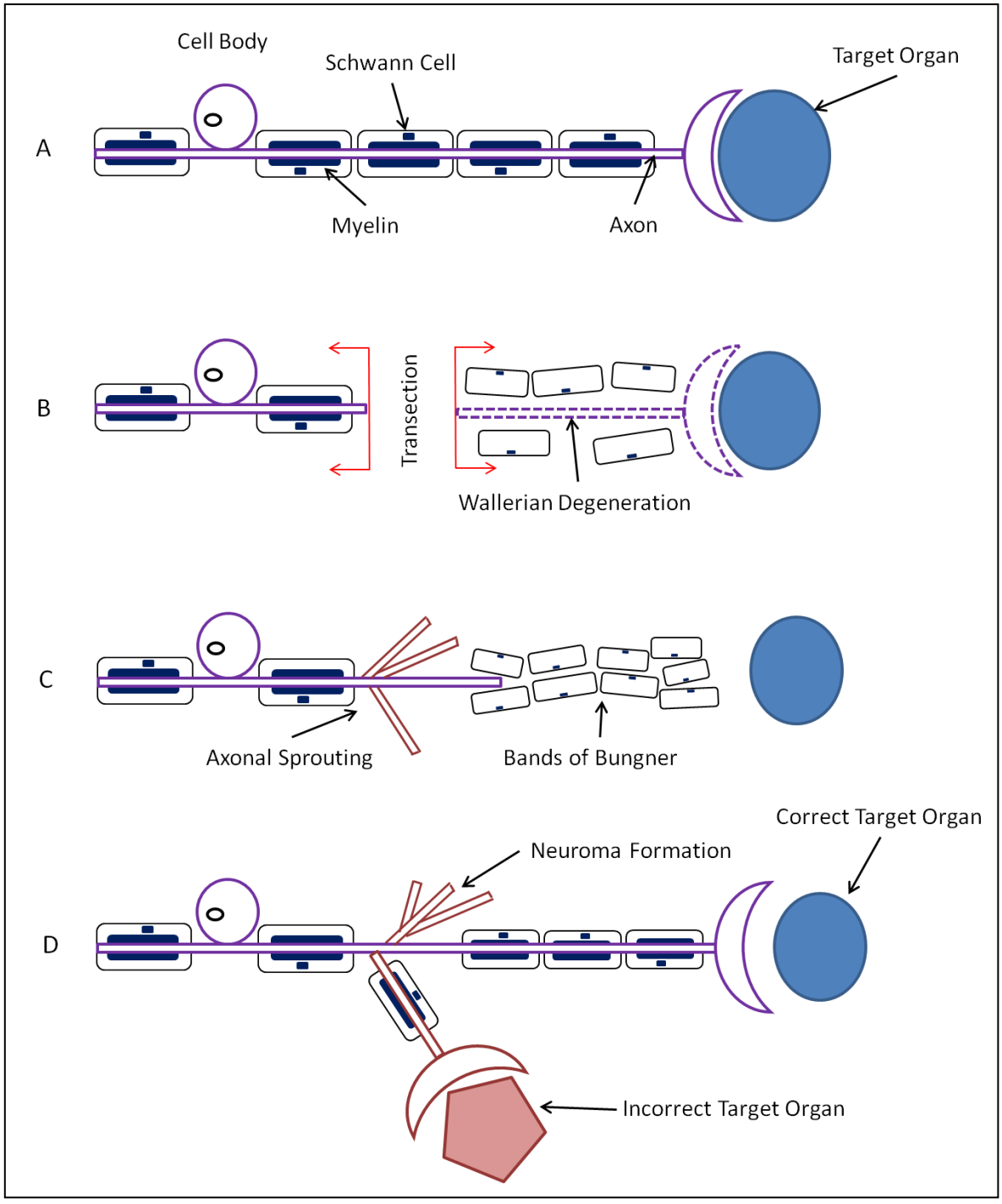

Figure 1.4: Axon regeneration following transection injury. A) Uninjured nerve. B) Transection injury to the nerve with retraction of severed nerve endings. C) Axon sprouting and attempting to find endoneurial tube. D) Potential outcomes for the regenerating axon - finds original endoneurial tube and regenerates to original target; enters incorrect endoneurial tube and fails to find original target; fails to enter any endoneurial tube and forms a neuroma. (Holland and Robinson, 1998).

1.5. A BRIEF HISTORY OF SURGICAL PERIPHERAL NERVE REPAIR

The surgical repair of injured peripheral nerves by direct suturing has long been used in order to improve the recovery of sensory and/or motor functionality. Gabriele Ferrara, a Milanese surgeon in the late 16th century, is often regarded as being the first to provide an accurate description of peripheral nerve suturing and is attributed with being the "father" of peripheral nerve reconstruction (Artico et al., 1996). Despite this there were actually many previous descriptions of the potential for peripheral nerve regeneration and repair throughout the previous centuries from the likes of Galen in the second century and Paul von Aegina in the seventh century (Battiston et al., 2009).

In the mid to late 17th century two early pioneers of microscopy, Robert Hooke and Antonio van Leeuwenhoek, ignited scientific interest in the microscopical world with accounts of their discovery's using their simple self made microscopes; van Leeuwenhoek giving accounts of, amongst many other things, nerve fibres (Gest, 2004, Wade, 2004). Van Leeuwenhoek noted that optic nerves happened to be made up of "many filamentous particles", rather than being hollow as claimed by anatomists of the period (Wade, 2004).

In the 19th century, thanks to significant developments in microscope construction (Wade, 2004), research into the nervous system began to gather pace and key discoveries about nerve injury and regeneration were made. In 1850 Augustus Waller published what would become a decisive paper in the development of understanding nerve injuries; in this paper Waller described events following nerve transection which included axon and myelin degeneration distal to the injury (Waller, 1850) - an event which would later be termed "Wallerian degeneration". Later in the 19th century the first descriptions of end-to-side nerve repair, autograft and allograft repair, and tubular nerve defect bridging were published (Battiston et al., 2009)

Early in the 20th century there was a great deal of interest and cooperation between clinical and basic scientists in the field of peripheral nerve repair and regeneration. However, as the

century progressed interest and cooperation began to fade due to doubts over the potential for improving nerve regeneration and differences in direction of clinical and basic research - with clinical research moving towards optimization of repair techniques and basic research moving towards molecular and chemical study (Battiston et al., 2009). In recent years the interest in peripheral nerve regeneration has undergone a resurgence with an increase in research related to understanding and improving peripheral nerve regeneration which, hopefully, will lead to new breakthroughs that can reduce the personal impact of peripheral nerve injury.

1.6. CURRENT CLINICAL REPAIR TECHNIQUES

Direct surgical intervention is usually limited to the more severe nerve injuries; mainly 5th degree nerve injuries in Sunderland's classification. Any surgery performed on a patient exhibiting symptoms of less severe nerve injuries [such as 1st or 2nd degree injuries] is usually to reduce pressure on the nerve from surrounding tissues or reduce internal pressure within the nerve (Sunderland, 1978, Matz et al., 1989).

1.6.1 Directly Sutured Repairs.

The choice of repair technique used is highly dependent on the extent of damage to the nerve but in a simple transection with no significant loss of nerve tissue the preferred repair method is end-to-end repair. The simplest form of end-to-end repair is epineural repair [fig. 1.5], which is used when the nerve injury is a clean full or partial transection where fascicles can be easily aligned correctly. This technique usually involves suturing the nerve ends together with sutures passing through the epineurium, although fibrin glue can be used as an alternative method with the benefit of less foreign material present and reduced potential for scar tissue formation (Ornelas et al., 2006a, b).

When minor trimming of the nerve ends is required grouped fascicle repair can be used. In this technique the epineurium is retracted allowing access to the fascicles and then groups of fascicles from the central end are approximated to their corresponding distal partners by passing sutures through the inter-fascicular epineural space (Siemionow and Brzezicki, 2009). A third end-to-end repair technique is fascicular repair; which uses sutures through the perineurium to align individual fascicles more precisely [fig. 1.6], however, due to its technical demands and high number of sutures required it is not a commonly used technique (Siemionow and Brzezicki, 2009). Although both grouped fascicular and fascicular repairs align the fascicles more precisely than epineural repair, which theoretically should lead to less misdirected axons, experimental studies have indicated little advantage when functional recovery is evaluated (Lundborg et al., 1997) and there is additional risk of fibrosis formation

in the nerve due to the significant increase in the amount of sutures required (Siemionow and Brzezicki, 2009).

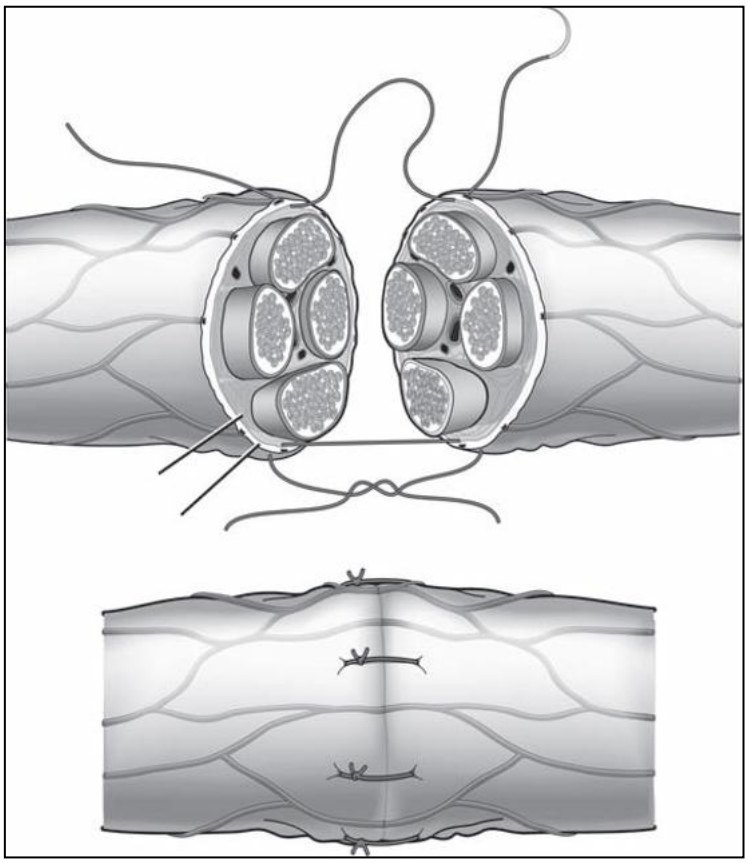

Figure 1.5: Epineural repair of transected peripheral nerve (Siemionow and Brzezicki, 2009). Used with permission from Elsevier Inc.

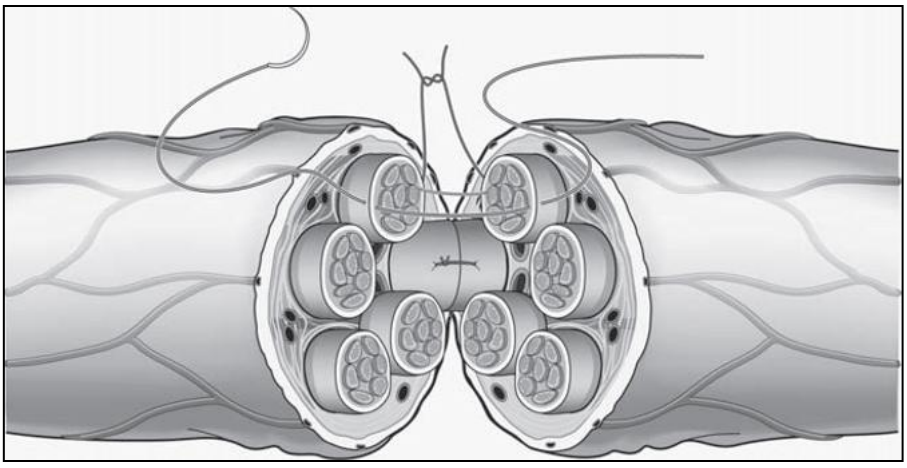

Figure 1.6: Individual fascicular repair of transected peripheral nerve (Siemionow and Brzezicki, 2009). Used with permission from Elsevier Inc.

An additional method of end-to-end repair is epineural sleeve repair. In this method the epineural sheath of the distal end of the nerve is turned back to expose approximately 2mm of nerve tissue, which is then removed. Two sutures are then passed through opposing sides of the now excess epineural sheath and it is pulled over the central nerve end and secured in position with two additional sutures [fig. 1.7](Lubiatowski et al., 2008). This method has been shown to improve the speed of functional recovery in studies when compared to the more established end-to-end techniques; with reasons such as the epineural sleeve providing a sealed neuro-permissive environment and the transfer of tension away from the lesion site both being postulated (Lubiatowski et al., 2008, Siemionow and Brzezicki, 2009).

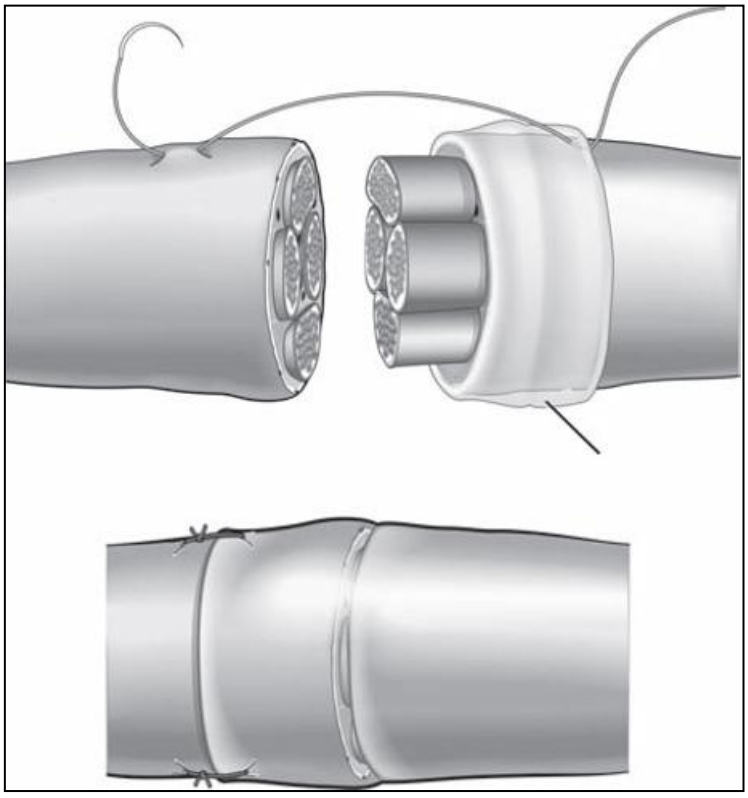

Figure 1.7: Epineural sleeve repair of transected peripheral nerve (Siemionow and Brzezicki, 2009). Used with permission from Elsevier Inc.

Often nerve injuries result in the loss of tissue to the extent that the nerve ends cannot be brought together without undue tension, in certain cases the nerve can be repositioned to reduce the gap between nerve ends to allow conventional end-to-end repair (Roganovic and Petkovic, 2004), if this is not possible the gap can be bridged using a nerve graft. The reason that undue tension following a repair is avoided is that the blood flow within the nerve is inversely proportionate to the tension in the nerve, with the result that an excessive increase of tension will cause ischemia around the repair site and inhibit the regeneration process (Siemionow and Brzezicki, 2009). Although nerve grafts allow repair with little or no tension they do include a second repair site for the regenerating axons to transverse which can cause further axon loss due to the increased potential for scar tissue and misdirection (Bratton et al., 1979, Hudson et al., 1979). A number of studies have compared results of direct repair under moderate tension with graft repairs and have reported similar outcomes in both repair techniques (Bratton et al., 1979, Hudson et al., 1979, Wong and Scott, 1991). Thus, direct repair with some tension is preferred, providing the negative impact of the tension is lower than the negative impact that the additional repair site in a graft would be (Siemionow and Brzezicki, 2009).

1.6.2 Nerve Graft Repairs.

Nerve autografts are currently the 'gold-standard' repair technique for bridging nerve gaps that would place excessive tension upon the repair site and they involve the harvesting of a sensory donor nerve of the correct size from the patient. The choice of donor nerve is influenced by factors such as the size of the nerve gap and the morbidity at the donor site, sensory nerves are used as the loss of sensation has less impact on a patient than a loss of mobility although the use of motor nerve grafts in a number of studies has revealed significantly better nerve regeneration in motor and mixed nerve repairs - potentially due to the larger diameter endoneurial tubes found in motor nerve grafts (Nichols et al., 2004, Moradzadeh et al., 2008). The sural nerve is the most commonly used for nerve autografts (Ray and Mackinnon, 2010) but other suitable nerves include: the medial cutaneous nerve of

the arm, medial and lateral cutaneous nerves of the forearm, superficial branch of the radial nerve and intercostal nerves; ideally the donor nerve will be in a convenient position for harvesting, located near to the proposed repair site and will result in the least amount of morbidity possible (Norkus et al., 2005). Although nerve autografts provide a method of successfully bridging larger nerve gaps than direct repair can there are more disadvantages than just donor site morbidity; there is an increased infection risk due to a second incision site being made, it is considered inferior to a tension-free direct repair and, probably most importantly, there is only a limited amount of nerve available to harvest (Ray and Mackinnon, 2010).

In cases where nerve autografts are not suitable, either because the length of nerve gap is too great or a large number of nerves require repair, then nerve allografts can be used as an alternative. Harvesting of donor nerves from cadavers can supply nerve grafts long enough to bridge almost any gap and as the graft can be taken from the relevant nerve required there is greater compatibility between the graft and regenerating nerve (Siemionow and Brzezicki, 2009). The major drawback of nerve allografts is the need for immunosuppression of the patient to avoid rejection of the graft, although, unlike in organ transplant where immunosuppression is required for the life of the patient, immunosuppression is only required for a limited time [varying between six and twenty-four months] following a nerve allograft due to the migration of host Schwann cells into the graft replacing those of the donor (Mackinnon et al., 2001, Ray and Mackinnon, 2010). As with organ transplantation, the donor and recipient need to be matched by MHC [major histocompatibility complex] in order to minimise the possibility of graft rejection, additionally matching by ABO blood type has shown improvements in functional recovery (Mackinnon et al., 2001).

1.6.3 Nerve Guide Conduit Repairs.

An alternative to bridging gaps with nerve grafts is to use artificially constructed biological or synthetic conduits, which can avoid the disadvantages associated with nerve autografts. The repairing of a nerve using a conduit is similar in concept to using a graft - provide a scaffold guiding axons across the gap between nerve ends - but uses alternative laboratory constructed materials [whether biological or synthetic in nature]. Clinical use of conduits is not as commonplace as nerve grafting currently, though there are a number of authorised products available [see table 1]. Currently all approved artificial conduits for use in nerve repair are simple hollow tubes which are effective for bridging relatively short nerve gaps (Ichihara et al., 2008).

A number of animal studies have demonstrated the potential for artificial conduits to improve nerve regeneration over small gaps (Meek et al., 1996, Den Dunnen et al., 1998, Meek et al., 2001) and there is evidence that larger gaps [e.g. 80mm] can also be bridged with certain types of conduit (Matsumoto et al., 2000). More detailed discussion on the use of conduits can be found in chapters 5 and 6.

Table 1: Clinically approved nerve repair conduits. PGA: polyglycolic acid. PDLLA/CL: poly-DL-lactide-co-ε-caprolactone.

Product Name	**Material**	**Company**
NeuraGen® Nerve Guide	Collagen (type 1)	Integra
Neuromatrix™ Conduit	Collagen (type 1)	Collagen Matrix inc
Neuro*flex*™ Conduit	Collagen (type 1)	Collagen Matrix inc
Neurotube®	PGA	Synovis
Neurolac®	PDLLA/CL	Polyganics
AxoGuard® Nerve Connector	Porcine small intestinal submucosa	AxoGen Inc.

1.7. FACTORS AFFECTING NERVE REGENERATION

It is clear from both Seddon's and Sunderland's classifications that the degree of nerve injury suffered is a critically important factor in determining the level of functional recovery that an injured nerve may achieve. Although the degree of nerve injury may have the most influence over the level of functional recovery it is not, by any means, the only factor that affects successful nerve regeneration. Many other factors are linked, some more strongly than others, to the ability of a nerve to successfully regenerate; such as the nerve injured, the position of the injury, the type of nerve injured [motor/sensory/mixed], the age of the patient, the delay between injury and surgical repair, the type of surgery and even the sex of the patient.

1.7.1 EFFECTS OF AGE ON NERVE REGENERATION

Many studies have shown age to be an important factor in the outcome of peripheral nerve injury (Gutmann et al., 1942, Navarro and Kennedy, 1988, Vaughan, 1992, Ruijs et al., 2005), with the reduced rate and extent of axonal regeneration along with impaired terminal and collateral sprouting of regenerated and intact axons observed in older nerves highlighted as limiting factors (Kovacic et al., 2009). The review by Kovacic et al. (2009) found that the literature suggested that, rather than a limited ability of aged neurons to regenerate or respond to trophic factors, changes in the peripheral neural pathways and target tissues were responsible for the reduced regeneration in older nerves; a further study by the same group demonstrated that older neurons still had the intrinsic ability to regenerate (Kovacic et al., 2010).

One important age related factor appears to be a delay in the Wallerian degeneration response, Vaughan (1992) found that in older rats [fifteen months old] injured nerves were undergoing Wallerian degeneration with little axonal sprouting ten days post injury whilst in younger rats [3 months old] at the same time point injured nerves were showing signs of axonal regeneration. The cause of the delay in Wallerian degeneration is thought to be

related to the reduced proliferation and activity of Schwann cells in older nerves following injury. As Schwann cells play an important role in Wallerian degeneration [see section 2.2] a reduction in their number or activity will affect the speed and efficiency of this necessary step in nerve regeneration (Verdu et al., 2000, Kovacic et al., 2009). The reduction in proliferation of Schwann cells can be linked to a reduction in mitogenic factors secreted by the macrophages that migrate to the site of injury (Komiyama and Suzuki, 1991). There is a suggestion that better functional recovery in the PNS of children is related to the ability of the immature CNS to adapt to changes in signalling from the PNS (Dahlin, 2008). Essentially this means that when axons are misguided following peripheral nerve injury, a child's CNS is better able to adjust to the new signalling pattern it receives from the PNS than an adult's; which can lessen the functional difficulties experienced.

1.7.2 EFFECTS OF SEX ON NERVE REGENERATION

Differences in nerve regeneration between males and females have also been noted in studies on peripheral nerves (Kujawa et al., 1991, Kovacic et al., 2003, Kovacic et al., 2004). In a study on the effects of testosterone, the male sex hormone, Kujawa *et al*. (1991) found that the application of exogenous testosterone improved regeneration rates in both male and female hamsters but that the regeneration rates of untreated female hamsters were higher (4.6mm/day) than untreated males [3.7mm/day]. Another difference noted was that the delay between injury and axonal sprouting was shorter in male hamsters [1.7 days] than in female hamsters [2.5 days], so over a short time period nerve regeneration in males would appear to be better but once sprouting begins in the females then the early advantage of the shorter delay in males is soon overcome by the increased rate of regeneration in females (Kujawa et al., 1991).

In the CNS patient sex is linked to differing recovery and impact of both stroke and traumatic brain injury: Alkayed et al. (1998) demonstrated that female rats had a more favourable outcome than male rats following stroke and they related this to the presence of estrogen in

female rats. They surmised that the reason human males and post-menopausal females have a higher risk of unfavourable outcome following stroke than age-matched pre-menopausal women is that endogenous estrogen acts in a neuroprotective manner. A study by Groswasser et al. (1998) identified that female patients were more likely to have a better predicted outcome following traumatic brain injury than males and noted the suggestion that progesterone acting in a neuroprotective manner may explain the difference. It is likely that this neuroprotective role of female sex hormones could also provide a benefit to injured nerves in the PNS.

A study by Jung-Testas et al. (1993) found that estrogen can stimulate proliferation of Schwann cells in the presence of cAMP which, given the important role played by Schwann cells in regeneration, would certainly have a positive effect on regeneration following injury. Their study also demonstrated that the effect of estrogen on Schwann cells was specific as no effect was observed with the use of progesterone instead (Jung-Testas et al., 1993). Estrogen has also been linked to neuroprotective effects in a number of studies (Behl and Manthey, 2000, Garcia-Segura et al., 2001) and also enhanced neurite outgrowth (Ferreira and Caceres, 1991).

Progesterone, a gonadal steroid hormone found in higher concentrations in females than males (Schumacher et al., 2007), is believed to have at least two effects on nerves that may contribute to improved peripheral nerve regeneration. Firstly, progesterone has been shown to reduce the loss of neurons following injury which would result in a higher quantity of intrinsic neurons being available to regenerate axons (Yu, 1989). Secondly, it has been demonstrated that Schwann cells have progesterone receptors (JungTestas et al., 1996) and that progesterone can promote Schwann cell myelin formation (Jungtestas et al., 1994), which is a vital step in regeneration of nerves.

The above examples indicate that the presence of certain steroid hormones found in naturally higher concentrations in females are responsible for the differences observed in

nerve regeneration between males and females, however, other studies have suggested that other intrinsic differences may have a part to play. One study by Kovacic et al. (2003) suggested that a gender-dependant difference in the level of retrograde transport of nerve growth factor [NGF] could be responsible for the higher sprouting capacity of female rat sensory axons that they observed. A later study by Kovacic et al. (2004) found that the reduction of female gonadal steroid hormones, via ovariectomy, did not have a significant effect upon the regeneration of female rat sensory nerves and indicates that these hormones alone are not the only factor in the difference between male and female nerve regeneration rates. Their hypothesised other factor was that, in female rats, more effective cell support in the distal portion of the nerve could improve regeneration rates (Kovacic et al., 2004)

1.7.3 EFFECTS OF NERVE TYPE ON REGENERATION

The addition [or neutralisation] of various beneficial [or detrimental] agents, as demonstrated in the studies mentioned, mean that although nothing can be done about the age or sex of a patient, something can potentially be done to counteract any detrimental effects of these factors upon nerve regeneration. Other factors that affect nerve regeneration, such as nerve type and position of injury, are more difficult to negate.

Differences in regeneration between motor and sensory nerves have been reported in many studies; some concluding better regeneration in sensory axons (Riley et al., 1988, Madorsky et al., 1998) and others in motor axons (Shawe, 1955, Kerns et al., 1991). Additionally regeneration of sudomotor axons [responsible for innervating sweat glands] and nociceptor axons [responsible for pain response] has been shown to be quicker than motor and other sensory axons (Navarro et al., 1994).

Studies assessing the potential for preferential motor reinnervation in mixed nerves have shown that motor axons can reach distal motor endoneurial tubes and reinnervate muscle at a rate higher than would be expected by chance alone (Brushart, 1988, Madison et al., 1999). Sensory axons however do not demonstrate this ability, with many more sensory

axons detected entering distal motor endoneurial tubes that motor axons entering distal sensory endoneurial tubes (Brushart, 1988). This would indicate that mixed nerves with high proportions of motor axons could regenerate better than mixed nerves with high proportions of sensory nerves due to both the effects of the preferential motor reinnervation and the lower number of misdirected sensory axons blocking distal motor endoneurial tubes. The mechanism for preferential motor reinnervation is believed to be a specific interaction between the regenerating axons and Schwann cells; possibly neurotropism [guidance by diffusible factors], specific recognition [axons select endoneurial tubes based upon surface proteins], or neurotrophism [axons only receive survival signals in appropriate endoneurial tubes] (Brushart, 1988). The location of the injury plays an important role in the speed and functionality of recovery as, due to the limited speed that regenerating axons advance distally, the greater distance regeneration is required to cover the longer it will be before regenerating axons reinnervate their original targets. Additionally, the diameter of distal endoneurial tubes is reduced over time, which can further reduce the speed of the regenerating axon's advance (Sunderland, 1991).

1.7.4 EFFECTS OF SCARRING ON REGENERATION

Scarring is a normal part of wound healing in mammals (Shah et al., 1992), however, the presence of scarring at the site of a nerve injury can be detrimental to the regeneration process (Sunderland, 1978, Atkins et al., 2006b). In a previous study by Atkins et al. (2006b) it was demonstrated that, in transgenic mice with an increased propensity for scar formation [IL-4/IL10 null], peripheral nerve regeneration was reduced compared to normal mice. On the other hand, in the same study, mice with a reduced propensity for scarring [M6PR/IGF2 null], regeneration was improved compared to normal mice (Atkins et al., 2006b).

Other studies have looked at the potential of treating nerve injuries with therapeutics that reduce the formation of scarring at the injury site. The main areas investigated so far have involved manipulating local levels of inflammation (Atkins et al., 2007, Ngeow et al., 2011a)

or transforming growth factor-β [TGF-β], which is linked to wound healing (Atkins et al., 2006a, Ngeow et al., 2011b).

1.7.4.1 The Role of TGF-β in Scarring and nerve regeneration.

TGF-β [transforming growth factor-β] is a cytokine associated with the repair of damaged tissue; it is considered have the widest range of activities of any cytokine involved in the tissue repair due to the range of effects that it induces and also the wide variety of cell types that either produce or respond to it (Roberts and Sporn, 1996).

The form of TGF-β secreted from cells is unable to bind to its signalling receptors as it is secreted in its latent form which can be one of two forms: the small latent complex which consists of TGF-β bound to the latency-associated protein [LAP] or the large latent complex which has an additional protein, the latent TGF-β binding protein [LTBP] - the LTBP is believed to promote binding of TGF-β to extracellular matrix and have a role in increasing the efficiency of secretion of TGF-β (Roberts and Sporn, 1996). In order for TGF-β to become activated it is widely reported that the LAP must bind to the cation independent mannose-6-phosphate/insulin-like growth factor receptor [CI-M6PR], this releases the TGF-β from the LAP and allows binding to TGF-β receptors [fig 1.8] (Dennis and Rifkin, 1991, Roberts and Sporn, 1996, Okane and Ferguson, 1997). Despite the level of importance placed on the CI-M6PR in TGF-β activation it is not the sole route of TGF-β activation. A study by Wong et al. (2011) found that although inhibiting the CI-M6PR inhibited activation of TGF-β in normal conditions, activation was less reliant on the CI-M6PR in hypoxic conditions. In addition, a number of mechanisms for activating TGF-β - acidification, alkalinization, detergents, urea and temperature - have been identified in vitro, though only acidification is thought to be utilized in vivo (Harpel et al., 1993).

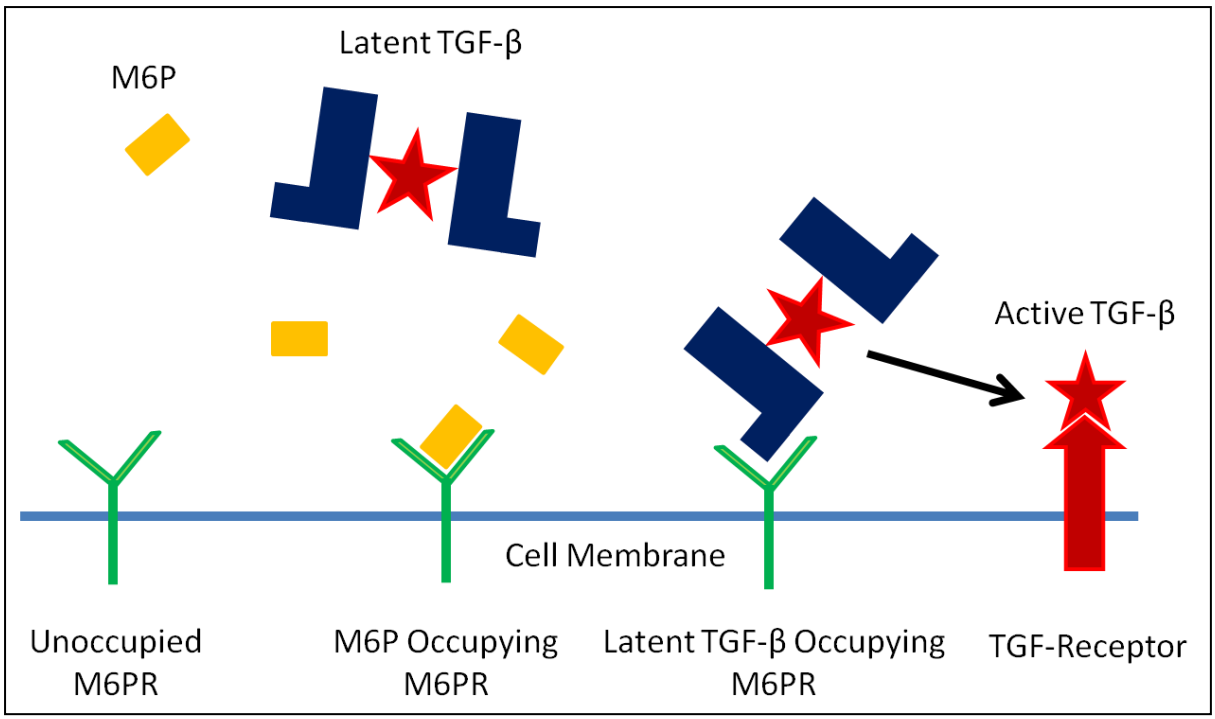

Figure 1.8: Diagram showing the role of M6P in preventing latent TGF-β activation. M6P in the local environment competes with latent TGF-β for access to M6P receptors, occupying the available receptors and preventing latent TGF-β activation.

In mammals there have been three iso-forms of TGF-β isolated, simply named TGF-β1, -β2 and β3; TGF-β1 is the most abundant as it is found in all tissues, whereas TGF-β2 and -β3 are less abundant (Roberts and Sporn, 1996). TGF-β is known to have a number of important roles in nerve regeneration; TGF-β1 has been shown to alter the phenotype of schwann cells from their relative inactive state during normal nerve function to the proliferative non-myelinating state favourable during nerve regeneration (Einheber et al., 1995) and a study by Gordon et al. (2003) demonstrated the potential for exogenous TGF-β to maintain chronically denervated Schwann cells in a state that would encourage axonal regeneration for a longer period of time. TGF-β is also well known as a stimulator of chemotaxis of numerous cell types, including monocytes [which become macrophages upon entering tissue] which have an important role in Wallerian degeneration (Wahl et al., 1987, Roberts and Sporn, 1996). In addition, the survival of neurons post-injury is improved by the

presence of TGF-β1 and -β2 - though TGF-β1 is by far the more potent (Chalazonitis et al., 1992), which obviously increases the potential for nerve function recovery.

The ratio between the different iso-types of TGF-β found in adult wounds has provoked a great deal of interest due to the differences between adult and embryonic wound repair and the altered ratio of TGF-β iso-types found in embryonic wounds. Adult wounds contain a high level of TGF-β1 and -β2 with very little TGF-β3 present and when healed contain scar tissue, however, early embryonic wounds - which repair without scarring (Whitby and Ferguson, 1991a, b) - contain very low levels of TGF-β1 and -β2 with high levels of TGF-β3 (Ferguson and O'Kane, 2004).

1.7.4.2 Antibodies to TFG-β as an Anti-Scarring Agent.

Studies on scar reduction using antibodies to TGF-β1 and -β2 have shown that neutralising these iso-forms can provide a significant reduction in scar formation in dermal wounds (Shah et al., 1994, 1995). In a study to test the effectiveness of exogenous application of TGF-β1 and -β2 antibodies on intra-neural scar reduction and, in addition, the impact of this scar reduction on nerve regeneration, Atkins et al. (2006a) found that scar formation at the injury site was reduced but nerve regeneration was not improved. It was hypothesised that the neutralisation of TGF-β1 and -β2 may have impacted upon the beneficial actions of TGF-β1 and -β2 related to nerve regeneration [see section 3.1 for further discussion]. An alternative approach to scar reduction has been the addition of exogenous TGF-β3; Shah et al. (1995) found that the addition of exogenous TGF-β3 significantly reduced levels of dermal scarring while neutralising all iso-forms of TGF-β negated the reduction in scarring shown by neutralising just TGF-β1 and -β2. On the basis of the results obtained by reducing TGF-β1 and -β2 levels and/or increasing TGF-β3 levels novel pharmaceutical agents have been developed and have shown comparable results to the earlier in vivo studies in early phase clinical trials conducted in skin (Ferguson and O'Kane, 2004). However, in a study by Atkins et al. (2007) the application of exogenous TGF-β3 did not appear to reduce intra-neural collagen formation or improve nerve regeneration.

1.7.4.3 Interleukin-10 as an Anti-Scarring Agent.

Interleukin-10 [IL-10] is a cytokine known to have a number of regulatory functions, including neutralising other cytokines, and is considered to be anti-inflammatory (Yamamoto et al., 2001). A number of studies have noted a connection between IL-10 and reduced levels of collagen; Yamamoto et al.(2001) found than IL-10 down regulated collagen I mRNA by over 30% and Liechty et al. (2000) demonstrated that skin grafts taken from normal C57BL/6 fetal mice heal without scarring or inflammation but scarring does occur when using skin grafts taken from IL-10 knockout fetal mice.

Atkins et al. (2007) were able to demonstrate that a low dose of IL-10 [125ng] injected beneath the epineurium and also into surrounding soft tissues reduced collagen formation and also improved nerve regeneration. A higher dose of IL-10 [500ng], however, did not reduce collagen formation or improve nerve regeneration (Atkins et al., 2007).

1.7.4.4 Mannose-6-Phosphate as an Anti-Scarring Agent.

An alternative approach to neutralising TGF-β with antibodies is to prevent or limit the activation of latent TGF-β, via the application of substances that interfere with the binding of latent TGF-β to receptors required to release the active form of TGF-β.

Mannose-6-phosphate [M6P] is a molecule that in previous studies has been linked to a reduction in the formation of scar tissue in dermal wounds. Studies by McCallion & Ferguson (1996) demonstrated that M6P does indeed reduce scar formation and they postulated a number of theories for this:

- Inhibition of activation of latent TGF-β [fig. 1.8].
- Reduction in the cellular sequestration of platelet-released latent TGF-β by cells at the wound site.
- Inhibition of formation of the large latent TGF-β complex by prevention of latent TGF-β-binding protein polymerisation to the LAP [latency associated peptide] at the M6P receptor.

- Induction of changes in the number or state of activation of inflammatory cells recruited to the wound site.

Additionally, recent studies (Ngeow, 2010, Ngeow et al., 2011a) have suggested that M6P has a beneficial effect upon early peripheral nerve regeneration in mice when injected at the site of sciatic nerve repair at a concentration of 600mM. Further discussion on M6P can be found in chapter 3 of this thesis.

1.8. METHODS OF ANALYSING IN VIVO PERIPHERAL NERVE REGENERATION

When researching ways to improve nerve regeneration it is vital to have some method of analysing whether the intervention used is better than the controls. The most common methods of doing this are behavioural observations, electrophysiology and direct visual observation of the nerve.

1.8.1 Behavioural Observations.

Behavioural observations are non-invasive techniques that assess the functional recovery of injured nerves and can be used to assess the progress of functional recovery over many time points. The nature of techniques can vary from simple observation using images and video of the experimental animals (Wang et al., 2005), to more complex systems that measure multiple parameters in an automated way - such as the CatWalk gait analysis system assessed by Deumens (2007) and Bozkurt (2008).

Analysis of functional recovery following sciatic injury in rodents can be analysed using gait analysis, of which the CatWalk [Noldus Information Technology, The Netherlands] is an advanced version. Walking track gait analysis can be used to measure toe spread, which decreases following sciatic injury and can be used to estimate functional loss (Menovsky and Beek, 2001) and is considered to be the most important measure of function of the sciatic nerve due to the reliance of toe spread on peroneal and tibial branches of the sciatic nerve (Bain et al., 1989). Additionally paw pressure, stride length and measurements of the duration a paw remains in position can also be measured to improve the overall picture of functionality gained by gait analysis.

1.8.2 Electrophysiological Assessment.

Much of the research into improving peripheral nerve regeneration is concerned with whether a treatment/technique will improve regeneration compared to standard nerve

suturing or autograft. Using behavioural observational techniques to find a difference between two injured nerves is far more difficult than finding differences between an injured and an uninjured nerve as often the difference in regeneration is quite small, so other techniques are needed in order to find any potential differences.

Electrophysiology is a technique that uses electrodes placed on the nerve to stimulate the nerve and make recordings of the compound action potentials [CAPs] proximal and distal to the injury site [fig. 1.9]. CAPs can be assessed for both motor and sensory axons separately through changing the position of the recording and stimulating electrodes - e.g. recording motor CAPs from the motor end plates (Archibald et al., 1995). Using the proximal and distal compound action potentials a ratio can be calculated which will give an indication of the number of functional axons crossing the injury site (Ashur et al., 1987). Conduction velocities, which indicate maturation of axons [reaching their target tissues or becoming myelinated], can also be calculated (Olivier et al., 1997)

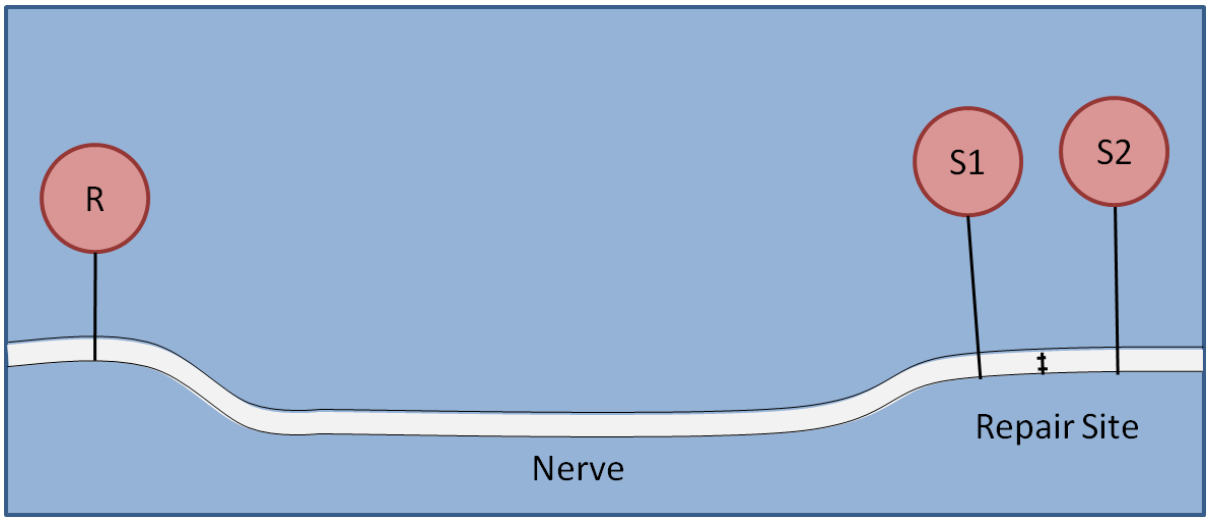

Figure 1.9: Basic setup of an electrophysiological reading; R= recording electrode, S1= proximal stimulation electrode, S2= distal stimulation electrode - the difference in reading between S1 and S2 provides a ratio which can be used to calculate the percentage of axons crossing the injury site (adapted from Atkins et al., 2006a)

1.8.3 Direct Observation.

Although electrophysiology can provide a more in depth analysis of peripheral nerve regeneration than behavioural observations such as gait analysis alone, it still does not explain what is happening at single axon levels and why, in a nerve with poor regeneration, axons are not crossing the injury site. In addition, when electrophysiology and walking track analyses are used in combination within a study, the results can contradict each other (Taha et al., 2004).

Various methods of directly observing experimental nerves with the use of a microscope can be used to visualise and measure many parameters, such as; axon numbers before and after the injury site, axon thickness, axon length and axon sprouting. Fibre counts of axons both central and distal to an injury site can be made following histological preparation of nerves; this typically consists of embedding the nerve tissue within a resin, wax or other suitable material and then sectioning the embedded tissue and finally staining the sections with a suitable stain prior to microscopical analysis. For example, myelinated axons are often stained using the general stain toluidine blue in order to enable nerve fibre counts to be made (Atkins et al., 2006a, Waitayawinyu et al., 2007).

Immunohistochemistry techniques - where antibodies to specific components of the nervous system are applied to the tissue - are used when increased information or differentiation between tissue types is desired. Antibodies to growth-associated protein-43 can be used to reveal axons with active growth cones, while antibodies to S-100 and peripheral myelin protein-22 can be used to reveal the location of Schwann cells and their myelin sheaths (Atsumi et al., 1999, D'Urso et al., 1999, Shin et al., 2003, Nie et al., 2014).

The main drawback of direct observation methods is that the nerves can only be assessed at a single time point as the nerve must be harvested and prepared in order to visualise it under the microscope. When using a standard animal model for nerve regeneration studies the harvested nerve will need to be cut into thin sections and have a specific stain applied as

its axons will not otherwise be visible under the microscope. However, genetically modified animals in which the axons inherently fluoresce have now been created which greatly reduce the level of preparation required to image nerves and can allow observations to be made of regeneration over multiple time points from the same nerve (Pan et al., 2003, Unezaki et al., 2009, Yan et al., 2011).

In the mid-1990's the jellyfish green fluorescent protein [GFP] was discovered to be an excellent marker of gene-expression that could be used to selectively stain specific components of living cells (Chalfie et al., 1994). Later work led to the generation of transgenic mice expressing GFP and additional mice expressing yellow [YFP], cyan [CFP] and red [RFP] fluorescent proteins [collectively termed XFP], incorporating regulatory elements from the thy-1 gene (Feng et al., 2000). Feng et al. (2000) demonstrated that the four variants of fluorescent protein satisfactorily label neurons in vivo, that they have no detrimental effect upon synaptic structure and that a unique, heritable pattern of expression occurs for offspring of a transgenic founder.

GFP was originally isolated from the Pacific Northwest jellyfish [*Aequoria victoria*] (Shimomura et al., 1962) and later work produced mutated varieties with different emission wavelengths, providing the ability to have living tissues double labelled (Ellenberg et al., 1999). The different emission wavelengths are produced by single amino acid substitutions at certain points, for example substituting tryptophan in place of tyrosine in the 66th position creates CFP (Heim et al., 1994) and substituting tyrosine in place of threonine at the 203rd position creates YFP (Ormo et al., 1996).

1.8.4 Generation of Transgenic Mice Expressing Spectral Variants of GFP.

To generate the transgenic mice mentioned above, Feng et al. (2000) used a modified thy-1 vector in which exon 3 and the introns alongside had been deleted using *Xho1* restriction enzymes to allow the insertion of a transgene into the deleted region [fig. 1.10] (Caroni, 1997) - this deletion had the additional benefit of preventing expression of the modified thy-1

gene in non-neuronal tissues, which the removed sequence is responsible for (Vidal et al., 1990). The modified thy-1 vector containing the relevant fluorescent protein transgene was then injected into a fertilized mouse oocyte using standard methods (Hogan et al., 1994) and animals positive for the transgene were used to found strains (Feng et al., 2000).

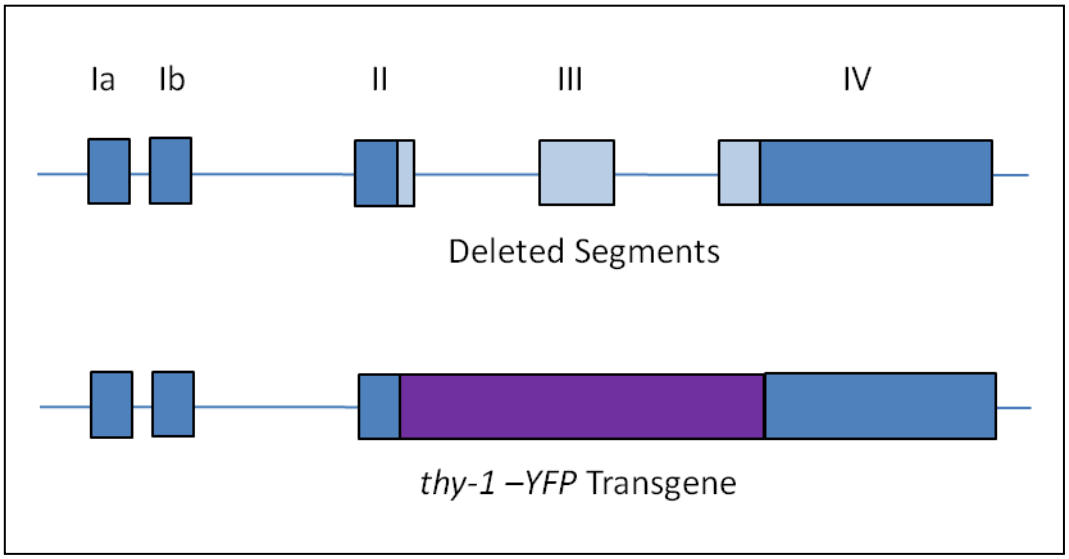

Figure 1.10: Modification of thy-1 gene - Top: thy-1 gene prior to removal of exon 3 by Xho1 restriction enzymes. Bottom: thy-1 gene with chosen transgene [i.e. YFP] in place. Adapted from Caroni (1997).

Also known as cluster differentiation 90 [CD90], thy-1 is a cell-adhesion molecule expressed on numerous cell types (Nakamura et al., 2006, Haack-Sorensen et al., 2008, Guillot-Delost et al., 2012) and has an important role in wound healing and inflammation through triggering the synthesis and release of cytokines and enzymes (Saalbach et al., 2008). For example, when neutrophils bind to thy-1 it triggers an increase in secretion and activation of MMP-9 [a matrix metalloproteinase important for leukocyte migration through the extra-cellular matrix (Opdenakker et al., 2001a, 2001b)] and secretion of the chemoattractant, CXCL8 - enhancing neutrophil migration to sites of inflammation (Saalbach et al., 2008).

Each XFP transgenic founder mouse generated by Feng et al. (2000) possessed a different, unique pattern of fluorescent protein expression [table 2]; which persisted consistently in the descendants of the founder mice, even when XFP mice were crossed with other strains.

Feng et al. (2000) stated that differences in transgene expression between founder mice were due to differences in the chromosomal integration of the transgene and/or the copy number of the transgene. The variation between strains came in two quantifiable types: firstly, the proportions of neurons located in specific tissues, and secondly, the intensity of the XFP labelling. The two types of variation were not correlated; labelling could be intense but limited to few neurones, or dim but labelling the all neurones of a specific type - homozygosity or heterozygosity also had no effect on the pattern of labelling, though labelling was stronger in homozygotes (Feng et al., 2000).

Table 2: Patterns of transgene expression in thy-1-XFP lines. All = expression in >80% of neurons; many = expression in 10-80%; few = expression in <10%. Numbers under 'cortex' = laminae in which somata of labelled neurons were present. RGC = retinal ganglion cells; INL = inner nuclear layer of the retina [A = amacrine cells, B = bipolar cells, M = Muller cells]; SCG = superior cervical ganglion; DRG = dorsal root ganglion; Mossy = mossy fibres in internal granulae layer of the cerebellum; Purk = cerebellar Purkinje cells; Molec = interneurons of the cerebellar molecular layer. Taken from Feng et al. (2000) and used with permission from Elsevier Inc.

Line	Motor Axon	Retina		SCG		DRG	Cortex	Cerebellum		
		RGC	INL	Pre	Post			Mossy	Purk	Molec
YFP-12	All	Many	A	None	None	Many	5,6	All	Many	Few
-16	All	All	A+B	All	Few	All	2-6	All	None	Few
-21	All	All	A	All	Many	All	2-6	All	All	None
-A	Many	Many	A	Many	None	Many	2-6	All	Many	Few
-C	All	All	A+B+M	All	Few	All	2-6	All	None	None
-D	All	All	A	All	None	All	2-6	All	None	Few
-F	All	Many	A	Many	None	All	2-6	All	Few	Few
-G	All	Many	A	All	Few	All	2-6	All	None	None
-H	Few	Few	None	Few	Few	Many	5	Many	None	None
GFP-F	All	All	A+B+M	All	None	All	2-6	All	Many	Few
-G	All	All	A+B+M	All	Few	All	2-6	All	Many	Few
-H	All	Many	None	All	None	Many	2-6	Many	None	None
-I	All	Few	None	All	None	Many	6	All	Many	None
-J	All	All	A+B+M	All	None	All	2-6	All	Many	None
-M	Few	Few	None	None	None	Few	Few	Many	None	None
-O	All	Few	None	None	None	Few	2-6	All	Many	None
-S	Few	Few	None	None	None	None	Few	Few	None	None
CFP-4	All	Many	None	None	Few	Many	5,6	All	Many	None
-11	All	Many	None	Few	Few	Many	2-6	All	Few	Few
-23	All	All	A	None	None	Many	2-6	All	None	None
-D	All	Few	None	None	None	All	5,6	All	All	None
-F	All	Many	None	All	None	All	2-6	All	None	Few
-H	All	Many	None	None	None	Many	2-6	Many	None	None
-I	All	All	None	None	None	All	2-6	All	None	None
-S	Few	None	None	None	None	Few	Few	Few	None	None

1.8.5 Use of *thy-1-XFP* Mouse Strains in Neuroscience Research.

The *thy-1-YFP-H* mouse model generated by Feng et al. (2000) has proven to be the most popular among the various XFP fluorescing strains they generated in terms of the number of published studies that have utilised it. Other strains generated by Feng et al. (2000) have been found to be particularly useful for certain types of research.

1.8.5.1 Studies Using *thy-1-CFP* Mice.

The *thy-1-CFP-23* strain - which express cyan rather than yellow fluorescent protein - has been used in a number of studies investigating optical nerve injuries (Bernstein et al., 2007, Leung et al., 2008a, Leung et al., 2008b, Wang et al., 2010, Chindasub et al., 2013). Feng et al. (2000) reported that more than 80% of retinal ganglion cells were labelled in the strain and this was backed up by Bernstein et al. (2007). Of particular note is the blue-light confocal scanning laser ophthalmoscope technique developed by Leung et al. (2008b) which allows non-invasive in vivo imaging to determine the integrity of retinal ganglion cells.

1.8.5.2 Studies Using *thy-1-RFP* Mice.

The use of *thy-1-RFP* strains - which express red fluorescent protein - is more limited to date, with a single study by Favero et al. (2009) the only published study making use of them at the time of writing. In that study, Favero et al. (2009) investigated the role of post-synaptic action potentials using over-expression of Kir2.1 and Kir2.2 potassium channels to hyperpolarise membranes and prevent those action potentials. The exact strain of *thy-1-RFP* mice that Favero et al. (2009) used is not made clear in the article and the mice are only used to determine the localisation of the Kir over-expression.

1.8.5.3 Studies Using *thy-1-GFP* Mice.

Studies which have used the *thy-1-GFP-M* strain (Trachtenberg et al., 2002, Holtmaat et al., 2006, Keck et al., 2008, Mostany et al., 2010, Singh et al., 2013) generated by Feng et al. (2000) have mostly concentrated on observing certain effects on neurones in the brain.

Trachtenberg et al. (2002) utilised the *thy-1-GFP-M* strain to study plasticity of individual pyramidal neurones in the cortex, with repeated imaging through a transparent skull cover taking place over a number of weeks. Also using a similar imaging technique were studies by Holtmaat et al. (2006) and Mostany et al. (2010), who investigated the effects of novel experiences, and the effects of stroke respectively. The relative popularity of this particular strain in studies of this type may be related to the fact that *thy-1-GFP-M* mice only have relatively few GFP labelled neurons in the cortex (Feng et al., 2000) - this prevents a potential issue where individual fluorescent neurons are difficult to separate for analysis (Lichtman and Sanes, 2003).

1.8.5.4 Studies Using *thy-1-YFP* Mice.

Of all the different colour variants Feng et al. (2000) used to generate strains of *thy-1*-XFP expressing mice, YFP [*thy-1-YFP-H* and *thy-1-YFP-16* strains] has proven the most popular in studies to date. In two studies the *thy-1-YFP-16* strain was used to observe retinal ganglion cell survival and changes in axon and dendrite arborisation (Leung et al., 2011, Li et al., 2011). These studies were derived from the previously discussed Leung et al. (2008b) study, which had used *thy-1-CFP-23* mice. An advantage of the *thy-1-YFP-16* mice used in these more recent studies appears to be that, with fewer positively stained retinal ganglion cells in the YFP model [reported in both studies as being <1% (Leung et al., 2011, Li et al., 2011)], details such as axon and dendrite arborisation can be determined (Leung et al., 2011). This assertion by Leung et al. (2011) and Li et al. (2011) contradicts the initial reports by Feng et al. (Feng et al., 2000), who indicated that >80% of retinal ganglion cells were labelled in the retina of the *thy-1-YFP-16* strain; however, the labelling profiles reported by Feng et al. (2000) are not overly precise and no detailed evidence is provided.

Conversely, the high levels of motor and sensory axon labelling in peripheral nerves has enabled non-invasive analysis of regeneration to be performed in some studies (Unezaki et al., 2009, Singh et al., 2012). A study by Unezaki et al. (2009) investigated the effects of

nerve growth factor and glial-cell derived neurotrophic factor on the regeneration of the sciatic nerve in *thy-1-YFP-16* mice. Unezaki et al. (2009) used a silicone conduit [with an osmotic pump to administer a continuous dose of the desired factor] for sciatic nerve repairs, which they partially assessed through imaging the injured limb over the course of 8-weeks [fig. 1.11]. A similar method was used by Singh et al. (2012) in a study investigating the effects of electrical stimulation on nerve regeneration, in which they used images of the injury site and toe pads to determine the rate and extent of sciatic nerve regeneration through a silicone conduit.

One strain of YFP mice, *thy-1-YFP-H* [YFP-H], generated by Feng et al. (2000) has been used successfully in a number of nerve regeneration studies by, among others, the Arthur W. English laboratory (English et al., 2005, Groves et al., 2005, Sabatier et al., 2008). In this strain the peripheral expression of YFP is limited to a subset of axons [table 2], but in those axons it is expressed along their entire length (Feng et al., 2000). An important consideration for using this strain in peripheral nerve studies is that the limited number of axons expressing YFP means that fluorescent axon density in the nerve is reduced, and as such individual axons are easier to discern. Groves et al. (2005) calculated that approximately 2.6% of all sensory axons are YFP labelled [based on 122.6 YFP labelled axons out of 4625 in the L4 spinal nerve] and that sensory axons make up approximately 58% of all labelled axons. The nerve most often used for nerve regeneration studies in YFP-H mice is the common fibular [CF], a branch of the sciatic nerve, which has been found to contain an average of 36.03 (±2.35) YFP labelled axons and is preferred to the tibular branch of the sciatic nerve as a higher proportion of fluorescent labelled nerves are located within the fibular branch of the sciatic nerve (Groves et al., 2005).

Further discussion on the use of *thy-1-YFP-H* mouse strain - both in the studies presented here and previous work by others - generated by Feng et al. (2000) is presented in chapter 7.

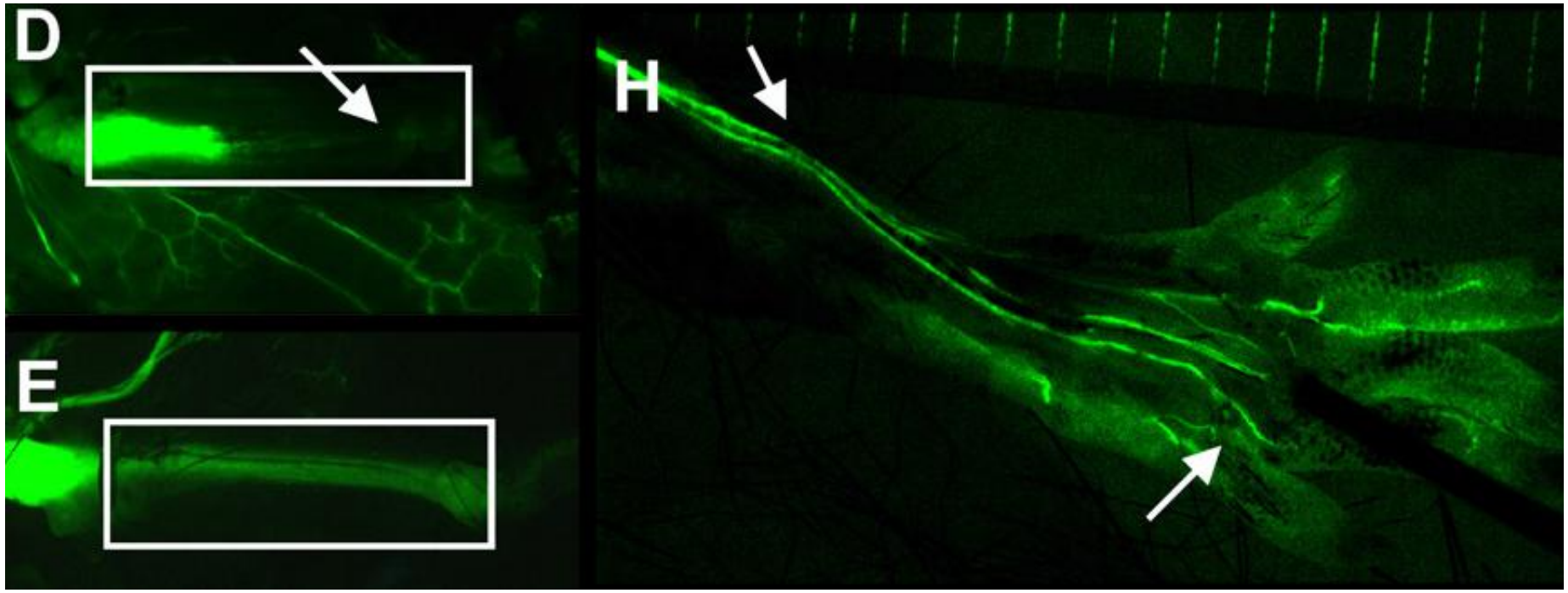

Figure 1.11: Non-invasive imaging of sciatic nerve regeneration in *thy-1-YFP-16* mice. D: regeneration through a nerve guide at 2-weeks post-injury; E: at 4-weeks post-injury; H: view of reinnervation of foot at 8-weeks post injury (Unezaki et al., 2009). Used with permission from Elsevier In

1.9 GENERAL AIMS AND OBJECTIVES

With the commonly used, more established methods of analysing peripheral nerve regeneration it is either impossible or extremely difficult to observe the fate of individual axons as they cross the repair site. Using a YFP-H mouse nerve injury model enables a representative sample of axons to be traced across the entirety of the nerve repair and beyond.

Despite the potential benefits of using YFP-H mice in peripheral nerve regeneration studies, there have been relatively few studies conducted with the strain [see section 7.1.2 for discussion of those studies]. Additionally, those studies that have used YFP-H mice do not appear to have fully utilised the potential of the strain - analysing only the number of axons regenerating into the repair and the length profiles of those axons (Groves et al., 2005).

Therefore, the general aim of the work contained within this thesis was to utilise the YFP-H mouse to investigate nerve repair at the level of the individual axon, following a range of different treatments and repair methods. In order to achieve this, new analysis methods have been developed to enable a much greater level of information to be gained from using the YFP-H mouse strain. The treatments/repair methods used to achieve this aim were:

- Graft repairs with/without a potential anti-scarring agent [M6P; chapter 3].
- Graft repairs with/without a potential regeneration enhancing/anti-scarring agent [EC23; chapter 4].
- Artificial nerve guide repair using a variety of nerve guide designs compared to graft repairs [chapter 5; chapter 6].

2.0 MATERIALS AND METHODS

2.1 ANIMALS

The experimental protocols were approved by the UK Home Office in accordance with the Animals (Scientific Procedures) Act 1986, as part of the project license numbers PPL 40/3070 [for anti-scarring agents experiments] and 40/3342 [for artificial nerve guides experiments]. Following my completion of the requisite Home Office License modules [1-4] I was granted a personal license [number PIL 40/10013] to undertake the work described within this thesis.

All experiments used *thy-1-YFP-H* transgenic mice [YFP-H], a strain possessing a subset of peripheral nerve cells expressing yellow fluorescent protein along the entire length of their axons [see section 1.8.4 for further details]. This strain was chosen in order to exploit the potential to trace the progress of individual regenerating axons through a repair. Four breeding pairs were purchased from JAX Mice in 2009 and all mice used in the experiments described here were descendants of those original breeding pairs. The YFP-H breeding pairs consisted of one heterozygous YFP-H mouse [possessing a single copy of the modified *thy-1* gene] and one wild-type [WT] mouse [lacking the modified *thy-1* gene and subsequently genetically identical to the C57BL-6J background strain used in the generation of the YFP-H strain] derived from previous YFP-H/WT matings. This mating arrangement is used in order to provide mixed litters containing approximately equal numbers of YFP-H and WT mice. In experiments that required nerve grafts, WT littermates of the experimental YFP-H mouse were used to provide the graft material. The mice used were aged between 8- and 20-weeks; typically mice aged between 8- and 16-weeks were used in the anti-scarring agents studies and mice aged between 12- and 20-weeks were used in the artificial nerve guide experiments. Mice were housed in soft wood chip lined plastic cages with a 12 hour light/dark cycle and an ambient temperature of between 19 and 21°C within a central animal

care facility [Biological Services Unit, University of Sheffield]. Mice were group housed where possible, depending on litter size and male-female ratio of the litter, prior to experiments being carried out. During the post-surgery recovery period mice were singly housed to minimize the incidence of suture removal. Standard rodent chow and water was provided for the mice ad libitum.

2.2 SURGICAL PROCEDURES

2.2.1 ANAESTHESIA FOR RECOVERY EXPERIMENTS

Animals involved in experiments requiring recovery from the surgical procedure were anaesthetised using an isoflurane [Isoflo, Abbot Laboratories, UK] and oxygen mixture [BOC, UK]. Anesthesia was induced by placing the animal within an induction box connected to an anesthetic machine [Harvard Apparatus LTD, Kent, UK] providing 4L/min of 4% isoflurane in 100% oxygen. Once induction was complete the animal was transferred to a thermostatically controlled heated blanket covered with a sterile surgical drape to maintain body temperature [Harvard Apparatus LTD, Kent, UK], while anesthesia was maintained by the use of a nosepiece connected to the anesthesia machine's vaporizer and providing 1-4L/min of 1.5-4% isoflurane in 100% oxygen, as required.

Following the successful completion of surgery animals were transferred to an enclosed incubator containing a thick blanket and heated to 37.5°C and allowed time to fully recover from the affects of anesthesia.

2.2.2 ANAESTHESIA FOR TISSUE HARVESTING

Animals used to provide nerve graft tissue were anaesthetised either as specified in section 2.2.1, or by inter-peritoneal injection [fluanisone, 0.8ml/kg; midazolam, 4mg/kg; ip] depending upon the specific study requirements.

In animals where tissue was harvested for analysis, anesthesia was induced by inter-peritoneal injection [fluanisone, 0.8ml/kg; midazolam, 4mg/kg; ip].

Following successful tissue harvest, animals were culled by cervical dislocation while under deep anesthesia.

2.2.3 NERVE GRAFT REPAIRS

The nerve grafts were obtained from WT littermates of the experimental YFP-H mouse under general anesthesia [as described in section 2.2.1] using the following procedure. The right rear leg of a WT mouse was shaved and disinfected with hibitane, an incision was made between mid-calf and mid-thigh level and the skin was freed by blunt dissection. The common fibular [CF] nerve was then exposed by separating the muscles behind the knee joint to allow access. The CF nerve was then freed from surrounding tissues and a section [5mm minimum length] extracted. Depending upon the specific study requirements, this section of nerve tissue was either transferred to a vial containing vehicle/therapeutic agent or into a prepared recipient YFP-H littermate.

YFP-H mice were prepared to receive grafts under anesthesia [as described in section 2.2.1]. The right CF nerve was exposed [as described above], carefully freed from the surrounding tissue and a 5mm silicone trough was inserted beneath the nerve prior to sectioning. The sectioned nerve endings were trimmed to create the required gap between central and distal ends, and graft tissue obtained from a WT littermate [as described above] was trimmed to fit the gap. The graft and nerve ends were aligned and the graft was secured in place with an application of fibrin glue; which was made up of fibrinogen [10mg/ml; Sigma Aldrich, UK] and thrombin [40IU/ml; Sigma Aldrich, UK] in a 1:1 ratio and allowed to set for five minutes. Once the repair was secured, the silicone trough was carefully removed and the wound closed using 6-O sutures [coated vicryl; Ethicon, UK]. A single dose of analgesic [0.01ml buprenorphine hydrochloride, 0.3mg/ml; Vetergesic®, Alstoe Animal Health, UK] was administered subcutaneously and the animals were allowed to recover for the length of time required by the specific experimental design.

2.2.4 NERVE GUIDE REPAIRS

Under general anaesthesia [as described in section 2.2.1] the right CF nerve of a YFP-H mouse was exposed and carefully freed from the surrounding tissue [as described in section 2.2.3]. The nerve endings were trimmed to create the required gap between central and distal ends. The sectioned nerve ends were placed approximately 0.5mm within a conduit and secured in place with an application of fibrin glue [fig 2.1], the wound was closed and animals allowed to recover for a 3-week period.

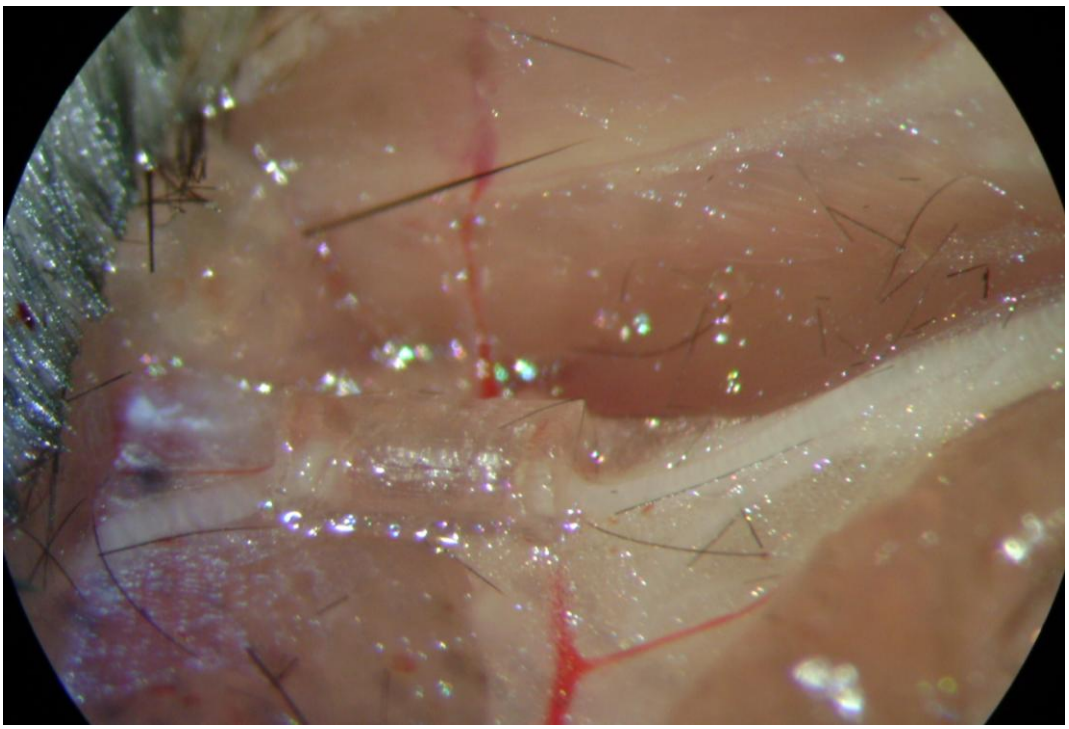

Figure 2.1: Nerve guide conduit repair. The CF nerve runs from right to left in this image and is sectioned midway between the branching of the sciatic [which starts a short distance from the right edge of this image] and the lateral edge of the knee joint [at the left edge of this image].

2.2.5 HARVESTING NERVE TISSUE FOR ANALYSIS

Following the appropriate recovery period, the repaired section of nerve tissue was harvested under general anesthesia [as described in section 2.2.2]. Following re-exposure and freeing of the CF nerve, the surrounding skin was sutured to an elevated brass ring to form a pool, which was then filled with 4% formaldehyde for 30 minutes to fix the nerve

tissue. The fixed nerve tissue was sectioned at a distance proximal [the branch point with the sciatic] and distal [where the CF nerve passed into the anterior region of the knee] to the repaired section, placed onto a microscope slide and coverslipped using Vectashield®.

For harvests of conduit repaired nerve, the process was as described above with the additional step of carefully removing the conduit material following fixation.

2.3 IMAGE ACQUISITION AND ANALYSIS

2.3.1 IMAGE ACQUISITION

Images of nerves were acquired with fluorescent microscopy (Zeiss Axioplan 2 imaging microscope with Qimaging Retiga 1300R camera) using Image Pro-Plus software (version 5; Media Cybernetics, Bethesda, MD). Images were acquired with a x10 objective in stacks consisting of thirty 10µm thick sections - throughout the entire thickness of the nerve - from which composite images were obtained. To obtain images of the full length of the nerve, stacks were acquired from multiple adjoining microscope fields and the composite images were joined using Adobe Photoshop.

Minimal image processing with Adobe Photoshop was applied to the joined images used for analysis, this consisted of adjusting brightness/contrast and image exposure in order to improve axon clarity.

2.3.2 IMAGE ANALYSIS

2.3.2.1 Sprouting Index.

In previous studies of nerve regeneration using YFP-H mice, one outcome measure used was the quantification of axons proximal and distal to the repair to generate a ratio - termed sprouting index - of axon sprouting into the repair (Groves et al., 2005, Sabatier et al., 2008). The equivalent outcome measure used in the studies discussed within this thesis builds upon the previously used sprouting index method by increasing the distal data points from a single reference to a total of eight [for graft only studies] or nine [for studies using conduits] separate intervals encompassing the entirety of the graft repair and the initial portion of the distal nerve ending. By calculating sprouting index ratios at multiple points along the repair the entire sprouting profile could be determined, giving an increased level of information compared to the previously used single point method.

For analysis the nerve images were marked at approximate 0.5mm intervals originating from the point where abnormal axon morphology began to the point where axons had entered the distal nerve ending, with one additional interval marked at 0.5mm prior to the first interval [fig 2.2]. The point where axons entered the distal nerve ending varied between studies: in graft only studies, 3.5mm from the first interval was sufficient to cover the distal nerve ending; in conduit studies 4.0mm from the first interval was required due to the slightly larger gap required between nerve endings in those studies.

The number of axons at each interval were counted and - in order to allow direct comparisons between different nerves - the number of axons at each interval were divided by the number of axons counted at the -0.5mm interval to give a sprouting index. Counts were made in triplicate and an average taken in order to minimise the effect of any miscounts [figs. 2.2 and 2.3].

2.3.2.2 Functional Axon Tracing.

Axons were then traced [using pseudo-colour tracing methods in Adobe Photoshop] from the final interval back along the repair to the first interval or a branch point with a previously traced axon, with a minimum of 75% of the axons present traced. Tracing was subsequently performed at all preceding intervals in turn to allow the percentage of axons from the start interval represented at each interval to be calculated [figs. 2.2 and 2.3].

2.3.2.2 Axon Disruption.

Finally, the direct path from the 0.0mm to 1.5mm intervals [the portion within repairs where axons typically appeared most disrupted] was accurately measured and the length of all traced axons between the two intervals was also measured. Axon lengths were compared to the direct path length to determine the average increase in axon length across the initial period of repair [fig. 2.4]. A greater average increase in traced axon length between the 0.0mm and 1.5mm intervals was considered indicative of greater axon disruption between the central nerve end and graft.

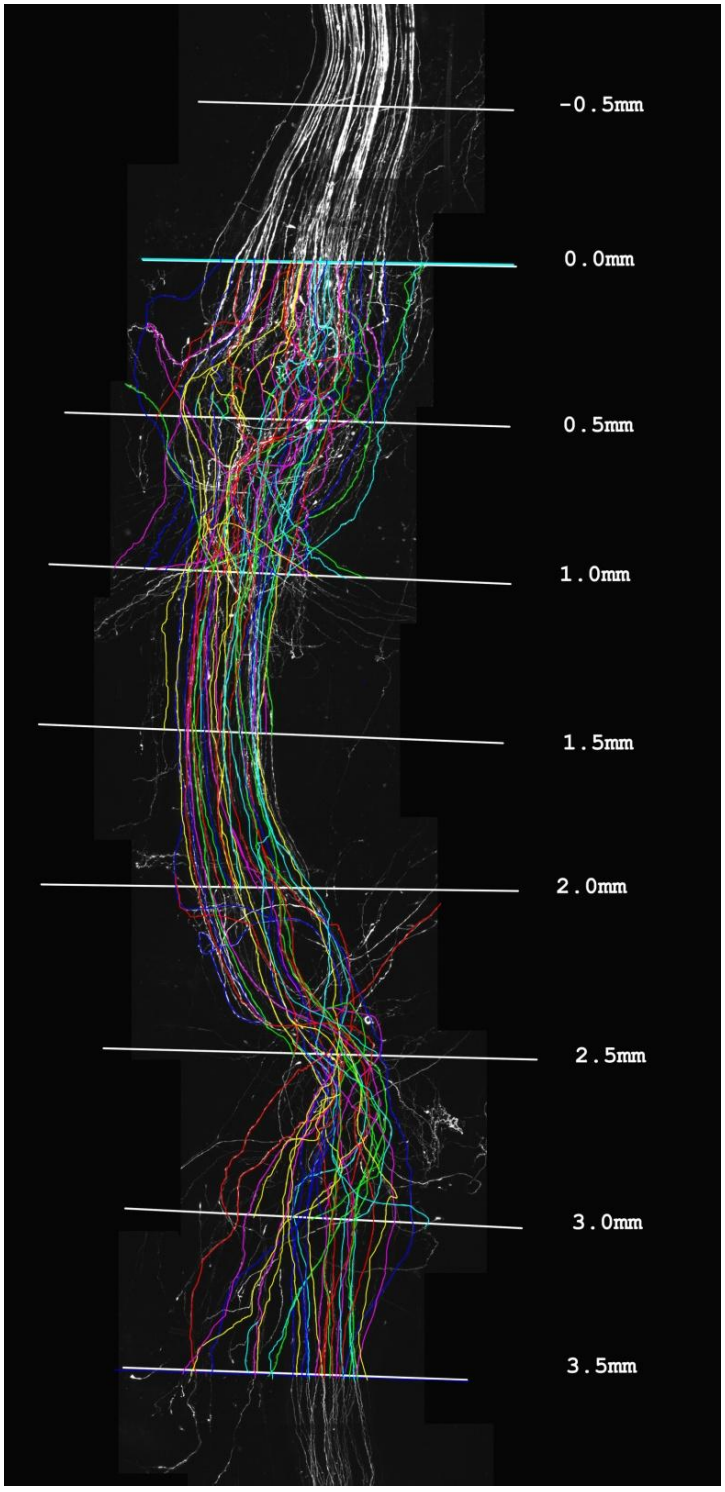

Figure 2.2: Fully reverse traced pseudo-colour nerve image - initially, 75% of axons at the 3.5mm interval were traced back to the 0.0mm interval, with further traces made at each preceding interval in turn to ensure 75% of axons present were traced.

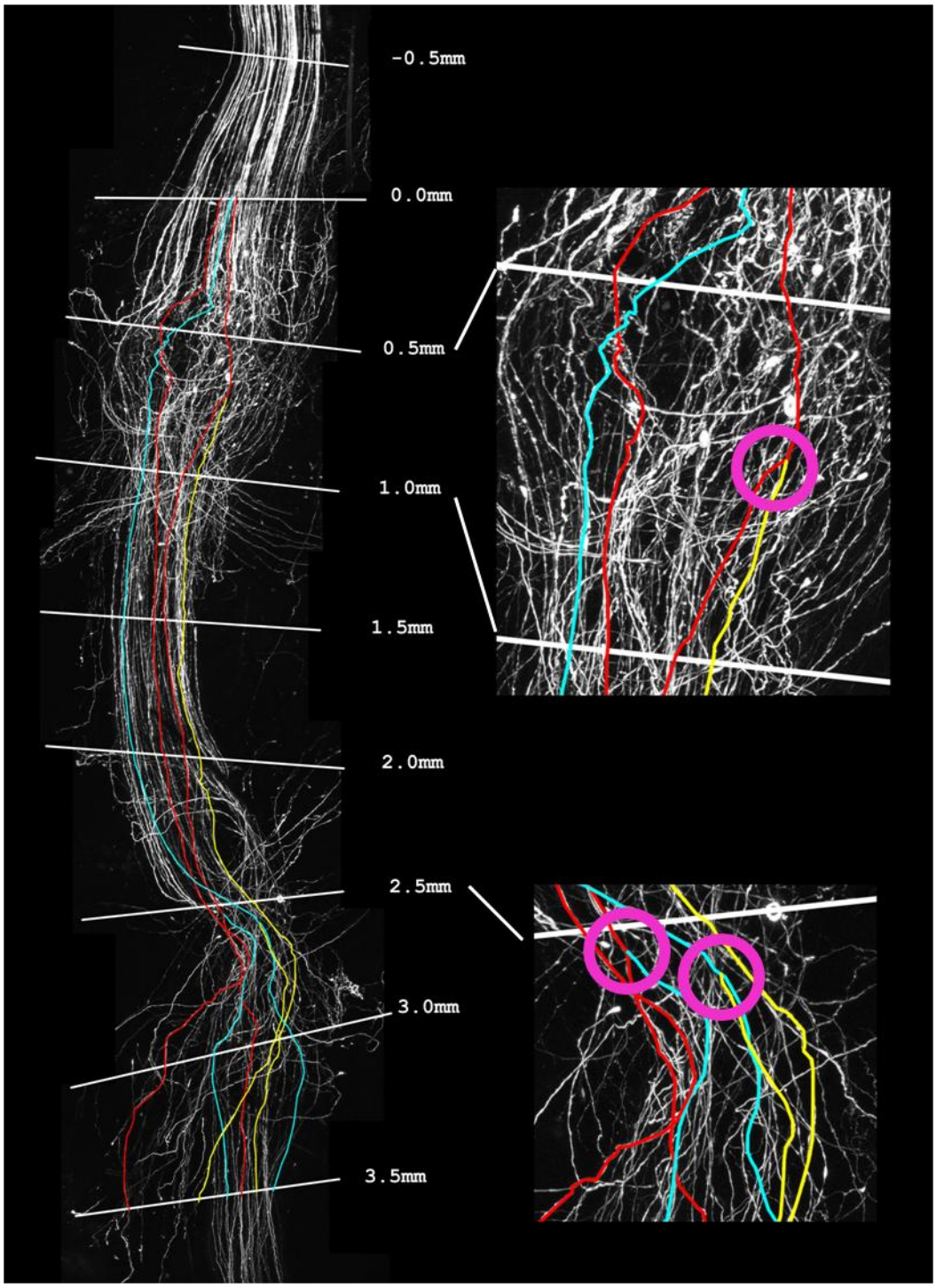

Figure 2.3: Nerve image with sample tracing from 3.5mm interval only. Three of the six axons traced from the 3.5mm interval were duplicate sprouts - branch points are highlighted in the expanded sections [magenta circles].

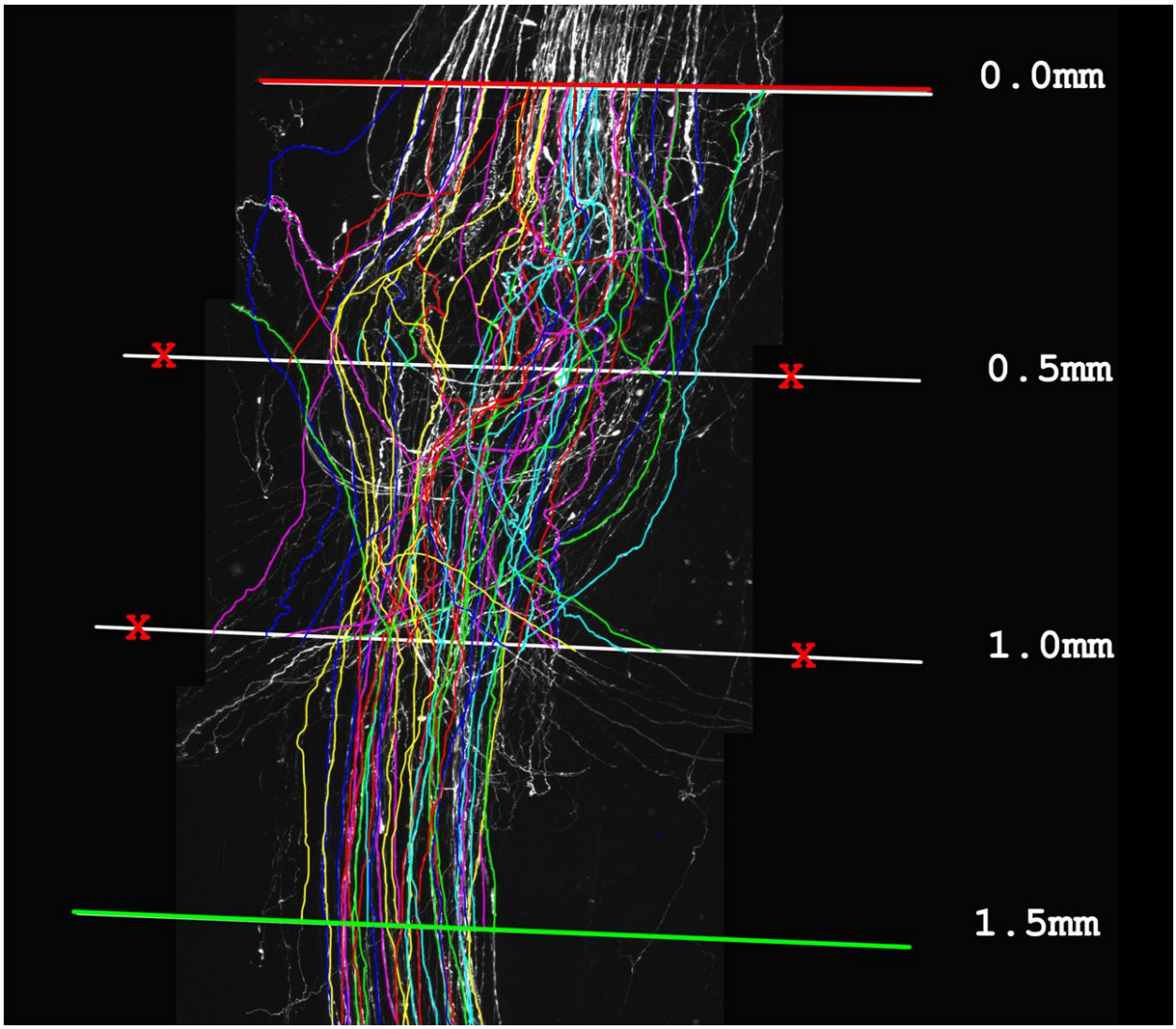

Figure 2.4: Enlarged view of the initial intervals of the repair with full axon tracing [~75% of the total number] at each interval. Traced axons from the 1.5mm interval back to the 0.0mm interval were measured and compared to the direct distance between intervals [axons traced from intervals marked with X back to 0.0mm were ignored].

2.3.3 STATISTICAL ANALYSIS

All statistical analysis of results was carried out using GraphPad Prism software [v.5.00, GraphPad Software Inc., California, USA].

For sprouting index and axon tracing results a 2-way analysis of variance [ANOVA] with post tests consisting of a series of t-tests with a Bonferroni correction applied [hereafter referred to as Bonferroni post-tests] was used in order to detect overall differences between experimental groups and differences between experimental groups at individual intervals.

For axon disruption results a 1-way ANOVA with Bonferroni post-tests was used in order to detect overall and individual interval differences between groups.

3.0 THE EFFECTS OF MANNOSE-6-PHOSPHATE ON NERVE REGENERATION

3.1 INTRODUCTION

A proof of concept study by Atkins et al. (2006b) - which assessed regeneration in the sciatic nerve of mice with an increased or decreased propensity for forming scar tissue - revealed an inverse correlation between the level of intraneural scarring and the level of success of peripheral nerve regeneration. Following this, further studies have been undertaken in the attempt to discover a therapeutic agent that can reduce the formation of scar tissue following peripheral nerve injury.

Atkins et al (2006a) conducted a study in which neutralising antibodies to TGF-β1 and -β2 were shown to reduce scarring in regenerating nerve tissue [see sections 1.7.4.1 and 1.7.4.2 for discussion on TGF-β and scarring] without improving overall nerve regeneration. It was suggested that, in the course of neutralising TGF-β1 and -β2, the positive roles that TGF-β is involved in during regeneration were impeded.

One of these roles is to attract monocytes from the blood stream to the injury site, where they become macrophages and assist with the removal of myelin and axon debris (Wahl et al., 1987, Perry and Brown, 1992).

Vargas et al. (2010) demonstrated the importance of myelin debris removal in a study using the JHD strain of mice. This strain is unable to produce antibodies [which would label degenerating myelin for targeting by macrophages] and as such 50% fewer macrophages were present at the injury site in JHD mice, with those present displaying a reduced phagocytic morphology. Vargas et al. (2010) found that myelin clearance was delayed in the JHD mice compared to wild-type mice and that the delay was in the second [macrophage

dependent] stage of clearance rather than the initial Schwann cell mediated [macrophage independent] stage of clearance. The result of this delay in clearance was a reduction in axon regeneration: in JHD mice crossed with YFP-H mice there were 50% fewer YFP labelled axons 16mm distal to the injury after 8-days and 9% fewer after 22-days compared to standard YFP-H mice. In addition, electrophysiological results indicated a 50% reduction in compound action potentials in the JHD mice compared to wild-types but no difference in the velocity of axon conduction; this indicates that although axons are inhibited from regenerating by the myelin debris, the process of re-myelination of regenerating axons is not affected.

TGF-β1 is also known to regulate many functions of Schwann cells, including inhibiting myelination (Mews and Meyer, 1993, Einheber et al., 1995, Guenard et al., 1995) and promoting both Schwann cell proliferation and death (D'Antonio et al., 2006). TGF-β1 has been shown to increase Schwann cell expression of leukemia inhibitory factor [LIF] mRNA (Matsuoka et al., 1997) - a cytokine linked to neurone survival (Cheema et al., 1994).

The phenotypic changes by Schwann cells following nerve injury [including downregulation of myelin production, expression of adhesion molecules, release of neurotrophic factors and proliferation] are understood to be a key stage in nerve regeneration and these changes are promoted by TGF-β1 (Einheber et al., 1995). The proliferation of Schwann cells following nerve injury would appear to be vital to successful nerve regeneration, as the application of anti-tumor necrosis factor-α [TNF-α] therapy following a sciatic crush injury has been shown to improve regeneration in rats (Kato et al., 2010). TNF-α is a cytokine linked to the transition of Schwann cells from their neural orientation to a more active immunological one following nerve injury (Schneiderschaulies et al., 1991) and has been shown to inhibit Schwann cell proliferation (Chandross et al., 1996) - though TNF-α has also been shown to adversely affect neurite outgrowth (Schneiderschaulies et al., 1991).

It is apparent that wholesale inhibition or removal of TGF-β1 and -β2 at the site of nerve injury to reduce intraneural scarring is inherently problematic due to the wide range of differing roles performed by the various TGF-β isoforms. However the mediation of TGF-β levels at the site of nerve injury still has potential, providing that it is performed in a more precise manner.

As discussed in chapter 1 [section 1.7.4.4], mannose-6-phosphate is a molecule with the ability to reduce scarring in dermal tissue (McCallion and Ferguson, 1996). The scar reducing potential of M6P is strongly linked to its to its ability to bind to the cation-independent M6P [CI-M6P] receptor, which latent TGF-β must bind to in order to cleave the LAP and become active (Dennis and Rifkin, 1991)[fig. 1.8]. M6P is found on the LAP as two of its three oligosaccharide side chains and binds with both high affinity and specificity to the CI-M6P receptor - it is this high affinity and specificity that allows non-LAP M6P to compete for receptor binding sites with latent TGF-β. The importance of the CI-M6P receptor to TGF-β activation and subsequent scar formation can be observed in mice with a deficiency in CI-M6P receptors, which demonstrate a reduced propensity for scarring and have also shown an improved ability to regenerate injured peripheral nerves (Atkins et al., 2006b). As a reduction in number of CI-M6P receptors is not a realistic clinical proposal, M6P could provide a simple method of achieving a similar result by preventing latent TGF-β from accessing the receptor without directly targeting TGF-β and affecting its suggested beneficial influence of nerve regeneration (Atkins et al., 2006a).

Previously, Ngeow et al. (2011b, 2011a) assessed the compound action potentials of the sciatic nerve six weeks post-repair and found them to be significantly higher in M6P treated nerves than controls, in addition conduction velocities were significantly higher - indicating both a greater number of functional axons crossing the repair and that more myelinated axons were present in M6P treated repairs. Interestingly, the levels of intraneural scarring in M6P treated nerves were not considered to be significantly reduced compared to controls in both Ngeow studies (Ngeow et al., 2011a, Ngeow et al., 2011b). Over a longer time period

[12-weeks] the difference between M6P treated repairs and controls was no longer considered significant (Ngeow et al., 2011b); indicating that M6P may only give an early boost to regeneration.

A number of suggestions were made by Ngeow et al. (2011a, 2011b) to account for the significantly improved regeneration in M6P treated repairs at 6-weeks post-injury compared to controls, and the subsequent equalisation of the difference between the two groups at 12-weeks post-injury. Whether axons in M6P repairs had a faster rate of initial regeneration, collagen remodelling occurred sooner in M6P repairs, or the reduction in collagen at later time points allowed formerly blocked axons in control repairs to successfully regenerate at that point could not be ascertained using the methods of analysis performed in the Ngeow et al. (2011a, 2011b) studies [electrophysiology and walking gait analysis].

3.1.1 AIM OF THIS STUDY

The aim of the study reported in this chapter was to investigate the effects of the application of 600nM M6P to graft repairs in YFP-H mice. The ability to view the fate of individual regenerating axons in nerve injury models using YFP-H mice [see section 1.8] should enable confirmation of what causes the initial improvement in regeneration within M6P treated repairs.

The hypothesis for this study was that the application of M6P would improve nerve regeneration, resulting in an axon sprouting profile closer to uninjured control nerves than injured controls, an increased proportion of unique axons regenerating through the repair and reduced disruption of axons entering the repair. The three groups in this study were:

- Graft repairs treated with M6P.
- Graft repairs treated with vehicle [PBS].
- Uninjured nerves.

3.2 MATERIALS AND METHODS

General materials and methods are detailed in chapter 2, more specific details for this chapter are detailed below.

3.2.1 SURGICAL PROCEDURES

In brief, common fibular nerve tissue was obtained from a wild-type littermate of the experimental YFP-H mouse and placed into a numbered vial containing a solution of 600nM M6P or PBS and left to soak for 30 minutes prior to being used to repair a 2.5mm defect created in the CF nerve of a YFP-H mouse. The vials were randomized by a colleague not involved in the analysis process. Following a two-week recovery period the repaired nerves were harvested and mounted onto slides. Uninjured nerves were harvested from YFP-H mice that had not been used in nerve repair experiments.

An small additional group of YFP-H mice were used to ensure that fluorescence distal to the injury degraded sufficiently within the two-week recovery period - it had previously been indicated that a significant level of distal fluorescence could persist between 10- and 14-days post injury (Groves et al., 2005, Witzel et al., 2005). In these mice the CF nerve was transected and then the central end was tied-off with silk suture to prevent axon regeneration. Following the recovery period both central and distal nerve endings were harvested and mounted onto slides.

3.2.2 ANIMAL NUMBERS AND GROUPINGS

In total 53 mice were used in the experiments described in this chapter, with equal numbers of WT and YFP-H mice used in the repair groups [WT mice used to provide graft tissue] and only YFP-H mice used in uninjured/non-repaired groups. All experiments were conducted under the UK Home Office project license number 40/3070.

The experimental groups for this chapter were: M6P (n=10 YFP-H and 10 WT), PBS (n=10 YFP-H and 10 WT), uninjured (n=10) and injured with no repair (n=3).

3.2.3 SAMPLE SIZE CALCULATIONS

Groups sizes for M6P, PBS and uninjured were determined based upon previous M6P work by Ngeow et al. (2011b), as our analysis methods for YFP-H mice had not been fully developed at this stage and as such no data was available to make calculations from.

3.2.4 STATISTICAL ANALYSIS

Statistical analysis of the results was carried out as stated in section 2.3.3. All sprouting index and functional axon tracing results used 2-way ANOVA with Bonferroni post-tests; axon disruption results used a 1-way ANOVA with Bonferroni post-tests. Differences were considered to be significant when $p<0.05$.

3.3 RESULTS

All animals recovered well following surgery, with no signs of infection or autotomy (self harm).

3.3.1 DEGRADATION OF DISTAL FLUORESCENCE

Fluorescence in the degenerating axons distal to the injury was almost completely degraded after the two-week recovery period [fig. 3.1]. All remaining fluorescence was limited to small flecks, indicating that analysis at the point where axons had re-entered the distal nerve ending would be unlikely to be adversely affected.

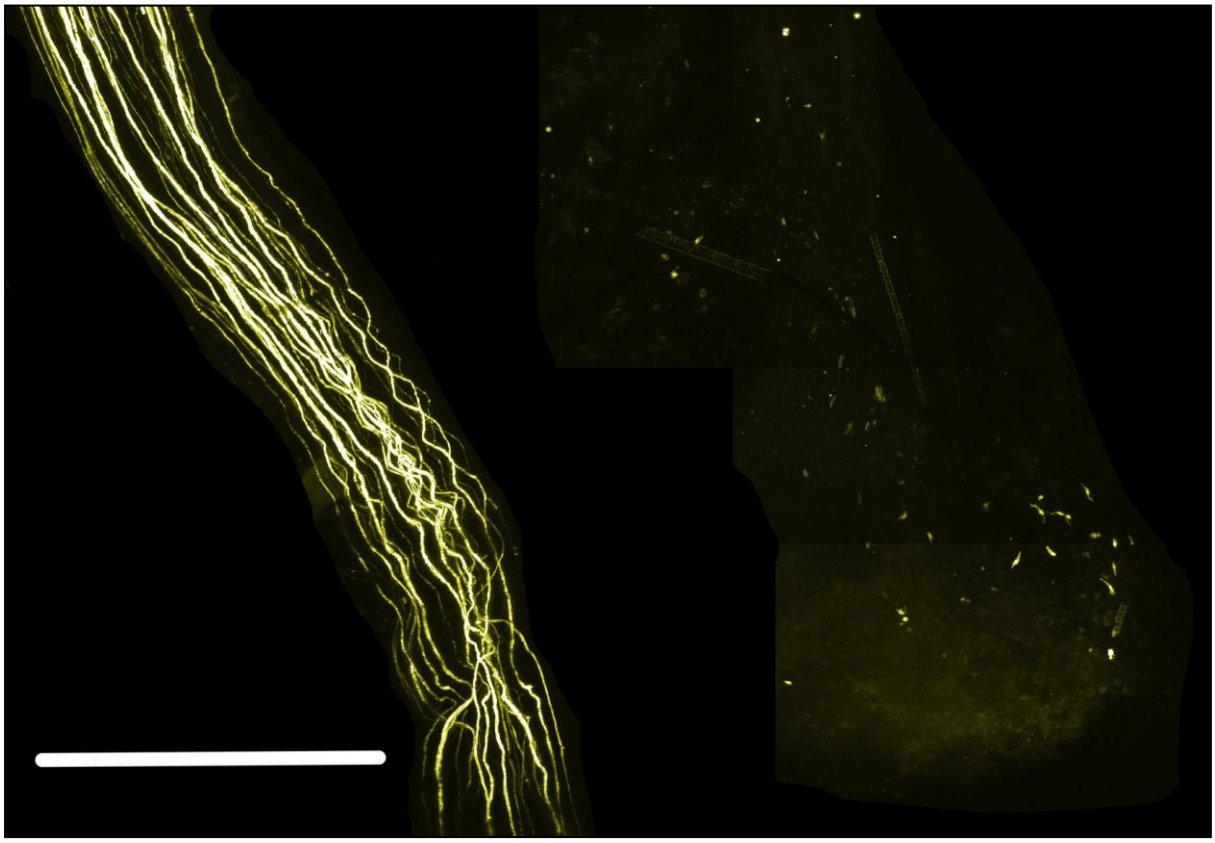

Figure 3.1: Central [left] and distal [right] nerve endings two-weeks after transection with no repair. Scale bar = 1.0mm.

3.3.2 QUALITATIVE DIFFERENCES BETWEEN GROUPS

Visually there was little difference between the two repair groups and no clear indicators that would allow the nerve images to be accurately separated into their respective groups [fig. 3.2].

Nerve images for both repair groups displayed an area of disrupted axons around the initial join between the central nerve ending and the graft, with axons then becoming more organised once within the graft [fig. 3.2]. At the join between the graft and the distal nerve ending another, smaller area of disrupted axons was present and again, once the axons had crossed this area and entered the distal nerve ending, they became more organised [fig. 3.2].

The difference between nerve images from both repair groups and those in the uninjured group is much clearer, with axons within the uninjured nerves running near parallel through the imaged length and no noticeable disruption [fig. 3.3]

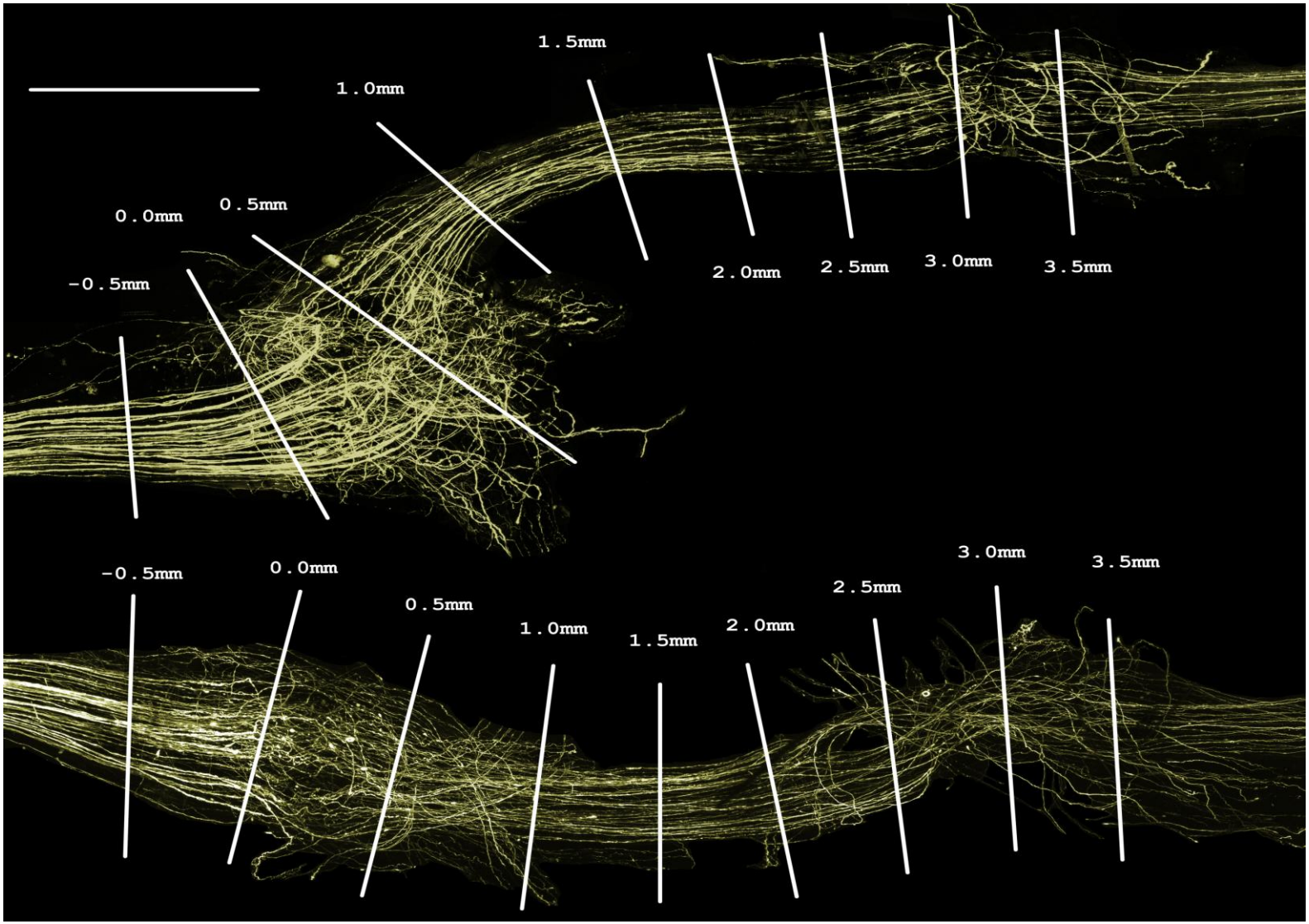

Figure 3.2: Typical images of vehicle (top) and M6P (bottom) treated nerve repairs with intervals marked. Scale bar = 1.0mm.

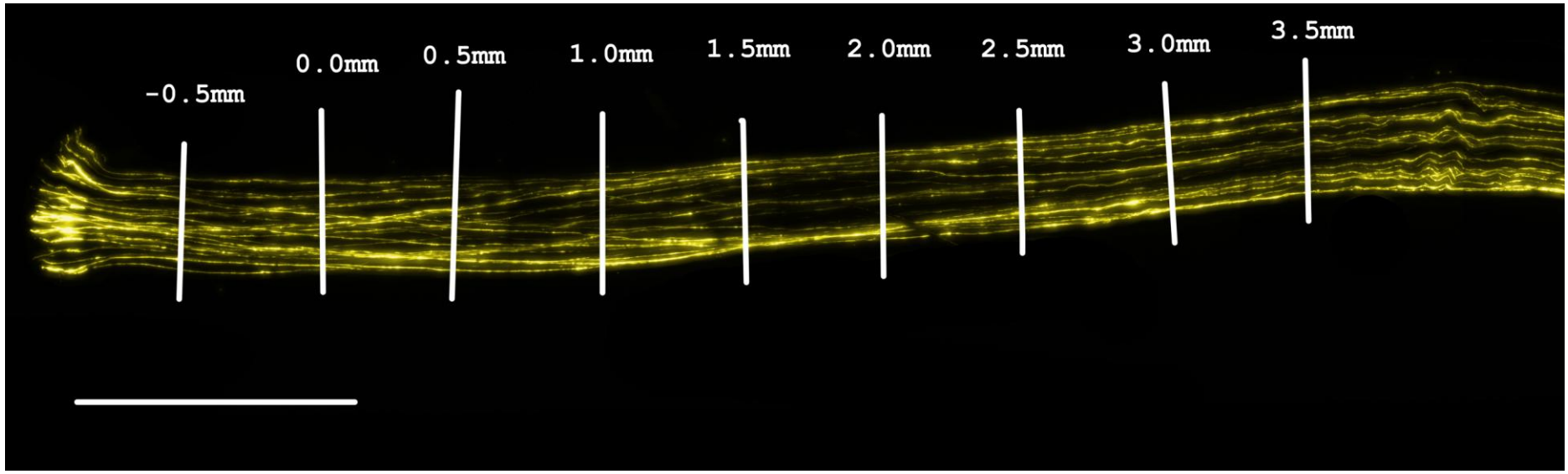

Figure 3.3: Typical uninjured nerve image with intervals marked. Scale bar = 1.0mm.

3.3.3 SPROUTING INDEX RESULTS

There were no significant differences detected between repair groups at any interval, however, the M6P group did display slightly lower initial sprouting at the 0.5mm and 1.0mm intervals and this difference between treatment groups was maintained for the remaining intervals [table 3 and fig. 3.4].

For both M6P and vehicle groups maximal sprouting was observed at the 0.5mm and 1.0mm intervals with sprouting in both groups significantly higher than the uninjured group. Minimal sprouting for both repair groups was observed at the 3.5mm [distal nerve stump] interval with sprouting in the M6P group significantly lower than the uninjured group [table 3 and fig. 3.4].

Table 3: Sprouting index levels for M6P, vehicle and uninjured groups [%].

Repair Position	Average Sprouting (M6P)	SEM (M6P)	Average Sprouting (Vehicle)	SEM (Vehicle)	Average Sprouting (Uninjured)	SEM (Uninjured)
-0.5	100.0	0.0	100.0	0.0	100.0	0.0
0	114.2	3.7	102.5	2.4	99.1	1.4
0.5	160.2	16.3	178.1	12.8	96.2	1.1
1	169.4	19.7	176.8	26.6	98.1	1.4
1.5	119.5	14.4	123.5	16.1	96.8	1.8
2	90.0	7.5	100.9	15.9	96.8	1.0
2.5	76.2	6.5	90.5	2.7	97.7	1.9
3	66.6	11.4	82.0	10.2	97.6	1.7
3.5	52.5	8.7	77.6	14.4	98.5	1.3

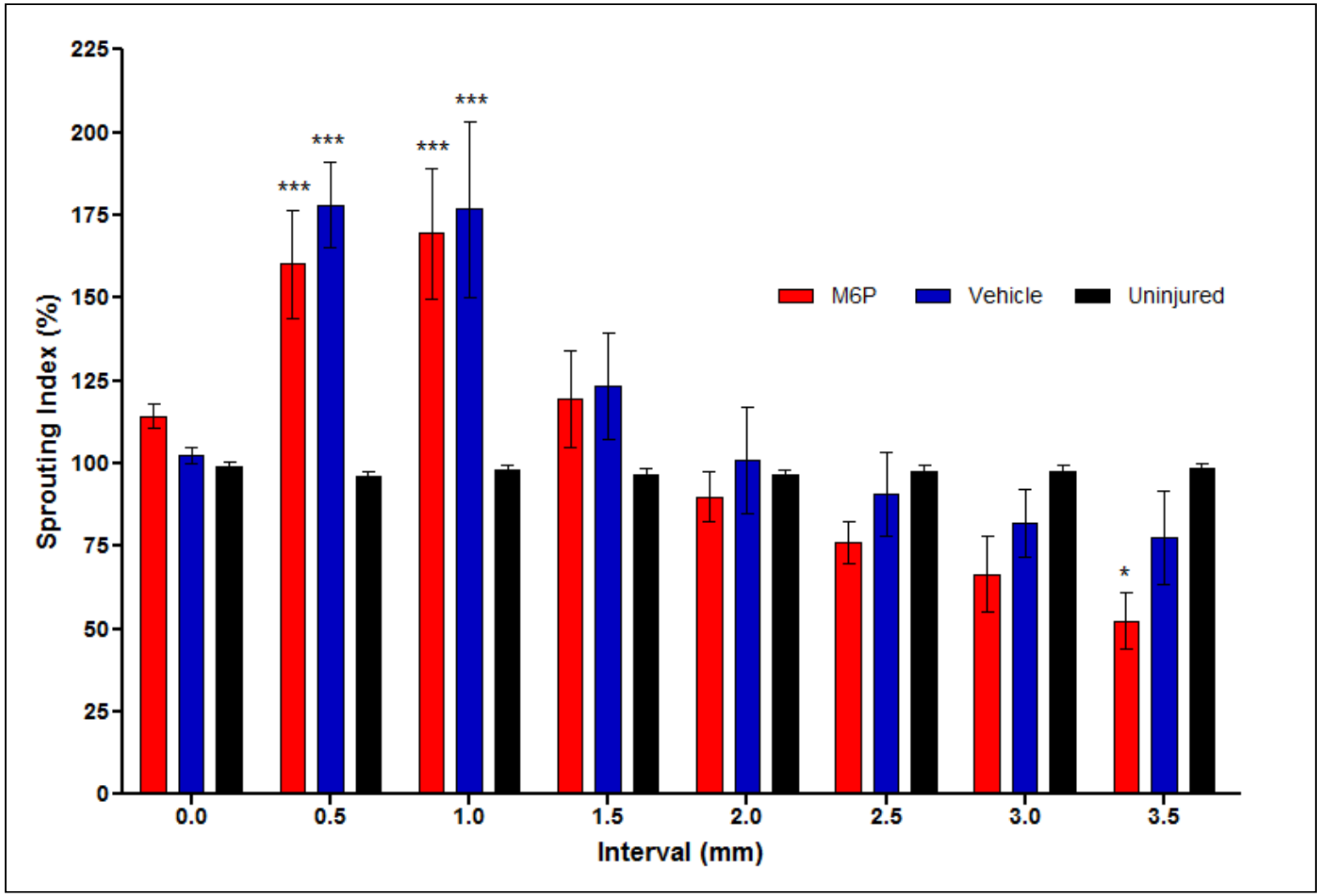

Figure 3.4: Sprouting index levels at 0.5mm intervals along the graft; * and * denote significant differences in value compared to uninjured controls, $p<0.05$ and $p<0.001$ respectively. Error bars denote SEM. Statistical test: 2-way ANOVA with Bonferroni post-tests.**

3.3.4 CHANGE IN SPROUTING INDEX BETWEEN INTERVALS

The maximum change in Sprouting index levels for both treatment groups occurred between the graft start and 0.5mm interval [fig. 3.5]; the difference between repair groups was considered significant between those intervals with a higher increase in sprouting index level observed in the vehicle group - the increase in sprouting index level in both repair groups was considered significant compared to uninjured controls. The sprouting index level in both repair groups remained stable between the 0.5mm and 1.0mm interval and then fell in both treatment groups between the 1.0mm and 1.5mm interval. The sprouting index level then continued to fall at a similar rate in both treatment groups between the remaining intervals [fig. 3.5].

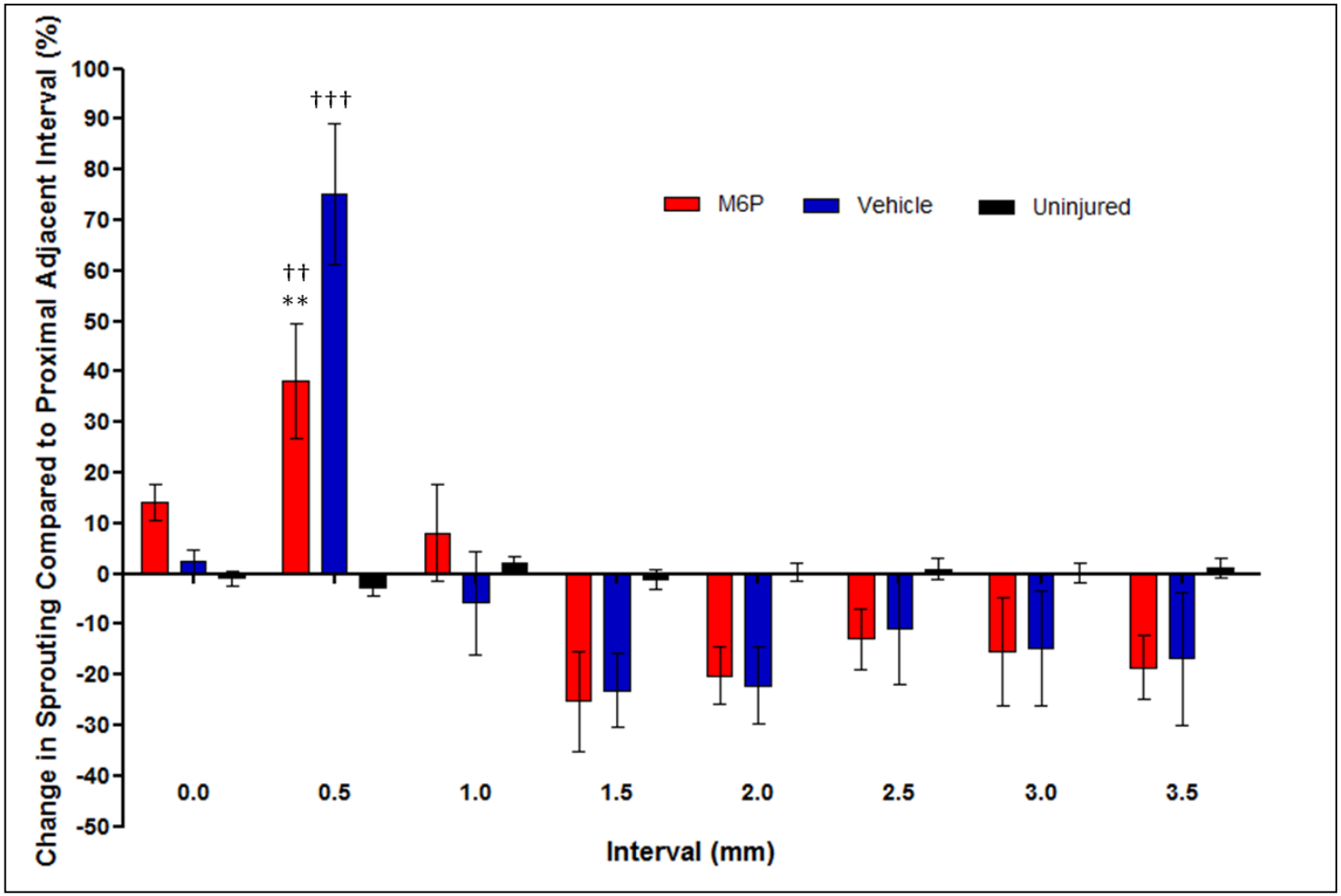

Figure 3.5: Changes in Sprouting index levels at each 0.5mm interval compared to the previous interval; †† and ††† denote significant differences in value compared to uninjured controls, *p*<0.01 and *p*<0.001 respectively; ** denotes significant difference in value compared to vehicle treated graft, *p*<0.01. Error bars denote SEM . Statistical test: 2-way ANOVA with Bonferroni post-tests.

3.3.5 FUNCTIONAL AXON TRACING

The proportion of unique axons from the from the start point [0.0mm] represented at each interval along the graft declined at a similar rate in both M6P and vehicle groups and no significant differences were found between groups at each individual interval [fig.18]. In both repair groups the largest loss of unique axons [25.1% in M6P; 25.2% in vehicle] occurred between the 0.5mm and 1.0mm intervals and from the 1.0mm interval onwards unique axon numbers in both repair groups were significantly lower than uninjured controls [fig. 3.6]. The proportion of unique axons continued to fall at a lower rate at each subsequent interval, resulting in a total of approximately 24% reaching the final 3.5mm interval in both repair groups [fig. 3.6].

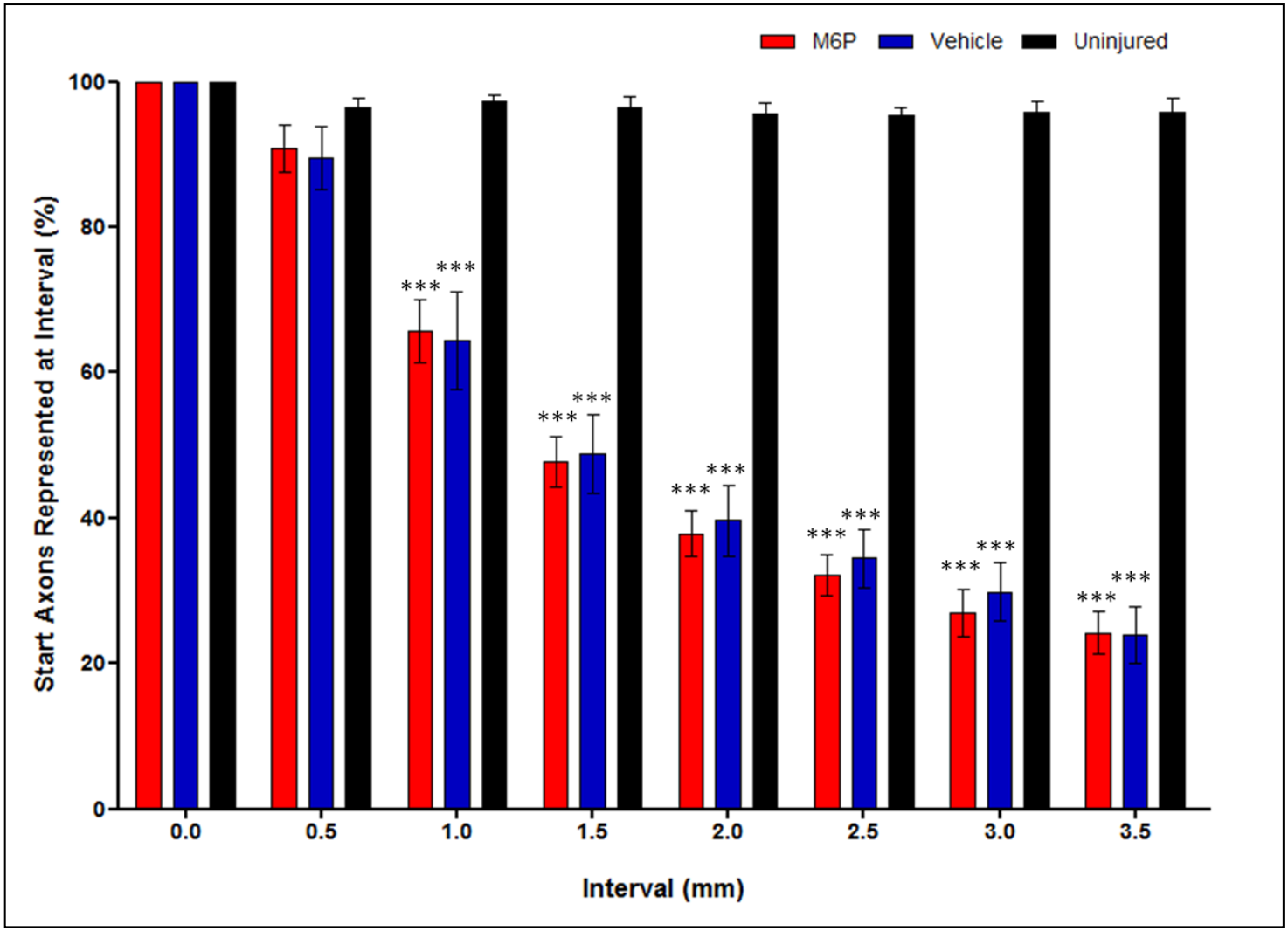

Figure 3.6: Percentages of start axons represented at subsequent 0.5mm intervals; * denotes significant difference compared to uninjured controls, *p*<0.001. Error bars denote SEM. Statistical test: 2-way ANOVA with Bonferroni post-tests.**

3.3.6 AXON DISRUPTION

When crossing the initial repair site from central nerve ending into the nerve graft [fig. 3.7] the average increase in axon length between the graft start and 1.5mm interval was significantly lower in the M6P group [13.6% ±1.2 SEM] than in the vehicle group [20.5% ±2.4][fig. 3.8]. In both repair groups the increase in axon length was significantly higher than in uninjured controls [2.3% ±1.6][fig. 3.8].

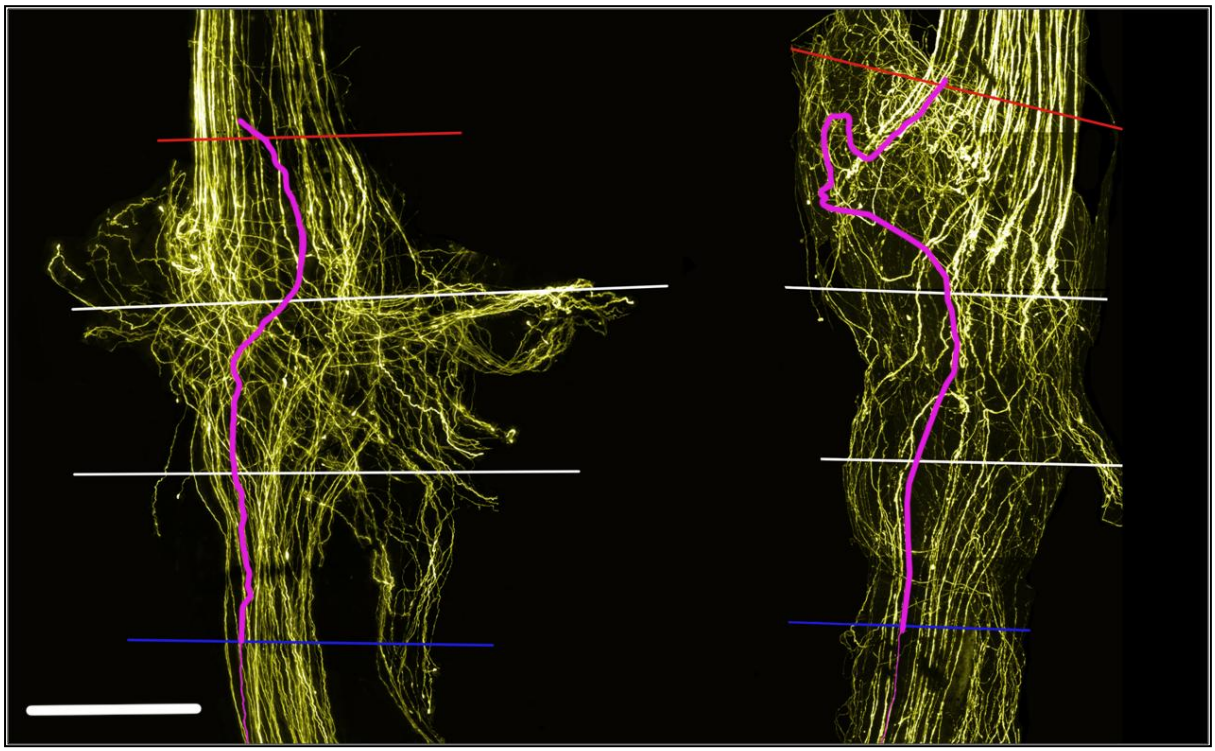

Figure 3.7: Comparison of axon disruption in M6P (left) and vehicle treated repairs (right) across the initial 1.5mm of the repair. An individual traced axon is used to indicate differences in axon length/disruption. Scale bar = 0.5mm.

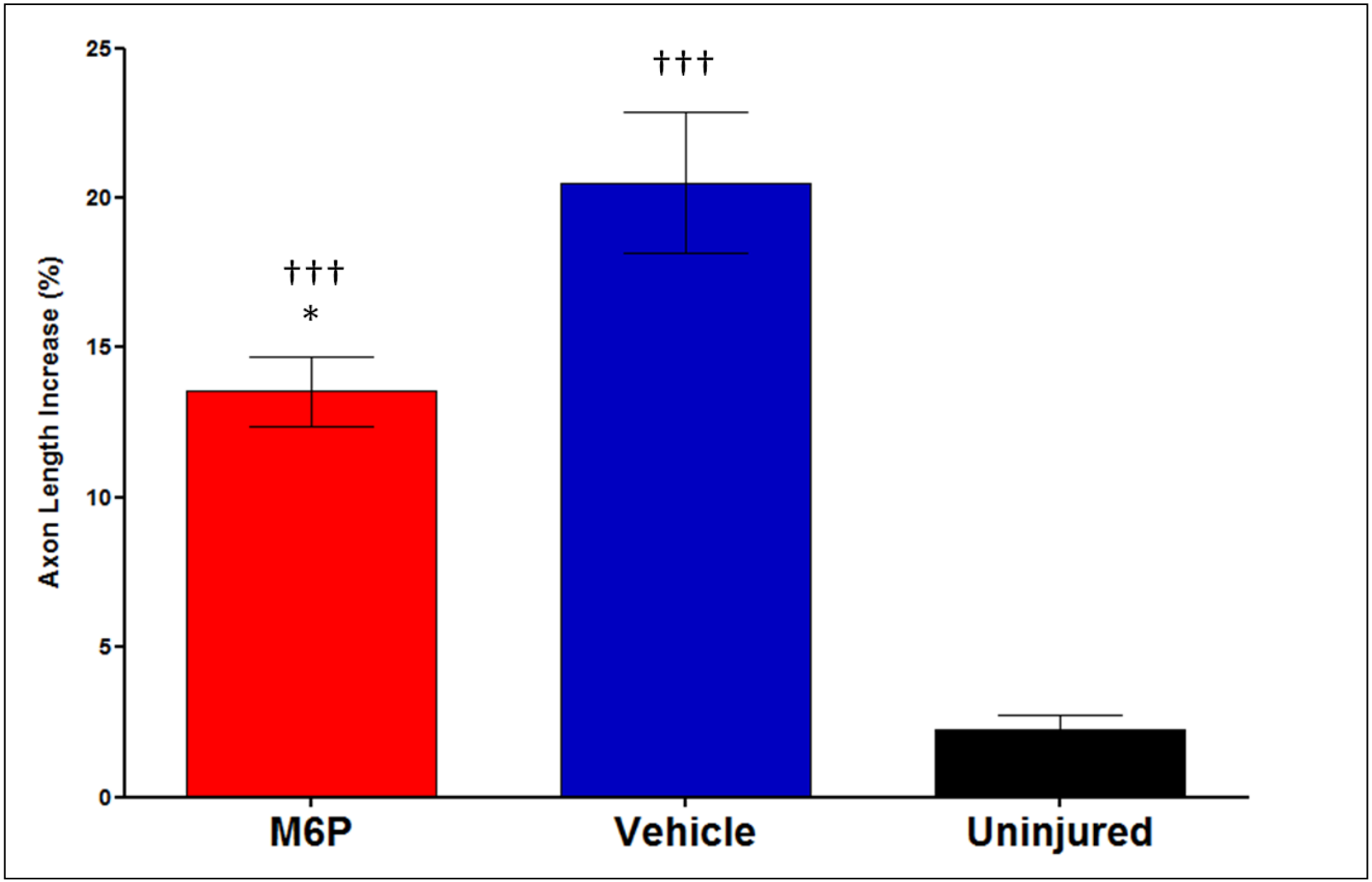

Figure 3.8: Percentage increase in axon length across the initial 1.5mm of repair; * denotes significant difference compared to vehicle group, *p*<0.05; ††† denotes significant difference compared to uninjured controls, *p*<0.001. Statistical test: 1-way ANOVA with Bonferroni post-tests.

3.4 DISCUSSION

3.4.1 AXON SPROUTING LEVELS THROUGH REPAIRS

It has long been recognised that injured axons sprout multiple branches which extend distally during the earlier stages of regeneration and it is also apparent that increases in the severity of an injury lead to increased axon sprouting (Bray and Aguayo, 1974, Sunderland, 1978, Toft et al., 1988, Giannini et al., 1989, Xu et al., 2008).

Xu et al. (2008) reported increased sprouting following 20mm long sciatic crush injuries than in 2mm injuries, with the level of sprouting measured at the same point distal to injury in both groups. This indicates that increased distal disruption can initiate an increase in sprouting in axons that have yet to encounter the disruption; whether the increase in sprouting is due to cytokine/chemokine signalling from the damaged tissues or axons encountering the disruption creating new sprouts proximal to the disruption is currently unclear.

Further evidence of axon sprouting as a response to disruption/scarring was provided in a study by Atkins et al. (2007) that investigated the anti-scarring potential of the anti-inflammatory cytokine interleukin-10 [IL-10]. In that study IL-10 was found to significantly reduce intra-neural scarring with a corresponding increase in axon regeneration across the repair site in electrophysiology results, however, axon count results were found to be similar in both IL-10 and saline controls. The reason given for this discrepancy between electrophysiology results and histomorphology results was that the relatively higher level of intra-neural scarring in saline controls caused an increase in axon sprouting resulting in more duplicated axons crossing the repair site (Atkins et al., 2007).

Following imaging of repaired nerves it appeared that a great deal of disruption and potential sprouting occurred in both M6P and vehicle groups at the joins between the central nerve end and the graft, and between the graft and distal nerve ending [fig. 3.2]

In previous studies of nerve regeneration using YFP-H mice, one outcome measure used was the quantification of axons proximal and distal to the repair to generate a ratio - termed sprouting index - of axon sprouting into the repair (Groves et al., 2005, Sabatier et al., 2008). The equivalent outcome measure used in this study [and the others reported within this thesis] built upon the previously used sprouting index method by increasing the distal data points from a single reference to a total of eight separate intervals encompassing the entirety of the graft repair and the initial portion of the distal nerve ending. By calculating sprouting index ratios at multiple points along the repair the entire sprouting profile could be determined, giving an increased level of information compared to the previously used single point method.

It was hypothesised that sprouting index profiles in the M6P groups would be closer to those in the uninjured group than the vehicle group, with lower initial sprouting followed by more stable sprouting index levels. However, sprouting index results for both repair groups were similar with significantly higher Sprouting index levels at the first two 0.5mm intervals of the repair compared to uninjured controls [fig. 3.4]. The M6P group also, interestingly, had a significantly lower sprouting index level at the distal nerve ending compared to the uninjured group - but not the vehicle group [fig. 3.4].

Further analysis comparing the change in sprouting index level at each interval compared to the level at the previous interval was conducted in an attempt to discover an explanation for the seemingly worse performance of the M6P group. The analysis revealed that the sprouting index level change between the 0.0mm and 0.5mm intervals was significantly lower in the M6P group when compared to vehicle treated repairs [fig. 3.5]. As the sprouting index level changes for all subsequent intervals was similar in both repair groups, this initial difference would be carried through the entire repair, resulting in the M6P group - but not the vehicle group - having a significantly lower sprouting index at the 3.5mm interval. This lower increase in early sprouting index levels could indicate that axons crossing into the graft in the

M6P group encountered fewer obstructions and, although not clearly indicated in these results, lower sprouting may have also occurred in the M6P group at the graft exit.

3.4.2 FUNCTIONAL AXON TRACING

Although a high number of total axons regenerating through a nerve graft repair can be considered indicative of a better recovery, increased sprouting can lead to higher axon numbers without improved functionality (Atkins et al., 2007). In fact, functional recovery can often contrast with morphological analysis of nerve regeneration - Pagnussat et al. (2012) reported on the effects of different training therapies on nerve regeneration in rats, with significantly better functional recovery observed following skilled and unskilled training compared to no training. However, in a number of morphological analyses [myelinated fibre area, myelin thickness, myelinated fibre and axon diameters] no differences were found between any of the nerve repair groups. Mirroring that study, Taha et al. (2004) reported significantly improved morphological regeneration [increased axon density] in rat tibial nerves when treated with retinoic acid but no improvement in functional outcome [walking track analysis].

In the study reported in this chapter, assessing functional recovery in terms of behavioural assessment was not viable due to the short recovery time period [2-weeks] chosen to assess early stage regeneration. In order to effectively estimate potential functional recovery axons were traced back from each interval to determine the proportion of axons from the 0.0mm interval that were represented at each subsequent interval - a higher proportion reaching the final 3.5mm interval would indicate better potential for future functional recovery.

Results indicated that there was no difference between the M6P or vehicle groups in terms of starting interval axons represented at each subsequent interval, with less than 25% of 0.0mm interval axons reaching the final 3.5mm interval in both groups [fig. 3.6]. That more

than 50% of axons from the 0.0mm interval were lost by the 1.5mm interval [fig. 3.6] further indicates the influence of the visible disruption observed at the graft entry point [fig. 3.2].

It had been anticipated that M6P treated repairs would have a higher proportion of starting interval axons represented at later intervals, especially the final interval.

An increase in 0.0mm interval axons reaching the 3.5mm interval in the M6P group would have tied in with electrophysiology results reported by Ngeow et al. (2011a, 2011b) in previous studies. In both of those studies M6P treatment resulted in significantly improved compound action potentials and conductance velocities compared to PBS treated controls at 6-weeks post repair - indicating a greater number of myelinated functional axons had crossed the repair. However, the number of axons crossing the repair is not the only factor needing consideration as other factors can affect functional recovery, such as misdirected sensory axons occupying distal motor axon endoneurial tubes and vice-versa [discussed in section 1.7.3]. In addition direct comparisons between this study and the Ngeow et al. (2011a, 2011b) studies are difficult due to the different methods of repair [graft vs. direct suture] and recovery periods [2-weeks vs. 6- and 12-weeks].

3.4.3 INITIAL AXON DISRUPTION AT GRAFT ENTRY

As reported in section 3.3.2 [fig. 3.2] a great deal of disruption was apparent between the 0.0mm and 1.5mm intervals in both repair groups, this disruption was further highlighted with the sprouting index results revealing the highest sprouting index levels to occur at the 0.5mm and 1.0mm [fig. 3.4] and that the majority of axons from the 0.0mm interval were lost by the 1.5mm interval [fig. 3.6].

Treatment with M6P appears to have a significant impact on the amount of disruption axons suffer at during the early stage regeneration into the graft. This is indicated by the significantly shorter average axon lengths over the initial 1.5mm portion of the graft [fig. 3.8] in the M6P group, indicating that axons were able to take a more direct path across this portion of the repair.

These results provide an explanation for the result observed by Ngeow et al. (2011b), where a significant improvement in regeneration was found at 6-weeks post-repair but not at 12-weeks post-repair. As axons in the M6P group take a shorter route across the repair they are likely to reach their target tissue in a shorter time on average than axons taking a longer route in vehicle treated repairs. This means that although axons in the M6P group would have a small head start over axons in the vehicle group, though this advantage would be negated once axons began to reach their target tissues.

As previous M6P studies did not show a significant reduction in intra-neural scarring (Ngeow et al., 2011a, Ngeow et al., 2011b) it would appear that the reduction in disruption shown in this study is not due to an overall reduction in collagen at the injury site. However, it is possible that the initial rate of collagen production and deposition was reduced by the impact of M6P on TGF-β activation immediately following the repair.

The impact of a reduction in collagen production in the early stages of regeneration could have a significant impact on the alignment of collagen fibres within the regenerating nerve tissue. When collagen density is low, fibroblasts responsible for collagen deposition are able to move through the extracellular matrix easier which results in improved collagen alignment (Dallon et al., 2001). Increased TGF-β1 levels - linked to increased production of collagen [see section 1.7.4] - have been shown to result in reduced collagen alignment, while increased levels of TGF-β3 - linked to decreased production of collagen - have been shown to promote collagen alignment (Henderson et al., 2012).

The alignment of collagen was not investigated within the Ngeow et al. (2011a, 2011b) studies but it is plausible that early reductions in collagen production resulted in alignment more favourable for regenerating axons, prior to the effects of M6P on TGF-β activation wearing off and collagen levels increasing to near normal by 6-weeks post injury.

As axon regeneration had proceeded to a point more distal than the excised segment of nerve examined in this study, it was not possible to determine whether the more direct path

taken by axons in M6P treated repairs had resulted in those axons regenerating significantly further than their counterparts in vehicle treated repairs. As regeneration in the leading axons proceeds at a rate of around 0.25mm/day through scar tissue and 1-3mm/day once axons cross the repair site (Gutmann et al., 1942, Al-Majed et al., 2000), any delay due to taking a longer path through areas of scarring can build up to a more significant difference.

For example, the difference between average axon length across the initial 1.5mm of the repair in M6P and vehicle groups was 6.9% or approximately 0.1mm. The difference in time between axons in the M6P group and axons in the vehicle group being able to exit the scar tissue and increase their regeneration rate from 0.25mm/day to 1-3mm/day could lead to the fastest regenerating axons in the M6P group being approximately 1.25mm further ahead than their equivalents in vehicle group by the time the axons in vehicle group exit the scar tissue.

3.4.4 CONCLUSIONS

The overall effect of M6P appears somewhat limited as no effects on overall sprouting or functional axon proportions were observed. It may be that M6P can only affect TGF-β activation for a short time following application before it is either cleared from the injury site or alternative TGF-β activation mechanisms activate sufficient TGF-β to negate the influence of M6P.

The shorter path taken by axons in the M6P group has the potential to improve regeneration by allowing those axons to reach their target tissues in a shorter time period. As discussed earlier [see section 1.7.3], delays in reinnervation can result in target tissues becoming unreceptive to regenerating axons and also the support for regenerating axons being withdrawn. As such enabling axons to regenerate through scar tissue quicker [due to shortened path length rather than increased regeneration speed] could result in a much better level of recovery.

In conclusion, this study provides further evidence of the ability of M6P to improve peripheral nerve regeneration within the initial period of time following nerve repair. The indication is that M6P helps to reduce the disruption axons encounter when crossing the repair site, with improved collagen alignment as a result of temporarily reducing collagen production the likely mechanism. Although the effects of M6P observed in this study do seem limited, M6P may prove useful therapeutically if used in combination with other regeneration enhancing agents.

4.0 THE EFFECTS OF EC23 ON NERVE REGENERATION

4.1 INTRODUCTION

Retinoic acid is a derivative of vitamin A that is involved in the development and regeneration of many different organs in many different animal species (Scadding and Maden, 1986a, b, c, Wion et al., 1987, Stratford et al., 1996, Maden and Hind, 2003). Inhibition of retinoic acid has been shown to have similar adverse effects upon heart development in both avian and mammalian species (Heine et al., 1985, Stratford et al., 1996, Niederreither et al., 2001), retinoic acid is also linked to the coordination of heart and limb development in zebrafish (Sorrell and Waxman, 2011).

Certain amphibians are capable of complete regeneration of severed limbs - such as axolotls and newts - and as such are of great interest for studying regeneration. The effects of vitamin A and its derivatives on regeneration in these animals have been studied in great detail, revealing contrasting effects of limb duplication and deletion depending upon the stage of development and concentrations used (Thoms and Stocum, 1984, Scadding and Maden, 1986a). In the axolotl, immersion in retinol palmitate has been shown to cause skeletal deletions in developing limbs in a dose dependent manner but conversely, in regenerating limbs it has been shown to cause proximodistal duplications (Thoms and Stocum, 1984, Scadding and Maden, 1986a). Retinol palmitate and retinoic acid have both been used to induce limb duplication in newt species such as *Pleurodeles waltl* and *Triturus vulgaris*, though complete duplicate limbs - unlike in the axolotl - were not observed (Lheureux et al., 1986).

In mammals regeneration in mature animals is not as straight forward as in an amphibian like the axolotl, with severance of a limb resulting in little more than wound healing. Research into development has revealed that the level of retinoic acid in specific locations

within an embryo is a critical factor, with excess levels being teratogenic and insufficient levels being deleterious (Duester, 2008). In one study (Niederreither et al., 2002), transgenic mice with a deficiency in retinaldehyde dehydrogenase 2 [*Raldh2*] - required for retinoic acid synthesis (Zhao et al., 1996) - were used to demonstrate that retinoic acid synthesis is responsible for both forelimb growth and anteroposterior patterning of the developing mouse embryo. The *Raldh2* knockout mice used by Niederreither et al. (2002) are not carried to term as they die at 10.5 days post coitum, with severe trunk defects present (Niederreither et al., 1999). Niederreither et al. (2002) were, by the maternal administration of retinoic acid, able to increase forelimb formation and extend survival times in *Raldh2* embryos.

In relation to nerve injuries, the application of exogenous retinoic acid has the potential to improve nerve regeneration through a number of effects, such as inhibiting inflammatory cytokines and increasing neurotrophin expression (Maden, 2007). For example, synthesis of the pro-inflammatory cytokine TNF-α has been show to be reduced in both primary and cell-line macrophage cultures exposed to retinoic acid (Motomura et al., 1996, Wang et al., 2007). TNF-α is known to be both helpful following nerve injury, through Schwann cell activation and macrophage recruitment (Gaudet et al., 2011), and detrimental due to inhibition of axon sprouting and the potential induction of demyelinating neuropathies (Said and Hontebeyriejoskowicz, 1992, Smith et al., 2009). Inhibition of TNF-α synthesis by means other than the application of all-trans retinoic acid has been shown to have a beneficial effect following nerve injury, with Lindenlaub et al. (2000) and Iwatsuki et al. (2013) both reporting reductions in neuropathic pain in mouse and rat models respectively - with Iwatsuki et al. (2013) also reporting improved nerve regeneration.

Various retinoids, including all-trans retinoic acid, have also been shown to have a beneficial effect on dermal scarring by reducing fibroblast proliferation and collagen production (Daly and Weston, 1986, Ogawa et al., 1998). Given that inhibiting TGF-β1 and -β2 to dermal wounds has previously been shown to reduce scarring (Shah et al., 1992) and then later was

shown to reduce intraneural scarring in nerve injuries (Atkins et al., 2006a) it can be surmised that retinoic acid may also be effective at reducing intraneural scarring.

There is evidence that retinoic acid can accelerate nerve regeneration, as a study by Yee and Rawson (2000) found that a single oral administration of retinoic acid following olfactory nerve transection led to the sense of smell in mice recovering significantly faster. However, the study by Yee and Rawson (2000) did not investigate the mechanism underlying the increased speed of recovery, so it is unclear whether the effect was due to an inherent speed increase in regenerating axons, less impedance of axons by intraneural scarring or improved nerve cell survival through increased neuronal support.

Despite the evidence for retinoic acid's beneficial effects on nerve regeneration, few studies have investigated the effects of direct application of retinoic acid on nerve regeneration. At the time of writing only one study had been published in which retinoic acid was directly applied to the site of a peripheral nerve lesion (Taha et al., 2004). In that study the tibial nerve in male Wistar rats was sectioned, treated with 10^{-8} mol/L retinoic acid or vehicle [meal oil], and then repaired using end-to-end or end-to-side anastomosis techniques. Taha et al. (2004) found that the application of retinoic acid improved regeneration in terms of the morphological parameters but not in terms of functional recovery.

A problem with the therapeutic use of all-trans retinoic acid is that it is relatively unstable and are easily photoisomerised into other, less effective retinoid isomers (Murayama et al., 1997, Suzuki et al., 1998). Given that the effects of retinoic acid have been shown to vary widely depending upon concentration (Thoms and Stocum, 1984, Scadding and Maden, 1986a) the instability of retinoic acid has the potential to cause adverse side effects when used as a therapeutic treatment.

EC23 is a stable synthetic form of all-trans retinoic acid with the chemical name 4-(5,5,8,8-tetramethyl-5,6,7,8-tetrahydronapthalen-2-ylethynyl)benzoic acid, which was synthesised and first reported by Christie et al. (2008). EC23 has displayed similar effects on human

pluripotent stem cell differentiation to those observed from all-trans retinoic acid treatment (Christie et al., 2008, Clemens et al., 2013) and also has improved photostability [EC23 is unaffected after 3-days exposure to fluorescent light, whereas all-trans retinoic acid degrades to just 37% of the original quantity (Christie et al., 2008)]. One other difference between EC23 and all-trans retinoic acid is that EC23 does appear to be more potent than retinoic acid (Christie et al., 2010); however, this may be a side-effect of EC23s increased stability, which would increase the probability of the administered dose remaining at the stated level rather than decreasing as all-trans retinoic acid would have the potential to do.

EC23 is believed to have the same mechanism of action as all-trans retinoic acid, based upon the shared ability of both compounds to differentiate human pluripotent stem cells into neural cells (Christie et al., 2008). Retinoic acid can act via the retinoic acid receptors [RAR] and retinoid X receptors [RXR] - with both receptor types having α, β and γ subtypes (Zhelyaznik and Mey, 2006) - though all-trans retinoic acid only interacts with RARs. Following a peripheral nerve crush injury there are local increases in transcript concentrations of RAR-α, RAR-β, RAR-γ, and RXR-α, with protein expression of RAR-α, RAR-β, and RXR-α upregulated during the subsequent nerve regeneration (Zhelyaznik and Mey, 2006). NGF has been shown to induce neurite outgrowth through activating RAR-β via inducing retinoic acid synthesis (Corcoran and Maden, 1999), and RAR-α and RXR-α have been shown to be upregulated in Schwann cells and macrophages, respectively, following nerve injury - with indications that retinoic acid regulates neuroglial interactions and Schwann cell differentiation (Zhelyaznik and Mey, 2006).

4.1.1 AIM OF THIS STUDY

The aim of the study reported in this chapter was to investigate the effects of the application of 10^{-8} mol/L EC23 to graft repairs in YFP-H mice. The following experimental groups were used in this study:

- Graft repairs treated with EC23.
- Graft repairs treated with vehicle [PBS].
- Uninjured nerves.

The hypothesis for this study was that the application of EC23 would improve nerve regeneration through a reduction in scarring and an increase in the regeneration speed of axons.

4.2 MATERIALS AND METHODS

General materials and methods are detailed in chapter 2, more specific details for this chapter are detailed below.

4.2.1 SURGICAL PROCEDURES

As described in chapter 2, nerve grafts of common fibular nerve tissue were obtained from a wild-type littermate of the experimental YFP-H mouse. These grafts were placed into a vial containing a solution of 10^{-8} mol/L EC23 dissolved in PBS and left to soak for 30 minutes [see 2.2.1 and 2.2.3 for general anaesthesia and surgical methods]. The concentration of EC23 [10^{-8} mol/L] was chosen as a previous study (Taha et al., 2004) had reported improved regeneration following the application of retinoic acid at that concentration directly to the recently sectioned tibial nerve in rats.

The treated nerve tissue was used to repair a 2.5mm defect created in the CF nerve of a YFP-H mouse [see 2.2.1 and 2.2.3 for general anaesthesia and surgical methods]. Following a 2-week recovery period, nerves were harvested and mounted onto slides [see 2.2.2 and 2.2.5 for general anaesthesia and surgical methods], imaged and analysed [see 2.3.1 and 2.3.2 for details]. Results for vehicle [PBS] repairs and uninjured controls were taken from those obtained in the mannose-6-phospate study discussed in chapter 3.

4.2.2 ANIMAL NUMBERS AND GROUPINGS

In total 40 mice were used in the experiments described in this chapter, with 16 used exclusively for EC23 experiments and 24 shared with the M6P experiments [see chapter 3]. Equal numbers of wild type and YFP-H mice were used in the repair groups and only YFP-H mice used in the uninjured group. All experiments were conducted under the UK Home Office project license number 40/3070.

The experimental groups for this chapter were: EC23 (n=8 YFP-H and 8 WT), vehicle (n=8 YFP-H and 8 WT), and uninjured (n=8). To maintain equal group sizes, only the first 8

completed vehicle and uninjured nerve results from the M6P study [see chapter 3] were used in this study.

4.2.3 SAMPLE SIZE CALCULATIONS

The sample sizes for this study were calculated using PiFace software [v1.76: *homepage.stat.uiowa.edu/~rlenth/Power*] with standard deviation data obtained from the M6P study discussed in the chapter 3.

4.2.3.1 Sample Size Choice and Justification.

The sample size chosen for the study discussed within this chapter was n=8, which would be sufficient to detect differences between groups of 32.35%, 11.34% and 7.37% for sprouting index [fig. 4.1], functional axon tracing [fig. 4.2] and axon disruption [fig. 4.3] respectively.

The functional axon tracing and axon disruption results were considered to be the more important analyses when considering sample size, as improved functional recovery and faster recovery speed are clinically relevant outcome measures. As such these two measures were used to determine the sample sizes for this study. Detectable differences of 12% and 8% were considered reasonable, which would be achievable with sample sizes of n=7, however, sample sizes were increased by one to n=8 to account for any failed repairs.

The large standard deviation levels for sprouting index results observed in the M6P study [see 3.3.1] meant that only a relatively large overall difference between groups [32.35% for n=8] could be detected without using an excessive number of animals. Despite this it was felt that sprouting index results could still provide a useful insight and identify potential trends of the differing sprouting profiles of the three repair groups [EC23, vehicle and uninjured].

4.2.3.2 Sample Size Calculation Results.

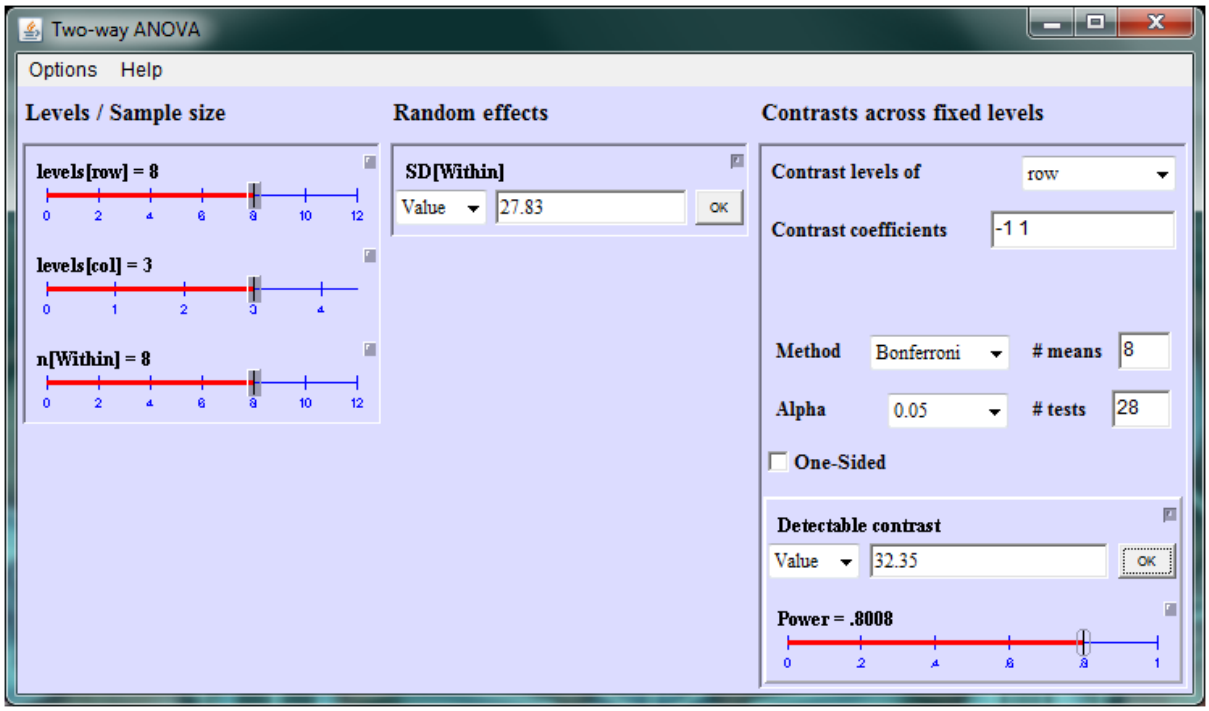

Figure 4.1: Sprouting index analysis power and detectable difference results when using a sample size of n=8. Levels[row] = number of intervals; levels[col] = number of groups; n[Within] = sample size; SD[Within] = standard deviation value derived from M6P study results. Number of intervals [# means] multiplied by number of repair groups minus one gives the number of t-tests required for the Bonferroni post-tests [# tests].

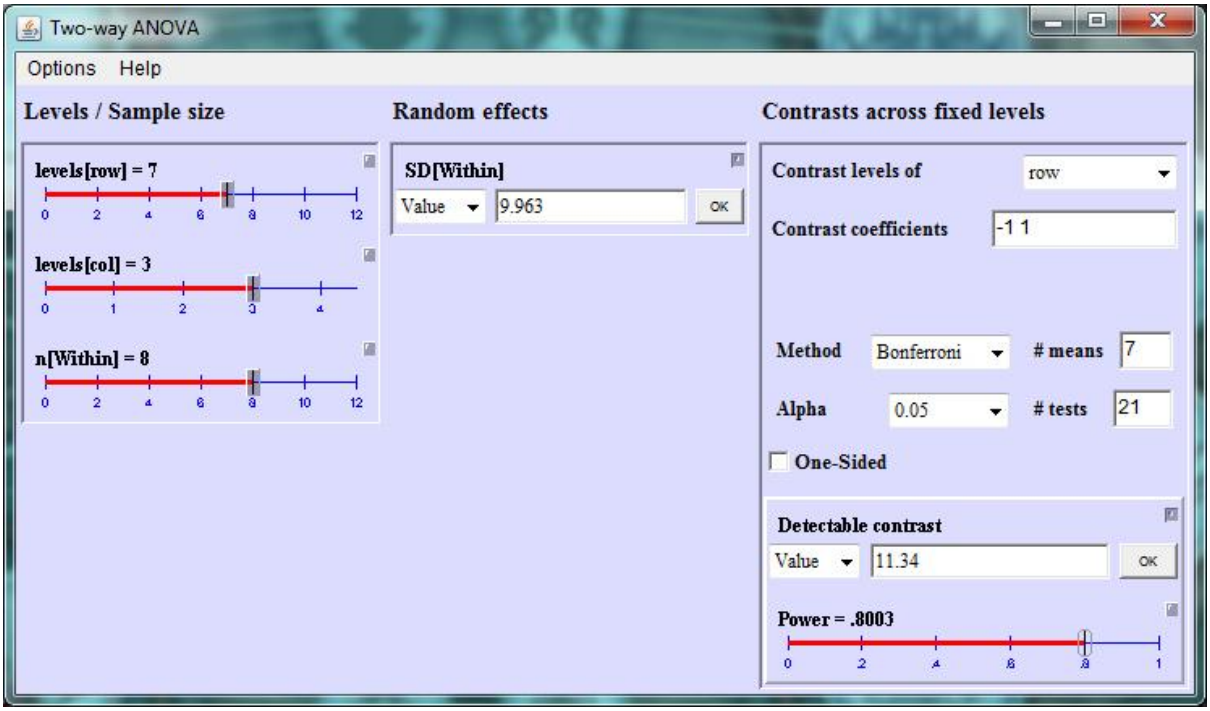

Figure 4.2: Functional axon tracing analysis power and detectable difference results when using a sample size of n=8.

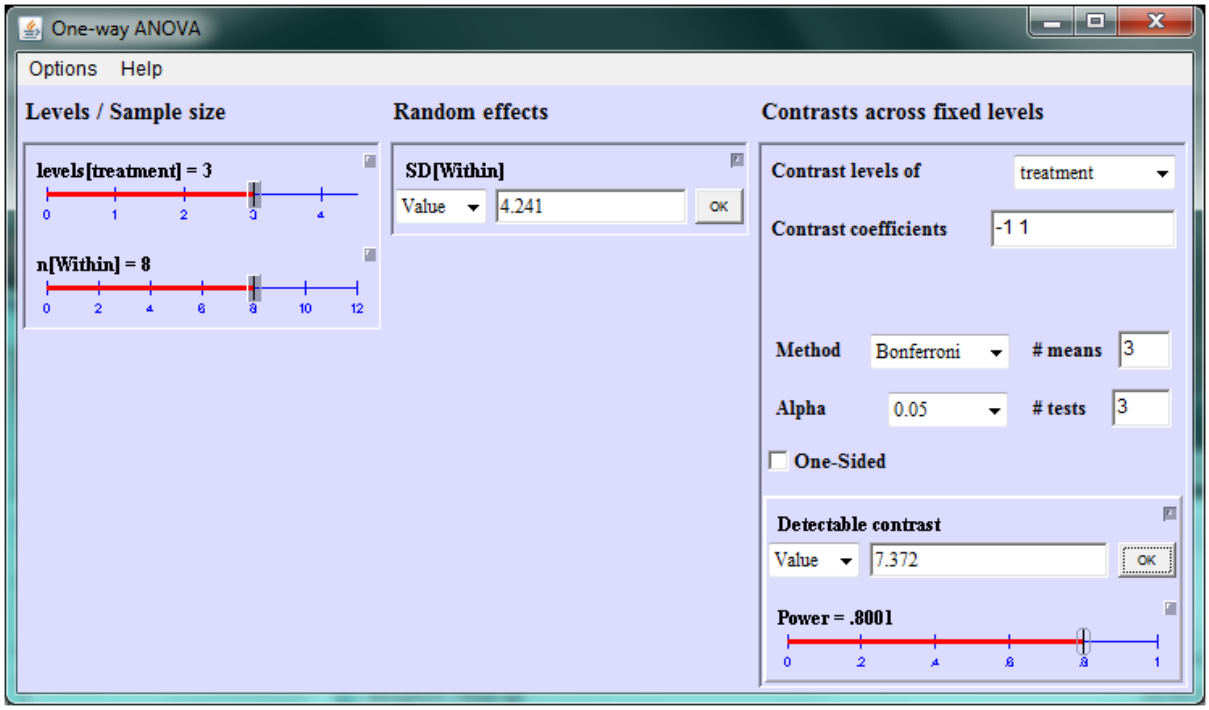

Figure 4.3: Axon disruption analysis power and detectable difference results when using a sample size of n=8. Levels [treatment] = number of groups; see fig. 15 for remaining definitions.

4.2.4 STATISTICAL ANALYSIS

Statistical analysis of the results was carried out as stated in section 2.3.3. All sprouting index and functional axon tracing results used 2-way ANOVA with Bonferroni post-tests; axon disruption results used a 1-way ANOVA with Bonferroni post-tests. Differences were considered to be significant when $p<0.05$.

4.3 RESULTS

All animals recovered well following surgery, with no signs of infection or autotomy (self mutilation of the denervated region).

4.3.1 QUALITIATIVE DIFFERENCES BETWEEN GROUPS

There was no clear difference between EC23 and vehicle treated repair images that would enable the images for the two groups to be separated accurately prior to the quantitative analysis. Though images of EC23 repairs typically appeared to have less axon sprouting at the join between central nerve end and graft than vehicle repairs [fig. 4.4].

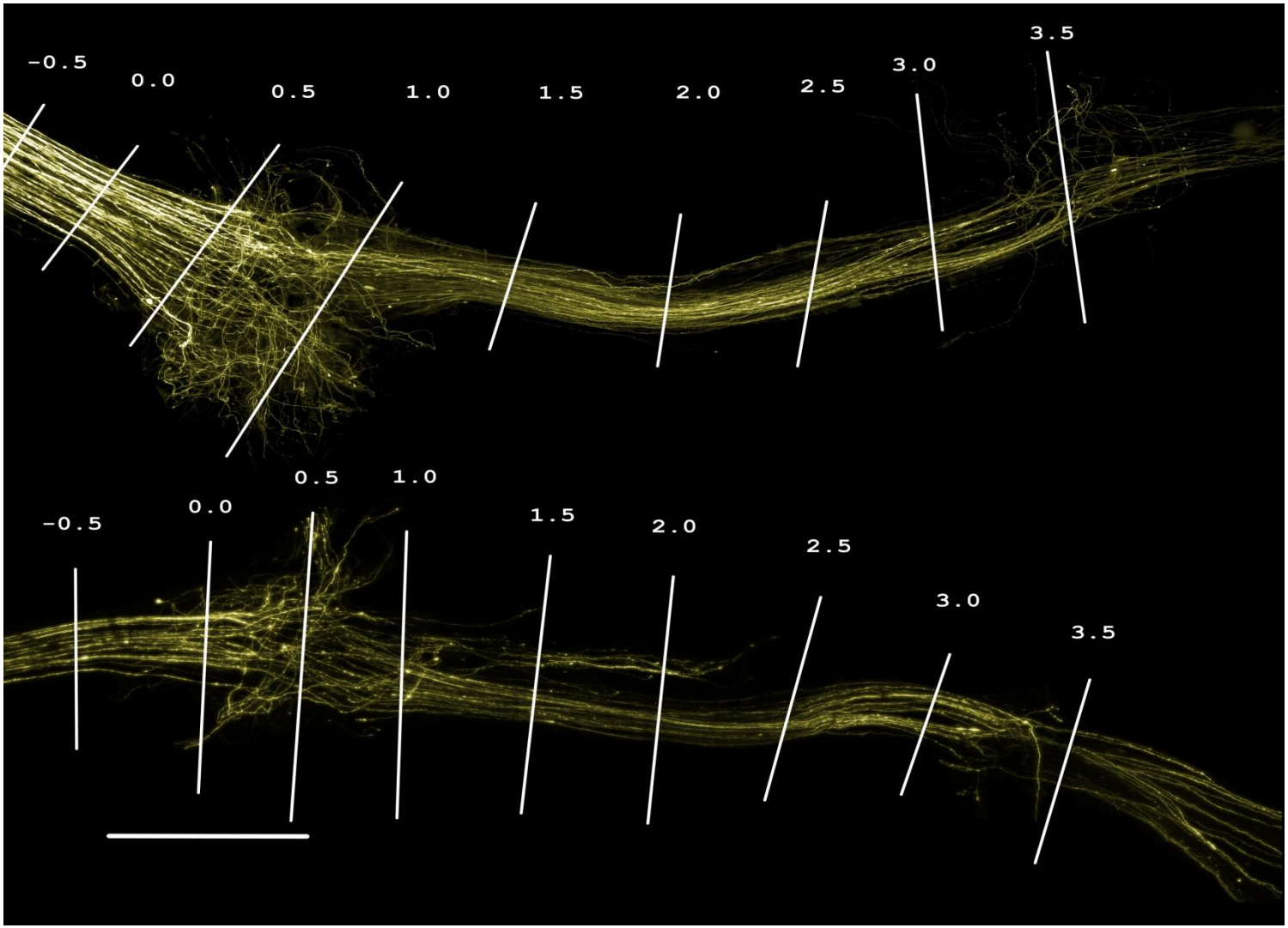

Figure 4.4: Typical nerve images with intervals marked for vehicle [top] and EC23 repairs [bottom]. Scale bar = 1.0mm.

4.3.2 SPROUTING INDEX RESULTS

In both repair groups sprouting index levels were at their highest at the 0.5mm and 1.0mm intervals, with both groups displaying significantly higher sprouting index levels than in the uninjured group at these intervals [table 4 and fig.4.5]. The EC23 group also had a higher sprouting index level at the 1.5mm interval when compared to the uninjured group.

No significant differences were detected between repair groups at any interval along the repair; though in the EC23 group an increased - but non-significant - sprouting index was noted at the 0.0mm interval [fig. 4.5].

In the EC23 group, sprouting index levels declined steadily from the 0.5mm interval to the 1.5mm interval, before a larger decline between the 1.5mm and 2.0mm intervals. Following that decline sprouting index levels in the EC23 group remained stable at the 2.0mm to 3.0mm intervals before declining slightly at the final 3.5mm interval [table 4 and fig. 4.5].

In contrast, the sprouting index levels in the vehicle group remained steady between the 0.5mm and 1.0mm intervals before a large decline at the 1.5mm interval. Following that decline, a smaller, steady decline was observed between each subsequent interval from the 1.5mm interval to 3.5mm interval [table 4 and fig. 4.5]

Table 4: Sprouting index levels for EC23, vehicle and uninjured groups [%].

Repair Position	Average Sprouting (EC23)	SEM (EC23)	Average Sprouting (Vehicle)	SEM (Vehicle)	Average Sprouting (Uninjured)	SEM (Uninjured)
-0.5	100	0	100	0	100	0
0	124.6	5.4	101	2.7	98.9	1.8
0.5	175.4	12.3	182.1	9.9	96.6	1.3
1	160.3	14	185.5	25.3	99	1.6
1.5	137.6	8.5	130.5	15.4	95.4	1.9
2	98.8	7.7	114.8	14.9	95.9	1
2.5	91.3	8.1	101.8	10	96.5	2
3	96.4	5.9	88.5	5	98	2.1
3.5	68.1	8.3	80	12	98.8	1.7

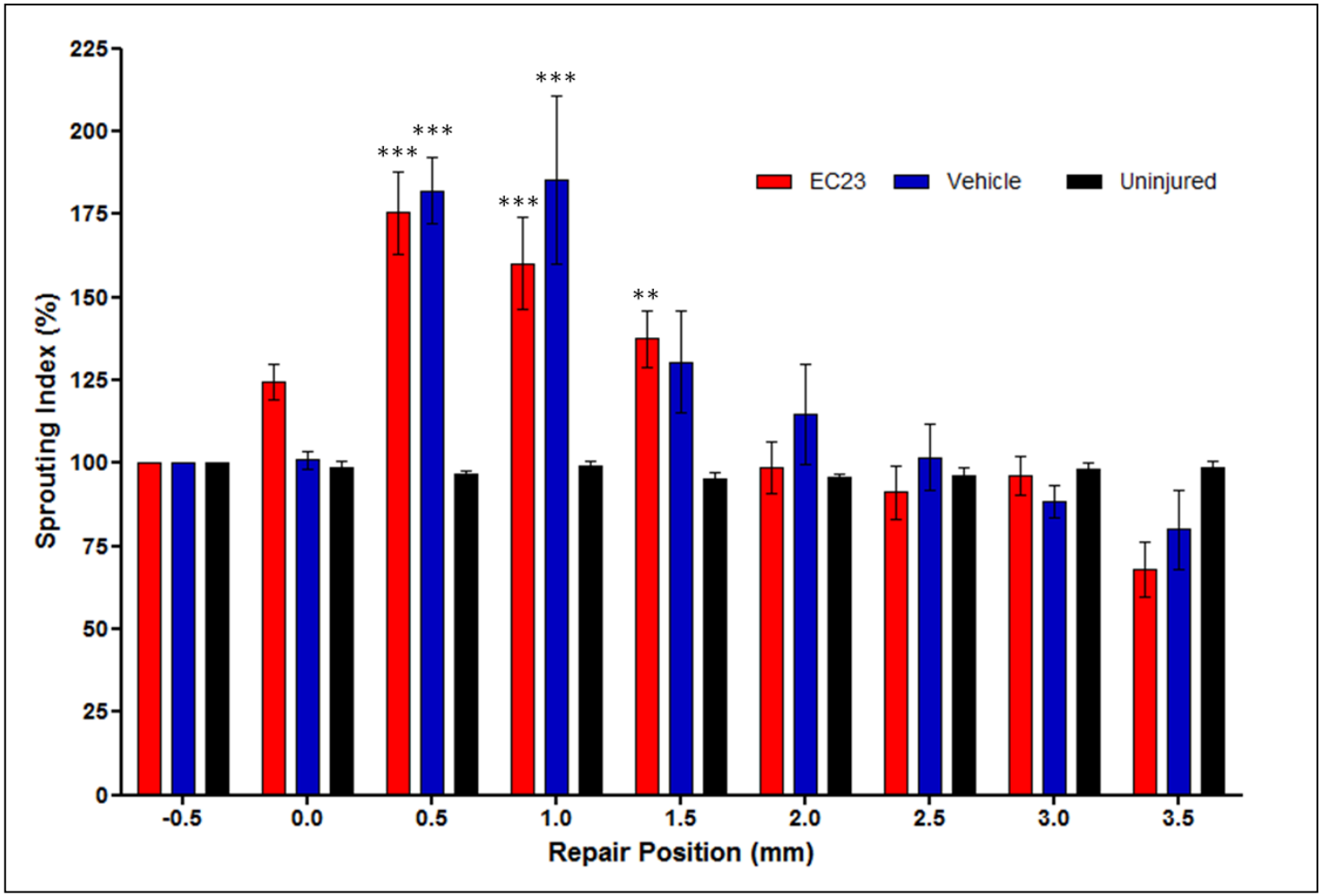

Figure 4.5: Sprouting index levels at 0.5mm along the repair; ** and * denote significant differences compared to uninjured controls, *p*<0.01 and *p*<0.001 respectively. Statistical test: 2-way ANOVA with Bonferroni post-tests.**

4.3.3 CHANGE IN SPROUTING INDEX BETWEEN INTERVALS

In both repair groups the change in sprouting index levels at the 0.5mm interval was considered to be significantly different than in the uninjured group; the difference between repair groups was also considered significant at that interval, with a higher increase in sprouting index level observed in the vehicle group [fig. 4.6].

There were no other significant differences between remaining intervals with regards to the change in sprouting index, though interestingly the 3.0mm interval in the EC23 group had a small overall increase in sprouting index level after the 0.5mm interval [fig. 4.6].

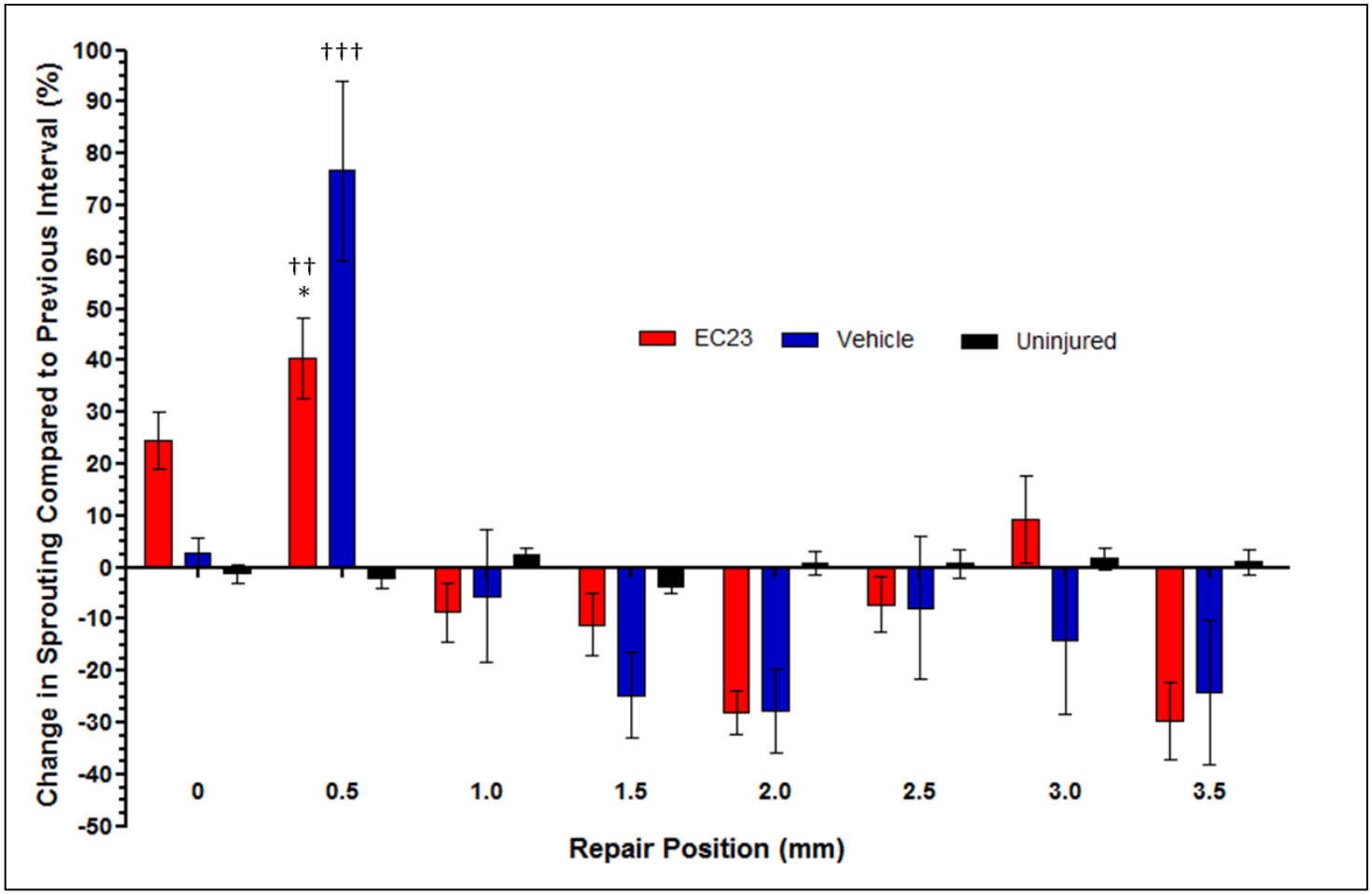

Figure 4.6: Changes in Sprouting index levels at each 0.5mm interval compared to the previous interval; †† and ††† denote significant differences in value compared to uninjured controls, *p*<0.01 and *p*<0.001 respectively; * denotes significant difference in value compared to vehicle treated graft, *p*<0.05. Statistical test: 2-way ANOVA with Bonferroni post-tests.

4.3.4 FUNCTIONAL AXON TRACING

The proportion of unique axons regenerating from the start interval [0.0mm] represented at the 0.5mm interval in the EC23 group was significantly lower than in both the vehicle and uninjured groups [fig.4.7]. Though the proportion of start interval axons represented at subsequent intervals continued to decline, the proportion was not significantly different to that observed in the vehicle group. In both repair groups the proportion of start axons represented at the 1.0mm interval onwards was considered to be significantly lower than the proportions observed for the uninjured group [fig. 4.7].

In both repair groups fewer than 50% of start axons were represented at the 1.5mm interval [49.7% in the EC23 group and 49.4% in the vehicle group] and at the 3.5mm interval the percentage had fallen to 20.3% in the EC23 group and 24.2% in the vehicle group [fig. 4.7].

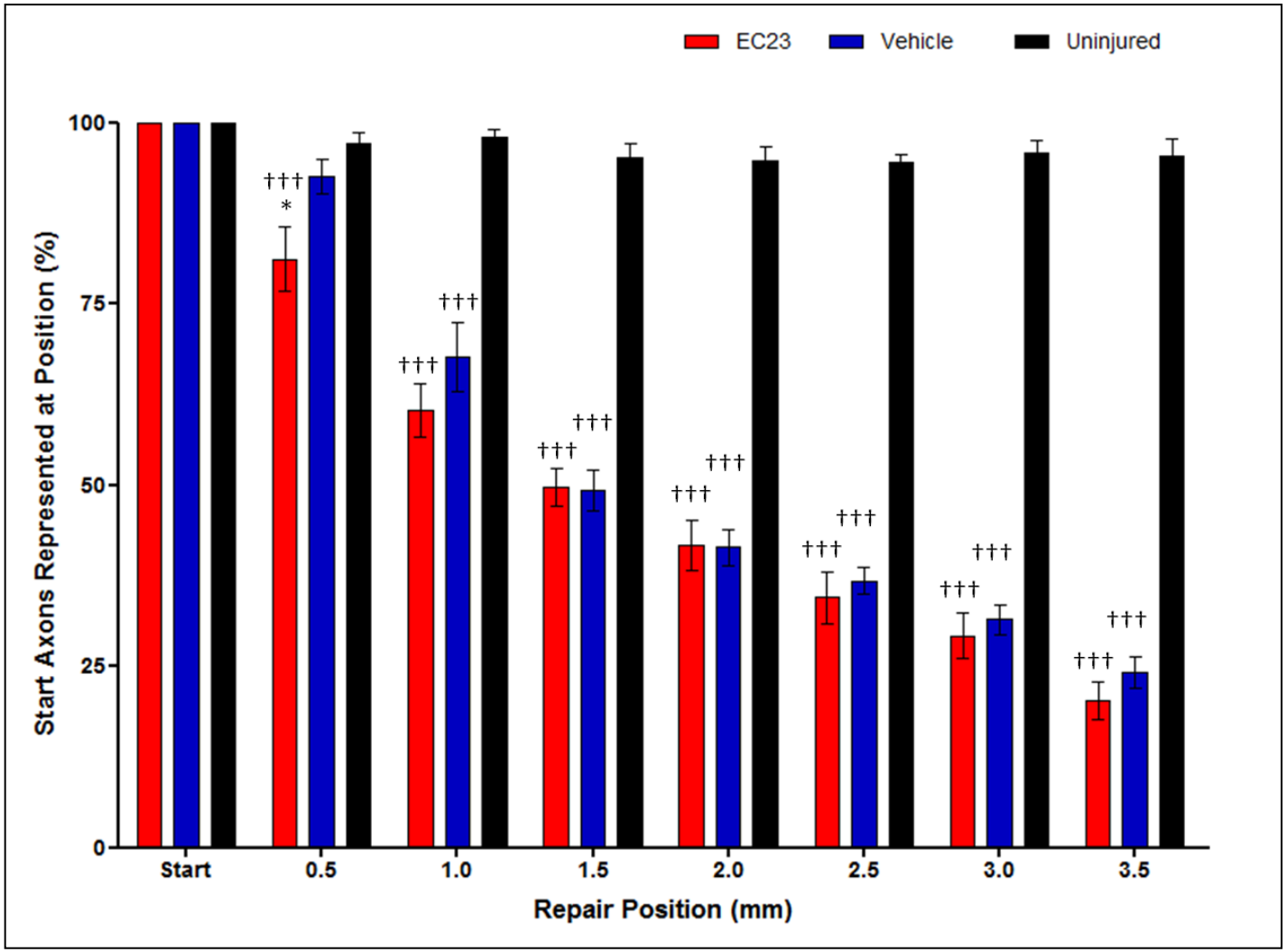

Figure 4.7: Percentages of start axons represented at subsequent 0.5mm intervals; ††† denotes significant difference compared to uninjured controls, $p<0.001$; * denotes significant difference to vehicle group, $p<0.05$. Statistical test: 2-way ANOVA with Bonferroni post-tests.

4.3.5 AXON DISRUPTION

When crossing the initial 1.5mm of the repair there was no significant difference in the increase in average axon length between either repair group, with an average axon length increase of 19.3% [SEM = 2.3] in the EC23 group and 21.0% [2.5] in the vehicle group [fig. 4.8].

Both repair groups were observed to have a significantly greater increase in average axon length compared to the uninjured group, which had a average increase of 2.4% [0.6] in axon length [fig. 4.8].

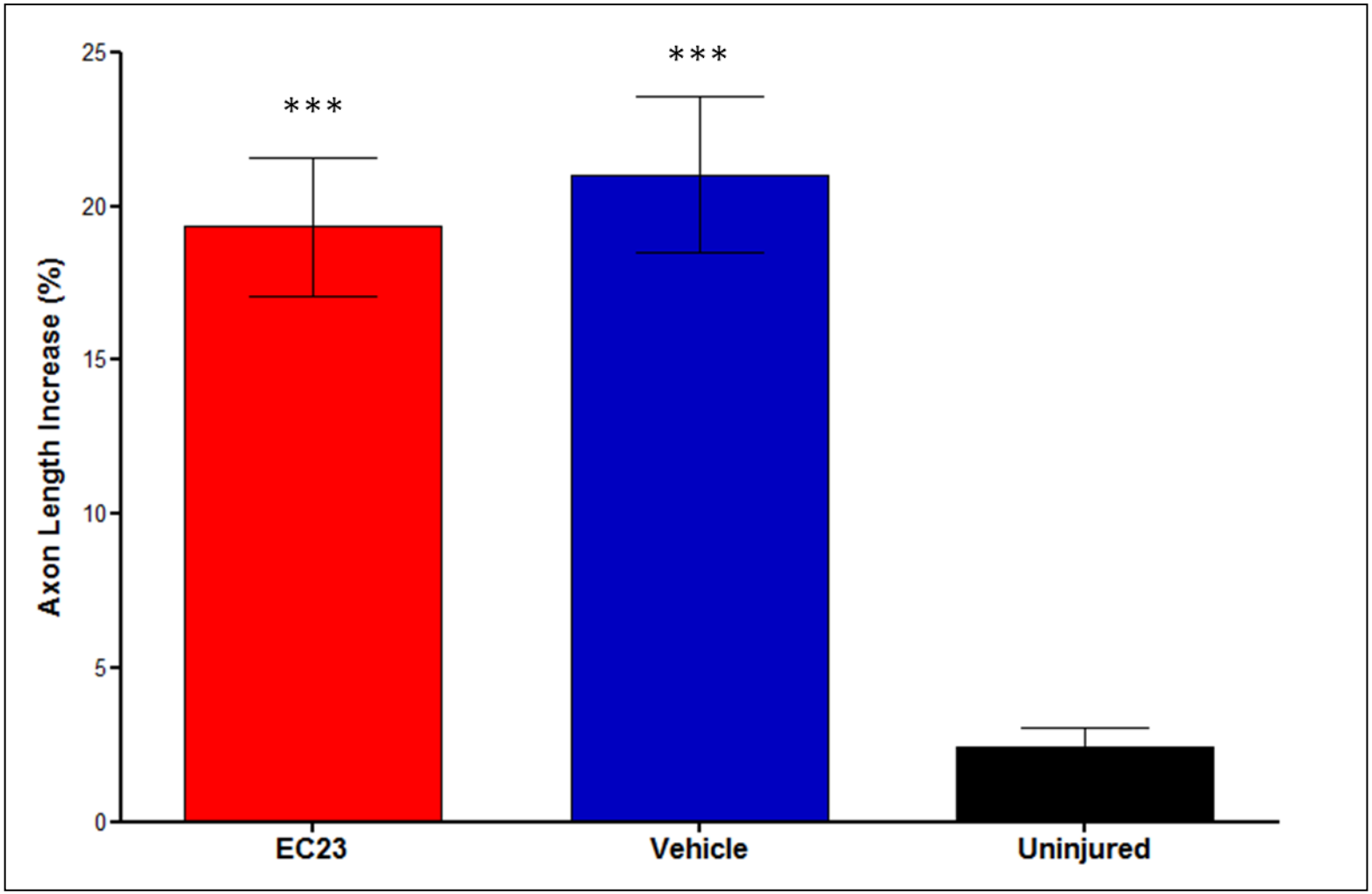

Figure 4.8: Percentage increase in axon length across the initial 1.5mm of repair; * denotes significant difference compared to uninjured controls, *p*<0.001. Statistical test: 1-way ANOVA with Bonferroni post-tests.**

4.4 DISCUSSION

4.4.1 AXON SPROUTING LEVELS THROUGH GRAFT REPAIRS

There was no overall difference between EC23 and vehicle repair groups, either in overall sprouting index levels or at individual intervals. Differences were noted between the two when compared to the uninjured controls [fig. 4.5].

One small difference in sprouting index levels was noted at the 1.5mm interval, where the sprouting index level for EC23 repairs was still considered to be significantly higher than uninjured controls, while in vehicle repairs there was no significant difference compared to uninjured controls [fig. 4.5]. This was reflected in the change in sprouting index results, with the change at 1.5mm smaller - though not significantly - in the EC23 group than in the vehicle group [fig. 4.6].

Based on the previous literature, which suggests that retinoic acid can enhance local levels of cytokines [or their receptors] beneficial for nerve regeneration (Ueno et al., 1993, Wang and Halvorsen, 1998), it had been expected that EC23 - as a synthetic form of retinoic acid - would have enhanced nerve regeneration.

One possible effect of retinoic acid application that would be beneficial in increasing the rate of regeneration would be via its effects on the local level of insulin-like growth factor II [IGF-II]. Treating neuroblastoma cells with concentrations of retinoic acid similar to those used in this study has been shown to increase IGF-II mRNA expression (Ueno et al., 1993).

The potential of IGF-II to increase regeneration rate was shown in a study by Glazner et al. (1993) in which locally applied exogenous IGF-II increased the regeneration rate of sensory axons following sciatic nerve crush injuries in rats. Additional evidence of the ability of IGF-II to increase regeneration speed was provided in a study by Near et al. (1992), in which motor axon regeneration rate was increased following IGF-II treatment of a sciatic nerve crush

injury. In both the Near et al (1992) and Glazner et al. (1993) studies regeneration was inhibited by anti-IGF-II antiserum, further implicating IGF-II as necessary for successful regeneration.

Ciliary neurotrophic factor [CNTF] is a cytokine whose effect on nerve regeneration is increased by retinoic acid in a different manner. Rather than increasing CNTF levels in the local environment, retinoic acid has been shown to increase CNTF receptor α subunit [CNTFRα] mRNA expression in nerve cells - resulting in an increased sensitivity to CNTF (Davis et al., 1993, Wang and Halvorsen, 1998, Weis et al., 1998).

There is a significant body of evidence demonstrating that CNTF has a beneficial effect following nerve injury. Amongst the beneficial effects attributed to CNTF are: promotion of axonal regeneration (Sahenk et al., 1994, Xu et al., 2009); promotion of Schwann cell proliferation, activation and migration (Xu et al., 2009); improved motoneuron survival and enabling of sprouting (Sendtner et al., 1990, Sendtner et al., 1997, Siegel et al., 2000).

Interestingly, while some studies have demonstrated improvements in nerve regeneration with the addition of exogenous CNTF (Sahenk et al., 1994, Xu et al., 2009) others have reported no effect. In a study by Mizisin et al (2004) the effects of CNTF in diabetic mice were examined, with the results of the study indicating that exogenous CNTF could ameliorate the effects of untreated diabetes on both uninjured and injured nerves. In diabetic rats treated with CNTF the outcomes measured indicated at least significant improvement compared to untreated diabetic rats, and in some outcomes - such as regeneration distance - there was no difference when compared to non-diabetic rats (Mizisin et al., 2004). However, non-diabetic rats treated with CNTF did not demonstrate any differences when compared to untreated non-diabetic rats - possibly due to sufficient CNTF being present naturally in those animals for the maximum effect possible to be reached (Mizisin et al., 2004).

The possibility that more CNTF is present in the local environment of regenerating nerves than can be used is also suggested by Sendtner et al. (1997). They state that "one trophic unit of CNTF supports half-maximal survival of responsive neurons in 1ml of cell culture medium" and report that 8191 ±2250 trophic units were present in the sciatic nerve of the *pmn* [progressive motor neuronopathy] mouse strain used in their study, meaning that only a very small amount of the available CNTF needs to be released in order to saturate available receptors.

CNTFRα expression has been shown to increase following nerve injury (Davis et al., 1993, Weis et al., 1998) and in a study by Lee et al. (2013) it was shown to promote both axonal and functional regeneration. Therefore, the reported ability of retinoic acid - and consequently EC23 - to further increase CNTFRα expression (Wang and Halvorsen, 1998) could result in an enhancement of the beneficial impact on nerve regeneration of CNTF.

The sprouting index profile for EC23 repairs indicates that the application of EC23 has no real effect on the number of axons reaching later intervals when compared to vehicle repairs. Although EC23 repairs did maintain a significantly higher sprouting index level compared to uninjured controls for an additional interval than vehicle repairs, the lack of a corresponding increase in unique axons at that interval [see section 4.4.2] indicates that this difference is not functionally important.

4.4.2 FUNCTIONAL AXON TRACING

The percentages of axons from the start of the repair represented at each 0.5mm interval were similar between both repair groups from the 1.0mm interval to the final 3.5mm interval, though at the 0.5mm interval the percentage was significantly lower in EC23 repairs [fig. 4.7].

It had been anticipated that EC23 would increase the rate that axons could regenerate into the repair, thus allowing misdirected axons in EC23 repairs to find a correct pathway into and along the repair quicker than their equivalents in vehicle repairs. This was expected to result in an increase in unique axons at later distal intervals in EC23 repairs compared to vehicle repairs, simply via the action of more unique axons in EC23 repairs managing to navigate their way to those later intervals within the experimental time period.

One potential effect that would have an impact on the percentage of unique axons reaching the 0.5mm interval is the influence of CNTF - the effects of which EC23 may enhance [see section 4.4.1] - on the ratio of motor axons and overall axon numbers. Dubovy et al. (2011) reported that CNTF treatment caused an increase in the number of retrograde labelled motoneurons extending axons into the repair, despite lower overall numbers of axons being observed within the repair. They proposed that the effect was due to selective pruning of sensory axons and earlier pruning of duplicate motor axons (Dubovy et al., 2011), an effect that is beyond the scope of this study to measure.

As the difference between unique axon percentages is negligible at the remaining intervals it would appear that the additional axons lost at the 0.5mm interval in EC23 repairs were also lost shortly afterwards in vehicle repairs [fig. 4.7]. This would appear to support the possibility that redundant axons were pruned sooner in EC23 repairs - perhaps as a result of sibling branches reaching distal endoneurial tubes and related trophic support quicker, or as a response to axons - that were later pruned - entering the incorrect type of endoneurial tube [i.e. motor to sensory/sensory to motor] and losing trophic support.

4.4.3 INITIAL AXON DISRUPTION AT GRAFT ENTRY

The increase in axon length over the initial proportion of the repair [0.0mm - 1.5mm] was similar in both repair groups, with the increase EC23 repairs only approximately 4% less than vehicle repairs [fig. 4.2]. Axon length in both repair groups was significantly increased compared to uninjured controls over the same distance [fig. 4.8].

It had been anticipated that EC23 would have a beneficial effect upon this early disruption through a reduction in levels of scar tissue at the join between central nerve ending and graft. This hypothesis was based on the evidence that retinoic acid can reduce local levels of the inflammatory cytokine TNF-α (Motomura et al., 1996, Wang et al., 2007) - with reductions in local inflammation linked to reduced intraneural scarring (Atkins et al., 2007) - and also reduce scarring in dermal tissues via reductions in fibroblast proliferation and collagen production (Daly and Weston, 1986, Ogawa et al., 1998).

However there is some contrasting evidence suggesting a role for retinoic acid in the increase of collagen production. Much of this evidence is related to studies on photo damaged skin in rodents and humans, in which retinoic acid was used to reduce surface wrinkles (Chen et al., 1992, Griffiths et al., 1993, Personelle et al., 1997, Bhawan, 1998).

4.4.4 CONCLUSIONS

In this study there were no strong indications that the application of EC23 improves the regeneration of peripheral nerves following graft repair. In 2004, Taha et al. reported the results of a study where retinoic acid was directly applied to repaired rat tibial nerves, with the conclusion that retinoic acid stimulated regeneration. However, their conclusion was drawn from results showing only a greater distal axon density in treated rat tibial nerve repairs without any improvement in functional recovery. It is therefore possible that the increased axon density that Taha et al. (2004) observed could have been a result of a larger

percentage of duplicated axon sprouts being present in the retinoic acid treated repairs at the point they used for their measurements.

The lack of prior data for both EC23 and retinoic acid in terms of direct, local application to a nerve injury made it difficult to determine an appropriate concentration for the EC23 dose within the study presented in this chapter. As discussed earlier [see section 4.1], at the time of writing only one study had been published where retinoic acid was directly applied at the site of a nerve injury in a rodent model (Taha et al., 2004) and it was from that study that the concentration of EC23 used in the present study [10^{-8} mol/L] was derived. However, it is possible - given the potential doubts over the conclusion reached by Taha et al. (2004) - that the concentration of EC23 used was not optimal for improved nerve regeneration to take place.

Alternatively, as EC23 has been shown to possess increased potency at similar concentrations to retinoic acid (Christie et al., 2010), - and the effects retinoic acid are dose-dependent [see section 4.1] - it may be that the concentration used in the presented study was sufficient to trigger a different, adverse response in some local cell types that negated any remaining beneficial effects of the treatment.

Finally, as retinoic acid acts within the cell nucleus (Maden and Hind, 2003), most of its effectiveness when applied locally will come from interactions with Schwann cells, fibroblasts and macrophages rather than the centrally located neurons. As retinoic acid applied systemically - via an oral dose - has been shown to accelerate functional recovery of injured nerves (Yee and Rawson, 2000) but local application did not demonstrate any effect on functional recovery (Taha et al., 2004) it is possible that a greater effect could have been observed administering EC23 systemically.

In conclusion, EC23 had no overall significant effects - beneficial or adverse - on nerve regeneration in YFP-H mice in terms of the outcomes measured within this particular study.

5.0 PERFORMANCE OF MICRO-STEREOLITHOGRAPHY CONDUITS IN VIVO

5.1 INTRODUCTION

As discussed in chapter 1 [see section 1.6.3], artificial nerve guide conduits are a potential alternative to nerve graft repairs. If conduits can be produced that equal the performance of nerve grafts over any distance in any nerve, they would likely become the "gold standard" repair for bridging nerve defects as they do not require the sacrifice of a donor nerve and thus avoid the associated potential complications.

A large variety of different materials have been trialled in nerve guide studies with varying levels of success. The main difference in material choices is whether they are natural, such as collagen (Archibald et al., 1991, Li et al., 1992, Archibald et al., 1995, Kitahara et al., 2000, Waitayawinyu et al., 2007, Farole and Jamal, 2008), or synthetic polymer based (Henry et al., 1985, Hurtado et al., 1987, Kiyotani et al., 1996, Matsumoto et al., 2000, Waitayawinyu et al., 2007).

5.1.1. CURRENT NERVE GUIDE CONDUITS IN ANIMAL STUDIES

Three of the currently approved nerve guide conduits are produced using type-1 collagen - Neuromatrix™, Neuro*flex*™ and NeuroGen®. Despite these three collagen conduits being approved for clinical use, only NeuroGen® conduits have featured in published animal or clinical studies. One early study (Archibald et al., 1991) compared NeuroGen® conduits to both direct suture and graft repairs in rat and *Macaca fascicularis* monkeys. The results of that study found no overall difference between conduit, graft or direct suture repairs in either animal model used at 12-weeks post-repair, though direct suture repairs were significantly better in rats at 4-weeks post-repair. A second study by Archibald et al. (1995) using a larger

cohort of *Macaca fascicularis* monkeys, over a longer period of time [42 months] also reported similar recoveries in the collagen conduits to graft and direct suture repairs. Interestingly, direct suture repairs displayed slower rates of recovery than conduit and graft repairs - indicating that even the small amount of tension in the repair of a 5mm gap can be detrimental to nerve regeneration.

A more recent study (Waitayawinyu et al., 2007) compared NeuroGen® conduits to both graft and polyglycolic acid [PGA] Neurotube® conduits. The results of the study by Waitayawinyu et al. (2007) indicated that there was little difference between regeneration when either grafts or NeuroGen® conduits were used to repair sciatic nerve injuries in rats. However, the results did indicate that the Neurotube® conduits performed significantly worse than both graft and NeuroGen® conduit repairs, with significantly lower axon counts, maximal muscle contraction and muscle weight recorded following Neurotube® conduit repairs.

5.1.2. CURRENT NERVE GUIDE CONDUITS IN CLINICAL STUDIES

The critical step for most conduit designs is the one from animal to human studies; if the in vivo results do not translate into clinical performance or conduits cannot be manufactured to the standards required clinically then they will fail to make the step up.

Neurotube® conduits have been used successfully in a number of clinical studies (Weber et al., 2000, Rinker and Liau, 2011, Mundinger et al., 2012) and a review by Meek and Coert (2008) concluded that the Neurotube® conduit should be the preferred choice over the three alternative FDA/CE approved conduits at the time of publishing [NeuroGen®, Neuro*Flex*™, Neurolac]. Their conclusion was based on the quantity and quality of clinical data available for each conduit as well as the available sizes and prices of the conduits.

A randomised prospective study comparing Neurotube® conduit repairs of the digital nerves against standard repairs [end-to-end suture or graft, depending upon nerve defect size]

found the conduits to perform better than standard repairs in certain circumstances (Weber et al., 2000). When nerve defects were 4mm or less, repairs that used Neurotube® conduits resulted in significantly better moving 2-point discrimination and sensory return grades than standard end-to-end suturing repairs. When used in repairing defects of 8mm or longer, Neurotube® conduits again fared significantly better in moving 2-point discrimination than the standard autograft repairs with a higher - though not quite significant - percentage of repairs considered to have excellent sensory return.

Another randomised prospective study on digital nerves compared Neurotube® conduits to autogenous vein conduits and found no significant differences between either treatment, though two Neurotube® conduit repairs did require reoperation following extrusion of the nerve endings (Rinker and Liau, 2011). A small study by Mundinger et al. (2012) on the repair of the inferior alveolar nerve with Neurotube® conduits found that all patients experienced a reduction in pain levels, with varying levels of sensory recovery - a prior, single participant study also reported reduction in pain levels along with excellent sensory recovery (Crawley and Dellon, 1992).

5.1.3. FUTURE NERVE GUIDE CONDUITS

Currently, all clinically approved conduits are simple, hollow tubes that are sufficient for use in repairing relatively short nerve defects. Work on the next generation of nerve guide conduits is focussed on extending the repair length possible when using conduits, with a range of passive and active ideas being trialled. Passive ideas focus on the physical structure of the conduits, providing physically supportive environments for both regenerating axons and support cells, while active ideas look at incorporating cells, neurotrophic factors and matrix proteins within the conduits that will have a therapeutic influence on nerve regeneration.

5.1.3.1 Physical Structure and Guidance.

One idea being investigated is the addition of intraluminal structures to provide physical support for regenerating axons and niches for migrating support cells to reside within. A study by Kim et al. (2008) demonstrated the potential benefit of topographical cues within conduits by producing hollow polymer conduits from rolled up sheets of aligned or random fibres and using them in repairs of rat tibial nerve injuries. In their study, Kim et al. (2008) found that the conduits produced from aligned fibre sheets performed similarly to nerve grafts over a 17mm defect in a number of outcomes, whilst the random fibre conduits performed significantly worse. Although fewer axons and Schwann cells were identified across the length of the conduit repair than across the length of the graft, functional recovery was similar in both repairs and the difference in the percentage of axons successfully reaching target tissue was minimal [45% in aligned fibre conduits compared to 55% in graft repairs].

A study conducted by Yao et al. (2010b) using rat sciatic nerves compared multi-lumen collagen conduits containing either 1-, 2-, 4- or 7-channels to both graft and NeuroGen® conduit repairs. Overall the performance of all conduits trialled within the study by Yao et al. (2010b) was poor when compared to the graft repairs across most outcomes reported. The NeuroGen® conduits performed worst with regards to myelinated fibre size, density and thickness, while 2-channel conduits (which performed best with regards to myelinated fibre density) and 7-channel conduits were worst when comparing myelinated fibre number and compound muscle action potentials respectively. Yao et al. (2010b) concluded by suggesting that their 4-channel conduit was the best of those trialled; however, given the relatively poor results for all the conduits in that study when compared to grafts, simply adding a number of channels to conduits is unlikely to improve the clinical outcomes of nerve repair when using conduits.

5.1.3.2 Addition of Supportive Factors and Cells.

More active approaches to improving conduit performance centre around the addition of supportive cells [Schwann cells/various stem cells], or individual trophic/tropic factors, or matrix proteins. Coating structural elements of conduits with proteins found in the extra-cellular matrix has the benefit of providing regenerating axons and support cells with a more biological surface than the inert conduit material alone.

Collagen and laminin are two proteins to have been used in this manner, with both having been shown to have beneficial effects on in vitro neurite growth and cell adhesion (Rangappa et al., 2000, Deister et al., 2007, Swindle-Reilly et al., 2012, Volkenstein et al., 2012). This is supported through my own unpublished observations, obtained during my final year undergraduate project at the University of Aston, in which neuroblastoma cells cultured on collagen coated tissue culture plastic displayed a flattened morphology [indicating better adhesion] and increased neurite outgrowth compared to cells cultured on uncoated plastic [fig. 5.1].

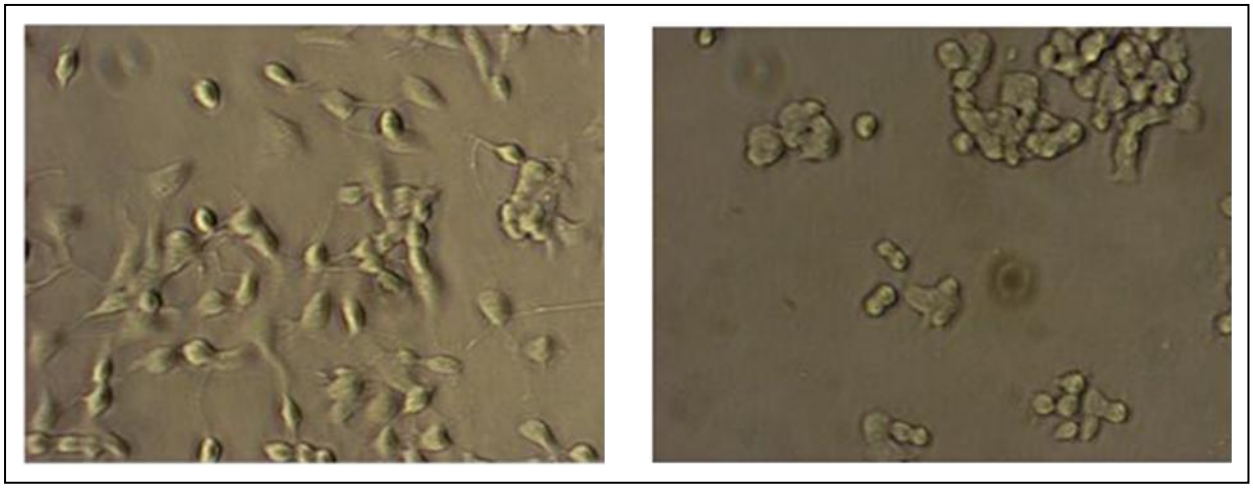

Figure 5.1: SH-SY5Y neuroblastoma cells cultured on collagen coated coverslip [left] and uncoated coverslip [right] - cells cultured on collagen show increased adhesion and neurite outgrowth (Harding, 2010. Unpublished observations).

Studies by two separate groups in Japan have investigated the performance of collagen based conduits containing laminin-coated collagen fibres, one using rats (Tong et al., 1994)

and the other using dogs [beagles] (Matsumoto et al., 2000). The earlier study by Tong et al (1994) reported good results in the conduit group compared to standard grafts over a 10mm sciatic nerve defect, with seemingly faster regeneration during the initial 30-days post-repair. The study by Matsumoto et al. (2000) reported regeneration across an 80mm peroneal nerve defect using similar conduits to Tong et al.(1994); however, the lack of a graft control to compare the conduit regeneration to in the study by Matsumoto et al (2000) limits their study to demonstrating that regeneration through conduits can take place over such long distances.

A common method used for adding cells or individual factors is to fill conduits with a gel containing various support factors and/or cells. A benefit of this method is that although most studies using it do so with simple, single lumen conduits, it is quite easy to move into more complex conduit designs at a later point. Indeed, there is wisdom in making sure that a specific composition of gel works as well as possible using simple conduits to minimise any confounding factors that may arise when using complex conduits.

A recent study by Nie et al. (2014) used a single lumen chitosan/gelatin-based conduit filled with a Schwann cell and TGF-β seeded collagen gel to repair 10mm rat sciatic nerve defects. The results of the study by Nie et al. (2014) indicated that chitosan/gelatin-based conduits containing the Schwann cell/TGF-β seeded gel performed equally well as autograft repairs for the outcome measures used (histological/electrophysiological/walking track analysis). The performance of the gel filled conduits was also considered to be significantly better than empty chitosan/gelatin-based conduits.

The addition of Schwann cells to conduits is an established theme in nerve guide studies, with many different approaches to their inclusion having been investigated over the last two decades (Kim et al., 1994, Ansselin et al., 1997, Hadlock et al., 2000, Mosahebi et al., 2002, Ao et al., 2011).

The seeding of a gel with Schwann cells is a commonly used solution for including them within a conduit (Mosahebi et al., 2002, Ao et al., 2011, Nie et al., 2014), most likely due to its simplicity and that the Schwann cell seeded gel can be prepared immediately prior to implantation - limiting the amount of time the Schwann cells spend between culture conditions and in vivo implantation. Another advantage of gels is that - provided they are sufficiently viscous - they can be used with porous conduits that allow the exchange of signalling factors between the external environment and interior of the conduit. An alternative method, used in some early nerve guide studies, was to fill conduits with a suspension of Schwann cells and seal both ends of the conduit to prevent leakage (Ansselin et al., 1997).

5.1.3.3 New Methods of Manufacture.

There are almost as many different methods of manufacturing conduits as there are types of conduit, with new techniques being developed continually. A full discussion on the different techniques used in conduit manufacture can be found in section 6.1.1, while this section will deal with the materials and techniques utilised for producing the conduits used within this specific study.

All conduits used within this study were manufactured using a micro-stereolithography [µSL] technique developed by the laboratories of Professor John Haycock and Dr. Frederik Claeyssens. To produce a conduit using their µSL technique, a bitmap image [created using Microsoft Paint] was used to set a digital micro-mirror device to project a laser beam in the desired shape - i.e. a hollow circle. Once the laser beam was projected through the digital micro-mirror device it was expanded and directed into a pre-polymer solution through the lens and mirror assembly, initially curing the pre-polymer solution at the point where the z-axis stage was located [fig. 5.2]. The z-axis stage then proceeded to descend at a rate of 0.01mm/s, moving the cured pre-polymer layer away from the laser beam and allowing subsequent layers to form. Once the desired length of conduit was achieved and the final layer had been given time to cure the conduit was immersed in denatured alcohol for 72

hours in order to ensure the removal of any remaining photo-initiator or non-cured pre-polymer. Conduits were sterilised via UV irradiation prior to implantation.

Initial work with this technique used a pre-polymer based on polyethylene-glycol [PEG], which was first tested in vitro by culturing NG108-15 [neuroblastoma/glioma hybrid] neuronal cells on coated glass coverslips and was found to enable similar cell morphology to uncoated coverslips (Pateman et al., 2014c). Prior to in vivo studies with µSL conduits, in vitro testing using excised rat dorsal root ganglia was conducted using µSL produced PEG channels to ensure that no toxic effects occurred following the µSL manufacturing process (Pateman et al., 2014c). These processes were later repeated using a poly-caprolactone pre-polymer (Pateman et al., 2014a).

The choice of µSL as a conduit manufacturing technique was made due to a number of beneficial properties of the technique. Firstly, the ability of the technique to create intricate microstructures (Choi et al., 2006) may allow guidance channels or cell niches to be incorporated within future conduits. The potential wide range of fabrication materials and possibility for scaling up the technique for mass production through automation of processes were also factors in choosing µSL (Pateman et al., 2014c).

The choice of conduit material [i.e. PEG and PCL] was based on two factors; the primary factor was the ability at the time to manufacture conduits using the µSL process, with a secondary important factor relating to the biological suitability of materials. Both PEG and PCL are already FDA approved for certain uses (Choi et al., 1998, Bender et al., 2004), which could prove beneficial if conduits of either material were later considered to have the potential to be used in clinical trials. Both PEG and PCL have been used previously in successful in vitro and in vivo conduit studies, supporting their suitability as conduit materials (Madison et al., 1985, DenDunnen et al., 1996, Goraltchouk et al., 2005, Chiono et al., 2008, Chang, 2009a, b)

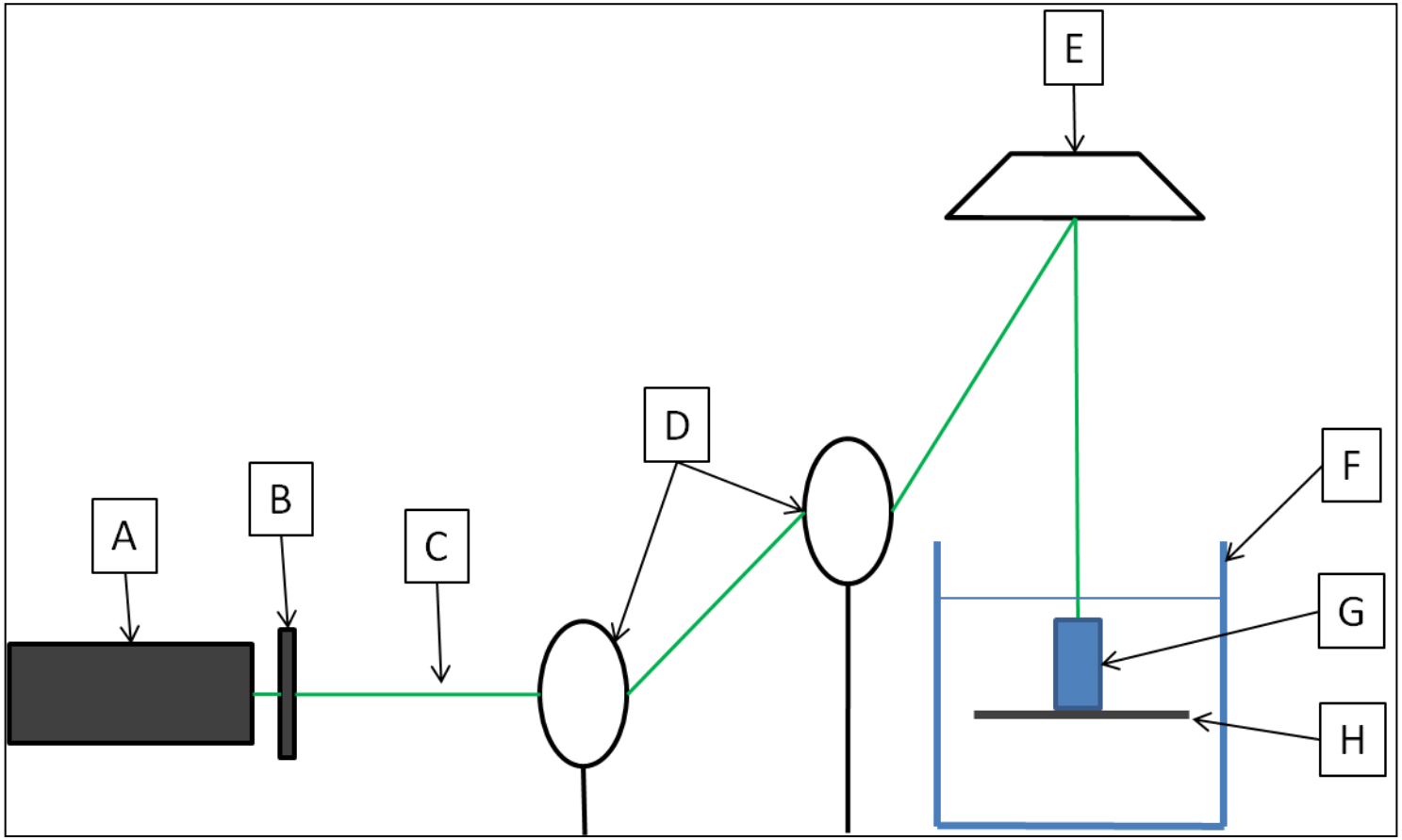

Figure 5.2: Diagram depicting micro-stereolithography setup. A: 405nm laser source; B: digital micromirror device; C: laser beam; D: focusing lenses; E: focusing mirror; F: glass vial containing pre-polymer solution of polyethylene-glycol; G: conduit; H: z-axis stage.

5.1.4 AIM OF THIS STUDY

The aim of the study reported in this chapter was to determine the ability of µSL conduits to support in vivo nerve regeneration. This study reports on the performance of three different designs of conduit:

1. Hollow PEG conduits.
2. Hollow PCL conduits.
3. PEG conduits filled with aligned electrospun PCL fibres.

Both designs of hollow conduit - differing only in material selection - were expected to display similar levels of performance to each other, while their performance compared to graft repairs was expected to be marginally worse. The reasoning for this expectation was that, while regeneration within hollow conduits would lack the innate structural and biological support found in graft repairs, the gap being bridged was relatively short - and previous studies have demonstrated the potential for hollow conduits to successfully bridge short gaps (Lundborg et al., 1997, Dahlin et al., 2001, Lundborg et al., 2004).

The fibre filled PEG conduits were expected to improve upon the performance levels observed in hollow conduits and rival the performance of graft repairs. The expectation was that the physical support of the aligned fibres would better help the guidance of regenerating axons across the repair.

5.2 MATERIALS AND METHODS

General materials and methods are detailed in chapter 2, more specific information related to the experiments discussed within this chapter is detailed below.

5.2.1 MICRO-STEREOLITHOGRAPHY PRODUCED CONDUITS

All conduits produced using micro-stereolithography [µSL] were provided by the laboratories of Professor John Haycock and Dr. Frederik Claeyssens [Kroto Research Institute, University of Sheffield, UK]. All µSL conduits used in the study discussed here measured 5mm long with an internal diameter of 1.0mm and a wall thickness of 0.25mm [giving a 1.5mm outside diameter].

The µSL conduits were made from a pre-polymer solution of either polyethylene-glycol or poly-caprolactone [Sigma Aldrich, UK].

The µSL setup consisted of a 405nm tunable laser source set to 5mW [Vortran Laser Technology Inc, CA, USA], a digital micro-mirror device [Texas Instruments Inc, TX, USA], a lens and mirror assembly [Thorlabs Ltd, Cambridgeshire, UK], and a motorised z-axis stage [Thorlabs Ltd, Cambridgeshire, UK].

Electrospun aligned poly-caprolactone fibres measuring 5µm in diameter were used in one set of conduits to improve axon guidance through the conduits. These electrospun fibres were produced using the methods previously described by Daud et al. (2012) which also refer to work performed by Wang et al. (2009). Briefly, a syringe with blunt needle and filled with poly-caprolactone dissolved in dichloromethane was connected to a syringe pump, with the needle connected to a high voltage power supply. A collector, consisting of aluminium foil wrapped around a grounded rotating drum was rotated at 2200rpm in order to collect produced fibres. When the syringe plunger is depressed, the poly-caprolactone forms into fibres which are collected by the rotating drum [fig. 5.3].

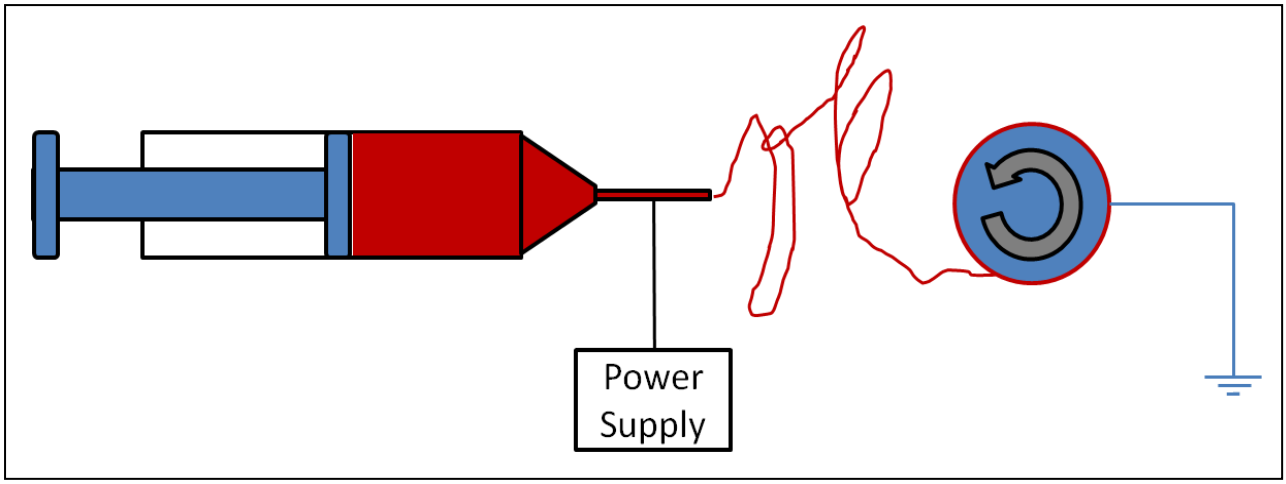

Figure 5.3: Depiction of electrospinning process.

5.2.2 SURGICAL PROCEDURES

For conduit repairs YFP-H mice were anaesthetised and the CF nerve exposed and a 3mm gap between central and distal nerve endings created [see 2.2.1 and 2.2.3 for full details]. The selected conduit was then used to repair the gap, with the nerve endings and conduit fixed in place using fibrin glue. Animals were allowed to recover for 3-weeks to allow regenerating nerve tissue in conduits to gain sufficient strength to survive harvesting [see section 2.2.4].

To obtain graft tissue, WT mice were anaesthetised and the CF nerve exposed, freed from surrounding tissue [see sections 2.2.2 and 2.2.3] and then covered with the muscle to prevent it from drying out prior to transplanting into a YFP-H mouse.

YFP-H mice were then anaesthetised and the CF nerve exposed and a 3mm gap between central and distal nerve endings created [see section 2.2.1 and 2.2.3]. Graft tissue was then obtained from the prepared WT mouse and used to repair the YFP-H mouse CF nerve [see section 2.2.3]. The WT mice were culled once graft tissue was obtained and the YFP-H mice allowed to recover for 3-weeks.

Following the recovery period, mice were anaesthetised [see section 2.2.2], the CF nerve re-exposed, harvested and prepared for image analysis [see section 2.2.5].

5.2.3 ANIMAL NUMBERS AND GROUPINGS

A total of 37 mice were used specifically for the in the experiments described in this chapter, with equal numbers of YFP-H and WT mice used in graft repairs and only YFP-H mice used in conduit repairs. Reused images from the M6P study [see chapter 3] provided data for the uninjured group [n=7] bringing the total number to 44 mice. Those images were completely reanalysed to take into account the increased repair length used in the studies discussed here and in chapter 6.

The groups for this chapter were: uninjured [n=7], graft [n=7 YFP-H and 7 WT to provide graft tissue], hollow polyethylene-glycol conduits [n=7], electrospun fibre filled polyethylene-glycol conduits [n=6, see section 5.3] and hollow poly-caprolactone conduits [n=7].

Two additional YFP-H mice were used in the fibre filled conduits group as early experiments revealed extremely poor regeneration [fig. 5.10] and it was decided that further experiments with the conduit in its original form were not viable. A change in the fibre packing density [50% reduction] was made and a pre-soaking of the fibres in Ringer's solution prior to implanting was performed in order to improve the performance of the fibre conduits.

5.2.4 SAMPLE SIZE CALCULATIONS

The sample sizes for this study were calculated using PiFace software [v1.76: *homepage.stat.uiowa.edu/~rlenth/Power*] with standard deviation data obtained from the M6P study discussed in the chapter 3.

5.2.4.1 Sample Size Choice and Justification.

The sample size chosen for the studies discussed within this chapter was n=7, which would be sufficient to detect differences between groups of 27.13%, 9.54% and 8.86% for sprouting index [fig. 5.4], functional axon tracing [fig. 5.5] and axon disruption [fig. 5.6] respectively. For justification see section 4.2.3.1.

5.2.4.2 Sample Size Calculation Results.

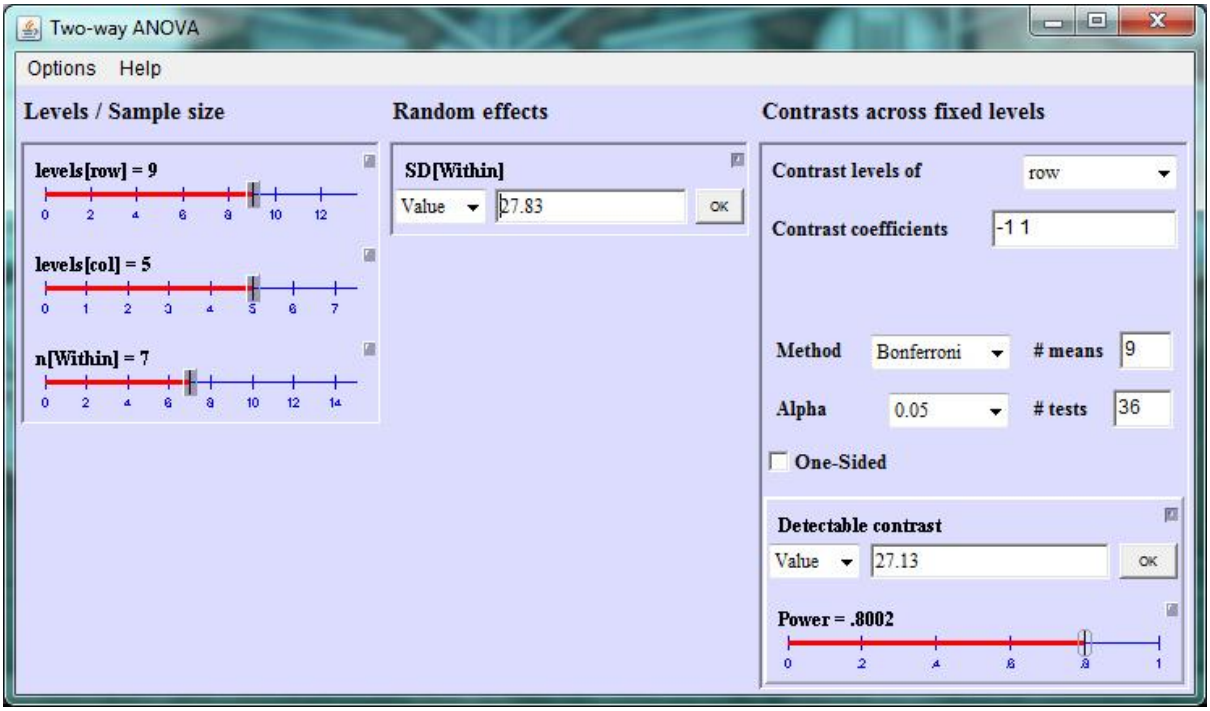

Figure 5.4: Sprouting index analysis power and detectable difference results for µSL conduit study when using a sample size of n=7. Levels[row] = number of intervals; levels[col] = number of groups; n[Within] = sample size; SD[Within] = standard deviation value derived from M6P study results. Number of intervals [# means] multiplied by number of repair groups minus one gives the number of t-tests required for the Bonferroni post-tests [# tests].

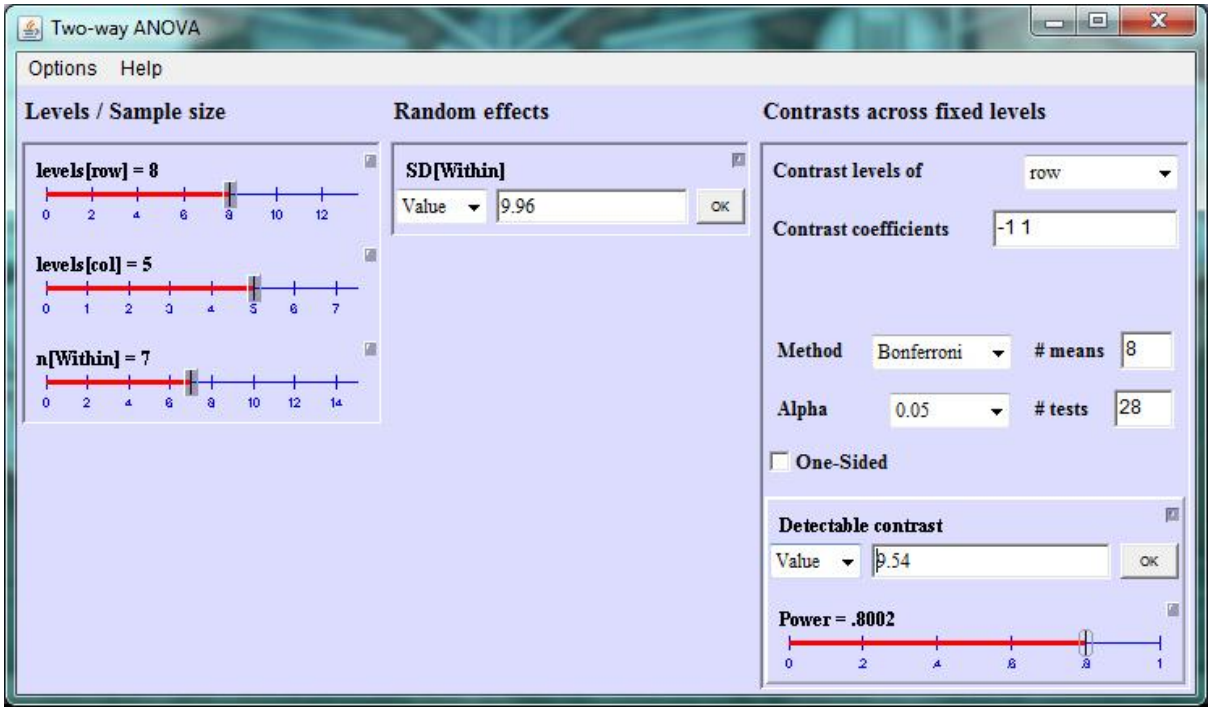

Figure 5.5: Functional axon tracing analysis power and detectable difference results for μSL conduit study when using a sample size of n=7.

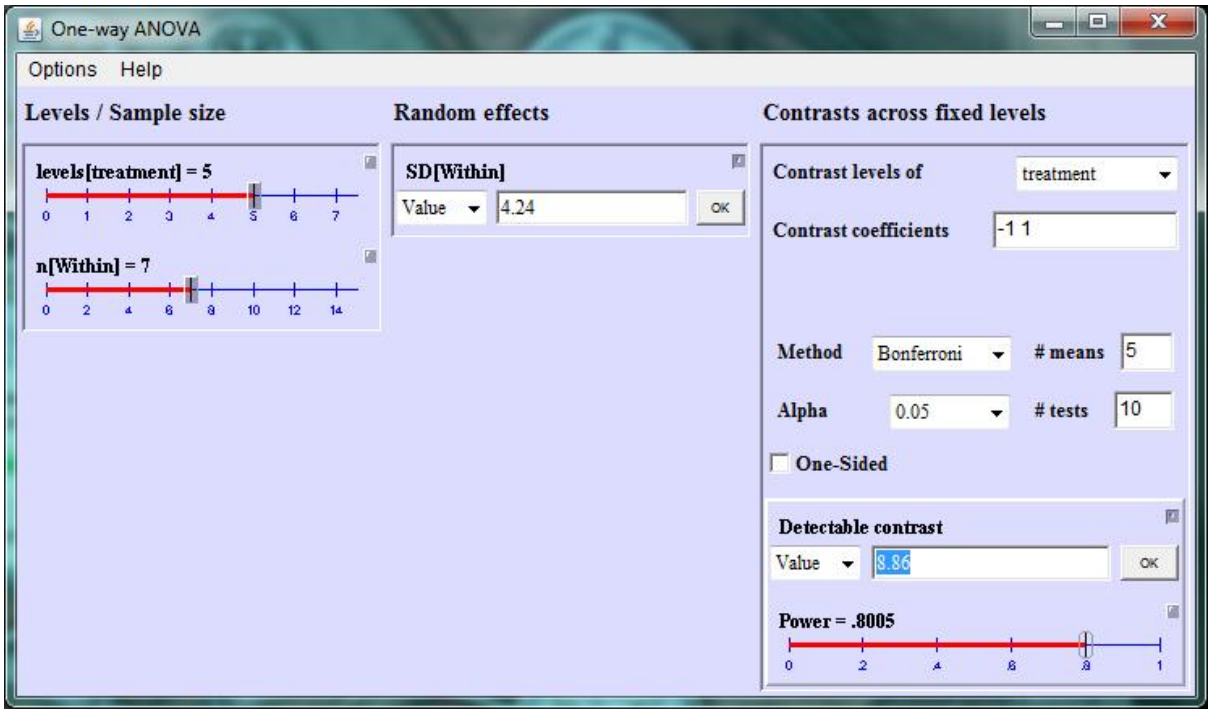

Figure 5.6: Axon disruption analysis power and detectable difference results for μSL conduit study when using a sample size of n=7. Levels[treatment] = number of groups.

5.2.5 STATISTICAL ANALYSIS

Statistical analysis of the results described in this chapter was carried out as stated in section 2.3.3. All sprouting index and functional axon tracing results used 2-way ANOVA with Bonferroni post-tests; axon disruption results used a 1-way ANOVA with Bonferroni post-tests. Differences were considered to be significant when $p<0.05$.

5.3 RESULTS

All animals recovered well following surgery with no signs of infection or autotomy. However, one fibre filled polyethylene-glycol conduit was found to have become dislodged at the central nerve ending during the recovery period and as a result was excluded from the results.

5.3.1 QUALITATIVE DIFFERENCES BETWEEN GROUPS

Axons in uninjured nerves tended to run almost parallel through the excised section with no notable increases or decreases in overall numbers [fig. 5.7]. In graft repairs there were two areas of disruption at the joins between the transected nerve endings and graft tissue, though axons within the graft were similarly organised to those in the uninjured nerves [fig. 5.8].

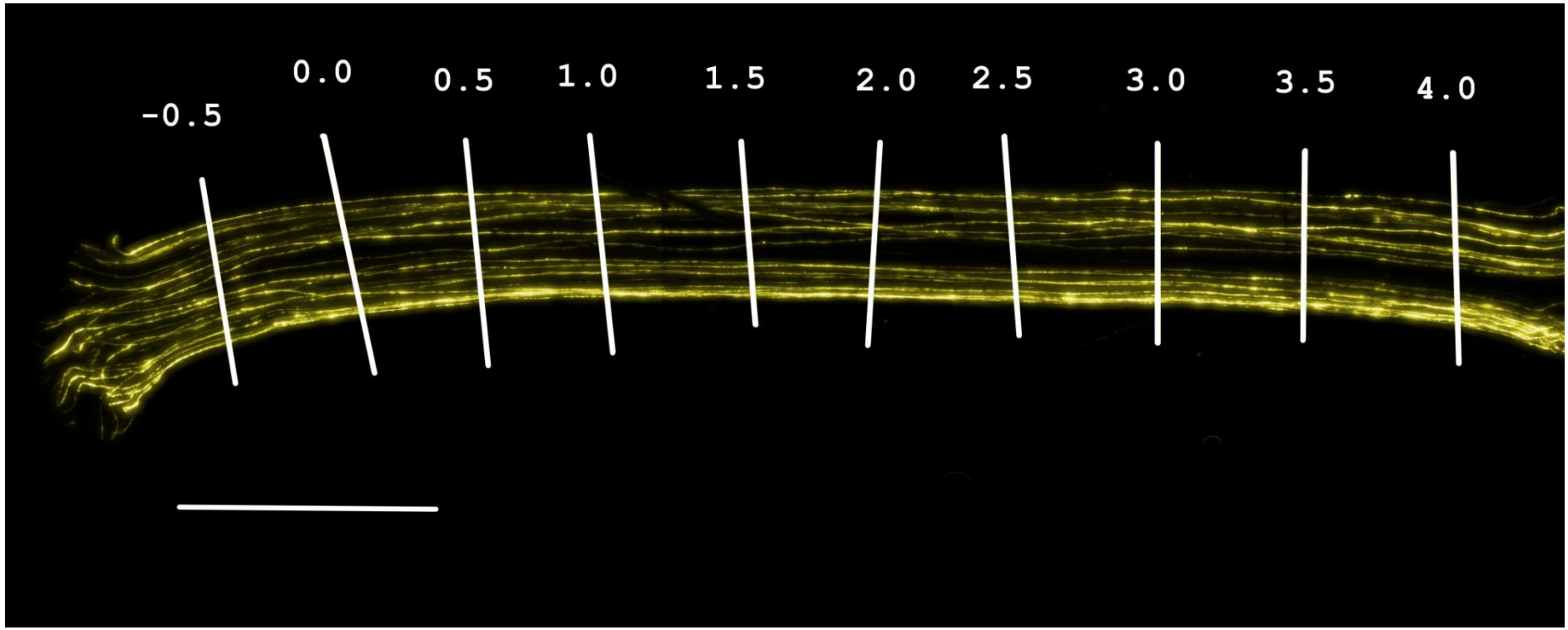

Figure 5.7: Typical uninjured nerve image with intervals marked. Scale bar = 1.0mm.

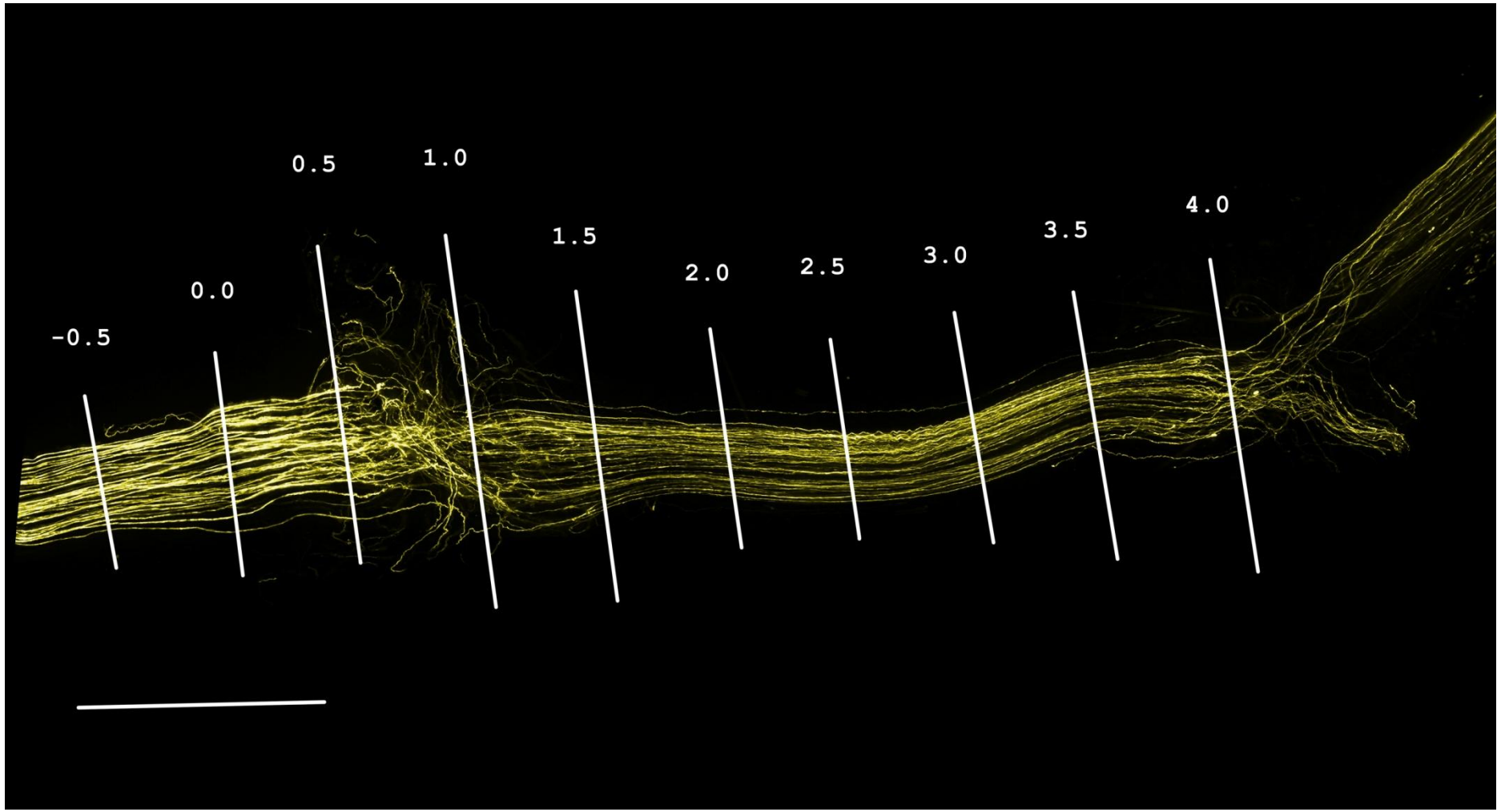

Figure 5.8: Typical graft repaired nerve image with intervals marked. Scale bar = 1.0mm.

5.3.1.1 Hollow Polyethylene-glycol Conduits.

Images obtained for hollow polyethylene-glycol [hPEG] conduits were quite varied in appearance. Typically axons became disrupted and disorganised upon regenerating out from the transected central nerve ending in a similar manner to that observed in graft repairs [figs. 5.8 and 5.9]. However, unlike in graft repairs, a large level of disorganisation remained in hPEG conduit repairs through the repair until the axons re-entered the distal nerve ending [fig. 5.9].

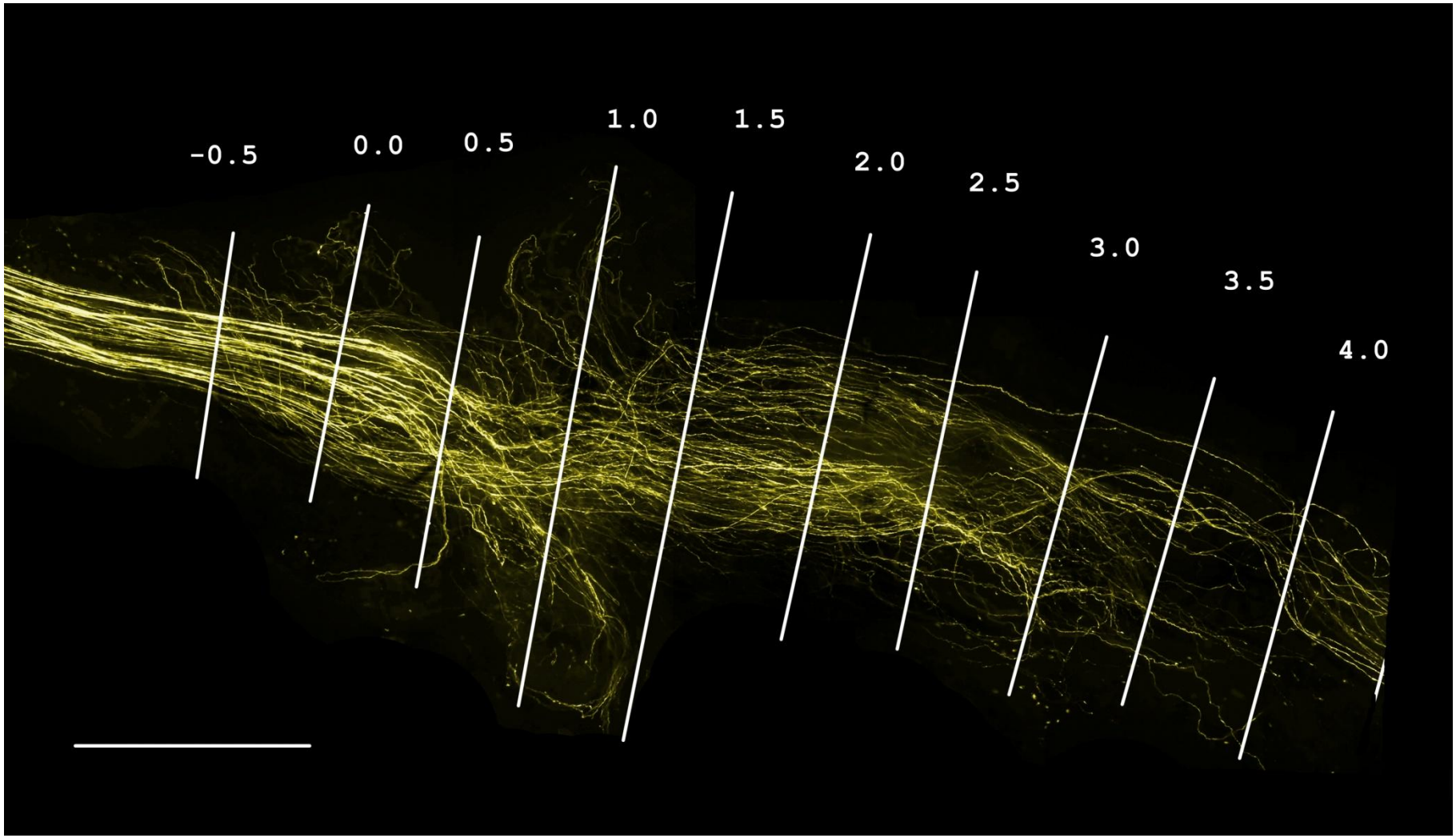

Figure 5.9: Typical hollow PEG conduit repaired nerve image with intervals traced. Scale bar = 1.0mm.

5.3.1.2 Electrospun Fibre Filled Polyethylene-glycol Conduits.

Initial repairs using fibre filled polyethylene-glycol [fPEG] conduits demonstrated no signs of successful regeneration, with few axons even appearing to enter the aligned fibres [fig. 5.10].

Following alterations to the fibre density and efforts to pre-soak the aligned fibres with Ringer's solution immediately prior to implantation regeneration appeared to improve to some degree, though in typical repairs no axons managed to regenerate through to the distal nerve ending [fig. 5.11]. A great deal of variation between repairs was noted and can clearly be demonstrated by comparing a more typical repair image [fig. 5.11] to that of the best performing repair, in which axons successfully regenerated to the distal nerve ending in large numbers [fig. 5.12]. This variation was also apparent from the large SEM values for most quantitative results in the fPEG group [table 4, figs. 5.14 to 5.16].

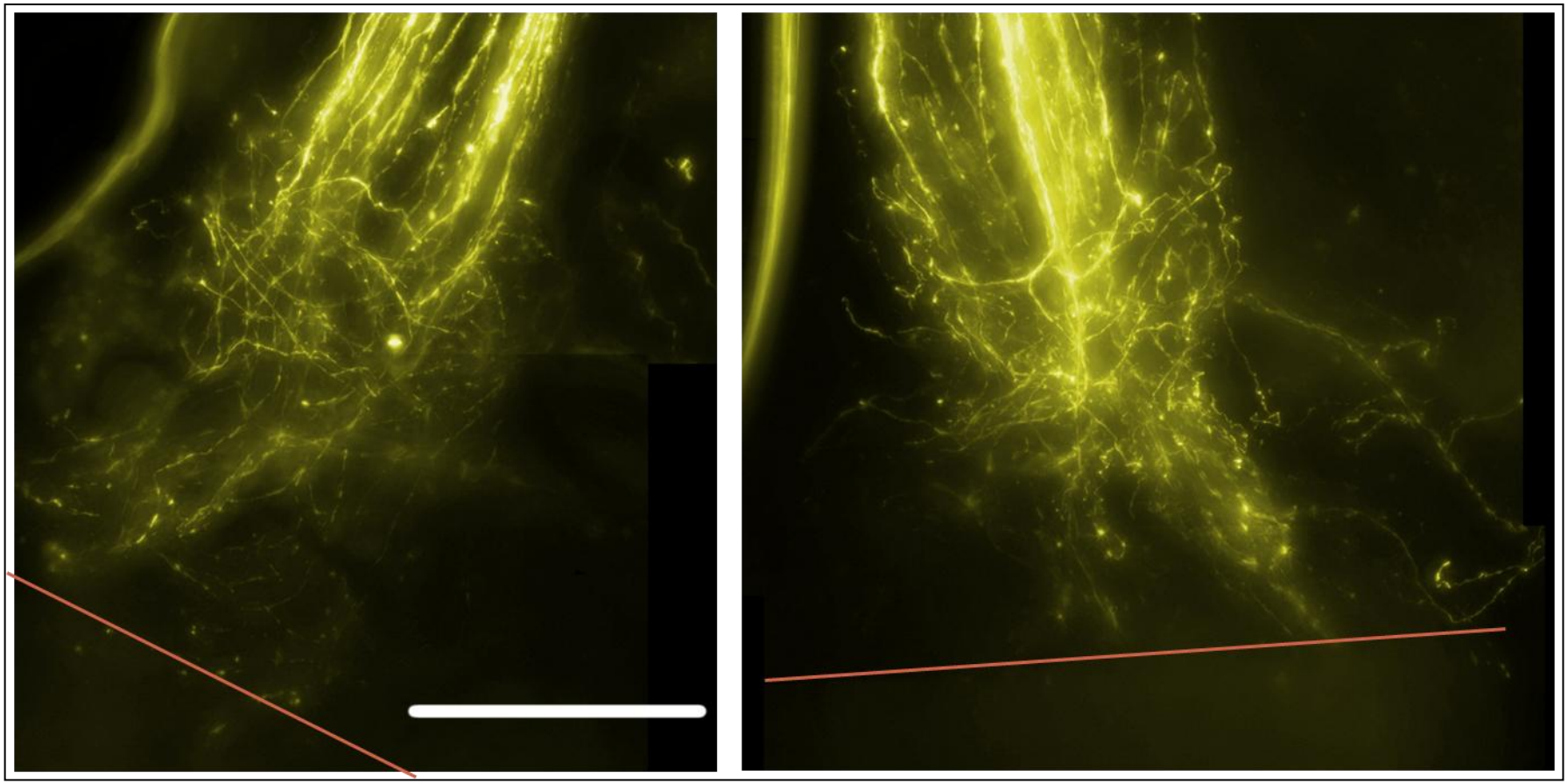

Figure 5.10: Failed early pilot fPEG repaired nerves - marked line indicates start of fibres. Scale bar = 0.5mm.

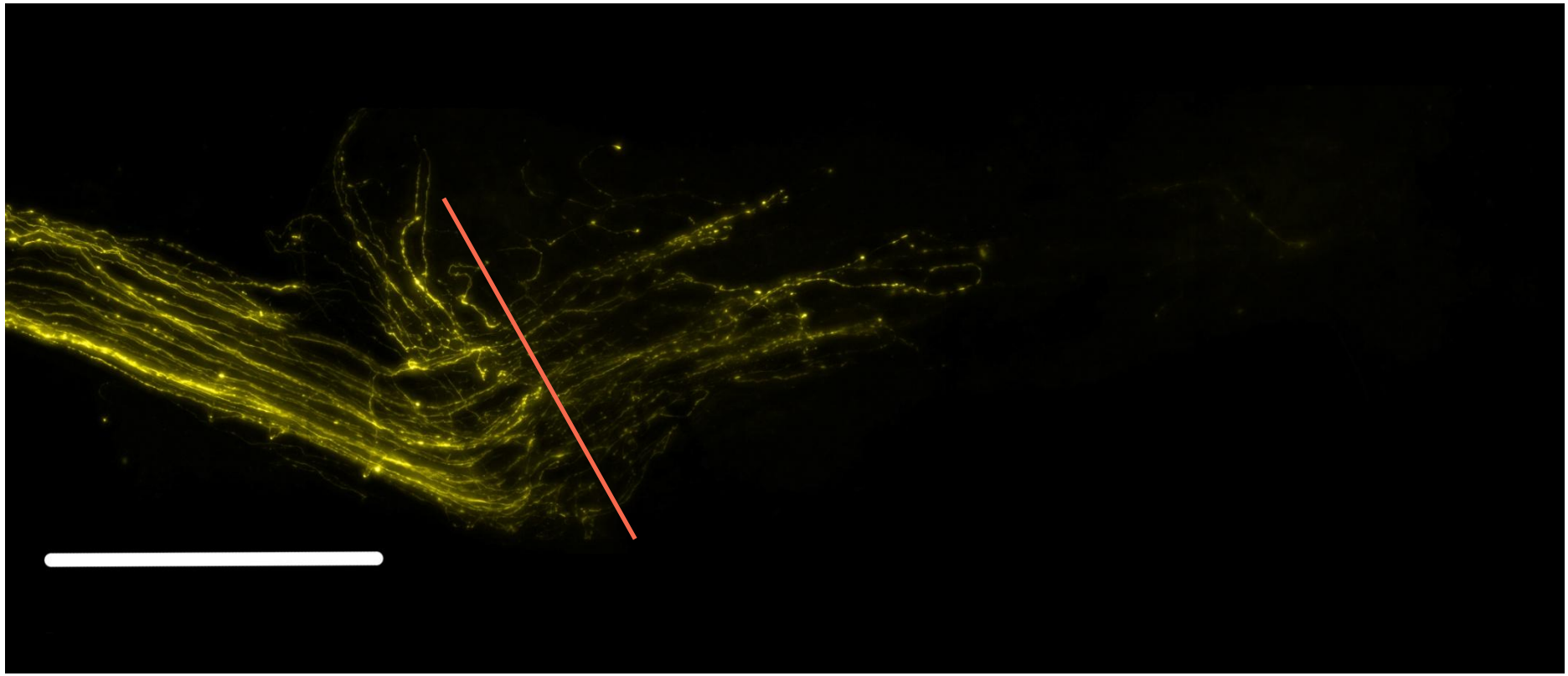

Figure 5.11: Typical fibre filled PEG conduit repaired nerve image - marked line indicates start of fibres. Scale bar = 1.0mm.

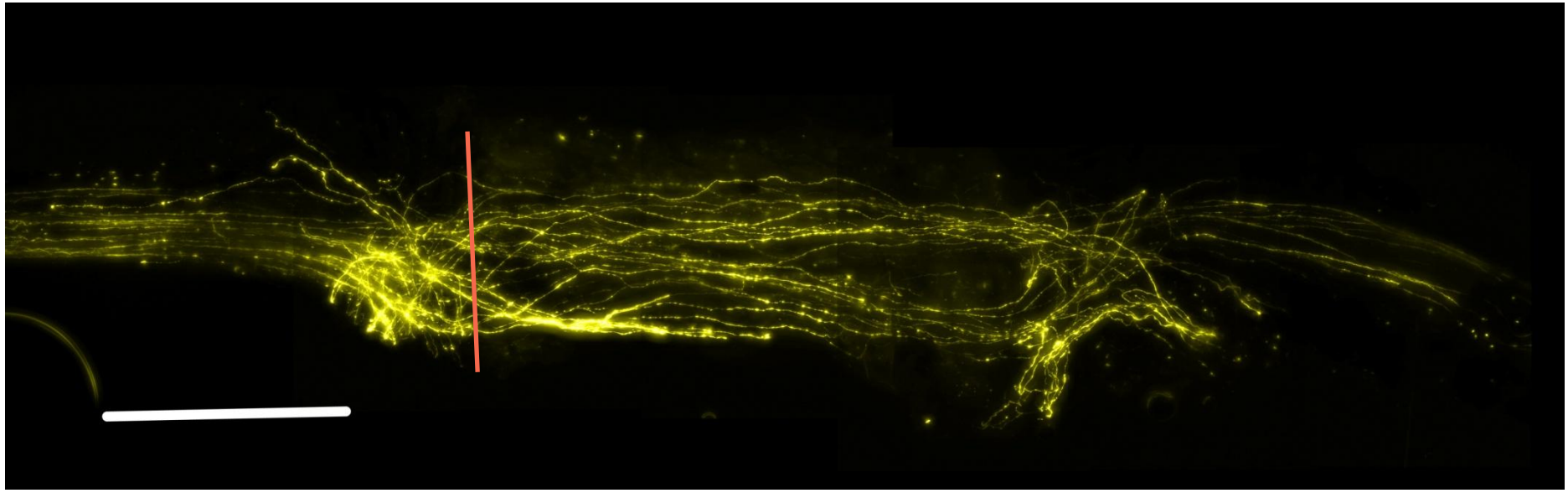

Figure 5.12: A fPEG repair where axons reached distal nerve ending - marked line indicates start of fibres. Axons appeared better organised than in hPEG [fig. 31] and hPCL repairs [fig. 35]. Scale bar = 1.0mm.

5.3.1.3 Hollow Poly-caprolactone Conduits.

Images obtained for hollow poly-caprolactone [hPCL] conduit repairs - like those for hPEG conduits - were quite varied in appearance compared to the graft repair images. As with hPEG conduits [fig. 5.9], axons typically became disrupted and disorganised upon regenerating out from the transected central nerve ending [fig. 5.13] in a similar manner to that observed in graft repairs [fig. 5.8]. Axons regenerating through the hPCL conduits tended to be more densely arranged than axons in hPEG conduits, giving the appearance of greater organisation [figs. 5.9 and 5.13].

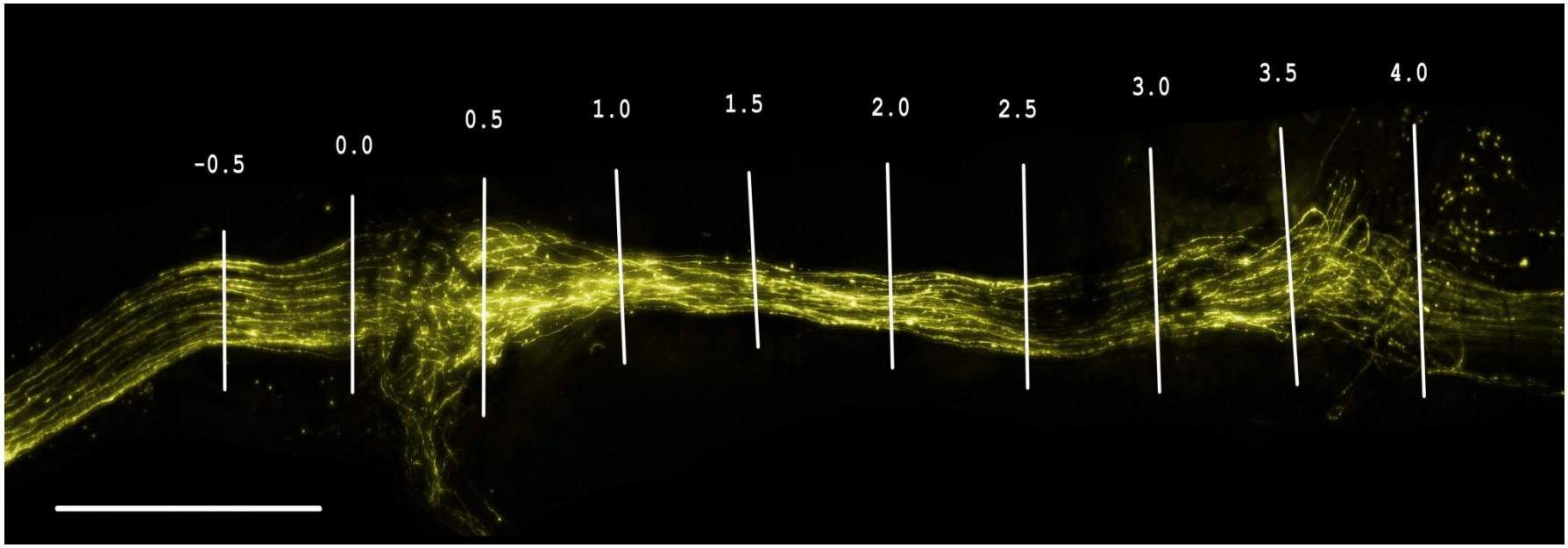

Figure 5.13: Typical hollow PCL conduit repaired nerve image. Scale bar = 1.0mm.

5.3.2 SPROUTING INDEX RESULTS

In all repair groups the highest sprouting index level observed was at the 0.5mm interval, with levels in fPEG, hPCL and graft groups significantly higher [$p<0.001$] than uninjured controls at this interval [fig. 5.14 and table 5]. In all repair groups the sprouting index levels declined at each interval between 0.5mm and 4.0mm - with the exception of the hPCL group where levels declined to the 2.5mm interval before increasing again at both 3.0 and 3.5mm intervals and finally declining again at the 4.0mm interval [fig. 5.14 and table 5].

In hPEG, fPEG and graft groups the lowest sprouting index levels were observed at the 4.0mm interval, and in the hPCL group it was at the 2.5mm interval [fig. 5.14 and table 5]. At the 4.0mm interval the sprouting index levels for both hPEG and fPEG groups were significantly lower [$p<0.05$ and $p<0.001$ respectively] than uninjured controls, with the level for the fPEG group also significantly lower [$p<0.01$] than that of the hPCL group [fig. 5.14].

Significant differences were also found at the 1.0mm and 2.0mm to 3.5mm intervals. At the 1.0mm interval the sprouting index level for the graft group was significantly higher [$p<0.05$] than in uninjured controls, while at the 2.0mm interval it was significantly higher [$p<0.05$] than in the fPEG group [fig. 5.14]. At the 2.5mm interval the sprouting index level for the fPEG group was significantly lower [$p<0.01$] than in both the graft and uninjured groups; the sprouting index level for the fPEG group remained significantly lower than in uninjured controls at the 3.0 and 3.5mm intervals [$p<0.01$ and $p<0.001$ respectively] and was also significantly lower [$p<0.01$] than in the hPCL group at the 3.5mm interval [fig. 5.14].

Table 5: Sprouting index levels for hPEG, fPEG, hPCL, vehicle and uninjured groups [%].

Repair Position (mm)	Average Sprouting % (hPEG)	SEM	Average Sprouting % (fPEG)	SEM	Average Sprouting % (hPCL)	SEM	Average Sprouting % (Graft)	SEM	Average Sprouting % (Uninjured)	SEM
-0.5	100.0	0.0	100.0	0.0	100.0	0.0	100.0	0.0	100.0	0.0
0	115.0	3.6	117.2	3.3	115.4	6.6	111.3	4.1	98.3	1.9
0.5	137.8	10.5	168.2	18.3	173.4	5.0	162.4	15.2	95.7	1.1
1	113.5	17.0	127.5	18.4	106.6	9.0	148.2	12.3	98.0	1.4
1.5	95.6	12.2	90.8	23.7	72.0	12.7	113.0	13.8	94.7	2.1
2	76.0	13.1	53.2	25.3	67.0	11.1	105.6	9.0	95.7	1.1
2.5	66.8	9.8	40.2	22.8	62.0	9.9	95.4	3.5	95.7	2.2
3	77.8	9.3	38.3	25.1	67.7	9.9	93.7	7.0	97.7	2.5
3.5	64.0	11.4	21.3	19.8	75.4	15.1	78.4	10.0	97.7	1.5
4	52.7	10.2	11.0	9.5	67.7	15.4	64.8	7.6	97.4	1.9

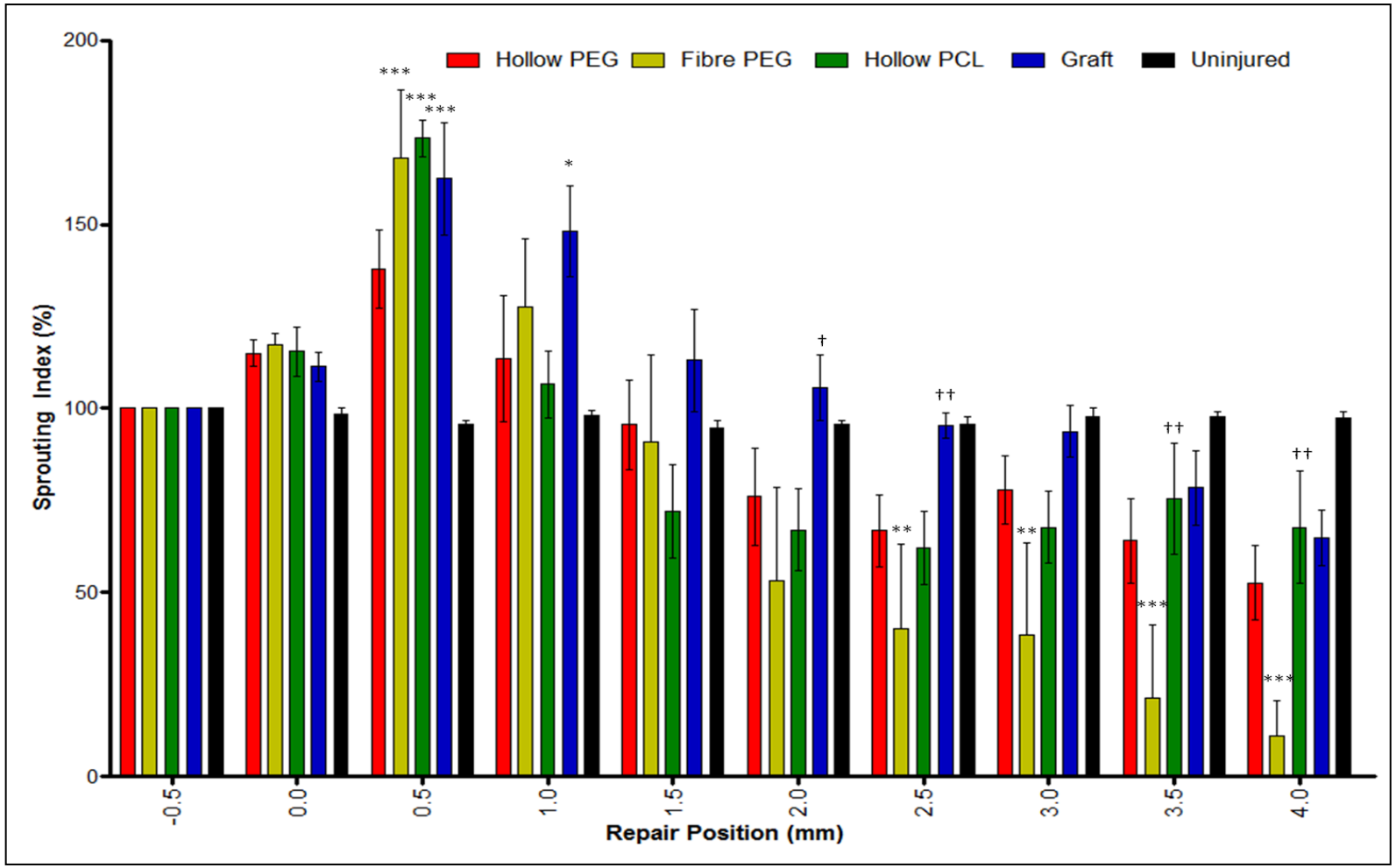

Figure 5.14: Sprouting index levels at 0.5mm intervals along the repairs; *, and *** denote significant differences compared to uninjured controls, *p*<0.05, *p*<0.01 and *p*<0.001 respectively; † and †† denote significant differences compared to fibre PEG conduit repairs. Statistical test: 2-way ANOVA with Bonferroni post-tests.**

5.3.3 CHANGE IN SPROUTING INDEX BETWEEN INTERVALS

The largest positive change in sprouting index level occurred at the 0.5mm interval in all repair groups, the level of change was significant [$p<0.001$] compared to uninjured controls in fPEG, hPCL and graft groups [fig. 5.15]. Only the level of change in sprouting in the hPEG group was not significantly greater than uninjured controls at the 0.5mm interval, though it was significantly lower [$p<0.05$] than the level of change observed in the hPCL group [fig. 5.15].

The largest negative change in sprouting index level for repair groups occurred at the 1.0mm interval - with the exception of the graft group, in which it occurred the 1.5mm interval [fig. 5.15]. At the 1.0mm interval the change in sprouting index level for both fPEG and hPCL groups was significantly greater [$p<0.01$ and $p<0.001$ respectively] than in uninjured controls - in addition the change in sprouting index level for hPCL was also significantly greater than both the hPEG [$p<0.01$] and graft [$p<0.001$] groups [fig. 5.15].

For the remaining intervals the change in sprouting index levels for the repair groups were negative - with the exceptions of hPEG and hPCL groups at the 3.0mm interval and the hPCL group at the 3.5mm interval, where small positive changes were observed [fig. 5.15].

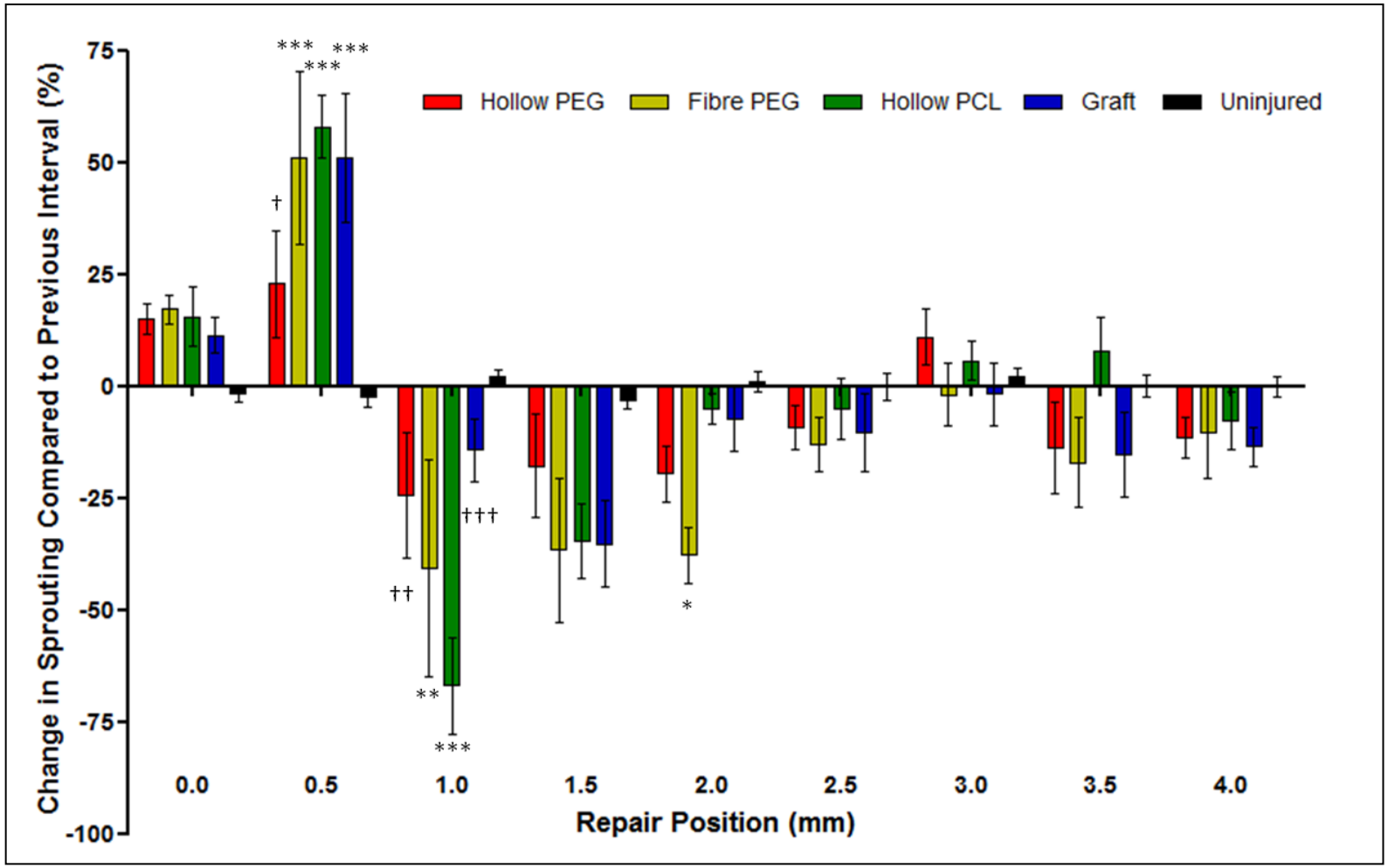

Figure 5.15: Changes in sprouting index levels at each 0.5mm interval compared to the previous interval; ** and * denote significant differences in level compared to uninjured controls, *p*<0.01 and *p*<0.001 respectively; †, †† and ††† denote significant differences in level compared to hollow PCL conduits, *p*<0.05, *p*<0.01 and *p*<0.001 respectively. Statistical test: 2-way ANOVA with Bonferroni post-tests.**

5.3.4 FUNCTIONAL AXON TRACING

No significant differences were detected between repair groups at any interval in terms of individual start axons present. Though there were some small differences between repair groups at points along the repair - a lower proportion of unique axons in hPCL repairs at the 1.5mm interval and both hPCL and hPEG lower than graft repairs at 2.0mm [fig. 5.16]. The percentage of unique start axons was significantly lower [$p<0.001$] in all repair groups compared to the uninjured controls at every interval from 1.0 to 4.0mm [fig. 5.16].

The largest loss of start axons occurred between the 0.5 and 1.0mm intervals in all repair groups, with 24% to 31% of unique start axons lost between those two intervals [fig. 5.16]. Between 49% and 61% of all unique start axons were lost between the 0.0mm and 1.5mm intervals with small losses continuing for the remainder of the repairs, so that at the final interval [4.0mm] the percentage of remaining start axons was between 4% and 20% [fig. 5.16]

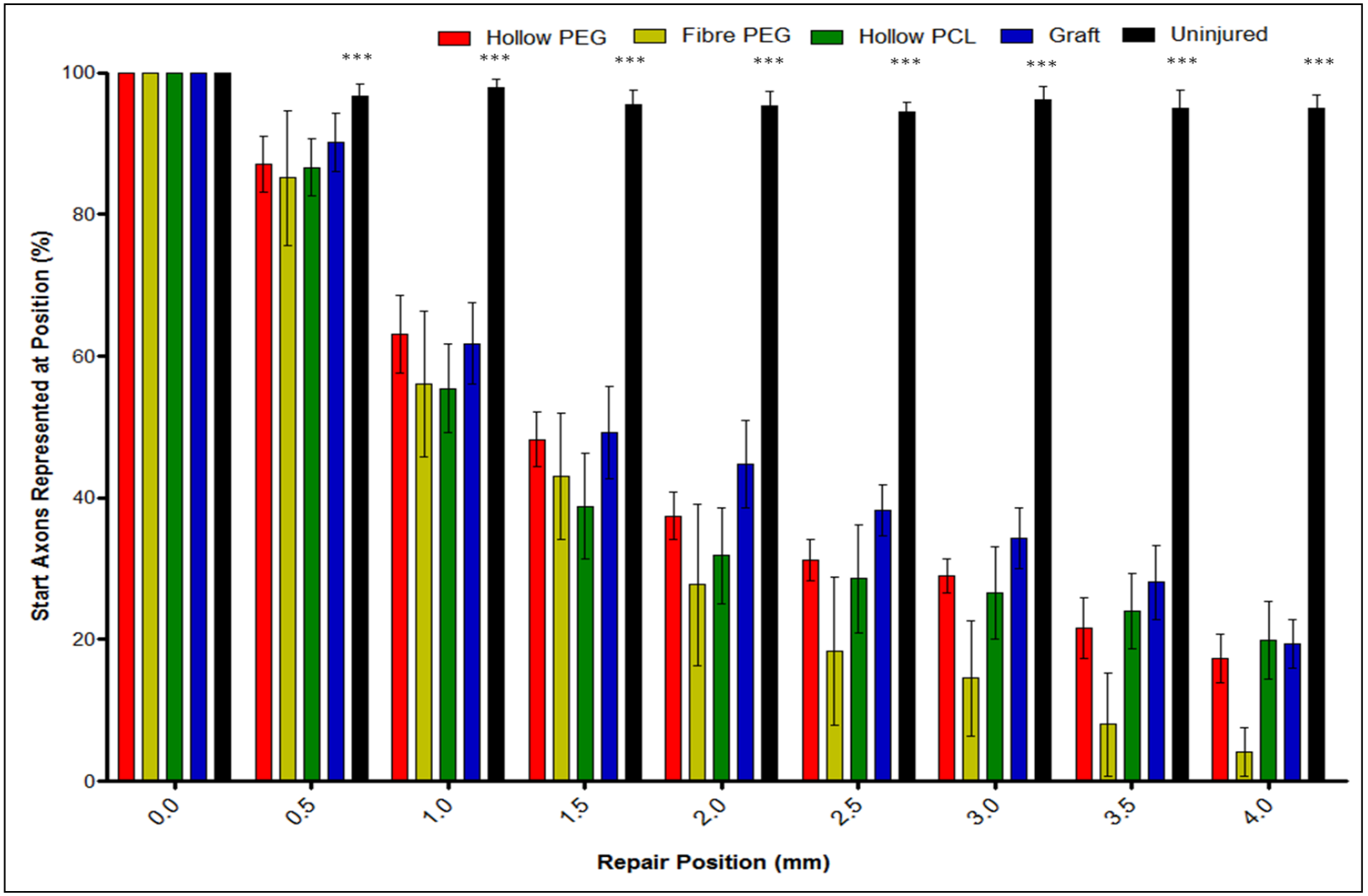

Figure 5.16: Percentages of start axons represented at subsequent 0.5mm intervals; * denotes significant difference compared to all repair groups, *p*<0.001. Statistical test: 2-way ANOVA with Bonferroni post-tests.**

5.3.5 AXON DISRUPTION

The average increase in axon length across the initial 1.5mm of repairs was significantly higher than uninjured controls in both the fPEG [$p<0.05$] and graft [$p<0.01$] groups [fig. 5.11]. However, in both the hPEG and hPCL groups the increases in average axon length were not significantly higher than uninjured controls [fig. 5.17].

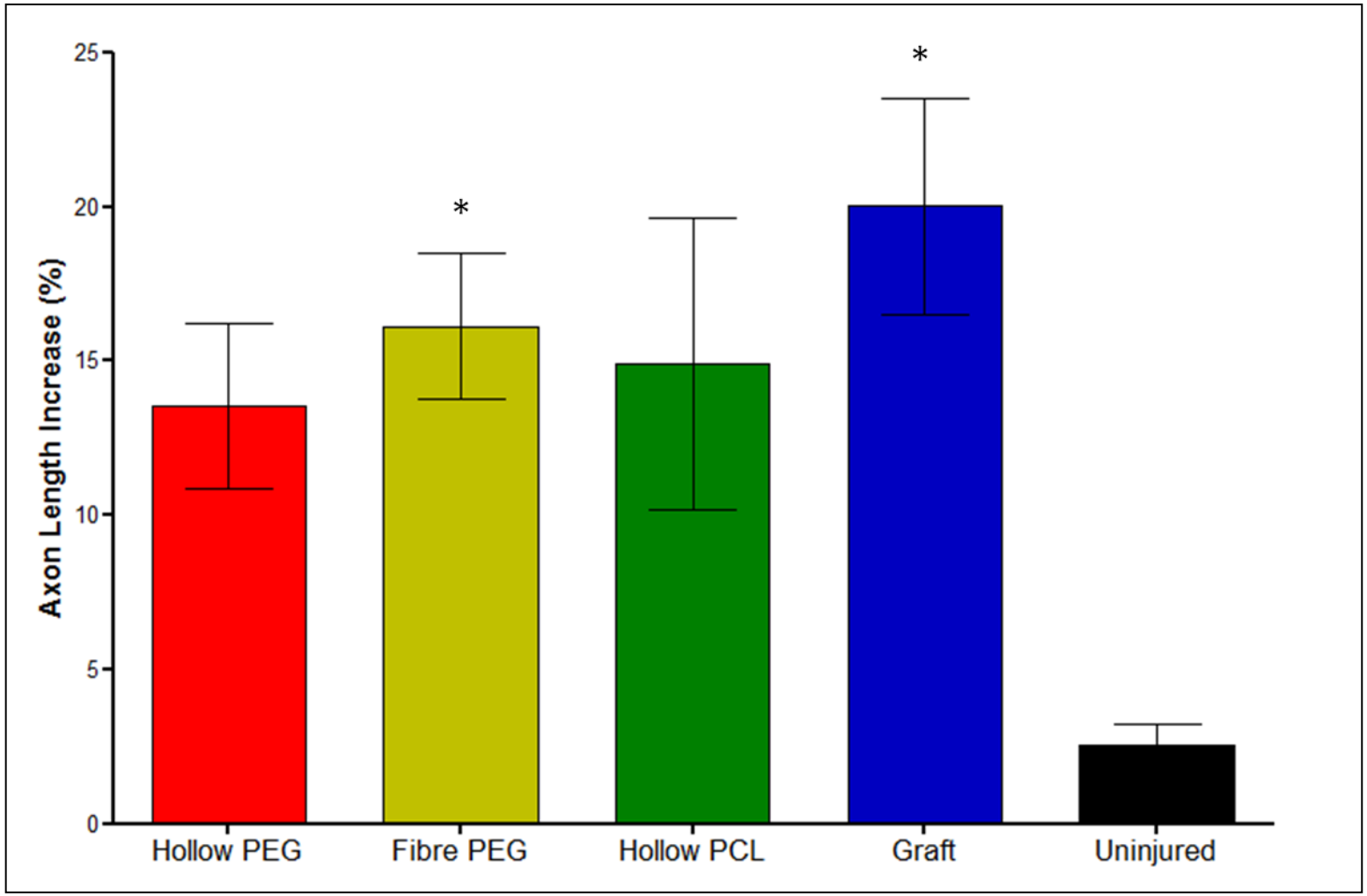

Figure 5.17: Percentage increase in axon length across the initial 1.5mm of repair; * and ** denote significant differences compared to uninjured controls, *p*<0.01. Statistical test: 1-way ANOVA with Bonferroni post-tests.

5.4 DISCUSSION

5.4.1 HOLLOW PEG AND PCL µSL CONDUITS

5.4.1.1 Visual Differences.

In terms of the visual appearance of the repaired nerves, hPCL repair images appeared similar to graft repair images [figs. 5.8 and 5.13] but hPEG repair images generally appeared to have a less organised appearance with axons more greatly spread out between the central and distal nerve endings [fig. 5.9]. Closer examination of the hPCL repair images does appear show that despite the similar appearance to graft images, the axons in hPCL repairs between central and distal nerve endings are less organised than those in graft repairs - which run fairly parallel through the graft [figs. 5.8 and 5.13].

It had been anticipated that axons within hollow conduits would, due to the lack of structural guidance, be somewhat less organised than those in grafts, where axons can be guided along existing endoneurial tubes. However, the difference between hPEG and hPCL conduits [axons spread out more in hPEG than hPCL] was not anticipated as both conduit types were similar dimensionally. One potentially key difference between the two conduit types is that while hPEG conduits are rigid, hPCL conduits are partially flexible, which leads to the possibility that the shape of hPCL conduits may have altered to a more elliptical shape due to pressure from surrounding tissues. This in turn may have restricted the spread of the regenerating nerve through hPCL conduits, providing that the path the nerve regenerated along was at one of the tighter radius ends of the ellipse.

5.4.1.2 Differences in Sprouting Index.

Quantitatively both types of hollow µSL conduits performed similarly to graft repairs overall, although there were some minor differences in the sprouting profiles between graft, hPEG conduits and hPCL conduits. In terms of sprouting there were no differences between

repairs [hPEG, hPCL and graft] at the start of the repair [0.0mm], with all three having a slightly higher sprouting index than uninjured controls [fig. 5.14].

The most interesting differences between the conduit repair groups occurred at the subsequent two intervals [0.5mm and 1.0mm]. At the 0.5mm interval the sprouting index levels for hPCL and graft repairs had increased significantly compared to the uninjured controls, whilst in the hPEG repairs the sprouting index level increased by a lower amount which was not considered to be significantly different to the uninjured controls [fig. 5.14]. In addition, the difference of the increase in sprouting index level between hPEG and hPCL was considered significant [fig. 5.14]. In terms of the overall sprouting index levels these differences in sprouting index levels increases led to both hPCL and graft repairs being significantly higher than uninjured controls while hPEG repairs were not.

At the next interval [1.0mm] the sprouting index levels for all repair groups decreased, though only in the hPCL group was this decrease considered significant when compared to the uninjured controls [fig 5.14]. The decrease in the hPCL group was also significantly different to both hPEG and graft repairs [fig. 5.14]. In terms of the overall sprouting index levels these changes resulted in hPEG and hPCL repairs having similar levels, not significantly higher than uninjured controls, at the 1.0mm interval - though graft repairs remained significantly higher than the uninjured controls [fig. 5.13].

The lower sprouting index level at the 0.5mm interval for hPEG would appear to indicate that axons regenerating into hPEG conduits encountered a reduced level of obstruction compared to those in grafts and hPCL conduits [see section 3.4.1 for discussion on sprouting/obstructions]. The expectation prior to starting these conduit studies was that axons would find regenerating into the hollow conduits easier than into the graft tissue, as upon exiting the central nerve ending they would not be faced with attempting to find a suitable endoneurial tube to regenerate along. This indeed appears to be the case in hPEG conduits but, despite the similarity in design between hPEG and hPCL conduits, it is not the

case for the hPCL conduits, which were observed to have a similar sprouting index level to grafts at the 0.5mm interval.

Other than the previously mentioned flexibility differences between hPEG [rigid] and hPCL [flexible] there is little obvious difference between these two conduit designs. Polyethylene-glycol has been shown to be biocompatible to a relatively high degree and, when in a hydrogel form, capable of supporting in vitro culturing of neural pre-cursor cells (Mahoney and Anseth, 2006, Mihai et al., 2011). The biocompatibility of poly-caprolactone has also been demonstrated to be very good (Sharma et al., 2011) and long-term it biodegrades in vivo without accumulation within tissues (Sun et al., 2006). Given that neither material is considered harmful and are often used in combination with each other (Cometa et al., 2010, Li et al., 2014) it appears unlikely that the differences in sprouting index levels at the initial repair intervals would be caused by the inherent properties of either material. So we need to consider, again, that the flexibility of hPCL conduits has a role to play here.

As discussed earlier, the flexible nature of the hPCL conduits could lead to them becoming slightly deformed via the pressure exerted by surrounding tissues. This deformation of the conduit may resulting in a larger gap between conduit and nerve endings at certain points - this gap may allow increased ingress of granular tissues from the surrounding environment. When granular tissue enters a conduit it can, in sufficient quantity, interfere with axonal regeneration into the conduit (Williams et al., 1984). It is possible that regenerating axons within hPCL conduits may have had to contend with increased ingress of granular tissue compared with hPEG conduits, resulting in greater initial sprouting to overcome the obstruction.

What may also impact upon the initial difference in sprouting index levels between hPEG and hPCL conduits is whether the nerve endings in hPCL conduits become damaged by any potential deformation of the conduit. Damage could be caused when a hPCL conduit deforms due to external pressures and pinches the regenerating nerve ending between its

walls. This is less likely than the previous hypothesis as no severe deformation was noted during extraction of the conduits and conduit/nerve ending positioning varied by a small amount in each surgical setup - which would alter the probability of the nerve ending becoming pinched. As the SEM for hPCL repairs at the 0.5mm and 1.0mm is relatively low compared to all other conduit repairs it is also unlikely that a small number of repairs with high sprouting index levels are skewing the results.

Following the initial differences between hPEG, hPCL and graft sprouting index levels at the 0.5mm and 1.0mm intervals, the sprouting index levels in both hPEG and hPCL repairs fall to similar levels, slightly lower than those in the graft repairs [fig. 5.14]. In both conduit repair groups there is a very small increase in sprouting at the 3.0mm interval, which in hPCL repairs continues at the 3.5mm interval [fig. 5.15]. This increase is likely to occur due to the regenerating axons meeting up with the distal nerve ending and then undergoing sprouting in order to locate suitable endoneurial tubes.

At the final interval [4.0mm] the sprouting index level for hPEG repairs is considered significantly lower than uninjured controls, while in hPCL and graft repairs it is not significantly lower [fig. 5.14]. As discussed in the M6P study [see section 3.4.1], this is likely as a result of the much lower initial increase in sprouting index level at the 0.5mm interval in hPEG repairs compared to the hPCL and graft repairs, as this difference was then roughly maintained throughout the remaining intervals [fig. 5.15].

It had been expected that axons would take longer to traverse the distance between central and distal nerve endings in conduit repairs as it has been reported that axon regeneration in hollow conduits requires an initial connective tissue bridge to form between the two nerve endings and migration of support cells (Lundborg et al., 1982a, Williams et al., 1984). There was, however, no evidence of this in the sprouting index results - the expectation being that significantly fewer axons would have reached the distal nerve ending in conduit repairs. This may be as a result of the majority of axons regenerating past the point where the nerve was

sectioned for removal - meaning that the difference does occur but is not revealed in the current model.

Alternatively, any difference may have been negated as axons in conduit repairs do not have to deal with entering and exiting graft tissue which may be obstructed with scar tissue formed by fibroblasts causing increased scarring within the graft tissue, which could also act as a source of additional inflammatory factors. As axons regenerate much slower through scar tissue (Gutmann et al., 1942, Al-Majed et al., 2000), the potentially reduced level in conduit repairs may allow regenerating axons in those repairs to make up for initial delays in regeneration.

5.4.1.3 Functional Axon Tracing.

As with previous studies [see sections 3.3.5 and 4.3.4], the majority of unique axon loss occurred within the initial 1.5mm of the repairs, with a large amount between the 0.5mm and 1.0mm intervals [fig. 5.16]. A post-hoc comparison does indicate a strong correlation between unique axon loss and the change in sprouting index level across hPEG, hPCL and graft repairs [fig. 5.18]. However, the large decline in sprouting index level [by approximately 66%] between the 0.5mm and 1.0mm intervals in hPCL repairs [fig. 5.15] does not appear to cause a proportionately large decline in unique axons at the 1.0mm interval [fig. 5.16]. A smaller sprouting index level decline [approximately 14%] in graft repairs resulted in only a 6% difference in unique axon numbers compared to hPCL repairs at the 1.0mm interval. Though there does appear a trend towards reduced predictability with greater unique axon loss or reduction in sprouting index levels based upon the comparison [fig. 5.18]

The apparent relationship between sprouting index level change and unique axon number is a relatively straightforward and expected one. A decrease in the overall number of axons at an interval should impact both unique and duplicate axons proportionately - so if there are 100 axons at a particular interval with 20 of them unique, then a 10% decline in total axons

at the next interval should result in 2 unique axons being lost compared to 8 duplicate sprouts.

These proportions may vary due to certain confounding factors - the pruning of excess axon sprouts would increase overall axon loss without affecting unique axon loss. While potential for preferential regeneration of certain axon subsets may increase or decrease unique axon loss, depending upon whether those axon subsets show increased or decreased levels of sprouting. However, it was not within the remit, or capability of this particular study to examine these possibilities.

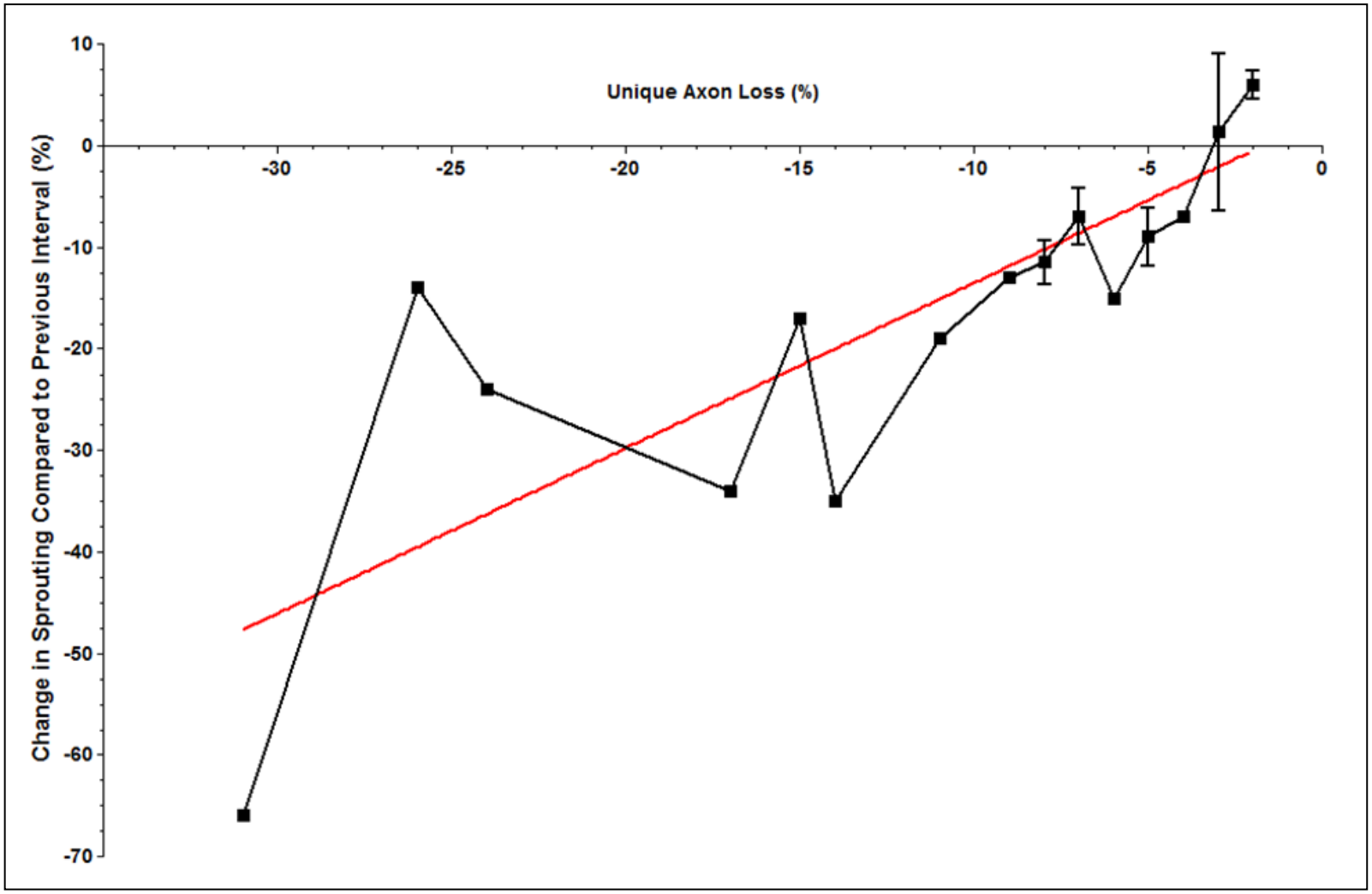

Figure 5.18: Comparison between unique axon loss and change in sprouting index at individual intervals - data pooled from hPEG, hPCL and graft results. A significant correlation between unique axon loss and change in sprouting was detected [p<0.0001] using Spearman's r correlation test. Error bars are SEM.

5.4.1.4 Initial Axon Disruption.

The average path length of axons across the initial 1.5mm of the repair in both hPEG and hPCL conduits was not considered to be significantly longer than that taken by axons in the uninjured controls [fig. 5.17]. In contrast the average path length in graft repairs was considered significantly longer than that taken by axons in uninjured controls, indicating a trend towards greater disruption in the initial stages of graft repairs compared to conduit repairs [fig. 5.17].

As discussed for the mannose-6-phosphate study [see section 3.4.3] the shorter the route taken by axons across a repair, the sooner they will reach their target tissue. This has the potential to improve regeneration through enabling axons to cover the distance between injury and target tissue while the environment and target tissues are still permissive to regeneration [see section 1.7.3].

It had been anticipated that using hollow conduits would reduce the disruption in the initial stages of repairs, mainly due to the axons in conduit repairs not having to regenerate directly into 'ready-made' tissue and find appropriate endoneurial tubes. Once axons in conduit repairs regenerate through any scar tissue at the exit of the central end they enter into a newly forming fibrin matrix, which by 5-7 days after conduit implantation forms a longitudinally organised link between the sectioned nerve endings (Williams et al., 1984, Dahlin and Lundborg, 2001). It is logical to assume that axons regenerating along with their supporting tissues would have less obstacles to regenerate around than axons attempting to regenerate into graft tissue where endoneurial tubes originally formed for a different arrangement of axons.

One drawback of hollow conduits may be that, because the structural tissues need to regenerate along with the axons, there is a longer delay between the repair being made and axons regenerating into the repair. It has been known since the early-to-mid 1980's that following implanting a conduit fills with a fluid rich in neurotrophic factors (Lundborg et al.,

1982b, Longo et al., 1983, Dahlin and Lundborg, 2001), typically within the first two days following implantation (Williams and Varon, 1985). It is then in the second week after implantation that Schwann cells and axons begin to enter the repair (Williams et al., 1983, Dahlin and Lundborg, 2001). This potential regeneration delay in conduit repairs may negate any gains made by axons taking a shorter route into, and across, the repair when compared to graft repairs.

5.4.2 FIBRE FILLED PEG µSL CONDUITS

5.4.2.1 Visual Differences.

It was immediately obvious from nerve images that the performance of the fPEG conduits - even following the changes discussed in section 5.2.3 - was disappointing [fig. 5.11]. Few axons regenerated more than 1.5mm into the conduits in most repairs and only in two repairs did axons reach the final [4.0mm] interval.

In one of the two repairs where axons reached the final interval the organisation of axons through the repair appeared to be better organised than those axons in both types of hollow conduit [fig. 5.12]. This indicates that the presence of the aligned fibres may have the potential to improve the organisation of axons regenerating through conduits - if the axons can actually manage to regenerate through the conduits.

5.5.2.2 Differences in Sprouting Index.

Quantitatively, the sprouting index results generally corresponded with the visual images, with only one repair contributing a noteworthy amount of axons to the final two intervals [table 5 and fig. 5.14]. Initially the sprouting index levels in fPEG repairs were similar to graft and hPCL repairs, with a small increase in sprouting index level at the start interval [0.0mm] followed by a significantly higher increase compared to uninjured controls at the 0.5mm interval [fig. 5.15]. The sprouting index level then decreased by an amount between that of hPEG and hPCL at the 1.0mm interval and decreased at the 1.5mm interval similarly to the other repair groups [fig. 5.15].

The main loss of overall axon numbers appears to occur at the 2.0mm interval - where fPEG repairs are the only repair to decrease significantly compared to uninjured controls - with similar changes in sprouting index levels to the other repair groups at the remaining intervals.

As the 0.0mm interval is determined by the first signs of abnormal axon morphology, not the end of the central nerve ending, the point where regenerating axons first meet PCL fibres is between the 0.5mm and 1.0mm intervals. Seeing that axons in fPEG repairs perform similarly to other conduit and graft repairs across these early intervals, there is an indication that axon regeneration is severely impacted once axons start regenerating into the aligned PCL fibres.

With the hPEG conduits demonstrating that a good level of nerve regeneration is achievable in conduits of the same design without any fibres, and PCL not appearing cause any detrimental effects when in the form of a conduit, it would appear that something about the electrospun PCL fibres is the cause of the failure.

An inherent disadvantage of any synthetic material used in artificial nerve guides is the lack of any naturally occurring cell adhesion proteins or recognition signals (Kim and Mooney, 1998). As the PCL fibres used in the fPEG conduits were not coated or treated with any matrix proteins it is likely that migrating Schwann cells would have found conditions to be sub-optimal at best.

An in vitro study by Schnell et al. (2007) demonstrated that electrospun PCL fibres do provide a favourable substrate for cell growth and attachment, though when PCL was combined with collagen [at a ratio of 75% PCL to 25% collagen] the biological benefits increased significantly. A study by Zhang et al. (2010), which investigated the potential for silk fibroin to be added to poly(L-lactic acid-co-ε-caprolactone) [PLLA-CL] electrospun fibres, found the electrospun fibres performance enhanced when coupled with the silk fibroin protein [especially the fibres with a 75% PCL to 25% silk fibroin ratio].

A later study by the same group (Wang et al., 2011) compared the performance of silk fibroin PLLA-CL fibres [SF/PLLA-CL] to pure PLLA-CL fibres in conduit repairs of the sciatic nerve. They used the best performing ratio for the electrospun fibres from the previous study [75% PCL to 25% silk fibroin] which resulted in significantly better conduction velocities and

compound action potentials when compared to pure PLLA-CL (Wang et al., 2011). Histological analysis also demonstrated the benefit of SF/PLLA-CL fibres, with greater overall and myelinated axon numbers and also apparently greater axon organisation in conduits filled with SF/PLLA-CL fibres (Wang et al., 2011).

It would appear that the use of uncoated PCL fibres, whilst not being quite as beneficial as matrix protein coated PCL fibres, should not be overly inhibitive to axon regeneration. One possible reason for the poor performance of fPEG conduits in this study could be related to how densely the fibres were packed into the PEG conduits. Two early pilot repairs used a higher density of PCL fibres [approximately double that used for subsequent experiments], with the result that no axons appeared to enter the fibres [fig. 5.10].

Following the initial two pilot repairs it was decided to reduce the density of the PCL fibres within the fPEG conduits. The amount that the density could be reduced by was limited, as reducing the density too much would lead to the fibres not fitting securely in the conduit and risk them falling out of the conduit once implanted.

A second issue noticed during the implantation of the two pilot fPEG conduits was that the fibres were extremely dry and tended to adsorb to any moist tissue. It was felt that this was likely to adversely impact regeneration through drying out and damaging the sectioned nerve endings and also impact the secretion of neurotrophin rich fluid into the conduit [see section 5.5.1.3]. Subsequently, for this study the fPEG conduits were soaked in Ringer's solution for one-hour prior to impact in an attempt to alleviate this issue.

These alterations [reduced fibre density and pre-soaking conduits] did improve the performance of fPEG conduits [though only compared to the pilot fPEG conduits], with the majority of repairs having sprouting index levels of 50% or greater at the 1.5mm interval and only two repairs failing to regenerate axons to the 3.0mm interval. One repair [fig. 5.12] performed remarkably well, having a sprouting index of 150% at the 0.5mm interval which

was maintained at a similar level throughout the entire length of the conduit and only declining significantly upon entering the distal nerve ending.

However, the large variation between fPEG conduit repairs [note the relatively large SEMs for table 5 and figs. 5.14 to 5.16] does indicate that the methods used to produce these alterations may require refinement in order to gain better homologated conduits. For example, simply placing the conduits in Ringer's solution may result in fibres in one conduit being completely soaked but fibres in another only being soaked at the ends, leaving the centre dry. Additionally, reducing variation between conduits in terms of fibre packing densities may also have an impact upon reducing variation between repairs.

5.4.2.3 Functional Axon Tracing.

Although the proportion of unique axons regenerating through fPEG was much lower than in hPEG, hPCL and graft repairs [~4% compared to ~20%; fig. 5.10], only two fPEG repairs actually had axons regenerating through the entire repair, with one of those [fig. 5.12] displaying similar levels to the three other repair groups.

Across all repair intervals the proportion of unique axons was not considered significantly different in fPEG repairs to the other repair groups, with little noticeable difference until after the 1.5mm interval [fig. 5.16]. As sprouting index results also show similar levels between the repair groups until after the 1.5mm interval [after which fPEG sprouting index levels begin to decline rapidly], this is indicates that regeneration within fPEG began in a similar fashion before failing midway into the repairs.

The one successful fPEG repair [fig. 5.12] did have similar proportions of unique axons at all intervals as the other three repair groups. This indicates that if the PCL fibres were treated to prevent the regeneration failure that occurred in the majority of fPEG repairs, then functional recovery would be similar to the other repair groups in fPEG repairs.

5.4.2.4 Initial Axon Disruption.

Average axon length increases over the initial 1.5mm of the repairs in fPEG conduits were similar to that in hPEG and hPCL conduits, though the slightly higher increase in fPEG repairs did result in the disruption being considered significant compared to uninjured controls [fig. 5.17].

It was anticipated that in fPEG repairs that this initial disruption would be reduced compared to graft repairs, the reasoning for this is mostly covered in section 5.4.1.4. The obvious difference between hPEG, hPCL and fPEG repairs is that axons in the hollow conduits exit the central nerve ending into a space containing only regenerating nerve tissue, associated cells and neurotrophic factors, while fPEG axons will also meet with PCL fibres. The

presence of the PCL fibres was not considered likely to increase disruption as, although they do provide a potential physical obstruction, they are flexible and do not contain their own population of inflammatory cells and factors as graft tissue does..

The average axon length increase in fPEG repairs does appear to indicate that this is indeed the case, as despite the significant difference between fPEG repairs and uninjured controls, the difference between fPEG and the other conduit repairs [<2.6%] was actually smaller than the difference between fPEG and graft repairs [>3.1%; fig. 5.17]. In addition, only one of the fPEG repairs had an average axon length increase above the mean value for average axon length increase, with that result actually lower than the maximum in hPCL repairs and less than 1% higher than that in hPEG repairs. This would indicate that the reason for fPEG repairs having a significantly greater disruption compared to uninjured controls - while hPEG and hPCL repairs do not - may result from less variation in the increase in average axon length between the fPEG repairs, likely resulting from the guidance provided by the aligned PCL fibres.

5.4.3 CONCLUSIONS

Both hollow conduit types used in this study enabled nerves to regenerate across a short defect in a similar manner to nerve grafts. Although this is certainly a promising start for µSL produced conduits, the major test of their suitability will come when faced with repairing larger nerve defects. Many conduit designs have been demonstrated to have graft-equalling performance over short defects less than 20mm (Lundborg et al., 1982a, Archibald et al., 1995, Francel et al., 1997, Bertleff et al., 2005, Sinis et al., 2005, Bushnell et al., 2008) but very few can maintain this across larger defects (Matsumoto et al., 2000).

However, the main aim of this study was to determine a baseline level of performance for hollow µSL conduits in the YFP-H mouse nerve injury model and to ensure that the conduits would allow regeneration to occur. This aim was successfully achieved, with the majority of hollow µSL conduits enabling regeneration across the defect [one hPEG and one hPCL

failed to regenerate axons all the way to the distal nerve ending] with no notable side-effects other than those also observed in graft repairs [mild loss of mobility and inflammation of the surgical site].

Of the two hollow µSL conduit materials PCL appears to be the more suitable for any future work, as it fits more of the desired qualities of artificial nerve guides (Ciardelli and Chiono, 2006): it is bioabsorbable, moderately flexible but still strong enough to resist collapsing and could be sutured in place if used on a larger nerve [though its resistance to tearing may require increasing]. The PEG conduits, despite their good performance in this study, are unlikely to ever be suitable for clinical use due to a number drawbacks of PEG: it is non-bioabsorbable, inflexible and brittle [a number of hPEG conduits were broken during attempts to implant them].

The performance of the fPEG conduits in this study was disappointing; however, the likely reasons for the poor performance of fPEG conduits [uncoated/dry PCL fibres] can be easily rectified. Although one fPEG conduit repair suffered a complete failure [central nerve ending dislodged from conduit], this is a potential eventuality in any conduit or graft repair where the repair is secured using fibrin glue rather than sutures and therefore does not reflect negatively upon fPEG conduits. Although the majority of fPEG repairs were disappointing, one [fig. 5.12] did manage to equal the performance of graft repairs and indicate that the aligned PCL fibres do improve the organisation and guidance of regenerating axons.

One area of future work using µSL conduits is likely to attempt to improve the performance of aligned PCL fibres within conduits by coating them with beneficial matrix proteins [e.g. collagen, laminin]. It is probable that the PEG conduits used to house the fibres in this study will be replaced by PCL conduits, which will result in fully bioabsorbable conduits.

A second area of future work could investigate the addition of Schwann cells [either from nerve tissue or derived from a suitable source of stem cells] or individual neurotrophic factors to the conduits. This may be trialled in similar length conduits to examine in the

addition of cells/factors can enable conduit regeneration to surpass graft repairs, or in much longer conduits to examine if it can enable regeneration similar to grafts over a long defect.

In conclusion, the μSL manufacturing technique has proved useful for producing conduits, with precise and reproducible conduit dimensions achievable at relatively small sizes. These conduits have generally performed well and have great potential to be developed further.

6.0 PERFORMANCE OF 3D-PRINTED CONDUITS IN VIVO

6.1 INTRODUCTION

Discussion of the benefits of using conduits in nerve repairs, and current and future conduit designs can be found in sections 1.6.3 and 5.1 respectively. The aim of this section is to briefly discuss prominent experimental techniques used for producing various designs of conduits.

6.1.1 MANUFACTURING ARTIFICIAL NERVE GUIDE CONDUITS

A wide variety of methods have been used in order to create conduits for peripheral nerve repair; a common theme is taking a cylindrical rod and coating it with a solution of the conduit material, once the material 'sets' the mould is removed to leave a hollow conduit (Ao et al., 2006, Huang et al., 2012).

The method used by Ao et al. (2006) was to create a mould into which a 2% chitosan solution in 1% acetic acid was injected and a Teflon coated steel rod was then inserted into the centre of the mould. The chitosan solution was filtered through a nylon mesh and degassed by reducing pressure prior to injection into the mould, once in the mould the chitosan solution was frozen for 12-hours at -20ºC. Following this the mould was removed and the conduit [with the rod still in place] was lyophilised and then immersed in sodium hydroxide to neutralise the remaining acetic acid. The final steps were to rinse with deionised water, equilibrate using PBS and then immersed in chitosan solution - this second layer of chitosan was dried in a ventilation oven prior to the steel rod being removed. Conduits produced using this method - or methods derived from this method - have since been used in a number of studies (Ao et al., 2011, Mohammadi et al., 2013, Azizi et al., 2014).

The conduits used by Huang et al. (2012) in their study investigating the benefits of silk fibroin were manufactured using a similar principle. A cylindrical rod was dipped into an 8-10% solution of dialysed regenerated *Bombyx mori* [silkworm] fibroin and this coating was then gelled using acetic acid and frozen to create a porous conduit.

A more complex version of this method was used by Yao et al. (2010a) in their study which produced multi-channelled collagen conduits. In that study a number of thin wires [relating to the number of channels desired] were passed through two end-caps 1cm apart in order for a collagen solution to self-assemble around. For the seven channel conduits they produced Yao et al. (2010a) inserted two wires at first, allowing the collagen solution to self-assemble around them and then air dry before repeating that step twice more, with a final repeated step for the single remaining wire. Once all wires were coated and the collagen had dried it was treated with a cross-linking solution overnight and then washed and freeze-dried; once the freeze-drying was complete the end-caps and wires were removed.

A different take on moulding a conduit around a central rod was used by Oh et al. (2013), who rolled an asymmetrical porous PCL/Pluronic F127 membrane around a rod and glued the ends of the membrane together. The main aim of the study by Oh et al. (2013) was to develop conduits with different surface pores - but the same membrane properties - to investigate the effects of pore size on nerve regeneration. In this they found nano-pores to perform better than micro-pores (Oh et al., 2013) - information which the same group then used to investigate the effects of ultrasound and NGF treatment on nerve regeneration through these conduits, determining that the combination of both ultrasound and NGF resulted in improved regeneration compared to either treatment in isolation (Kim et al., 2013).

Electrospinning is a popular method used to create conduits (Panseri et al., 2008, Mottaghitalab et al., 2013) and a brief overview of the basics of the technique can be found in chapter 5 of this thesis [see section 5.2.1]. Electrospinning was used successfully to

create the conduits used by Panseri et al. (2008) in a study assessing their performance in a rat sciatic nerve injury model. The conduits were made by electrospinning PCL fibres onto the rotating grounded collector and then electrospinning PCL/Poly(DL-lactide-co-glycolide) [PCL/PLGA] fibres on top of the PCL fibres. This created a strong mechanical base through the PCL fibres surrounded with the tight-nit outer mesh of the PCL/PLGA fibres (Panseri et al., 2008).

Mottaghitalab et al. (2013) also used electrospinning techniques in the fabrication of conduits, although their technique differed in that fibronectin containing silk fibroin nano-fibres was electrospun onto a silk fibroin/single walled carbon nano-tube substrate [SF/SWNT], which was then rolled up to form a conduit. The SF/SWNT substrate was formed by freeze-drying a SF/SWNT solution; once the electrospun fibres were in place the substrate was soaked in PBS for 4-hours to improve flexibility prior to rolling up the substrate with the electrospun fibres forming the interior of the conduit (Mottaghitalab et al., 2013).

Many of the current experimental procedures for producing conduits have certain key limitations that limit the potential to commercially produce conduits for clinical use. For example, it is clear in the methods described above that the relatively slow production rates and number of complex production stages would hamper any attempts to scale up production to a suitable level.

Additionally, both experimental and current commercial nerve guides are generally limited in the variety of sizes produced. Experimental conduits are generally sized according to the nerve injury model they will be used in and commercially produced conduits tend to be available in set diameter/length combinations (Meek and Coert, 2008). This may be an issue for surgeons when during the initial treatment of traumatic nerve injuries, as the injured nerve may require a particular diameter/length combination that is not catered for.

In recent years additive manufacturing technologies [generally termed 3D printing] have garnered a great deal of interest across a broad range of industries. The main reason for this is that much more complex and intricate designs can be manufactured using additive techniques than traditional casting or subtractive techniques [where being able to remove casts and tooling access are limiting factors]. Potential medical uses range from educational and surgery planning applications (Rengier et al., 2010, Watson, 2014) to cell scaffolds and replacement organs (Gruene et al., 2011, Serra et al., 2013, Schubert et al., 2014).

The µSL [micro-stereolithography] technique used to manufacture the conduits used in the study reported in chapter 5 is considered to be an additive manufacturing technique [through the curing of liquid polymer in layers] and clearly demonstrates good potential in the production of nerve guide conduits. With current µSL techniques conduit wall thicknesses of 50µm and surface features of 25µm are achievable (Pateman et al., 2014b). This suggests that very precise structures can be created, such as niches and guiding channels, which could benefit regenerating axons. However, µSL still has some of the same drawbacks as the previously discussed techniques: the setup and manufacture of the conduits is a complex process - making true homogeneity between batches potentially difficult to obtain - and the rate of production is limited due to difficulties in producing multiple conduits simultaneously.

Another additive manufacturing technique that may prove more suitable to commercial scale conduit production is selective laser sintering [SLS]. Complex structures can be created using SLS, with models of skeletal and tissue structures having been created in order to plan surgical procedures (Suzuki et al., 2010). However, the resolution required for creating a skull model - as Suzuki et al. (2010) used in one study - is much lower than would be required for creating topographical guidance in a conduit. The ability of SLS to produce many conduits of varying combinations of sizes simultaneously may prove commercially beneficial in the event that suitable nerve guide conduits can be produced using the technique. An additional benefit is that a range of conduit sizes could be produced attached

to a single 'Airfix kit' style frame, allowing surgeons to simply select the most appropriately sized conduit from the range.

6.1.2 AIM OF THIS STUDY

The aim of the study reported in this chapter was to investigate the potential of a 3D printing manufacturing technique [SLS] to produce conduits suitable for repairing peripheral nerve injury. The work carried out within this study was made possible following a successful grant application I made to the MRC Centenary Fund.

The primary aims of the study were to:

- Assess the ability of a SLS machine to produce suitably sized conduits to use with the YFP-H mouse CF [common fibular] nerve injury model.
- Assess the performance of SLS produced conduits when used to repair a CF nerve injury in YFP-H mice.

Following initial technical discussions it was expected that the available SLS machine would be able to produce suitably sized conduits, though the ideal sizes would be near to the limits of its capabilities.

The performance of the SLS produced conduits was expected to be similar to that predicted for the µSL produced conduits in that they would facilitate regeneration almost to the same standard as graft repairs [see section 5.1.4].

6.2 MATERIALS AND METHODS

General materials and methods are detailed in chapter 2, more specific information related to the experiments discussed within this chapter is detailed below.

6.2.1 SELECTIVE LASER SINTERING PRODUCED CONDUITS

All conduits produced using SLS techniques were produced in collaboration with the laboratory of Professor Neil Hopkinson [Department of Mechanical Engineering, University of Sheffield, UK].

The SLS machine that produced the conduits [EOS Formiga P100] used in this study uses a scanning system to direct a laser beam at a layer of fine nylon-12 powder [this material is currently the standard for this machine (Johnson et al., 2013)] and melt [sinter] it into a pattern determined by a CAD image file [fig. 6.1]. Once the desired pattern is sintered the powder stage descends by a predetermined distance, a new layer of nylon-12 powder is spread on top of the previous powder layer by a dispensing hopper and the next layer of the pattern is sintered [fig. 6.1]. Once the sintering process is complete, the conduits are removed from the non-sintered powder and pressurised air is used to remove loose powder, the non-sintered powder can then be reused - either on its own or mixed with a proportion of unused powder (Dotchev and Yusoff, 2009).

Due to the small internal diameter size required for the conduits it was not possible to clear all non-sintered powder from inside the conduits using pressurised air. Instead, an appropriately sized hypodermic needle filled with denatured alcohol was used to force this remaining powder out of the conduits. The conduits were then soaked for 48 hours in denatured alcohol to remove any remaining loose powder prior to sterilisation by autoclaving.

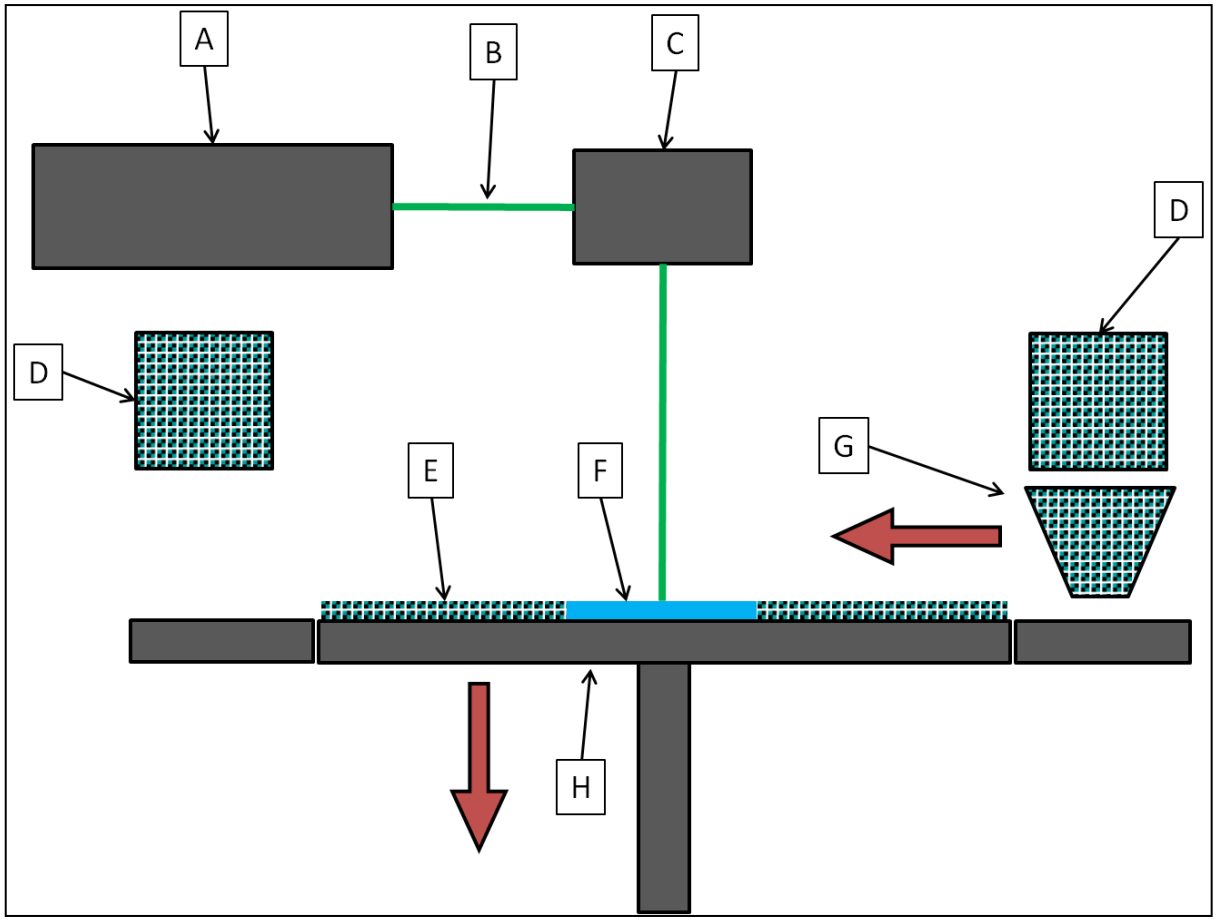

Figure 6.1: Diagram depicting selective laser sintering process. A: laser source [30w CO2]; B: laser beam; C: scanning system; D: powder dispenser; E: fresh powder spreader; F: sintered powder; G: powder spreader; H: moveable powder stage.

Initial SLS conduit designs consisted of a range of differently sized conduits attached to a frame [fig. 6.2]. Examination of the conduits found that the powder occupying the centre of conduits with an internal diameter of 0.5mm could not be removed, in the 1.0mm internal diameter conduits with 0.25mm thick walls powder was also difficult to clear [fig. 6.2]. Although a 1.0mm internal diameter would have been comparable with that used for the µSL conduits [see section 5.2.1], the wall thickness requirement for the SLS conduits necessitated a smaller internal diameter to be used. This was in order to reduce the outside diameter of the SLS conduits to a suitable size to fit within the repair location. A range of conduits 4.0mm long with 0.5mm thick walls and internal diameters ranging from 0.5mm to 1.0mm was then produced to determine a suitable size - with a 0.8mm internal diameter decided upon and produced for experimental repair.

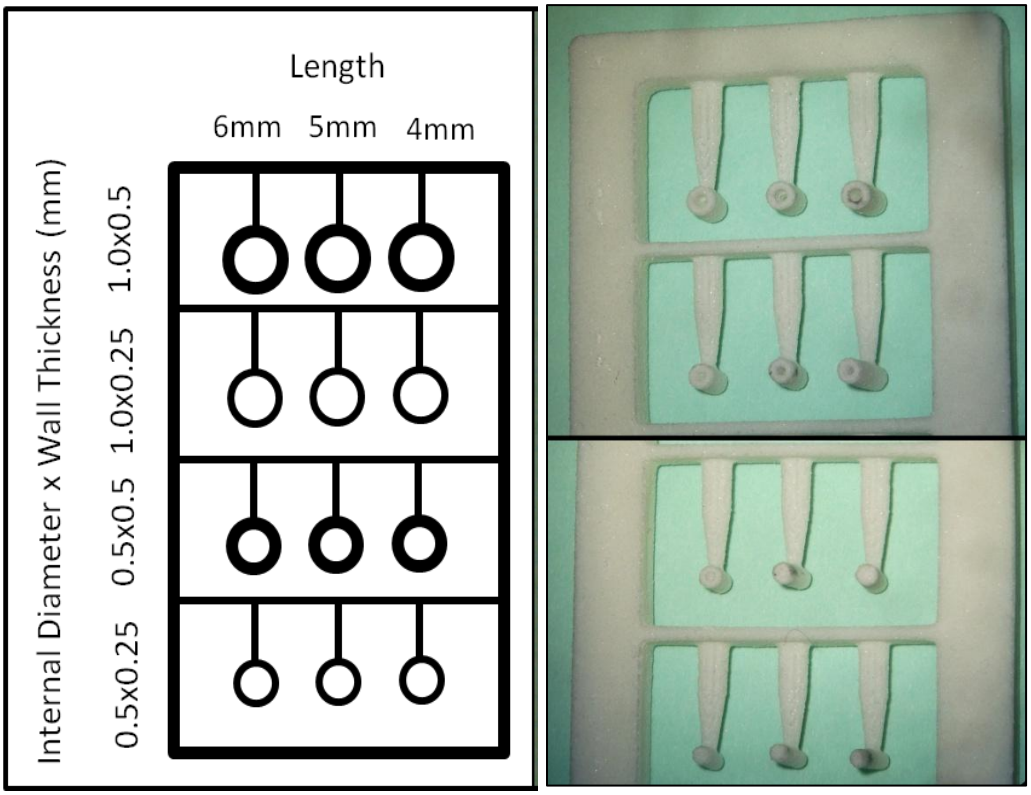

Figure 6.2: Diagrammatical representation of SLS conduit grid layout [left] and actual SLS produced conduits attached to frame [right].

6.2.2 SURGICAL PROCEDURES

All surgical procedures were identical to those discussed in section 5.2.2.

6.2.3 ANIMAL NUMBERS AND GROUPINGS

A total of 28 mice were used in the experiments described in this chapter - with 7 specific to this study, with the remaining 21 being controls shared with the separate but concurrently performed µSL study. Equal numbers of YFP-H and WT mice were used in graft repairs and only YFP-H mice used in conduit repairs and uninjured controls.

The groups for this chapter were: uninjured [n=7], graft [n=7 YFP-H and 7 WT] and SLS conduits [n=7].

6.2.4 SAMPLE SIZE CALCULATIONS

The sample sizes for this study were calculated using PiFace software [v1.76: *homepage.stat.uiowa.edu/~rlenth/Power*] with standard deviation data obtained from the M6P study discussed in the chapter 3.

6.2.4.1 Sample Size Choice and Justification.

Due to this study sharing controls with the µSL study the sample size chosen for the SLS conduit study was n=7 [see 5.2.4.1]. This would be sufficient to detect differences between groups of 35.25%, 12.62% and 7.98% for sprouting index [fig. 6.3], functional axon tracing [fig. 6.4] and axon disruption [fig. 6.5] respectively. For justification see section 4.2.3.1.

6.2.4.2 Sample Size Calculation Results.

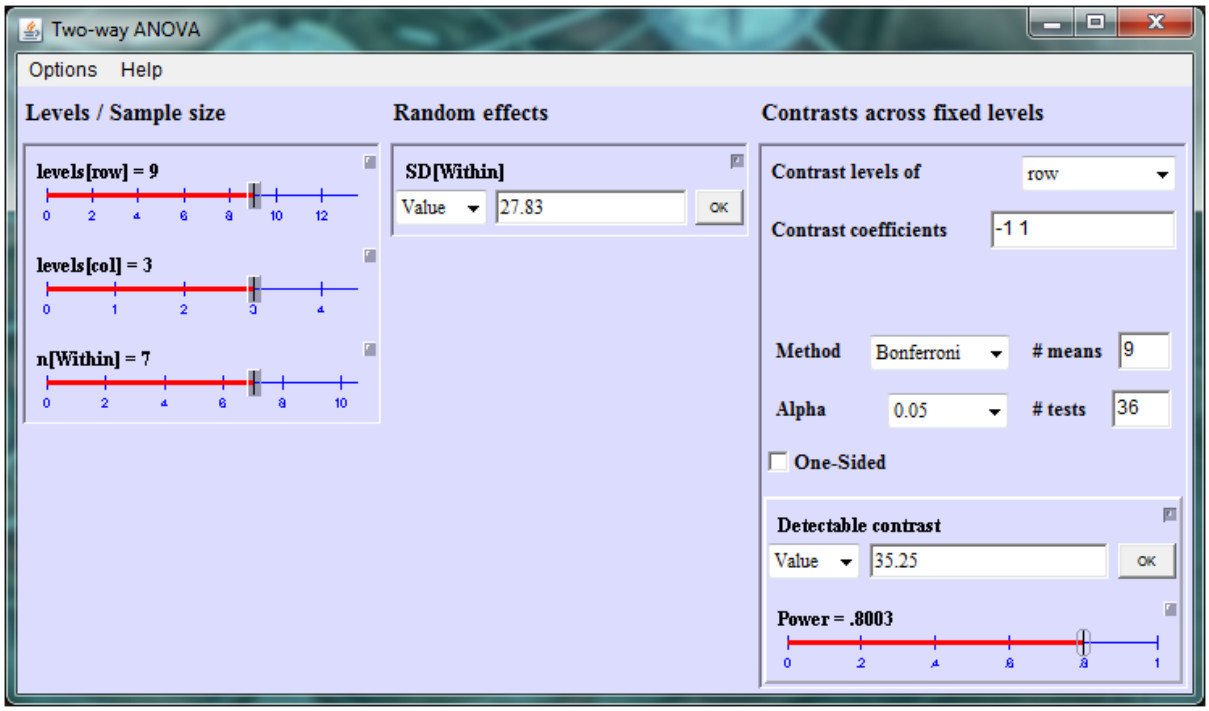

Figure 6.3: Sprouting index analysis power and detectable difference results for SLS conduit study when using a sample size of n=7. Levels[row] = number of intervals; levels[col] = number of groups; n[Within] = sample size; SD[Within] = standard deviation value derived from M6P study results. Number of intervals [# means] multiplied by number of repair groups minus one gives the number of t-tests required for the Bonferroni post-tests [# tests].

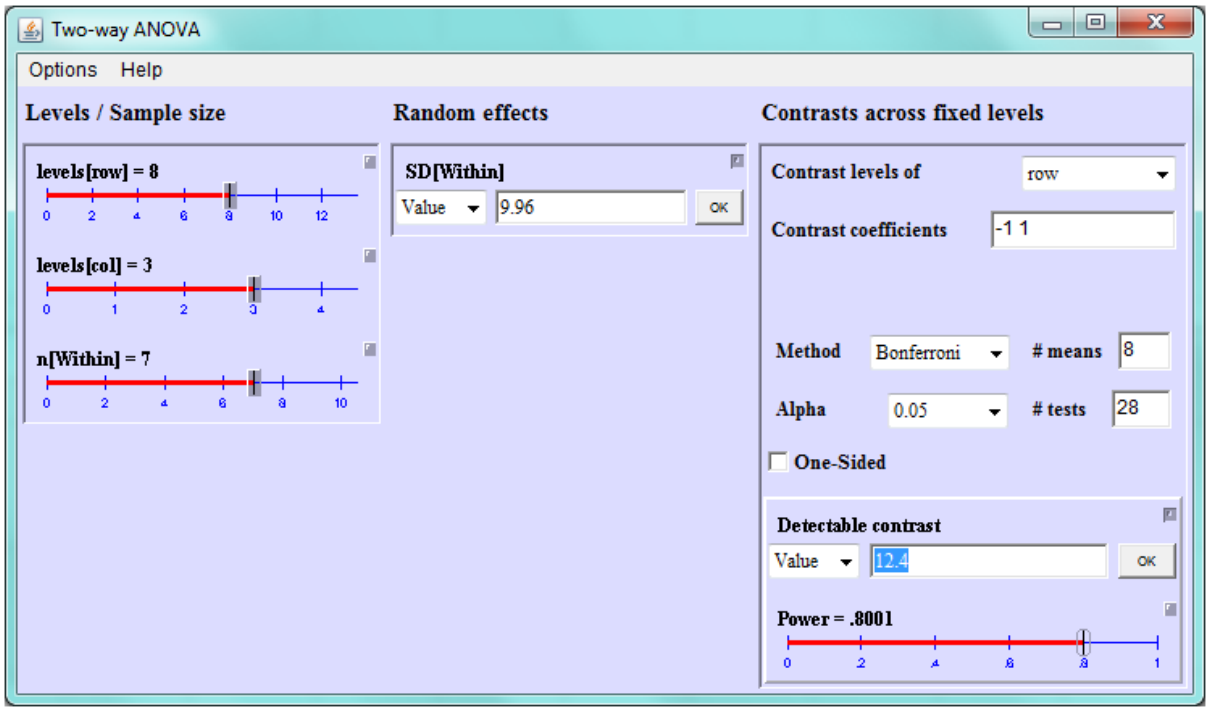

Figure 6.4: Functional axon tracing analysis power and detectable difference results for SLS conduit study when using a sample size of n=7. See fig. 43 for definitions.

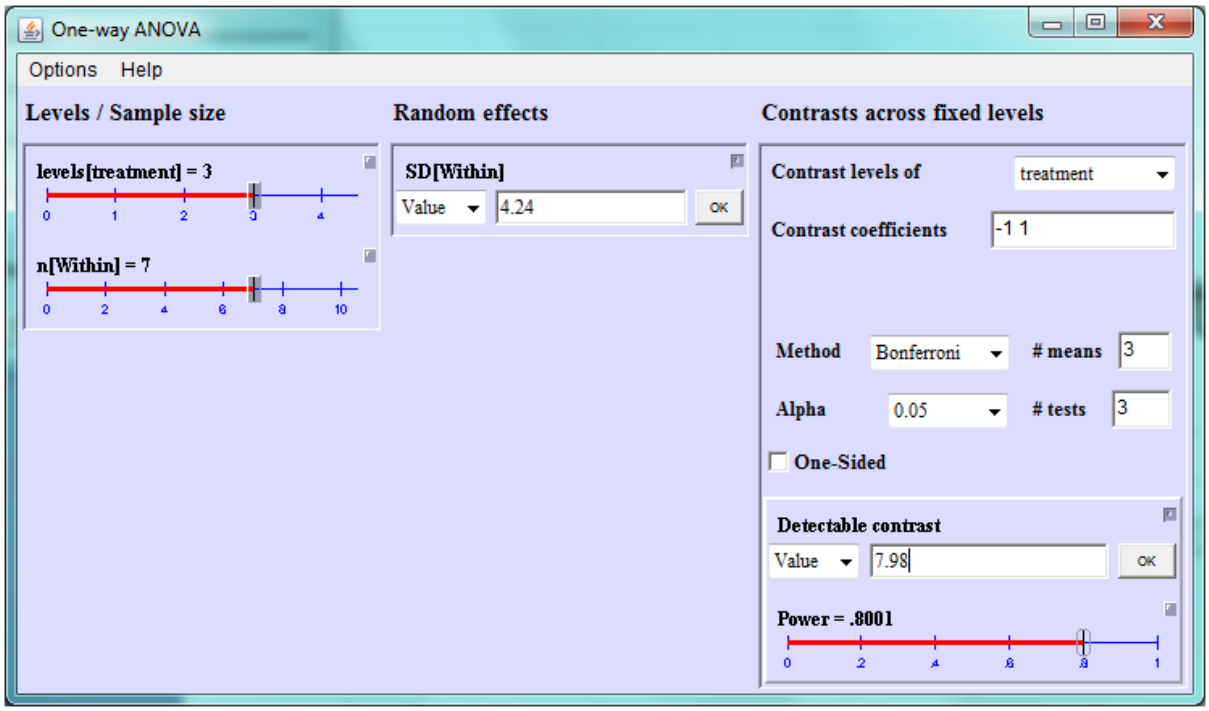

Figure 6.5: Axon disruption analysis power and detectable difference results for SLS conduit study when using a sample size of n=7. Levels[treatment] = number of groups; see fig. 43 for remaining definitions.

6.2.5 STATISTICAL ANALYSIS

Statistical analysis of the results described in this chapter was carried out as stated in section 2.3.3. All sprouting index and functional axon tracing results used 2-way ANOVA with Bonferroni post-tests; axon disruption results used a 1-way ANOVA with Bonferroni post-tests. Differences were considered to be significant when $p<0.05$.

6.3 RESULTS

The SLS process was able to produce conduits of a suitable size for use in repairing the mouse common fibular nerve. A range of different conduit sizes were produced in order to determine what size of conduits the SLS machine could produce best, with internal diameter and wall thickness proving more critical than length when considering viable designs.

When wall thicknesses below 0.5mm were trialled the powder compacted within the conduit lumen became too difficult to remove, this was also the case when internal diameters smaller than 0.8mm were trialled.

The final design choice of conduit size was 4mm long, with an internal diameter of 0.8mm and a wall thickness of 0.5mm. Due to resolution issues the actual internal diameter of the conduits used was reduced to approximately 0.6mm, with small increases to the wall thickness caused by additional powder becoming attached to the intended conduit wall.

6.3.1 QUALITATIVE DIFFERENCES BETWEEN GROUPS

All images obtained for SLS conduits were similar in appearance, with most axons only extending a short distance - less than 1.5mm - out from the central nerve ending and displaying limited sprouting [fig. 6.6]. Additionally, loose nylon-12 powder - visible as clumps of a light haze - was observed within the repaired nerve tissue [fig. 6.6]. In all cases the appearance was markedly different to graft repairs [fig. 6.7]

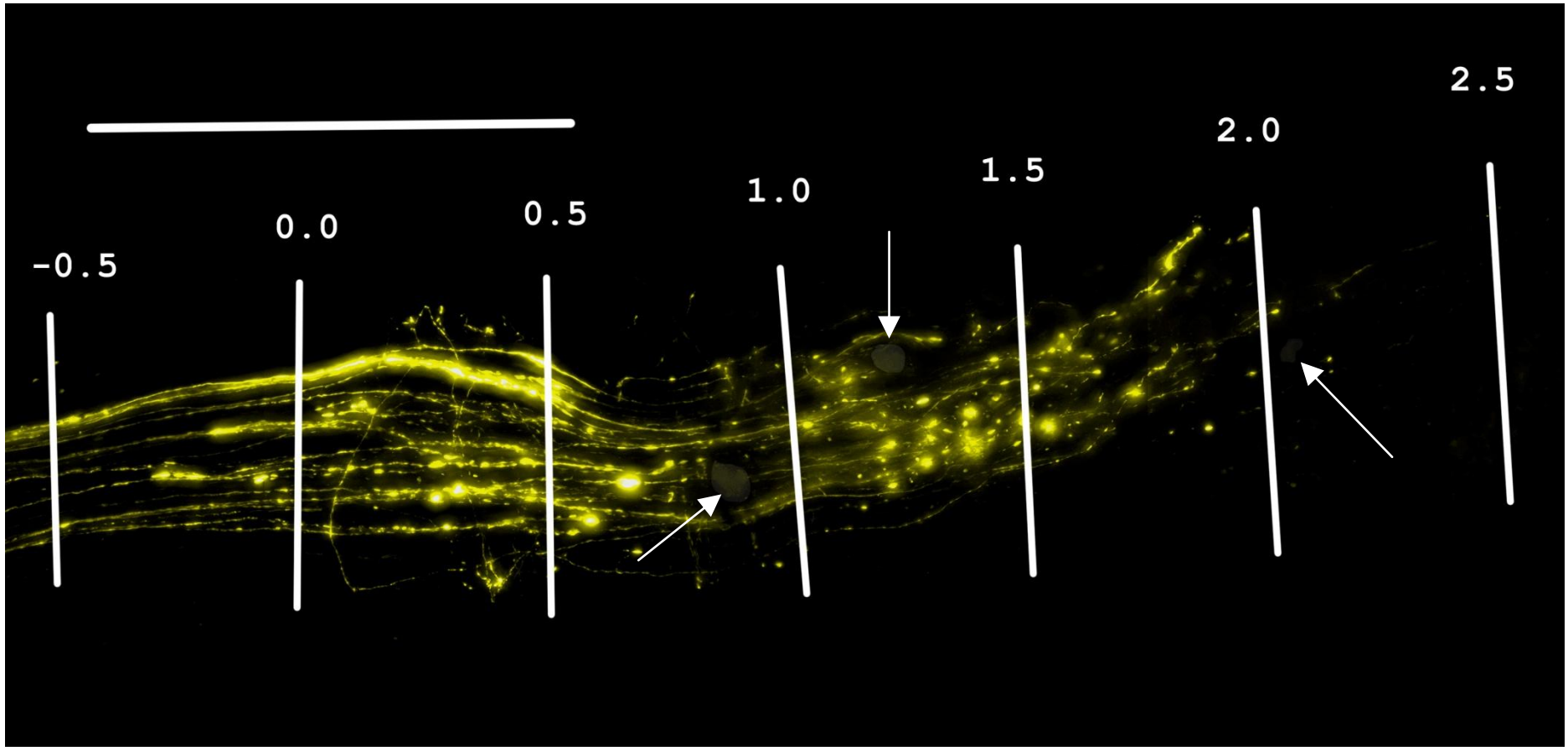

Figure 6.6: Typical SLS conduit repair image with intervals marked. Areas of loose nylon-12 powder can be seen around the axons [examples marked by white arrows]. Scale bar = 1.0mm.

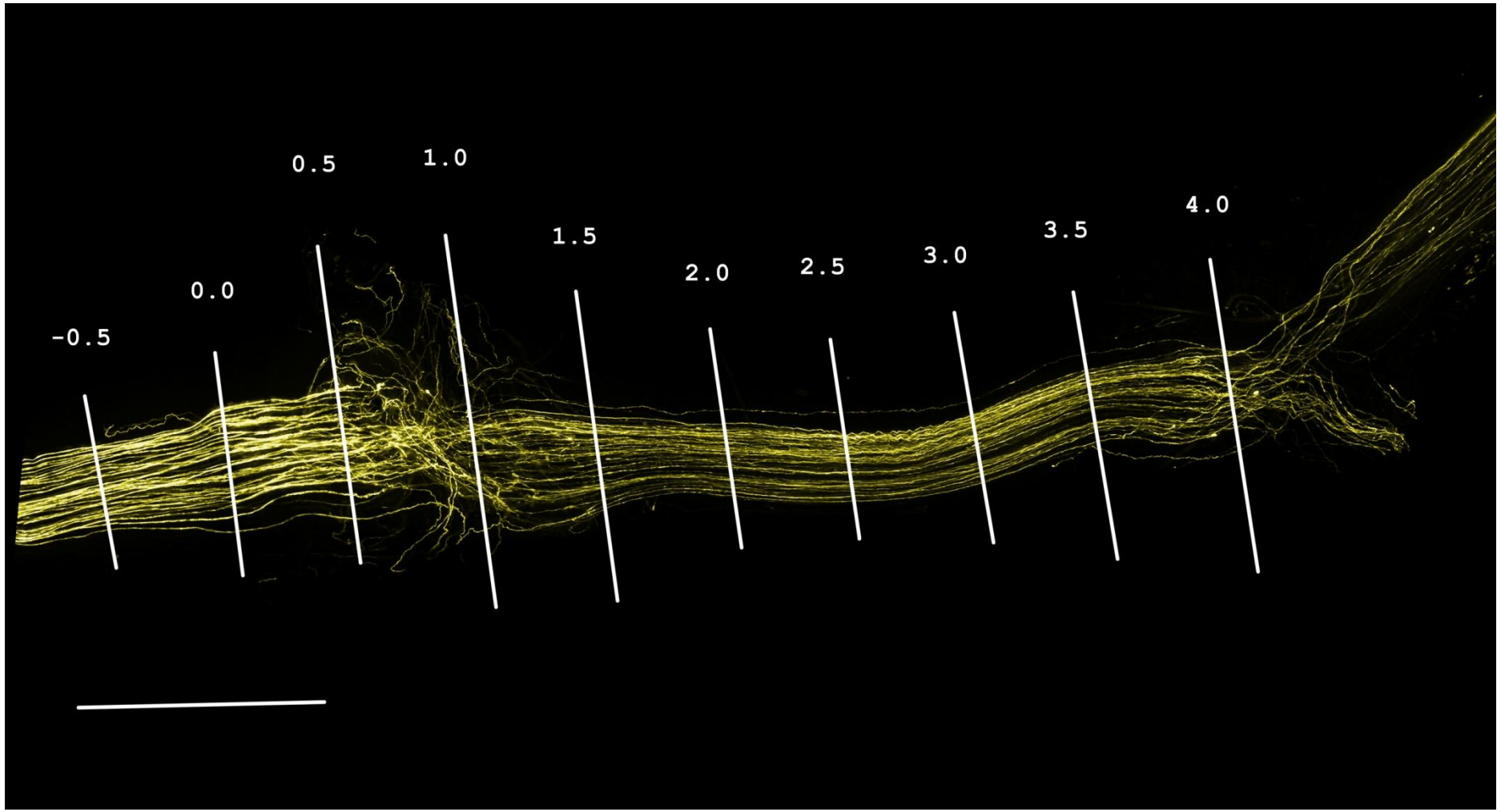

Figure 6.7 [repeat of 5.8]: Typical graft repaired nerve image with intervals marked. Scale bar = 1.0mm.

6.3.2 SPROUTING INDEX RESULTS

Sprouting index levels for SLS conduits ranged from 0.0% to 140.3% [table 6]. The maximal sprouting index level for the SLS conduits - as in grafts - was at the 0.5mm interval, where the level was significantly higher than uninjured controls [$p<0.001$][fig. 6.8]. Unlike in the graft repairs, the sprouting index levels in the SLS conduits fell markedly at the subsequent 1.0mm interval back to near uninjured levels and significantly lower than the level observed for graft repairs [$p<0.001$][fig. 6.8]. At the 1.5mm interval the sprouting index level for SLS conduits fell again, becoming significantly lower than uninjured levels [$p<0.001$] while remaining significantly lower than graft repairs [$p<0.05$][fig. 6.8]. At all remaining intervals the SLS conduit sprouting index levels were significantly lower than in both graft and uninjured groups [$p<0.001$], with levels falling to almost zero at the 3.0mm interval and then reaching zero for the final two intervals.

Table 6: Sprouting index levels for SLS, vehicle and uninjured groups [%].

Repair Position (mm)	Average Sprouting % (SLS)	SEM	Average Sprouting % (Graft)	SEM	Average Sprouting % (Uninjured)	SEM
-0.5	100	0.0	100.0	0.0	100.0	0.0
0	107.6	5.7	111.3	4.1	98.3	1.9
0.5	140.3	14.1	162.4	15.2	95.7	1.1
1	90.1	13.1	148.2	12.3	98.0	1.4
1.5	61.7	15.1	113.0	13.8	94.7	2.1
2	26.4	6.4	105.6	9.0	95.7	1.1
2.5	7.1	2.9	95.4	3.5	95.7	2.2
3	0.7	0.7	93.7	7.0	97.7	2.5
3.5	0.0	0.0	78.4	10.0	97.7	1.5
4	0.0	0.0	64.8	7.6	97.4	1.9

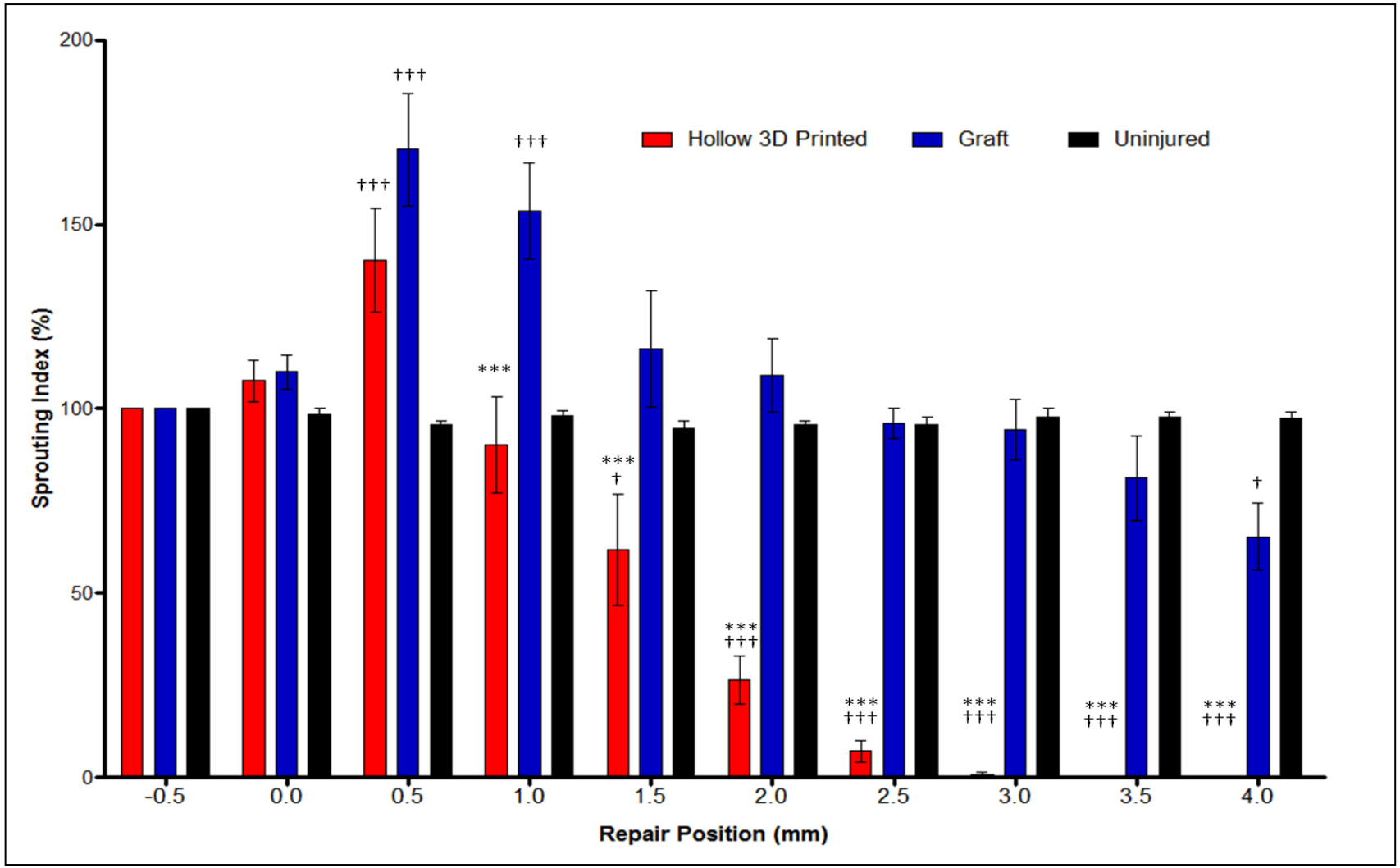

Figure 6.8: Sprouting index levels at 0.5mm intervals along the repairs; * denotes significant difference compared to graft repairs, *p*<0.001; ††† denotes significant difference compared to uninjured controls. Statistical test: 2-way ANOVA with Bonferroni post-tests.**

6.3.3 CHANGE IN SPROUTING INDEX BETWEEN INTERVALS

The maximum increase in sprouting levels occurred at between the 0.0mm and 0.5mm intervals in both SLS conduit and graft repairs, with this increase significantly higher than the uninjured group [$p<0.01$ and $p<0.001$ respectively][fig. 6.9].

The largest decrease in sprouting index level in the SLS conduit group occurred between the 0.5mm and 1.0mm intervals, this decrease was significant compared to both graft repairs [$p<0.01$] and uninjured group [$p<0.001$][fig. 6.9]. This decrease in the SLS conduit group occurred earlier than the equivalent decrease in the graft group, which occurred between the 1.0mm and 1.5mm intervals [fig. 6.9]. An additional significant decrease [$p<0.01$, compared to uninjured] was observed in the SLS conduit group between the 1.5mm and 2.0mm intervals [fig. 6.9].

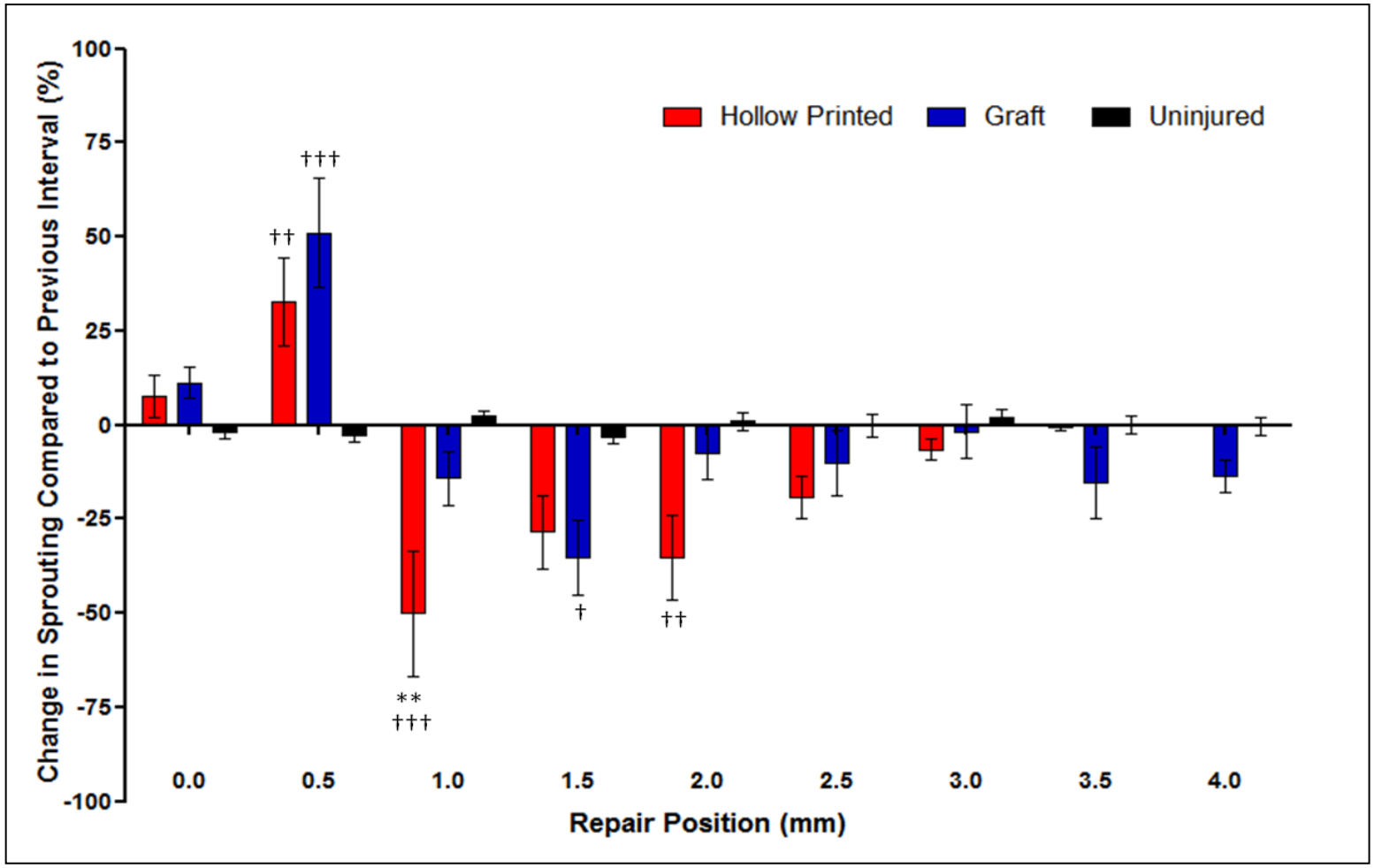

Figure 6.9: Changes in sprouting index levels at each 0.5mm interval compared to the previous interval; ** denotes significant differences in level compared graft repairs, *p*<0.01; †, †† and ††† denote significant differences in level compared to uninjured controls, *p*<0.05, *p*<0.01 and *p*<0.001 respectively. Statistical test: 2-way ANOVA with Bonferroni post-tests.

6.3.4 FUNCTIONAL AXON TRACING

Significantly fewer individual start axons were present from the 1.5mm interval onwards in the SLS conduit group compared to the graft group [$p<0.05$ at 1.5mm and $p<0.001$ at 2.0mm to 4.0mm][fig. 6.10]. As no axons had reached either the 3.5mm or 4.0mm intervals the proportion of start axons at these intervals was obviously zero.

Unlike in the graft group - where the start axon percentage first became significantly lower than in the uninjured group at the 1.0mm interval [$p<0.001$] - the start axon percentages for the SLS conduit group were significantly lower immediately at the 0.5mm interval [$p<0.05$][fig. 6.10]. Start axon percentages for the SLS conduit group, along with the graft group, were then significantly lower than the uninjured group from the 1.0mm interval onwards [$p<0.001$][fig. 6.10].

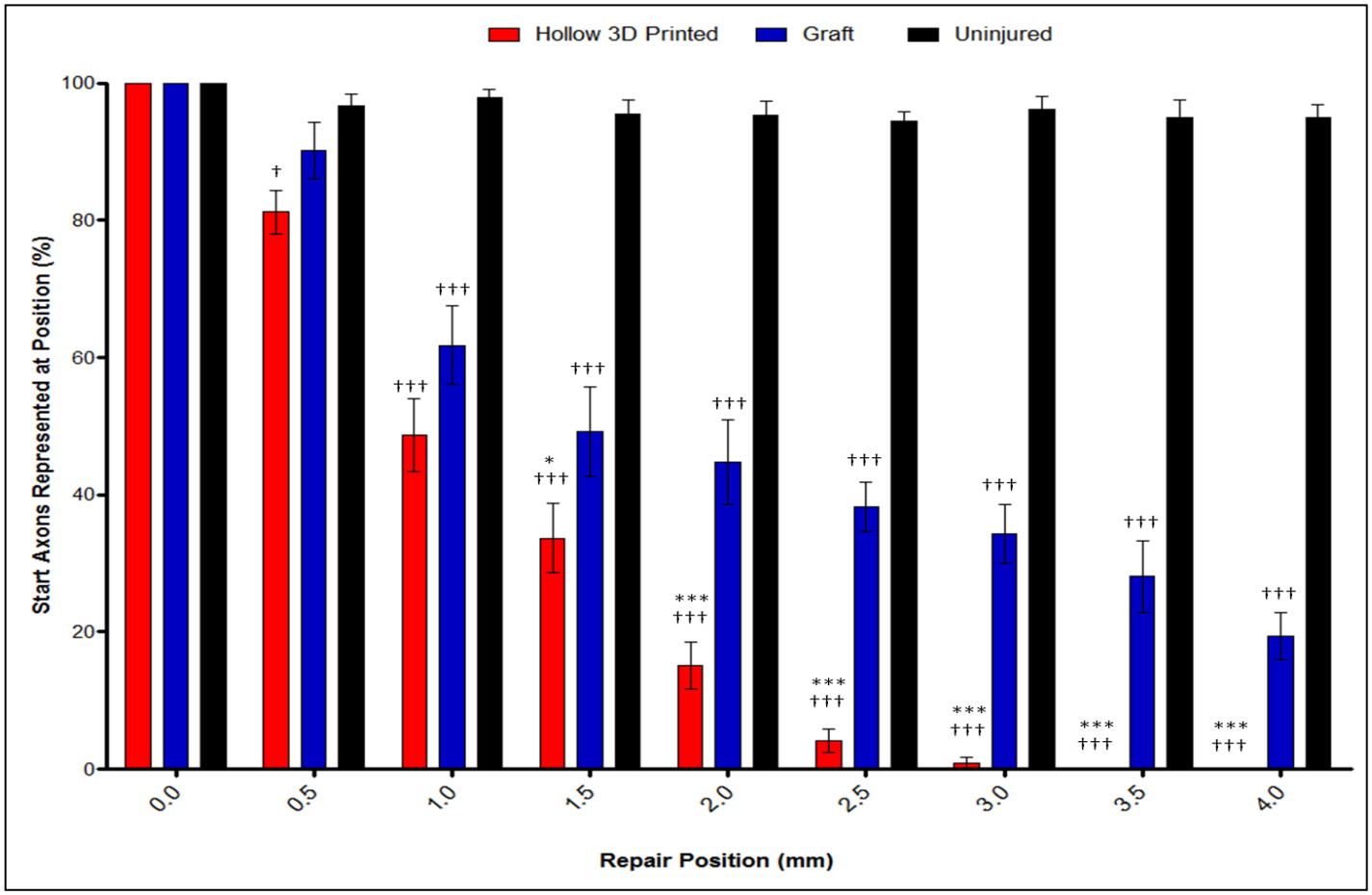

Figure 6.10: Percentages of start axons represented at subsequent 0.5mm intervals; * and * denote significant difference compared to graft repairs, *p*<0.05 and *p*<0.001 respectively; † and ††† denote significant difference compared to uninjured controls, *p*<0.05 and *p*<0.001 respectively. Statistical test: 2-way ANOVA with Bonferroni post-tests.**

6.3.5 AXON DISRUPTION

No significant differences were detected between the SLS conduit and graft groups in terms of increased axon length across the initial repair disruption [$p>0.05$][fig. 6.11].

Axon length increases across the initial repair disruption in both repair groups were significantly higher than for the uninjured group [$p<0.05$][fig. 6.11].

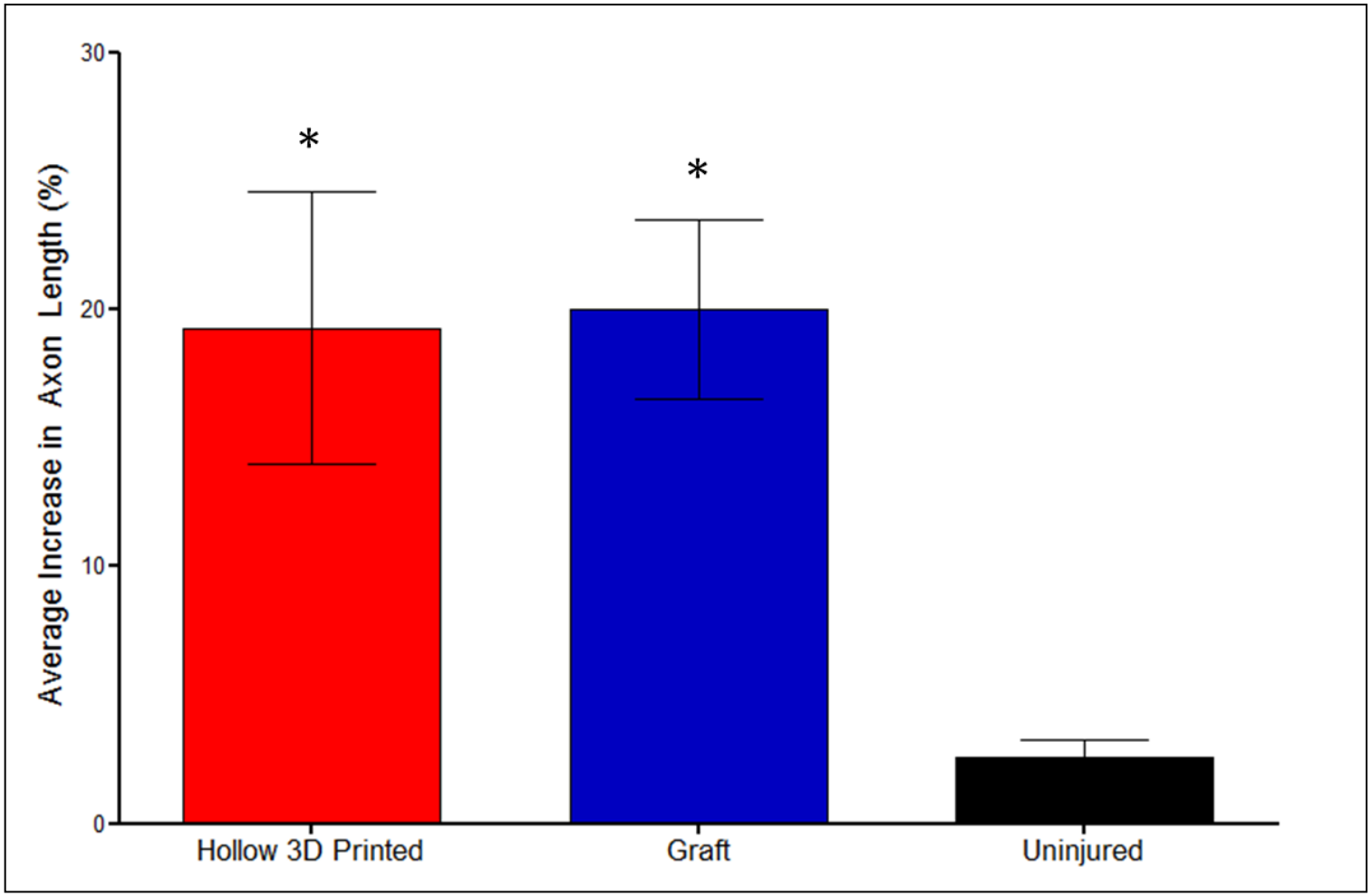

Figure 6.11: Percentage increase in axon length across the initial 1.5mm of repair; * denotes significant difference compared to uninjured controls, *p*<0.05. Statistical test: 2-way ANOVA with Bonferroni post-tests.

6.4 DISCUSSION

6.4.1 VISUAL DIFFERENCES

The major differences between SLS conduits and grafts were obvious from visual images alone, with axons only regenerating part-way into the SLS conduits and none reaching the distal nerve ending in any SLS conduit repair [figs. 6.6 and 6.7].

One interesting observation noted on the images of nerves repaired with SLS conduits was the inclusion of opaque specks within the regenerated tissue and around the axons [fig. 6.6]. These specks were considered to be unsintered nylon-12 powder from the conduits.

The potential presence of unsintered nylon-12 powder remaining after production was known about prior to implantation, as SLS conduits required packed powder to be removed from the conduit lumen. This powder was removed by flushing conduits with 70% IMS using a hypodermic needle, with conduits then thoroughly rinsed with alcohol to remove remaining powder. Based on what can be seen in SLS conduit images, and also observations made at the time that nerves were extracted from the conduits, it would appear that the procedure to remove loose nylon-12 powder was unsuccessful.

6.4.2 DIFFERENCES IN SPROUTING INDEX

Sprouting index levels in SLS conduits were similar to those in graft repairs at the start [0.0mm] and 0.5mm intervals and significantly higher than uninjured controls at the 0.5mm interval [fig. 6.8]. The increase in sprouting index at the 0.5mm interval in SLS conduits, while not quite as large as that in grafts, was still significantly greater than uninjured controls [fig. 6.9].

The similarity to grafts did not extend beyond the 0.5mm interval indicating that - as the 0.5mm interval is considered to be the point where axons have recently exited the central nerve ending - regeneration began to fail almost immediately once axons entered the

conduit. At the 1.0mm interval the sprouting index levels for SLS conduit repairs significantly decreased compared to both graft repairs and uninjured controls [fig. 6.9] and were significantly lower than the level in graft repairs overall [fig. 6.8]. Sprouting index levels continued to decline in SLS conduit repairs at subsequent intervals, being significantly lower than both graft repairs and uninjured controls at all remaining intervals, with only a few axons at the 3.0mm interval and no axons regenerating any further [fig. 6.8].

Taken together with the visual observations these results strongly suggest that something in the SLS conduit design has either an inhibitive effect on regeneration or considerably slows the rate of regeneration. Comparing the SLS conduits to the hollow µSL conduits that performed equally to graft repairs [see section 5.3.2], three clear differences are present: the material conduits are made from [notably the presence of unsintered powder], the internal diameter of the conduit and the thickness of the conduit walls.

The difference in material is unlikely to have caused such a decline in performance, as the SLS material [nylon-12] is generally considered to be a biologically inert material (Williams and Blayney, 1987). However, the presence of unsintered micro-particles of nylon-12 within the conduit and the fact that these particles have been incorporated within the regenerating tissue is much more likely to have an adverse effect.

The size of conduit produced by SLS was close to the limit achievable by the SLS machine, resulting in the specified design sizes and actual conduit sizes differing in terms of wall thickness and lumen diameter. Additionally, the internal diameter used was the maximum possible - due to the required wall thickness - that allowed the conduits to be of a suitable size for implantation in the repair location. The SLS conduit design used stated a 0.8mm lumen diameter with a 0.5mm thick wall; however, once the nylon-12 powder blocking the lumen was removed the actual lumen diameter was approximately 0.6mm [a 0.6mm gauge needle could be pushed through with force], much smaller than the internal diameter in the µSL [1.0mm].

One issue that has been noted in both experimental and clinical conduit repairs [along with general studies on nerve regeneration] is that when the regenerating nerve is compressed or constricted by the conduit, regeneration is adversely impacted and/or localised pain necessitates the removal of the conduit (Krarup and Gilliatt, 1985, Krarup et al., 1988, Itoh et al., 2002). This is a particular problem in non-degradable conduits such as silicone tubes (Lundborg et al., 1997, Dahlin et al., 2001, Lundborg et al., 2004), as due to increases in the myelination of axons occurring over time the axons become constrained by the size of the conduit (Schlosshauer et al., 2006). Additionally, as noted in section 3.3.1, tying a suture tightly around the end of the sectioned central nerve ending completely prevents regeneration from occurring.

The ideal internal diameter of conduits is debateable, with early studies indicating a diameter 2.5 to 3 times the size of the nerve (Ducker and Hayes, 1968) and more recent studies claiming 1.3 times the size of the nerve to be suitable (Lundborg et al., 2004). Considering that the diameter of the mouse common fibular nerve is typically around 0.35mm [based on surgical and microscope observations] and in many of the graft repairs the width of the nerve was observed to increase to ~0.8-1.0mm, then it does seem likely that regenerating nerves within SLS conduits were constrained to some degree by the conduits. Although as some axons have managed to regenerate partially across the repair, the level of compression from the conduit is probably sufficient to restrict the regeneration of many, but not all, axons [fig. 6.12].

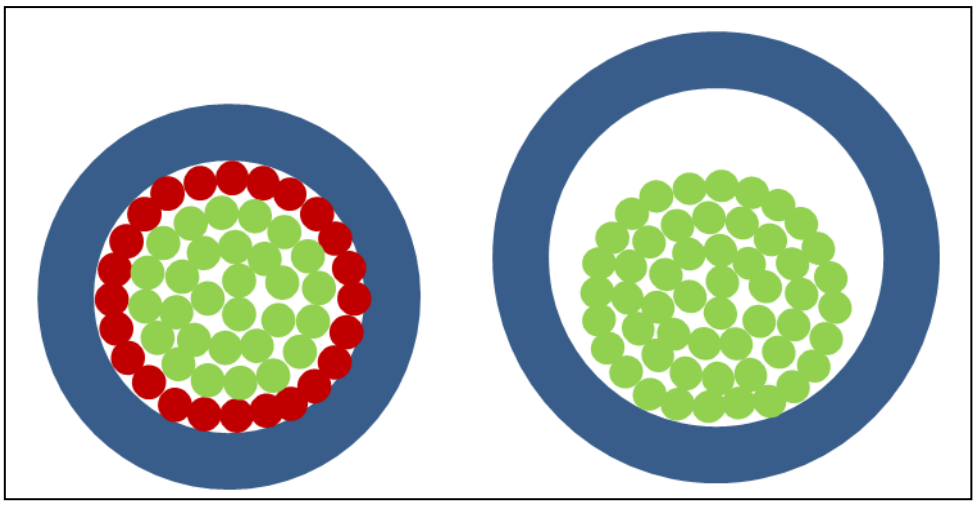

Figure 6.12: Effects of conduit compression on nerve regeneration. Left: Narrow internal diameter of conduit [blue] constricts regenerating nerve, impeding regeneration of outer axons [red] while inner axons [green] are cushioned by connective tissue. Right: Wider internal diameter allows nerve to regenerate unimpeded.

The reduced internal diameter for SLS conduits indicates that the wall thickness is at least 0.65mm, with a strong possibility that additional material was also added to the outer portion of the wall further increasing the wall thickness. The detrimental effects of thicker conduit walls have been established for many decades, with Ducker and Hayes (1968) noting that thicker-walled conduits [1.65mm] resulted in neuroma build up at both central and distal nerve endings, an effect absent in thinner-walled conduits [0.13mm]. Den Dunnen et al. (1995, 1998) have also reported on the detrimental effects of thicker walled conduits; however, in those cases the detrimental effects were caused by the swelling of the conduit material constricting the regenerating nerves.

In most other cases thick conduit walls have a negative effect on regeneration by limiting the exchange of nutrients and neurotrophic factors between the conduit interior and surrounding tissues (Kokai et al., 2009). As all conduits used in the studies discussed in this chapter and chapter 5 were considered non-porous the poor level of regeneration in SLS conduits is unlikely to be due to this effect. A possible physical effect of the thicker conduit walls in SLS conduits is that the sectioned nerve endings are positioned at a steeper angle when entering the conduits [fig. 6.13], this may increase the pressure on the nerve at the edge of the

conduit, causing a similar effect to compression on the nerve at that site [see above for discussion on effects of excess compression on regeneration].

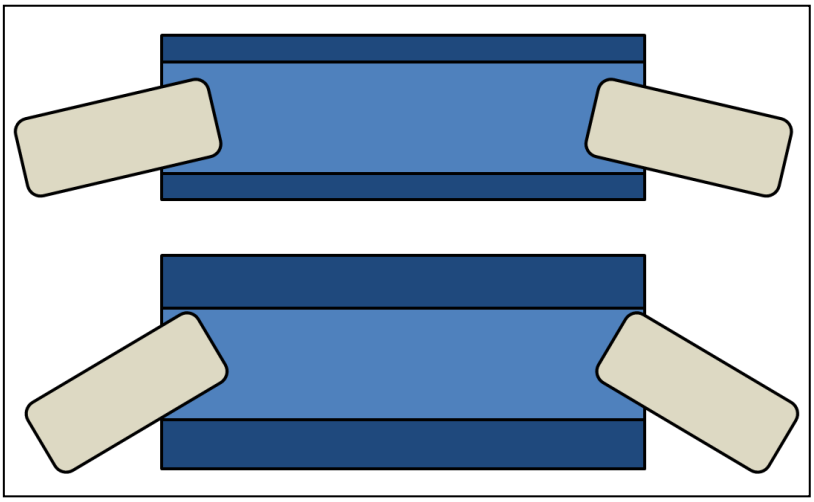

Figure 6.13: Representation of the impact of conduit wall size on sectioned nerve ending positioning.

6.4.3 FUNCTIONAL AXON TRACING.

Due to the lack of axons regenerating through to the latter portions of the SLS conduits only the proportions of unique axons at the first few intervals are of any real interest for comparing to grafts.

It is difficult to directly compare the significant differences displayed in these results with those in the previous chapter due to the effects on statistical analysis of different numbers of groups in each study. Additionally, the differences in conduit sizes between the µSL and SLS studies is likely to impact on the ability to compare differences between the studies. However, it is interesting to note that while both hPEG and SLS conduit repairs have a lower [though not significant] sprouting index level than graft repairs at the 0.5mm interval, the proportion of unique axons at that interval in SLS repairs was lower than in grafts and significantly lower than uninjured controls but in hPEG repairs the proportion remained at a similar level to grafts [figs 5.16 and 6.10].

The immediate loss of unique axons in SLS conduit repairs suggests that axons are failing to regenerate immediately after exiting the central nerve ending, rather than simply regenerating slower than grafts. As discussed in section 6.4.1.2, compression of the regenerating nerve can adversely affect regeneration, this compression may also impact upon the proportion of unique axons regenerating into the SLS conduits. Regenerating axons at the outer edges of the nerve are more likely to be impacted by compression due to having a lower quantity of connective tissue surrounding and protecting them [fig. 6.12]. Conversely, the regenerating axons closer to the centre of the nerve will be less impacted by any compression due to a greater quantity of surrounding connective tissues and other axons protecting them [fig. 6.12].

This selective inhibition of axons would be more likely to result in greater loss of unique axons early in the repairs than an effect causing indiscriminate inhibition of axons. This would be due to individual axons and their sprouts being closer together at earlier points in the repairs, increasing the chance of all sprouts of one axon being inhibited.

6.4.4 INITIAL AXON DISRUPTION.

That disruption across the initial 1.5mm of repairs in SLS conduits is the same as in grafts shows that, despite having no clear structural obstacles in their path [such as graft scar tissue and endoneurial tube location], axons were still diverted to a similar degree as grafts.

With SLS conduits being of a similar design - although with different dimensions - to the hollow µSL conduits used in the chapter 5 study [i.e. single lumen hollow tubes], the disruption levels should, hypothetically, be similar to those conduits. However, in the µSL study both hollow conduit designs were not considered to have significantly increase axon lengths compared to uninjured controls across the initial portion of repairs and had lower [though not significantly] increases compared to grafts [see section 5.3.5].

The presence of loose nylon-12 powder within the regenerating nerve tissue [fig. 6.6] may have had an influence on the paths taken by regenerating axons. The images obtained from SLS conduit repairs indicate that clusters of the powder were situated throughout the repairs, which would have created numerous obstacles for regenerating axons to navigate around.

6.4.5 CONCLUSIONS

It is clear from the results presented here that at the current time the SLS process is not suitable for producing nerve guide conduits. This is due to issues with size tolerance, conduit quality and available materials.

One important issue was that the actual internal diameters of the SLS conduits were smaller than the designs had called for, potentially compressing the regenerating nerves and retarding axon regeneration. The internal diameter size had been specified as being 0.8mm with 0.5mm wall thickness to give an outer diameter of 1.8mm - which was the largest that could be suitably positioned in the repair area. When wall thicknesses below 0.5mm were trialled the internal diameters were severely reduced and in some cases entirely blocked.

As the minimum wall thickness was limited by the production method, any increase in internal diameter would result in a larger outer diameter conduit. The size of the conduits used in both SLS and µSL studies [see chapter 5] was close to the limit of what could be implanted using the common fibular nerve injury model and required the minimum age of mice at setup time to be increased from 8-weeks [used in M6P and EC23 studies] to 12-weeks to allow mice to grow to a sufficient size. As such any increases in conduit size would risk causing the mice undue discomfort and increase the risk of the conduit becoming dislodged by the movement of the joint.

Another issue is that nylon-12 powder came loose from the conduit and became absorbed into the regenerating nerve tissue. This would appear similar to an issue in SLS commonly termed the 'orange peel' phenomenon, where surfaces of manufactured objects have an

undesirable rough texture. This effect is generally considered to be caused by the use of powder that had previously been used but not sintered - though supplementing the used powder with new can bring it back up to acceptable levels [48-50% new powder](Dotchev and Yusoff, 2009).

However, in the study discussed here a 50/50 blend of new and used powder was used, which should have prevented the 'orange peel' effect. This suggests that the loose powder could have been an effect caused by the SLS machine used to produce the conduits being near the limit of its resolution when producing such small sized objects.

Finally, although nylon-12 is considered biologically inert (Williams and Blayney, 1987), it does not fit with the desired properties of an artificial nerve guide - it is rigid, non-bioabsorbable and non-porous, where the opposite is considered desirable (Ciardelli and Chiono, 2006). Nylon-12 [also referred to as polyamide-12] is currently the standard material in SLS when using commercially available SLS machines such as the EOS Formiga P100 used in this study (Johnson et al., 2013). Although other materials can be used in SLS [e.g. PCL, nano-hydroxyapatite, calcium phosphate (Bose et al., 2013)] there is a tendency for 'in house' purpose built SLS machines to be used rather than commercially available ones (Chen et al., 2014).

Despite the poor results of this study, SLS manufacturing of conduits may still be of use in the future. Though in order to be able to provide suitable conduits it is critical that more biologically favourable materials can be found to work within the SLS process and that manufacturing tolerances can be improved significantly.

7.0 GENERAL DISCUSSION

The aim of this chapter is to:

- Summarise the previous studies YFP-H mice [sections 7.1.1].
- Discuss observations on the use of YFP-H mice within the studies contained within this thesis [section 7.1.2]
- Discuss possible future work that could lead on from the studies contained within this thesis [section 7.2]
- Give a general conclusion on the use of the YFP-H mouse common fibular nerve injury model [section 7.3].

7.1. USE OF THE *THY-1-YFP-H* MOUSE STRAIN

The previous uses of the YFP-H mouse strain and its performance in the studies discussed in this thesis will be discussed in this section, the generation of this strain and others is discussed in section 1.8.4.

7.1.1 PREVIOUS STUDIES USING *THY-1-YFP-H* MICE

Amongst all of the transgenic mouse strains generated by Feng et al. (2000), the *thy-1-YFP-H* strain is by far the most utilised - with the laboratory of Arthur W. English responsible for a significant number of studies using the strain (English et al., 2005, Groves et al., 2005, Sabatier et al., 2008, English et al., 2011).

The study by Groves et al. (2005), which investigated the effects of proteoglycan degradation on peripheral nerve regeneration, was used as the basis for the development of the model used in the studies described within this thesis. Groves et al. (2005) harvested graft tissue from both CF nerves of WT mice and soaked tissue from the left CF nerve in 10µl of PBS and tissue from the right CF nerve in 10µl of chondroitinase ABC, keratinase, heparinase I or heparinase III. The graft tissue was allowed to soak for one-hour prior to

being used to repair both CF nerves in YFP-H mice, the graft tissue was secured using equal ratios of fibrinogen, fibronectin and thrombin and once the surgical site was closed the mice were allowed to recover for one-week. Following recovery the repaired nerves were exposed and fixed *in situ* prior to being removed and placed on slides for imaging.

The analysis methods used by Groves et al. (2005) were based around the number of axons regenerating and their length. The first method compared the number of axons prior to the injury with the number of axons that had entered the graft, creating a single point sprouting index (Groves et al., 2005). The axon length analysis was presented in a more complex manner, but essentially measured the entire profile length of the axons entering the graft and presented these as cumulative percentage of axons against axon lengths, and percentage of all axons reaching four different lengths [100, 200, 500 and 1000µm]. In terms of the outcomes of these analyses, Groves et al. (2005) considered increased single point Sprouting index levels and a greater proportion of longer axons to represent improved regeneration. They concluded that treatment with chondroitinase or heparinase I improved regeneration due to significantly higher proportions of axons longer that 1000µm being present in those repairs and the significantly higher sprouting index result in heparinase I treated repairs [both compared to PBS treated repairs](Groves et al., 2005).

In addition to the results reported as the main objective for their study [effects of proteoglycan degradation on nerve regeneration], Groves et al. (2005) also reported on some aspects of the YFP labelling in the YFP-H mouse strain. By investigating the makeup of the appropriate dorsal and ventral roots [those at L4 and L5] Groves et al. (2005) were able to determine that significantly more sensory axons [58%] were labelled with YFP than motor axons [42%], and that the profile of neurone sizes was skewed towards medium and large sized neurones in the YFP labelled population.

However, a separate study by Witzel et al. (2005) - which investigated the pathway sampling of axons regenerating through a sciatic nerve graft - reported that 72% of YFP labelled

axons in the sciatic nerve were sensory, with motor axons making-up 28%. Both Witzel et al. (2005) and Groves et al. (2005) used relatively low numbers of YFP-H mice [4 and 3 respectively] which may have introduced some discrepancy between the two studies, though the pattern of YFP labelling is reportedly unchanged between mice of the same transgenic strain (Feng et al., 2000).

A more likely cause for the discrepancy in sensory/motor neurone labelling ratios between the studies by Witzel et al. (2005) and Groves et al. (2005) is how each study investigated this. Witzel et al. (2005) used Fluoro-Gold retrograde labelling in order to dual-label any YFP labelled neurons with axons in the sciatic nerve, they then fixed and sectioned [40µm] the appropriate dorsal and ventral root sections and counted any double labelled neurons. Groves et al. (2005) instead whole mounted the dorsal and ventral roots and used confocal microscopy to acquire images of 10µm sections through the entire thickness of the mounted tissue. Of the two methods, that of Witzel et al. (2005) appears to have the greater potential for error - with the thicker sections perhaps obscuring the fluorescence of some neurones or the fact that sections were physically sectioned contributing to possible error. Indeed, issues with differing tissue shrinkage between nerve sections were reported to have prevented the counting of axons across the sciatic nerve injuries within the study by Witzel et al. (2005). Though how these sort of errors would lead to selective bias against detection of YFP labelled motor neurones is unclear, as any obscuring of neurones would be expected to be random in both dorsal and ventral roots.

Discrepancies when investigating the patterns of YFP labelling do appear unexpectedly common between studies using YFP-H mice. The earliest published study that utilised YFP-H mice, which investigated the potential for the strain to be used as a tool for investigating Wallerian degeneration (Beirowski et al., 2004), differed again to both Groves et al. (2005) and Witzel et al. (2005) when reporting on YFP labelling.

The study by Beirowski et al. (2004) reported no significant difference between the ratio of YFP labelled sensory and motor axons from the L4 dorsal and ventral roots [55% sensory to 45% motor] - closer to the ratio reported by Groves et al. (2005) [58% to 42%] than that reported by Witzel et al. (2005) [72% sensory to 28% motor]. However, unlike the study by Groves et al. (2005), Beirowski et al. (2004) reported much lower YFP labelled axon numbers overall - an average of 30.5 in the L4 dorsal root and 24.5 in the L4 ventral root, compared to the 122.6 and 87.2 respectively reported by Groves et al. (2005). This four-fold difference between the studies is difficult to understand but is unlikely to be due to variations between mice within the strain - as this would show up in both studies as extremely large error values - so must be due to either a difference in techniques or investigator error. The main difference reported in the techniques used by Beirowski et al. (2004) and Groves et al. (2005) to fix, harvest and image the dorsal and ventral roots was that following transcardial perfusion of the mice and tissue harvesting, Beirowski et al. (2004) proceeded to further process the tissue prior to whole mounting, whereas Groves et al. (2005) proceeded directly to whole mounting the tissue.

In addition to the large differences in YFP labelled axons reported in the L4 dorsal and ventral roots by Beirowski et al. (2004) and Groves et al. (2005), there is a notable difference between the studies in terms of the number of YFP axons reported in the sciatic nerve. Although only Beirowski et al. (2004) actually reported the quantity of YFP labelled axons in the sciatic [28.5 ±8.3 SEM], the number of YFP axons that Groves et al. (2005) reported in the CF nerve [36.02 ±2.35] - a branch of the sciatic - makes it clear that, again, there is a large discrepancy between the findings of the two studies. Again it is unclear why Beirowski et al. (2004) appear to be observing consistently lower YFP labelled axon numbers than Groves et al. (2005), despite using similar techniques. Considering that for the studies discussed within this thesis, the average number of YFP axons observed in the CF nerve prior to the injury site [~30] was similar to that reported by Groves et al. (2005), it would

appear that something in the experimental setup used by Beirowski et al. (2004) prevented them from observing all YFP axons that were present.

As mentioned at the start of this section, the laboratory of Arthur W. English has been responsible for a large proportion of the studies utilising the *thy-1-YFP-H* mouse strain. The study by Groves et al. (2005) was the second using this particular strain that they had published, following shortly after a study demonstrating that neurotrophin-4/5 is required during peripheral nerve regeneration (English et al., 2005). In that study, English et al. (2005) used graft tissue from wild-type, neurotrophin-4/5$^{-/-}$, neurotrophin-4/5$^{+/-}$ and BDNF$^{+/-}$ mice to repair CF nerve injuries in YFP-H mice. English et al. (2005) concluded that regeneration through both neurotrophin-4/5$^{-/-}$ and neurotrophin-4/5$^{+/-}$ grafts was significantly worse than through wild-type grafts.

As with the study by Groves et al. (2005), English et al. (2005) used a single point sprouting index and cumulative profile lengths of the axons entering the graft to assess the differences between repairs. Also used was the percentage of axons of different profile lengths, presented as a histogram with 100µm bin sizing.

Studies by the same group include a number investigating the effects of treadmill training, starting with Sabatier et al. (2008) reporting its beneficial effects on nerve regeneration and later following up with studies looking at the effects of neurotrophin-4/5 (English et al., 2011), BDNF (Wilhelm et al., 2012) and sex differences (Wood et al., 2012) in combination with treadmill training.

Other laboratories have also successfully used YFP-H mice in a wide range of study types. In investigations of peripheral nerve regeneration using YFP-H mice the saphenous nerve has proved useful when imaging the same regenerating nerve over a time-course. Pan et al. (2003) used transcutaneous imaging in a YFP-H saphenous nerve injury model [using transection, crush and crush following a conditioning lesion injuries] to reveal the potential of the immunosuppressive drug FK506 to ameliorate the regeneration blocking effects of the

chemotherapeutic drug vincristine. A study by Yan et al.(2011) used YFP-H mice to investigate the effect of different FK506 dosing regimens on saphenous nerve regeneration following crush injury. They reported that in groups where FK506 was administered prior to the nerve crush, axon regeneration rate and overall length was improved compared to control groups and groups where FK506 administration was delayed, regardless of the FK506 concentration (Yan et al., 2011).

Cheng et al. (2010) reported an interesting effect of hair clipping on the local pattern of cutaneous axons. Following hair clipping in YFP-H mice where no skin damage occurred the local levels of YFP expression increased, particularly around the hair follicles - this was used to demonstrate the plasticity of cutaneous axons (Cheng et al., 2010).

As with other strains of *thy-1-XFP* mice [see sections 1.8.5.1 and 1.8.5.4], there has been interest in using the YFP-H strain to investigate effects of various insults on retinal ganglion cells (Dursun et al., 2011, Kalesnykas et al., 2012, Oglesby et al., 2012, Feng et al., 2013). A study by Dursun et al. (2011) investigated the effects of early post-natal ethanol intoxication on retinal ganglion cells in YFP-H mice, reporting an overall decrease in cell numbers along with altered morphology [reduced soma size and increased dendritic tortuosity].

A study by Oglesby et al. (2012) used YFP-H mice to develop a semi-automated quantitative analysis method of assessing retinal ganglion cell morphology, mapping out the distribution of YFP labelled retinal ganglion cells in the retina in the process. This was followed up with a study using the developed analysis method to assess retinal ganglion cell morphology following optic nerve crush or experimentally induce glaucoma (Kalesnykas et al., 2012). The study by Kalesnykas et al. (2012) reported large reductions in YFP labelled retinal ganglion cells, axons and dendrite structure following optic nerve crush injuries, and reductions in axons but not retinal ganglion cells along with increases in soma size and dendritic structure following experimental glaucoma.

7.1.2 OBSERVATIONS ON USING THE *THY-1-YFP-H* MOUSE NERVE INJURY MODEL

In using the YFP-H mouse CF nerve injury model of mice exclusively for the studies contained within this thesis both the benefits and limitations of the model can be revealed.

A key benefit - and one used to great effect in many of the studies discussed in the previous section (English et al., 2005, Groves et al., 2005, Sabatier et al., 2008) - is the ability to trace the path taken by regenerating axons across the entire repair. Prior to the studies presented within this thesis, this tracing generally took the form of tracing axons from the point where they exited the central nerve ending to where their regeneration had ended (Groves et al., 2005). This tracing method was investigated as a potential analysis method when looking at how to obtain the best data from the YFP-H model; however, concerns over its accuracy and the quantity of analysis-hours required were raised.

Tracing axons in images from early pilot repairs revealed that many axons took a convoluted path through the early stages and many sprouted numerous times across the repair. This results in analysers having to decide which sprout to follow and could end up skewing results based on the analyser's preference for choosing long/short sprouts. In addition, many axons managed to regenerate further into the distal nerve ending than was feasible to excise [the CF nerve ultimately passes around the knee joint and becomes difficult to access] so the entire length of those axons could not be measured. This, coupled with the convoluted routes taken by many axons, results in actual axon length data becoming almost meaningless.

Although marking set intervals onto the images allows a more accurate measure of regeneration length to be taken [e.g. every interval crossed by an axon adds 0.5mm to its length regardless of if it took a much longer route between intervals], tracing from the central nerve ending towards the distal still has an issue with the analyser's choice of which axon branches to follow. Thus, the decision was made to trace axons in the opposite direction

[distal to central] to take advantage of the convergence of axon branches to improve the repeatability of the analysis.

The addition of the initial axon disruption analysis was made in an attempt to quantify the average amount of disruption that traced axons underwent while in the initial stages of the repair. Throughout all the studies reported in this thesis the greatest visual disruption in repairs occurred between the 0.0mm and 1.5mm intervals, and as such the average path length of axons that successfully regenerated between these two intervals was used to assess early disruption. A minor issue experienced when using this analysis method was that a small number of axons in some repairs doubled back on themselves to re-cross the 1.5mm interval. In these cases it was decided to measure axon length from the first crossing of the interval only to maintain consistency. This also prevented instances where a small number of very long doubled back axons could result in a repair with very little other disruption being considered to be worse than one with no doubled back axons but much greater disruption overall.

One problem encountered with axon tracing during these studies is that on some occasions the fluorescent axons were obscured by excess tissue - such as blood vessels - that had not been removed from the nerve prior to mounting [fig 7.1]. Although the removal of as much excess tissue as possible was performed upon extracting the nerve, it was not always possible to remove all of this tissue due to difficulties in discriminating excess tissue from nerve tissue. As some early attempts to remove all excess tissue resulted in damage to the nerve tissue it was decided that risking small areas of obscured fluorescence would be preferable.

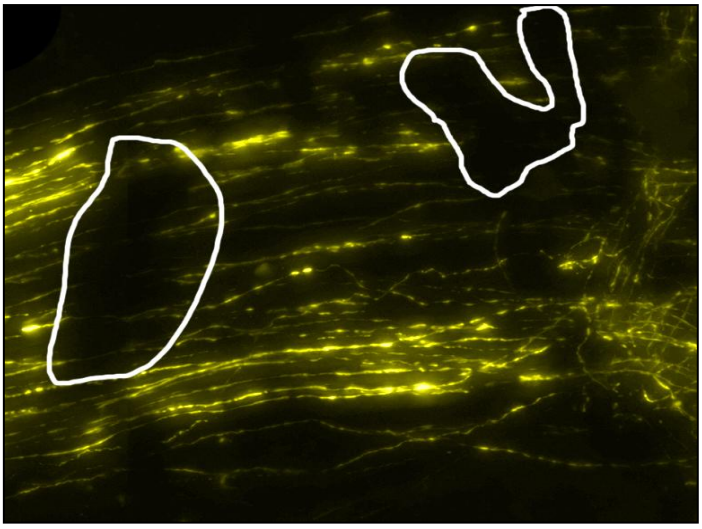

Figure 7.1: Close-up view of YFP nerve with suspected blood vessels obscuring fluorescent axons.

Another common issue noted with axon fluorescence were variations in brightness between different areas of the nerve [high vs. low axon density] and also between different axons [large vs. small axons]. This causes difficulties when obtaining images of the nerves as too much brightness results in overexposure and too little results underexposure [both making axons difficult to view]. As such the brightness balance used when acquiring images needs to be carefully chosen in order to ensure the best possible image is obtained.

The fact that the YFP fluorescence persists through repeated imaging with no noticeable fading is of great benefit for two main reasons. Firstly, acquiring a stack of images through the nerve usually takes 30-60 seconds and if the fluorescence faded quickly then the images making up the stack would have vastly differing brightness levels - adversely effecting the resultant composite image. Secondly, on some occasions the composite images from some microscope fields were found to not line up correctly with adjacent fields, necessitating the reacquisition of images.

It was observed during these studies that, although the YFP fluorescence persists through repeated imaging, there is a tendency for it begin to leach from the axons into the surrounding tissues after approximately 3 to 6 months [fig. 7.2]. Although axons can still be made out at this point, the high levels of background fluorescence does make the images

difficult to use in analysis. However, the time between nerve harvesting and this leaching should be sufficient to obtain any required images.

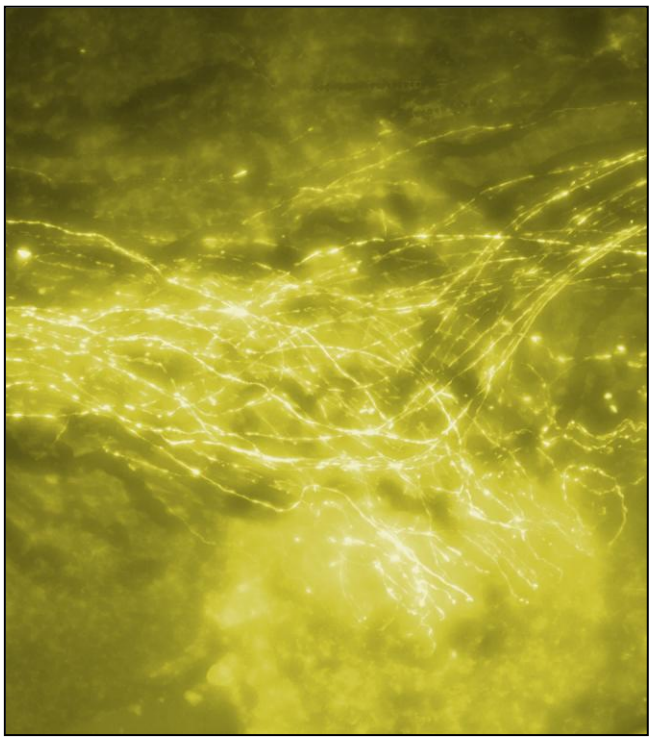

Figure 7.2: Example of fluorescence leaching into non-axonal tissues in 6-month post-harvest nerve.

7.2 FUTURE WORK SUGGESTIONS

7.2.1: INVESTIGATION OF DIFFERENT EC23 CONCENTRATIONS

Although EC23 did not demonstrate any beneficial effects in the study discussed here there are valid doubts as to whether the concentration used was optimal [see chapter 4]. To determine whether EC23 is biologically active at the chosen dose [10^{-8} mol/L], a reporter assay - such as a luciferase reporter assay - could be performed on appropriate cells [such as nerve, fibroblast and Schwann cell lines]. These assays work by transfecting cells with a gene vector containing a promoter response element that produces a bioluminescent enzyme when bound to the desired transcription factor [in this case, retinoic acid receptors] (Ho et al., 2013).

A series of in vitro experiments to investigate whether different concentrations have a greater influence on regeneration may also be of use. These could take the form of culturing intact or dissociated DRGs to determine the effects of various EC23 concentrations on neurite outgrowth and Schwann cell migration. If the application of a particular EC23 concentration proves to be beneficial in terms of increased neurite growth/length or faster migration of Schwann cells, then further in vivo experiments may be warranted.

7.2.2: IMPROVEMENT OF ALIGNED PCL FIBRES

The use of PCL fibres within conduits in the study discussed in chapter 5 gave disappointing results overall, though the one apparently successful repair in those conduits [fig. 5.12] does suggest that fibre filled conduits have promise. The poor performance may have been a result of the uncoated fibres affecting the dispersal of neurotrophic factors through the conduit, poor migration of Schwann cells into the conduit, or simply that axons were unable to satisfactorily interact with the fibres [see section 5.4.2]. Coating the fibres with matrix proteins, such as collagen or laminin, may help with Schwann cell migration into the conduits and axons may be able to interact better with the coated surface.

7.2.3: INCORPORATION OF REGENERATION ENHANCING AGENTS AND/OR CELLS INTO NERVE GUIDES

Adding various neurotrophic factors or support cells to conduits is currently considered to be necessary to enable successful regeneration over longer distances than current conduits can support [see section 5.1.3.2]. The µSL conduits used in chapter 5 may benefit from the addition neurotrophic factors/Schwann cells if they are to be trialled over significantly longer nerve defects, with the possibility of incorporating regeneration enhancing agents - such as M6P - also worth considering. The question of how to incorporate such things into the conduits is one requiring much thought: the simplest way is to combine the desired factors/cells/agents with a hydrogel insert; another - requiring a more technical approach - would be to incorporate factors/agents into a bioabsorbable conduit material, which would then release the factors in a controlled manner to boost regeneration.

7.2.4: FURTHER CHARACTERISATION OF FLUORESCENCE IN THE YFP-H MOUSE STRAIN

As discussed in section 7.1.2, previous studies have attempted to characterise numbers of YFP-H labelled axons in different nerves; however, those studies have tended to vary greatly in their conclusions and have generally only dealt with either the sciatic or common fibular nerves. In addition, the study by Feng et al. (2000) which reported the generation of this strain gave only extremely approximate information regarding fluorescent labelling within the different neuronal tissues. Therefore it would be of great interest to use any spare tissue from experimental mice to build up a greater level of detail about the levels of YFP-H labelling in various neuronal tissues. This information could then be used by investigators to design future studies investigating different aspects of the nervous system.

7.2.5: INVESTIGATE THE POTENTIAL OF A SCIATIC NERVE INJURY MODEL IN YFP-H MICE

Although the CF nerve injury model in YFP-H mice has proven successful in the studies within this thesis and elsewhere [see section 7.1.2], sciatic nerve injury models are much more common due to the increased size of the sciatic nerve. The advantage of the sciatic over the CF nerve is that regeneration across much longer nerve defects can be assessed and the nerve is easier to handle during repair. In addition, using the sciatic in a YFP-H mouse model would allow better comparisons between this model and others [such as electrophysiological ones]. The obvious drawback with a YFP-H sciatic nerve injury model is the greatly increased number of YFP axons that would need to be analysed. Whether the large number of YFP axons in sciatic nerves can be analysed accurately or not would be the main topic an investigation into a YFP-H sciatic nerve injury model.

7.3 CONCLUSIONS

Although this model does have some minor drawbacks, the benefits it offers easily outweigh them - especially if this model is used in collaboration with other models to gain a broader view of the effects of different interventions. This is often the case with other models and methods, such as the pairing of electrophysiology with walking gait analysis and histological techniques (Ngeow et al., 2011a, Ngeow et al., 2011b).

In the studies presented within this thesis a number of effects were observed [i.e. decreased axon disruption in M6P treated repairs and reduced axons organisation in hollow conduits] that would have been either very difficult or impossible to have observed using other methods.

This model also appears to lend itself well to the screening a number of promising interventions prior to moving forward with the better performing interventions into longer-term studies - mainly as results can be obtained within 2-weeks.

So in conclusion, the YFP-H mouse CF nerve injury model provides a valuable tool for investigating peripheral nerve regeneration and further use and development of the model should be encouraged.

REFERENCES

Al-Majed AA, Neumann CM, Brushart TM, Gordon T (2000) Brief electrical stimulation promotes the speed and accuracy of motor axonal regeneration. Journal of Neuroscience 20:2602-2608.

Alkayed NJ, Harukuni I, Kimes AS, London ED, Traystman RJ, Hurn PD (1998) Gender-linked brain injury in experimental stroke. Stroke 29:159-165.

Ansselin AD, Fink T, Davey DF (1997) Peripheral nerve regeneration through nerve guides seeded with adult Schwann cells. Neuropathology and Applied Neurobiology 23:387-398.

Ao Q, Fung C-K, Tsui AY-P, Cai S, Zuo H-C, Chan Y-S, Shum DK-Y (2011) The regeneration of transected sciatic nerves of adult rats using chitosan nerve conduits seeded with bone marrow stromal cell-derived Schwann cells. Biomaterials 32:787-796.

Ao Q, Wang AJ, Cao WL, Zhang L, Kong LJ, He Q, Gong YD, Zhang XF (2006) Manufacture of multimicrotubule chitosan nerve conduits with novel molds and characterization in vitro. Journal of Biomedical Materials Research Part A 77A:11-18.

Archibald SJ, Krarup C, Shefner J, Li ST, Madison RD (1991) A Collagen-Based Nerve Guide Conduit For Peripheral-Nerve Repair - An Electrophysiological Study Of Nerve Regeneration In Rodents And Nonhuman-Primates. Journal of Comparative Neurology 306:685-696.

Archibald SJ, Shefner J, Krarup C, Madison RD (1995) Monkey Median Nerve Repaired By Nerve Graft Or Collagen Nerve Guide Tube. Journal of Neuroscience 15:4109-4123.

Artico M, Cervoni L, Nucci F, Giuffre R (1996) Birthday of Peripheral Nervous System Surgery: The Contribution of Gabriele Ferrara (1543-1627). [Miscellaneous Article]. Neurosurgery August 39:380-383.

Ashur H, Vilner Y, Finsterbush A, Rousso M, Weinberg H, Devor M (1987) EXTENT OF FIBER REGENERATION AFTER PERIPHERAL-NERVE REPAIR - SILICONE SPLINT VS SUTURE, GAP REPAIR VS GRAFT. Experimental Neurology 97:365-374.

Atkins S, Loescher AR, Boissonade FM, Smith K, Occleston N, O'Kane S, Ferguson MJ, Robinson PP (2007) Interleukin-10 reduces scarring and enhances regeneration at a site of sciatic nerve repair. Journal of the Peripheral Nervous System 12:269-276.

Atkins S, Smith KG, Loescher AR, Boissonade FM, Ferguson MWJ, Robinson PP (2006a) The effect of antibodies to TGF-beta 1 and TGF-beta 2 at a site of sciatic nerve repair. Journal of the Peripheral Nervous System 11:286-293.

Atkins S, Smith KG, Loescher AR, Boissonade FM, O'Kane S, Ferguson MWJ, Robinson PP (2006b) Scarring impedes regeneration at sites of peripheral nerve repair. Neuroreport 17:1245-1249.

Atsumi Y, Matsumoto K, Sakuda M, Maeda T, Kurisu K, Wakisaka S (1999) Altered distribution of Schwann cells in the periodontal ligament of the rat incisor following resection of the inferior alveolar nerve: an immunohistochemical study on S-100 proteins. Brain Research 849:187-195.

Azizi A, Azizi S, Heshmatian B, Amini K (2014) Improvement of functional recovery of transected peripheral nerve by means of chitosan grafts filled with vitamin E, pyrroloquinoline quinone and their combination. International Journal of Surgery 12:76-82.

Bailey R, Kaskutas V, Fox I, Baum CM, Mackinnon SE (2009) Effect of Upper Extremity Nerve Damage on Activity Participation, Pain, Depression, and Quality of Life. Journal of Hand Surgery-American Volume 34A:1682-1688.

Bain JR, Mackinnon SE, Hunter DA (1989) FUNCTIONAL-EVALUATION OF COMPLETE SCIATIC, PERONEAL, AND POSTERIOR TIBIAL NERVE LESIONS IN THE RAT. Plastic and Reconstructive Surgery 83:129-136.

Battiston B, Papalia I, Tos P, Geuna S (2009) Peripheral Nerve Repair and Regeneration Research: A Historical Note. Essays on Peripheral Nerve Repair and Regeneration 87:1-7.

Behl C, Manthey D (2000) Neuroprotective activities of estrogen: An update. Journal of Neurocytology 29:351-358.

Beirowski B, Berek L, Adalbert R, Wagner D, Grumme DS, Addicks K, Ribchester RR, Coleman MP (2004) Quantitative and qualitative analysis of Wallerian degeneration using restricted axonal labelling in YFP-H mice. Journal of Neuroscience Methods 134:23-35.

Bender MD, Bennett JM, Waddell RL, Doctor JS, Marra KG (2004) Multi-channeled biodegradable polymer/CultiSpher composite nerve guides. Biomaterials 25:1269-1278.

Bernstein SL, Guo Y, Slater BJ, Puche A, Kelman SE (2007) Neuron stress and loss following rodent anterior ischemic optic neuropathy in double-reporter transgenic mice. Investigative Ophthalmology & Visual Science 48:2304-2310.

Bertleff M, Meek MF, Nicolai JPA (2005) A prospective clinical evaluation of biodegradable neurolac nerve guides for sensory nerve repair in the hand. Journal of Hand Surgery-American Volume 30A:513-518.

Beuche W, Friede RL (1984) The Role Of Non-Resident Cells In Wallerian Degeneration. Journal of Neurocytology 13:767-796.

Bhawan J (1998) Short- and long-term histologic effects of topical tretinoin on photodamaged skin. International Journal of Dermatology 37:286-292.

Bisby MA, Chen S (1990) Delayed Wallerian Degeneration In Sciatic-Nerves Of C57bl/Ola Mice Is Associated With Impaired Regeneration Of Sensory Axons. Brain Research 530:117-120.

Bose S, Vahabzadeh S, Bandyopadhyay A (2013) Bone tissue engineering using 3D printing. Materials Today 16:496-504.

Boycott AE (1903) On the number of nodes of Ranvier in different stages of the growth of nerve fibres in the frog. Journal of Physiology-London 30:370-380.

Bozkurt A, Deumens R, Scheffel J, O'Dey DM, Weis J, Joosten EA, Fuehrmann T, Brook GA, Pallua N (2008) CatWalk gait analysis in assessment of functional recovery after sciatic nerve injury. Journal of Neuroscience Methods 173:91-98.

Bratton BR, Kline DG, Coleman W, Hudson AR (1979) EXPERIMENTAL INTERFASCICULAR NERVE GRAFTING. Journal of Neurosurgery 51:323-332.

Bray GM, Aguayo AJ (1974) REGENERATION OF PERIPHERAL UNMYELINATED NERVES - FATE OF AXONAL SPROUTS WHICH DEVELOP AFTER INJURY. Journal of Anatomy 117:517-529.

Brueck W (1997) The role of macrophages in Wallerian degeneration. Brain Pathology 7:741-752.

Brushart TME (1988) Preferential Reinnervation Of Motor Nerves By Regenerating Motor Axons. Journal of Neuroscience 8:1026-1031.

Bushnell BD, McWilliams AD, Whitener GB, Messer TM (2008) Early clinical experience with collagen nerve tubes in digital nerve repair. Journal of Hand Surgery-American Volume 33A:1081-1087.

Caroni P (1997) Overexpression of growth-associated proteins in the neurons of adult transgenic mice. Journal of Neuroscience Methods 71:3-9.

Chalazonitis A, Kalberg J, Twardzik DR, Morrison RS, Kessler JA (1992) Transforming Growth-Factor-Beta Has Neurotrophic Actions On Sensory Neurons Invitro And Is Synergistic With Nerve Growth-Factor. Developmental Biology 152:121-132.

Chalfie M, Tu Y, Euskirchen G, Ward WW, Prasher DC (1994) Green Fluorescent Protein As A Marker For Gene-Expression. Science 263:802-805.

Chandross KJ, Spray DC, Cohen RI, Kumar NM, Kremer M, Dermietzel R, Kessler JA (1996) TNF alpha inhibits Schwann cell proliferation, Connexin46 expression, and gap junctional communication. Molecular and Cellular Neuroscience 7:479-500.

Chang C-J (2009a) Effects of nerve growth factor from genipin-crosslinked gelatin in polycaprolactone conduit on peripheral nerve regeneration-in vitro and in vivo. Journal of Biomedical Materials Research Part A 91A:586-596.

Chang C-J (2009b) The Effect of Pulse-Released Nerve Growth Factor from Genipin-Crosslinked Gelatin in Schwann Cell-Seeded Polycaprolactone Conduits on Large-Gap Peripheral Nerve Regeneration. Tissue Engineering Part A 15:547-557.

Cheema SS, Richards L, Murphy M, Bartlett PF (1994) Leukemia Inhibitory Factor Prevents The Death Of Axotomised Sensory Neurons In The Dorsal-Root Ganglia Of The Neonatal Rat. Journal of Neuroscience Research 37:213-218.

Chen C, Lee M, Shyu V, Chen Y, Chen C, Chen J (2014) Surface modification of polycaprolactone scaffolds fabricated via selective laser sintering for cartilage tissue engineering. Materials Science and Engineering C 40.

Chen S, Kiss I, Tramposch KM (1992) Effects Of All-Trans Retinoic Acid On Uvb-Irradiated And Nonirradiated Hairless Mouse Skin. Journal of Investigative Dermatology 98:248-254.

Cheney FW, Domino KB, Caplan RA, Posner KL (1999) Nerve injury associated with anesthesia - A closed claims analysis. Anesthesiology 90:1062-1069.

Cheng C, Guo GF, Martinez JA, Singh V, Zochodne DW (2010) Dynamic Plasticity of Axons within a Cutaneous Milieu. Journal of Neuroscience 30:14735-14744.

Chindasub P, Lindsey JD, Duong-Polk K, Leung CK, Weinreb RN (2013) Inhibition of Histone Deacetylases 1 and 3 Protects Injured Retinal Ganglion Cells. Investigative Ophthalmology & Visual Science 54:96-102.

Chiono V, Ciardelli G, Vozzi G, Cortez J, Barbani N, Gentile P, Giusti P (2008) Enzymatically-modified melt-extruded guides for peripheral nerve repair. Engineering in Life Sciences 8:226-237.

Choi JW, Ha YM, Lee SH, Choi KH (2006) Design of microstereolithography system based on dynamic image projection for fabrication of three-dimensional microstructures. Journal of Mechanical Science and Technology 20:2094-2104.

Choi YH, Liu F, Kim JS, Choi YK, Park JS, Kim SW (1998) Polyethylene glycol-grafted poly-L-lysine as polymeric gene carrier. Journal of Controlled Release 54:39-48.

Christie VB, Barnard JH, Batsanov AS, Bridgens CE, Cartmell EB, Collings JC, Maltman DJ, Redfern CPE, Marder TB, Przyborski S, Whiting A (2008) Synthesis and evaluation of synthetic retinoid derivatives as inducers of stem cell differentiation. Organic & Biomolecular Chemistry 6:3497-3507.

Christie VB, Maltman DJ, Henderson AP, Whiting A, Marder TB, Lako M, Przyborski SA (2010) Retinoid supplementation of differentiating human neural progenitors and embryonic stem cells leads to enhanced neurogenesis in vitro. Journal of Neuroscience Methods 193:239-245.

Ciardelli G, Chiono V (2006) Materials for peripheral nerve regeneration. Macromolecular Bioscience 6:13-26.

Clemence A, Mirsky R, Jessen KR (1989) Non-Myelin-Forming Schwann-Cells Proliferate Rapidly During Wallerian Degeneration In The Rat Sciatic-Nerve. Journal of Neurocytology 18:185-192.

Clemens G, Flower KR, Henderson AP, Whiting A, Przyborski SA, Jimenez-Hernandez M, Ball F, Bassan P, Cinque G, Gardner P (2013) The action of all-trans-retinoic acid (ATRA) and synthetic retinoid analogues (EC19 and EC23) on human pluripotent stem cells differentiation investigated using single cell infrared microspectroscopy. Molecular Biosystems 9:677-692.

Coleman MP, Perry VH (2002) Axon pathology in neurological disease: a neglected therapeutic target. Trends in Neurosciences 25:532-537.

Cometa S, Bartolozzi I, Corti A, Chiellini F, De Giglio E, Chiellini E (2010) Hydrolytic and microbial degradation of multi-block polyurethanes based on poly(epsilon-caprolactone)/poly(ethylene glycol) segments. Polymer Degradation and Stability 95:2013-2021.

Corcoran J, Maden M (1999) Nerve growth factor acts via retinoic acid synthesis to stimulate neurite outgrowth. Nature Neuroscience 2.

Cragg BG, Thomas PK (1964) Conduction Velocity Of Regenerated Peripheral Nerve Fibres. Journal of Physiology-London 171:164-&.

Crawley WA, Dellon AL (1992) Inferior Alveolar Nerve Reconstruction With A Polyglycolic Acid Bioabsorbable Nerve Conduit. Plastic and Reconstructive Surgery 90:300-302.

D'Antonio M, Droggiti A, Feltri ML, Roes J, Wrabetz L, Mirsky R, Jessen KR (2006) TGF beta type II receptor signaling controls Schwann cell death and proliferation in developing nerves. Journal of Neuroscience 26:8417-8427.

D'Urso D, Ehrhardt P, Muller HW (1999) Peripheral myelin protein 22 and protein zero: a novel association in peripheral nervous system myelin. Journal of Neuroscience 19:3396-3403.

Dahlin LB (2008) (ii) Nerve injuries. Current Orthopaedics 22:9-16.

Dahlin LB, Anagnostaki L, Lundborg G (2001) Tissue response to silicone tubes used to repair human median and ulnar nerves. Scandinavian Journal of Plastic and Reconstructive Surgery and Hand Surgery 35:29-34.

Dahlin LB, Lundborg G (2001) Use of tubes in peripheral nerve repair. Neurosurgery Clinics of North America 12:341-+.

Dallon JC, Sherratt JA, Maini PK (2001) Modeling the effects of transforming growth factor-beta on extracellular matrix alignment in dermal wound repair. Wound Repair and Regeneration 9:278-286.

Daly TJ, Weston WL (1986) Retinoid Effects On Fibroblast Proliferation And Collagen-Synthesis Invitro And On Fibrotic Disease In vivo. Journal of the American Academy of Dermatology 15:900-902.

Daud MFB, Pawar KC, Claeyssens F, Ryan AJ, Haycock JW (2012) An aligned 3D neuronal-glial co-culture model for peripheral nerve studies. Biomaterials 33:5901-5913.

Davis S, Aldrich TH, Ip NY, Stahl N, Scherer S, Farruggella T, Distefano PS, Curtis R, Panayotatos N, Gascan H, Chevalier S, Yancopoulos GD (1993) Released Form Of Cntf Receptor-Alpha Component As A Soluble Mediator Of Cntf Responses. Science 259:1736-1739.

De S, Aviles Trigueros M, Kalyvas A, David S (2003) Phospholipase A2 plays an important role in myelin breakdown and phagocytosis during Wallerian degeneration. Molecular and Cellular Neuroscience 24:753-765.

Deister C, Aljabari S, Schmidt CE (2007) Effects of collagen 1, fibronectin, laminin and hyaluronic acid concentration in multi-component gels on neurite extension. Journal of Biomaterials Science-Polymer Edition 18:983-997.

Den Dunnen WFA, Meek MF, Robinson PH, Schakernraad JM (1998) Peripheral nerve regeneration through P(DLLA-epsilon-CL) nerve guides. Journal of Materials Science-Materials in Medicine 9:811-814.

Dendunnen WFA, Vanderlei B, Robinson PH, Holwerda A, Pennings AJ, Schakenraad JM (1995) Biological Performance Of A Degradable Poly(Lactic Acid-Epsilon-Caprolactone) Nerve Guide - Influence Of Tube Dimensions. Journal of Biomedical Materials Research 29:757-766.

DenDunnen WFA, VanderLei B, Schakenraad JM, Stokroos I, Blaauw E, Bartels H, Pennings AJ, Robinson PH (1996) Poly(DL-lactide-epsilon-caprolactone) nerve guides perform better than autologous nerve grafts. Microsurgery 17:348-357.

Dennis PA, Rifkin DB (1991) Cellular Activation Of Latent Transforming Growth-Factor-Beta Requires Binding To The Cation-Independent Mannose 6-Phosphate Insulin-Like Growth-Factor Type-Ii Receptor. Proceedings of the National Academy of Sciences of the United States of America 88:580-584.

Deumens R, Jaken RJP, Marcus MAE, Joosten EAJ (2007) The CatWalk gait analysis in assessment of both dynamic and static gait changes after adult rat sciatic nerve resection. Journal of Neuroscience Methods 164:120-130.

Dotchev K, Yusoff W (2009) Recycling of polyamide 12 based powders in the laser sintering process. Rapid Prototyping Journal 15:192-203.

Dubovy P, Raska O, Klusakova I, Stejskal L, Celakovsky P, Haninec P (2011) Ciliary neurotrophic factor promotes motor reinnervation of the musculocutaneous nerve in an experimental model of end-to-side neurorrhaphy. Bmc Neuroscience 12.

Dubuisson AS, Kline DG (2002) Brachial plexus injury: A survey of 100 consecutive cases from a single service. Neurosurgery 51:673-682.

Ducker TB, Hayes GJ (1968) Experimental Improvements In Use Of Silastic Cff For Peripheral Nerve Repair. Journal of Neurosurgery 28:582-&.

Duester G (2008) Retinoic acid synthesis and signaling during early organogenesis. Cell 134:921-931.

Dursun I, Jakubowska-Dogru E, van der List D, Liets LC, Coombs JL, Berman RF (2011) Effects of Early Postnatal Exposure to Ethanol on Retinal Ganglion Cell Morphology and Numbers of Neurons in the Dorsolateral Geniculate in Mice. Alcoholism-Clinical and Experimental Research 35:2063-2074.

Einheber S, Hannocks MJ, Metz CN, Rifkin DB, Salzer JL (1995) Transforming Growth-Factor-Beta-1 Regulates Axon-Schwann Cell-Interactions. Journal of Cell Biology 129:443-458.

Ellenberg J, Lippincott-Schwartz J, Presley JF (1999) Dual-colour imaging with GFP variants. Trends in Cell Biology 9:52-56.

English AW, Cucoranu D, Mulligan A, Rodriguez JA, Sabatier MJ (2011) Neurotrophin-4/5 is implicated in the enhancement of axon regeneration produced by treadmill training following peripheral nerve injury. European Journal of Neuroscience 33:2265-2271.

English AW, Meador W, Carrasco DI (2005) Neurotrophin-4/5 is required for the early growth of regenerating axons in peripheral nerves. European Journal of Neuroscience 21:2624-2634.

Farole A, Jamal BT (2008) A Bioabsorbable collagen nerve cuff (NeuraGen) for repair of lingual and inferior alveolar nerve injuries: A case series. Journal of Oral and Maxillofacial Surgery 66:2058-2062.

Favero M, Massella O, Cangiano A, Buffelli M (2009) On the mechanism of action of muscle fibre activity in synapse competition and elimination at the mammalian neuromuscular junction. European Journal of Neuroscience 29:2327-2334.

Feng GP, Mellor RH, Bernstein M, Keller-Peck C, Nguyen QT, Wallace M, Nerbonne JM, Lichtman JW, Sanes JR (2000) Imaging neuronal subsets in transgenic mice expressing multiple spectral variants of GFP. Neuron 28:41-51.

Feng L, Zhao Y, Yoshida M, Chen H, Yang JF, Kim TS, Cang J, Troy JB, Liu X (2013) Sustained Ocular Hypertension Induces Dendritic Degeneration of Mouse Retinal Ganglion Cells That Depends on Cell Type and Location. Investigative Ophthalmology & Visual Science 54:1106-1117.

Ferguson MWJ, O'Kane S (2004) Scar-free healing: from embryonic mechanisms to adult therapeutic intervention. Philosophical Transactions of the Royal Society of London Series B-Biological Sciences 359:839-850.

Fernandez E, Pallini R, LaMarca F, Lauretti L, Scogna A (1996) Neurosurgery of the peripheral nervous system .1. Basic anatomic concepts. Surgical Neurology 46:47-48.

Fernandezvalle C, Bunge RP, Bunge MB (1995) Schwann-Cells Degrade Myelin And Proliferate In The Absence Of Macrophages - Evidence From In-Vitro Studies Of Wallerian Degeneration. Journal of Neurocytology 24:667-679.

Ferreira A, Caceres A (1991) Estrogen-Enhanced Neurite Growth - Evidence For A Selective Induction Of Tau And Stable Microtubules. Journal of Neuroscience 11:392-400.

Fowler TJ, Danta G, Gilliatt RW (1972) Recovery Of Nerve-Conduction After A Pneumatic Tourniquet - Observations On Hind-Limb Of Baboon. Journal of Neurology Neurosurgery and Psychiatry 35:638-&.

Francel PC, Francel TJ, Mackinnon SE, Hertl C (1997) Enhancing nerve regeneration across a silicone tube conduit by using interposed short-segment nerve grafts. Journal of Neurosurgery 87:887-892.

Fried K, Bongenhielm U, Boissonade FM, Robinson PP (2001) Nerve injury-induced pain in the trigeminal system. Neuroscientist 7:155-165.

Friede RL, Bischhausen R (1980) Fine-Structure Of Stumps Of Transected Nerve-Fibers In Sub-Serial Sections. Journal of the Neurological Sciences 44:181-203.

Galbraith KA, McCullough CJ (1979) Acute Nerve Injury As A Complication Of Closed Fractures Or Dislocations Of The Elbow. Injury-International Journal of the Care of the Injured 11:159-164.

Garcia-Segura LM, Azcoitia I, DonCarlos LL (2001) Neuroprotection by estradiol. Progress in Neurobiology 63:29-60.

Gaudet AD, Popovich PG, Ramer MS (2011) Wallerian degeneration: Gaining perspective on inflammatory events after peripheral nerve injury. Journal of Neuroinflammation 8.

George EB, Glass JD, Griffin JW (1995) Axotomy-Induced Axonal Degeneration Is Mediated By Calcium Influx Through Ion-Specific Channels. Journal of Neuroscience 15:6445-6452.

Gest H (2004) The discovery of microorganisms by Robert Hooke and Antoni Van Leeuwenhoek, fellows of the Royal Society. Notes and Records of the Royal Society of London 58:187-201.

Geuna S, Raimondo S, Ronchi G, Di Scipio F, Tos P, Czaja K, Fornaro M (2009) Histology of the Peripheral Nerve and Changes Occurring During Nerve Regeneration. Essays on Peripheral Nerve Repair and Regeneration 87:27-46.

Giannini C, Lais AC, Dyck PJ (1989) Number, Size, And Class Of Peripheral-Nerve Fibers Regenerating After Crush, Multiple Crush, And Graft. Brain Research 500:131-138.

Glazner GW, Lupien S, Miller JA, Ishii DN (1993) Insulin-Like Growth Factor-Ii Increases The Rate Of Sciatic-Nerve Regeneration In Rats. Neuroscience 54:791-797.

Goraltchouk A, Freier T, Shoichet MS (2005) Synthesis of degradable poly(L-lactide-co-ethylene glycol) porous tubes by liquid-liquid centrifugal casting for use as nerve guidance channels. Biomaterials 26:7555-7563.

Gordon T, Sulaiman O, Boyd JG (2003) Experimental strategies to promote functional recovery after peripheral nerve injuries. Journal of the Peripheral Nervous System 8:236-250.

Griffiths CEM, Russman AN, Majmudar G, Singer RS, Hamilton TA, Voorhees JJ (1993) Restoration Of Collagen Formation In Photodamaged Human Skin By Tretinoin (Retinoic Acid). New England Journal of Medicine 329:530-535.

Groswasser Z, Cohen M, Keren O (1998) Female TBI patients recover better than males. Brain Injury 12:805-808.

Groves ML, McKeon R, Werner E, Nagarsheth M, Meador W, English AW (2005) Axon regeneration in peripheral nerves is enhanced by proteoglycan degradation. Experimental Neurology 195:278-292.

Gruene M, Deiwick A, Koch L, Schlie S, Unger C, Hofmann N, Bernemann I, Glasmacher B, Chichkov B (2011) Laser Printing of Stem Cells for Biofabrication of Scaffold-Free Autologous Grafts. Tissue Engineering Part C-Methods 17:79-87.

Guenard V, Gwynn LA, Wood PM (1995) Transforming Growth-Factor-Beta Blocks Myelination But Not Ensheathment Of Axons By Schwann-Cells In-Vitro. Journal of Neuroscience 15:419-428.

Guillot-Delost M, Le Gouvello S, Mesel-Lemoine M, Cherai M, Baillou C, Simon A, Levy Y, Weiss L, Louafi S, Chaput N, Berrehar F, Kerbrat S, Klatzmann D, Lemoine FM (2012) Human CD90 Identifies Th17/Tc17 T Cell Subsets That Are Depleted in HIV-Infected Patients. Journal of Immunology 188:981-991.

Gutmann E, Guttmann L, Medawar PB, Young JZ (1942) The rate of regeneration of nerve. Journal of Experimental Biology 19:14-44.

Haack-Sorensen M, Friis T, Bindslev L, Mortensen S, Johnsen HE, Kastrup J (2008) Comparison of different culture conditions for human mesenchymal stromal cells for clinical stem cell therapy. Scandinavian Journal of Clinical & Laboratory Investigation 68:192-203.

Hack CE, Wolbink GJ, Schalkwijk C, Speijer H, Hermens WT, vandenBosch H (1997) A role for secretory phospholipase A(2) and C-reactive protein in the removal of injured cells. Immunology Today 18:111-115.

Hadlock T, Sundback C, Hunter D, Cheney M, Vacanti JP (2000) A polymer foam conduit seeded with Schwann cells promotes guided peripheral nerve regeneration. Tissue Engineering 6:119-127.

Hall SM, Gregson NA (1971) In-Vivo And Ultrastructural Effects Of Injection Of Lysophosphatidyl Choline Into Myelinated Peripheral Nerve Fibres Of Adult Mouse. Journal of Cell Science 9:769-&.

Harpel JG, Metz CN, Kojima S, Rifkin DB (1993) Control of transforming growth factor-beta activity: Latency vs activation. Progress in Growth Factor Research 4:321-335.

Heim R, Prasher DC, Tsien RY (1994) Wavelength Mutations And Posttranslational Autoxidation Of Green Fluorescent Protein. Proceedings of the National Academy of Sciences of the United States of America 91:12501-12504.

Heine UI, Roberts AB, Munoz EF, Roche NS, Sporn MB (1985) Effects Of Retinoid Deficiency On The Development Of The Heart And Vascular System Of The Quail Embryo. Virchows Archiv B-Cell Pathology Including Molecular Pathology 50:135-152.

Henderson J, Ferguson MWJ, Terenghi G (2012) The reinnervation pattern of wounds and scars after treatment with transforming growth factor beta isoforms. Journal of Plastic Reconstructive and Aesthetic Surgery 65:E80-E86.

Henry EW, Chiu TH, Nyilas E, Brushart TM, Dikkes P, Sidman RL (1985) Nerve Regeneration Through Biodegradable Polyester Tubes. Experimental Neurology 90:652-676.

Hillerup S (2007) Iatrogenic injury to oral branches of the trigeminal nerve: records of 449 cases. Clinical Oral Investigations 11:133-142.

Ho P-i, Yue K, Pandey P, Breault L, Harbinski F, McBride AJ, Webb B, Narahari J, Karassina N, Wood KV, Hill A, Auld DS (2013) Reporter Enzyme Inhibitor Study To Aid Assembly of Orthogonal Reporter Gene Assays. Acs Chemical Biology 8:1009-1017.

Hogan B, Constantini F, Lacey E (1994) Manipulating the Mouse Embryo: A Laboratory Manual. New York: Cold Spring Harbour Laboratory Press.

Holland GR, Robinson PP (1998) Peripheral Nerve Damage and Repair. In: Clinical Oral Science (Harris, M. et al., eds), pp 274-289 Oxford, UK: John Wright.

Holtmaat A, Wilbrecht L, Knott GW, Welker E, Svoboda K (2006) Experience-dependent and cell-type-specific spine growth in the neocortex. Nature 441:979-983.

Huang W, Begum R, Barber T, Ibba V, Tee NCH, Hussain M, Arastoo M, Yang Q, Robson LG, Lesage S, Gheysens T, Skaer NJV, Knight DP, Priestley JV (2012) Regenerative potential of silk conduits in repair of peripheral nerve injury in adult rats. Biomaterials 33:59-71.

Hudson AR, Hunter D, Kline DG, Bratton BR (1979) Histological Studies Of Experimental Interfascicular Graft Repairs. Journal of Neurosurgery 51:333-340.

Hurtado H, Knoops B, Deaguilar PV (1987) Rat Sciatic-Nerve Regeneration In Semipermeable Artificial Tubes. Experimental Neurology 97:751-757.

Ichihara S, Inada Y, Nakamura T (2008) Artificial nerve tubes and their application for repair of peripheral nerve injury: an update of current concepts. Injury-International Journal of the Care of the Injured 39:S29-S39.

Itoh S, Takakuda K, Kawabata S, Aso Y, Kasai K, Itoh H, Shinomiya K (2002) Evaluation of cross-linking procedures of collagen tubes used in peripheral nerve repair. Biomaterials 23:4475-4481.

Iwatsuki K, Arai T, Ota H, Kato S, Natsume T, Kurimoto S, Yamamoto M, Hirata H (2013) Targeting Anti-Inflammatory Treatment Can Ameliorate Injury-Induced Neuropathic Pain. Plos One 8.

Johnson A, Bingham GA, Wimpenny DI (2013) Additive manufactured textiles for high-performance stab resistant applications. Rapid Prototyping Journal 19:199-207.

Jung-Testas I, Schumacher M, Bugnard H, Baulieu EE (1993) Stimulation of rat Schwann cell proliferation by estradiol: synergism between the estrogen and cAMP. Brain Res Dev Brain Res 72:282-290.

Jungtestas I, Schumacher M, Robel P, Baulieu EE (1994) Actions Of Steroid-Hormones And Growth-Factors On Glial-Cells Of The Central And Peripheral Nervous-System. Journal of Steroid Biochemistry and Molecular Biology 48:145-154.

JungTestas I, Schumacher M, Robel P, Baulieu EE (1996) Demonstration of progesterone receptors in rat Schwann cells. Journal of Steroid Biochemistry and Molecular Biology 58:77-82.

Kalesnykas G, Oglesby EN, Zack DJ, Cone FE, Steinhart MR, Tian J, Pease ME, Quigley HA (2012) Retinal Ganglion Cell Morphology after Optic Nerve Crush and Experimental Glaucoma. Investigative Ophthalmology & Visual Science 53:3847-3857.

Kaplan S, Odaci E, Unal B, Sahin B, Fornaro M (2009) DEVELOPMENT OF THE PERIPHERAL NERVE. Essays on Peripheral Nerve Repair and Regeneration 87:9-26.

Karanth S, Yang G, Yeh J, Richardson PM (2006) Nature of signals that initiate the immune response during Wallerian degeneration of peripheral nerves. Experimental Neurology 202:161-166.

Kato K, Liu H, Kikuchi S-i, Myers RR, Shubayev VI (2010) Immediate Anti-tumor Necrosis Factor-alpha (Etanercept) Therapy Enhances Axonal Regeneration After Sciatic Nerve Crush. Journal of Neuroscience Research 88:360-368.

Keck T, Mrsic-Flogel TD, Afonso MV, Eysel UT, Bonhoeffer T, Hubener M (2008) Massive restructuring of neuronal circuits during functional reorganization of adult visual cortex. Nature Neuroscience 11:1162-1167.

Kemp AS, Turner MW (1986) The Role Of Opsonins In Vacuolar Sealing And The Ingestion Of Zymosan By Human-Neutrophils. Immunology 59:69-74.

Kerns JM, Braverman B, Mathew A, Lucchinetti C, Ivankovich AD (1991) A Comparison Of Cryoprobe And Crush Lesions In The Rat Sciatic-Nerve. Pain 47:31-39.

Kim BS, Mooney DJ (1998) Development of biocompatible synthetic extracellular matrices for tissue engineering. Trends in Biotechnology 16:224-230.

Kim DH, Connolly SE, Kline DG, Voorhies RM, Smith A, Powell M, Yoes T, Daniloff JK (1994) Labeled Schwann-Cell Transplants Versus Sural Nerve Grafts In Nerve Repair. Journal of Neurosurgery 80:254-260.

Kim JR, Oh SH, Kwon GB, Namgung U, Song KS, Jeon BH, Lee JH (2013) Acceleration of Peripheral Nerve Regeneration through Asymmetrically Porous Nerve Guide Conduit Applied with Biological/Physical Stimulation. Tissue Engineering Part A 19:2674-2685.

Kim Y-t, Haftel VK, Kumar S, Bellamkonda RV (2008) The role of aligned polymer fiber-based constructs in the bridging of long peripheral nerve gaps. Biomaterials 29:3117-3127.

Kitahara AK, Nishimura Y, Shimizu Y, Endo K (2000) Facial nerve repair accomplished by the interposition of a collagen nerve guide. Journal of Neurosurgery 93:113-120.

Kiyotani T, Teramachi M, Takimoto Y, Nakamura T, Shimizu Y, Endo K (1996) Nerve regeneration across a 25-mm gap bridged by a polyglycolic acid collagen tube: A histological and electrophysiological evaluation of regenerated nerves. Brain Research 740:66-74.

Kokai LE, Lin Y-C, Oyster NM, Marra KG (2009) Diffusion of soluble factors through degradable polymer nerve guides: Controlling manufacturing parameters. Acta Biomaterialia 5:2540-2550.

Komiyama A, Suzuki K (1991) Age-related changes in attachment and proliferation of mouse Schwann cells in vitro. Brain Res Dev Brain Res 62:7-16.

Kouyoumdjian JA (2006) Peripheral nerve injuries: A retrospective survey of 456 cases. Muscle & Nerve 34:785-788.

Kovacic U, Sketelj J, Bajrovic FF (2003) Sex-related difference in collateral sprouting of nociceptive axons after peripheral nerve injury in the rat. Experimental Neurology 184:479-488.

Kovacic U, Sketelj J, Bajrovic FF (2009) Age-Related Differences In The Reinnervation After Peripheral Nerve Injury. Essays on Peripheral Nerve Repair and Regeneration 87:465-482.

Kovacic U, Zele T, Mars T, Sketelj J, Bajrovic FF (2010) Aging impairs collateral sprouting of nociceptive axons in the rat. Neurobiology of Aging 31:339-350.

Kovacic U, Zele T, Osredkar J, Sketelj J, Bajrovic FF (2004) Sex-related differences in the regeneration of sensory axons and recovery of nociception after peripheral nerve crush in the rat. Experimental Neurology 189:94-104.

Krarup C, Gilliatt RW (1985) Some Effects Of Prolonged Constriction On Nerve Regeneration In The Rabbit. Journal of the Neurological Sciences 68:1-14.

Krarup C, Loeb GE, Pezeshkpour GH (1988) conduction studies in peripheral cat nerve using implanted electrodes .2. The effects of prolonged constriction on regeneration of crushed nerve-fibers. Muscle & Nerve 11:933-944.

Kretschmer T, Antoniadis G, Braun V, Rath SA, Richter HP (2001) Evaluation of iatrogenic lesions in 722 surgically treated cases of peripheral nerve trauma. Journal of Neurosurgery 94.

Kroll DA, Caplan RA, Posner K, Ward RJ, Cheney FW (1990) Nerve Injury Associated With Anesthesia. Anesthesiology 73:202-207.

Kubota A, Komiyama A, Matsumoto M, Suzuki K (1998) Effect of macrophage suppression with silica on the proliferation of Schwann cells during Wallerian degeneration. Brain Research 802:254-258.

Kujawa KA, Emeric E, Jones KJ (1991) Testosterone Differentially Regulates The Regenerative Properties Of Injured Hamster Facial Motoneurons. Journal of Neuroscience 11:3898-3906.

Lascelle RG, Thomas PK (1966) Changes Due To Age In Internodal Length In Sural Nerve In Man. Journal of Neurology Neurosurgery and Psychiatry 29:40-&.

Lee H, Jo EK, Choi SY, Oh SB, Park K, Kim JS, Lee SJ (2006) Necrotic neuronal cells induce inflammatory Schwann cell activation via TLR2 and TLR3: Implication in Wallerian degeneration. Biochemical and Biophysical Research Communications 350:742-747.

Lee N, Spearry RP, Leahy KM, Robitz R, Trinh DS, Mason CO, Zurbrugg RJ, Batt MK, Paul RJ, Maclennan AJ (2013) Muscle ciliary neurotrophic factor receptor promotes axonal regeneration and functional recovery following peripheral nerve lesion. Journal of Comparative Neurology 521:2947-2965.

Leung CK-s, Lindsey JD, Crowston JG, Chen L, Chiang S, Weinreb RN (2008a) Longitudinal Profile of Retinal Ganglion Cell Damage after Optic Nerve Crush with Blue-Light Confocal Scanning Laser Ophthalmoscopy. Investigative Ophthalmology & Visual Science 49:4898-4902.

Leung CKS, Lindsey JD, Crowston JG, Ju W-K, Liu Q, Bartsch D-U, Weinreb RN (2008b) In vivo imaging of murine retinal ganglion cells. Journal of Neuroscience Methods 168:475-478.

Leung CKS, Weinreb RN, Li ZW, Liu S, Lindsey JD, Choi N, Liu L, Cheung CYL, Ye C, Qiu KL, Chen LJ, Yung WH, Crowston JG, Pu ML, So KF, Pang CP, Lam DSC (2011) Long-Term In Vivo Imaging

and Measurement of Dendritic Shrinkage of Retinal Ganglion Cells. Investigative Ophthalmology & Visual Science 52:1539-1547.

Lheureux E, Thoms SD, Carey F (1986) The Effects Of 2 Retinoids On Limb Regeneration In Pleurodeles-Waltl And Triturus-Vulgaris. Journal of Embryology and Experimental Morphology 92:165-182.

Li G, Li D, Niu Y, He T, Chen KC, Xu K (2014) Alternating block polyurethanes based on PCL and PEG as potential nerve regeneration materials. Journal of Biomedical Materials Research Part A 102:685-697.

Li ST, Archibald SJ, Krarup C, Madison RD (1992) Peripheral Nerve Repair With Collagen Conduits. Clinical Materials 9:195-200.

Li Z-w, Liu S, Weinreb RN, Lindsey JD, Yu M, Liu L, Ye C, Cui Q, Yung W-h, Pang C-P, Lam DSC, Leung CK-s (2011) Tracking Dendritic Shrinkage of Retinal Ganglion Cells after Acute Elevation of Intraocular Pressure. Investigative Ophthalmology & Visual Science 52:7205-7212.

Lichtman JW, Sanes JR (2003) Watching the neuromuscular junction. Journal of Neurocytology 32:767-775.

Liechty KW, Kim HB, Adzick NS, Crombleholme TM (2000) Fetal wound repair results in scar formation in interleukin-10-deficient mice in a syngeneic murine model of scarless fetal wound repair. Journal of Pediatric Surgery 35:866-872.

Lindenlaub T, Teuteberg P, Hartung T, Sommer C (2000) Effects of neutralizing antibodies to TNF-alpha on pain-related behavior and nerve regeneration in mice with chronic constriction injury. Brain Research 866:15-22.

Liu T, van Rooijen N, Tracey DJ (2000) Depletion of Macrophages Reduces Axonal Degeneration and Hyperalgesia Following Nerve Injury. Pain 86:25-32.

Longo FM, Manthorpe M, Skaper SD, Lundborg G, Varon S (1983) Neuronotrophic Activities Accumulate Invivo Within Silicone Nerve Regeneration Chambers. Brain Research 261:109-116.

Lowery LA, Van Vactor D (2009) The trip of the tip: understanding the growth cone machinery. Nature Reviews Molecular Cell Biology 10:332-343.

Lubiatowski P, Unsal FM, Nair D, Ozer K, Siemionow M (2008) The epineural sleeve technique for nerve graft reconstruction enhances nerve recovery. Microsurgery 28:160-167.

Lubinska L (1982) Patterns of Wallerian Degeneration of Myelinated Fibers in Short and Long Peripheral Stumps and in Isolated Segments of Rat Phrenic-Nerve - Interpretation of the Role of Axoplasmic Flow of the Trophic Factor. Brain Research 233:227-240.

Lundborg G, Dahlin LB, Danielsen N, Gelberman RH, Longo FM, Powell HC, Varon S (1982a) Nerve Regeneration In Silicone Chambers - Influence Of Gap Length And Of Distal Stump Components. Experimental Neurology 76:361-375.

Lundborg G, Longo FM, Varon S (1982b) NERVE REGENERATION MODEL AND TROPHIC FACTORS INVIVO. Brain Research 232:157-161.

Lundborg G, Rosen B, Dahlin L, Danielsen N, Holmberg J (1997) Tubular versus conventional repair of median and ulnar nerves in the human forearm: Early results from a prospective, randomized, clinical study. Journal of Hand Surgery-American Volume 22A:99-106.

Lundborg G, Rosen B, Dahlin L, Holmberg J, Rosen I (2004) Tubular repair of the median or ulnar nerve in the human forearm: A 5-year follow-up. Journal of Hand Surgery-British and European Volume 29B:100-107.

Lunn ER, Perry VH, Brown MC, Rosen H, Gordon S (1989) Absence Of Wallerian Degeneration Does Not Hinder Regeneration In Peripheral-Nerve. European Journal of Neuroscience 1:27-33.

Mackinnon SE, Doolabh VB, Novak CB, Trulock EP (2001) Clinical outcome following nerve allograft transplantation. Plastic and Reconstructive Surgery 107:1419-1429.

Maden M (2007) Retinoic acid in the development, regeneration and maintenance of the nervous system. Nature Reviews Neuroscience 8:755-765.

Maden M, Hind M (2003) Retinoic acid, a regeneration-inducing molecule. Developmental Dynamics 226:237-244.

Madison R, Dasilva CF, Dikkes P, Chiu TH, Sidman RL (1985) Increased Rate Of Peripheral-Nerve Regeneration Using Bioresorbable Nerve Guides And A Laminin-Containing Gel. Experimental Neurology 88:767-772.

Madison RD, Archibald SJ, Lacin R, Krarup C (1999) Factors contributing to preferential motor reinnervation in the primate peripheral nervous system. Journal of Neuroscience 19:11007-11016.

Madorsky SJ, Swett JE, Crumley RL (1998) Motor versus sensory neuron regeneration through collagen tubules. Plastic and Reconstructive Surgery 102:430-436.

Mahoney MJ, Anseth KS (2006) Three-dimensional growth and function of neural tissue in degradable polyethylene glycol hydrogels. Biomaterials 27:2265-2274.

Martini R, Fischer S, Lopez-Vales R, David S (2008) Interactions Between Schwann Cells and Macrophages in Injury and Inherited Demyelinating Disease. Glia 56:1566-1577.

Matsumoto K, Ohnishi K, Kiyotani T, Sekine T, Ueda H, Nakamura T, Endo K, Shimizu Y (2000) Peripheral nerve regeneration across an 80-mm gap bridged by a polyglycolic acid (PGA)-collagen tube filled with laminin-coated collagen fibers: a histological and electrophysiological evaluation of regenerated nerves. Brain Research 868:315-328.

Matsuoka I, Nakane A, Kurihara K (1997) Induction of LIF-mRNA by TGF-beta 1 in Schwann cells. Brain Research 776:170-180.

Matthews MA (1968) An Electron Microscopic Study Of Relationship Between Axon Diameter And Initiation Of Myelin Production In Peripheral Nervous System. Anatomical Record 161:337-&.

Matz SO, Welliver PS, Welliver DI (1989) Brachial plexus neuropraxia complicating a comminuted clavicle fracture in a college football player. The American Journal of Sports Medicine 17:581-583.

McCallion RL, Ferguson MWJ (1996) Fetal Wound Healing. In: The Molecular and Cellular Biology of Wound Repair (Clarke, R. A. F., ed) New York: Plenum Press.

Meek MF, Coert JH (2008) US Food and Drug Administration/Conformit Europe-approved absorbable nerve conduits for clinical repair of peripheral and cranial nerves. Annals of Plastic Surgery 60:466-472.

Meek MF, Den Dunnen WFA, Schakenraad JM, Robinson PH (1996) Evaluation of functional nerve recovery after reconstruction with a poly (DL-lactide-epsilon-caprolactone) nerve guide, filled with modified denatured muscle tissue. Microsurgery 17:555-561.

Meek MF, Van der Werff JFA, Nicolai JPA, Gramsbergen A (2001) Biodegradable p(DLLA-epsilon-CL) nerve guides versus autologous nerve grafts: Electromyographic and video analysis. Muscle & Nerve 24:753-759.

Menovsky T, Beek JF (2001) Laser, fibrin glue, or suture repair of peripheral nerves: a comparative functional, histological, and morphometric study in the rat sciatic nerve. Journal of Neurosurgery 95:694-699.

Mews M, Meyer M (1993) Modulation Of Schwann-Cell Phenotype By Tgf-Beta-1 - Inhibition Of P0 Messenger-Rna Expression And Down-Regulation Of The Low-Affinity Ngf Receptor. Glia 8:208-217.

Midha R (1997) Epidemiology of brachial plexus injuries in a multitrauma population. Neurosurgery 40:1182-1188.

Mihai R, Florescu IP, Coroiu V, Oancea A, Lungu M (2011) In vitro biocompatibility testing of some synthetic polymers used for the achievement of nervous conduits. Journal of medicine and life 4:250-255.

Mitchison T, Kirschner M (1988) Cytoskeletal Dynamics And Nerve Growth. Neuron 1:761-772.

Mizisin AP, Vu Y, Shuff M, Calcutt NA (2004) Ciliary neurotrophic factor improves nerve conduction and ameliorates regeneration deficits in diabetic rats. Diabetes 53:1807-1812.

Mohammadi R, Amini K, Yousefi A, Abdollahi-Pirbazari M, Belbasi A, Abedi F (2013) Functional Effects of Local Administration of Thyroid Hormone Combined With Chitosan Conduit After Sciatic Nerve Transection in Rats. Journal of Oral and Maxillofacial Surgery 71:1763-1776.

Moradzadeh A, Borschel GH, Luciano JP, Whitlock EL, Hayashi A, Hunter DA, Mackinnon SE (2008) The impact of motor and sensory nerve architecture on nerve regeneration. Experimental Neurology 212:370-376.

Mosahebi A, Fuller P, Wiberg M, Terenghi G (2002) Effect of allogeneic Schwann cell transplantation on peripheral nerve regeneration. Experimental Neurology 173:213-223.

Mostany R, Chowdhury TG, Johnston DG, Portonovo SA, Carmichael ST, Portera-Cailliau C (2010) Local Hemodynamics Dictate Long-Term Dendritic Plasticity in Peri-Infarct Cortex. Journal of Neuroscience 30:14116-14126.

Motomura K, Isobe H, Sakai H, Nawata H (1996) Suppressive effects of all-trans retinoic acid on the lipopolysaccharide-stimulated release of tumor necrosis factor-alpha and nitric oxide by rat Kupffer cells in vitro. International Hepatology Communications 5:177-183.

Mottaghitalab F, Farokhi M, Zaminy A, Kokabi M, Soleimani M, Mirahmadi F, Shokrgozar MA, Sadeghizadeh M (2013) A Biosynthetic Nerve Guide Conduit Based on Silk/SWNT/Fibronectin Nanocomposite for Peripheral Nerve Regeneration. Plos One 8.

Mullervahl H (1984) Iatrogenic Lesions Of Peripheral-Nerves In Surgery. Langenbecks Archiv Fur Chirurgie 364:321-323.

Mundinger GS, Prucz RB, Rozen SM, Tufaro AP (2012) Reconstruction of the Inferior Alveolar Nerve with Bioabsorbable Polyglycolic Acid Nerve Conduits. Plastic and Reconstructive Surgery 129:110E-117E.

Murayama A, Suzuki T, Matsui M (1997) Photoisomerization of retinoic acids in ethanol under room light: A warning for cell biological study of geometrical isomers of retinoids. Journal of Nutritional Science and Vitaminology 43:167-176.

Nakamura Y, Muguruma Y, Yahata T, Miyatake H, Sakai D, Mochida J, Hotta T, Ando K (2006) Expression of CD90 on keratinocyte stem/progenitor cells. British Journal of Dermatology 154:1062-1070.

Navarro X, Kennedy WR (1988) Effect Of Age On Collateral Reinnervation Of Sweat Glands In The Mouse. Brain Research 463:174-181.

Navarro X, Verdu E, Buti M (1994) Comparison Of Regenerative And Reinnervating Capabilities Of Different Functional Types Of Nerve-Fibers. Experimental Neurology 129:217-224.

Near SL, Whalen LR, Miller JA, Ishii DN (1992) Insulin-Like Growth Factor-Ii Stimulates Motor-Nerve Regeneration. Proceedings of the National Academy of Sciences of the United States of America 89:11716-11720.

Ngeow WC (2010) The Effect of Scar Reducing Agents on the Outcome of Peripheral Nerve Repair. In: Academic Unit of Oral and Maxillofacial Medicine and Surgery, vol. Ph.D., p 268 Sheffield: University of Sheffield.

Ngeow WC, Atkins S, Morgan CR, Metcalfe AD, Boissonade FM, Loescher AR, Robinson PP (2011a) A Comparison Between The Effects Of Three Potential Scar-Reducing Agents Applied At A Site Of Sciatic Nerve Repair. Neuroscience 181:271-277.

Ngeow WC, Atkins S, Morgan CR, Metcalfe AD, Boissonade FM, Loescher AR, Robinson PP (2011b) The effect of Mannose-6-Phosphate on recovery after sciatic nerve repair. Brain Research 1394:40-48.

Nichols CM, Brenner MJ, Fox IK, Tung TH, Hunter DA, Rickman SR, Mackinnon SE (2004) Effect of motor versus sensory nerve grafts on peripheral nerve regeneration. Experimental Neurology 190:347-355.

Nie X, Deng M, Yang M, Liu L, Zhang Y, Wen X (2014) Axonal Regeneration and Remyelination Evaluation of Chitosan/Gelatin-Based Nerve Guide Combined with Transforming Growth Factor-beta 1 and Schwann Cells. Cell Biochemistry and Biophysics 68:163-172.

Niederreither K, Subbarayan V, Dolle P, Chambon P (1999) Embryonic retinoic acid synthesis is essential for early mouse post-implantation development. Nature Genetics 21:444-448.

Niederreither K, Vermot J, Messaddeq N, Schuhbaur B, Chambon P, Dolle P (2001) Embryonic retinoic acid synthesis is essential for heart morphogenesis in the mouse. Development 128:1019-1031.

Niederreither K, Vermot J, Schuhbaur B, Chambon P, Dolle P (2002) Embryonic retinoic acid synthesis is required for forelimb growth and anteroposterior patterning in the mouse. Development 129:3563-3574.

Norkus T, Norkus M, Ramanauskas T (2005) Donor, recipient and nerve grafts in brachial plexus reconstruction: anatomical and technical features for facilitating the exposure. Surgical and Radiologic Anatomy 27:524-530.

Ogawa A, Maeguchi M, Uchida Y, Yoshioka T, Kawashima M, Muraki T (1998) Effect of tazarotene, an acetylenic retinoid, on human dermal fibroblast. Japanese Journal of Pharmacology 76:317-319.

Oglesby E, Quigley HA, Zack DJ, Cone FE, Steinhart MR, Tian J, Pease ME, Kalesnykas G (2012) Semi-automated, quantitative analysis of retinal ganglion cell morphology in mice selectively expressing yellow fluorescent protein. Experimental Eye Research 96:107-115.

Oh SH, Kim JR, Kwon GB, Namgung U, Song KS, Lee JH (2013) Effect of Surface Pore Structure of Nerve Guide Conduit on Peripheral Nerve Regeneration. Tissue Engineering Part C-Methods 19:233-243.

Okane S, Ferguson MWJ (1997) Transforming growth factor beta s and wound healing. International Journal of Biochemistry & Cell Biology 29:63-78.

Olivier E, Edgley SA, Armand J, Lemon RN (1997) An electrophysiological study of the postnatal development of the corticospinal system in the macaque monkey. Journal of Neuroscience 17:267-276.

Opdenakker G, Van den Steen PE, Dubois B, Nelissen I, Van Coillie E, Masure S, Proost P, Van Damme J (2001a) Gelatinase B functions as regulator and effector in leukocyte biology. Journal of Leukocyte Biology 69:851-859.

Opdenakker G, Van den Steen PE, Van Damme J (2001b) Gelatinase B: a tuner and amplifier of immune functions. Trends in Immunology 22:571-579.

Orebaugh SL, Williams BA (2009) Brachial Plexus Anatomy: Normal and Variant. Thescientificworldjournal 9:300-312.

Ormo M, Cubitt AB, Kallio K, Gross LA, Tsien RY, Remington SJ (1996) Crystal structure of the Aequorea victoria green fluorescent protein. Science 273:1392-1395.

Ornelas L, Padilla L, Di Silvio M, Schalch P, Esperante S, Infante RL, Bustamante JC, Avalos P, Varela D, Lopez M (2006a) Fibrin glue: An alternative technique for nerve coaptation - Part I. Wave amplitude, conduction velocity, and plantar-length factors. Journal of Reconstructive Microsurgery 22:119-122.

Ornelas L, Padilla L, Di Silvio M, Schalch P, Esperante S, Infante RL, Bustamante JC, Avalos P, Varela D, Lopez M (2006b) Fibrin glue: An alternative technique for nerve coaptation - Part II. Nerve regeneration and histomorphometric assessment. Journal of Reconstructive Microsurgery 22:123-128.

Pagnussat AS, Michaelsen SM, Achaval M, Ilha J, Hermel EES, Back FP, Netto CA (2012) Effect of skilled and unskilled training on nerve regeneration and functional recovery. Brazilian Journal of Medical and Biological Research 45:753-762.

Pan YA, Misgeld T, Lichtman JW, Sanes JR (2003) Effects of neurotoxic and neuroprotective agents on peripheral nerve regeneration assayed by time-lapse imaging in vivo. Journal of Neuroscience 23:11479-11488.

Panseri S, Cunha C, Lowery J, Del Carro U, Taraballi F, Amadio S, Vescovi A, Gelain F (2008) Electrospun micro- and nanofiber tubes for functional nervous regeneration in sciatic nerve transections. Bmc Biotechnology 8.

Pateman C, Harding A, Plenderleith R, Boissonade F, Rimmer S, Haycock J, Claeyssens F (2014a) Nerve Guides from Photocurable Polymers for Peripheral Nerve Repair. In: TERMIS-EU Annual Meeting Genova, Italy.

Pateman C, Harding A, Rimmer S, Boissonade F, Claeyssens F, Haycock J (2014b) Photocurable Polymeric Nerve Guides For Peripheral Nerve Repair.

Pateman C, Harding A, Rimmer S, Boissonade F, Claeyssens F, Haycock J (2014c) Photocurable Polymeric Nerve Guides For Peripheral Nerve Repair. Awaiting publication.

Perrin FE, Lacroix S, Aviles-Trigueros M, David S (2005) Involvement of Monocyte Chemoattractant Protein-1, Macrophage Inflammatory Protein-1α and Interleukin-1β in Wallerian Degeneration. Brain 128:854-866.

Perry VH, Brown MC (1992) Role Of Macrophages In Peripheral-Nerve Degeneration And Repair. Bioessays 14:401-406.

Personelle J, DeCampos S, Ruiz RD, Ribeiro GQ (1997) Injection of all-trans retinoic acid for treatment of thin wrinkles. Aesthetic Plastic Surgery 21:196-204.

Rangappa N, Romero A, Nelson KD, Eberhart RC, Smith GM (2000) Laminin-coated poly(L-lactide) filaments induce robust neurite growth while providing directional orientation. Journal of Biomedical Materials Research 51:625-634.

Ray WZ, Mackinnon SE (2010) Management of nerve gaps: Autografts, allografts, nerve transfers, and end-to-side neurorrhaphy. Experimental Neurology 223:77-85.

Rengier F, Mehndiratta A, von Tengg-Kobligk H, Zechmann CM, Unterhinninghofen R, Kauczor HU, Giesel FL (2010) 3D printing based on imaging data: review of medical applications. International Journal of Computer Assisted Radiology and Surgery 5:335-341.

Riley DA, Sanger JR, Matloub HS, Yousif NJ, Bain JLW, Moore GH (1988) Identifying Motor And Sensory Myelinated Axons In Rabbit Peripheral-Nerves By Histochemical Staining For Carbonic-Anhydrase And Cholinesterase Activities. Brain Research 453:79-88.

Rinker B, Liau JY (2011) A Prospective Randomized Study Comparing Woven Polyglycolic Acid and Autogenous Vein Conduits for Reconstruction of Digital Nerve Gaps. Journal of Hand Surgery-American Volume 36A:775-781.

Roberts AB, Sporn MB (1996) Transforming Growth Factor-β. New York: Plenum Press.

Robinson PP, Loescher AR, Smith KG (2000) A prospective, quantitative study on the clinical outcome of lingual nerve repair. British Journal of Oral and Maxillofacial Surgery 38:255-263.

Roganovic Z, Petkovic S (2004) Missile severances of the radial nerve. Results of 131 repairs. Acta Neurochirurgica 146:1185-1192.

Rudge P, Ochoa J, Gilliatt RW (1974) Acute Peripheral-Nerve Compression In Baboon. Journal of the Neurological Sciences 23:403-420.

Ruijs ACJ, Jaquet J-B, Kalmijn S, Giele H, Hovius SER (2005) Median and Ulnar Nerve Injuries: A Meta-Analysis of Predictors of Motor and Sensory Recovery after Modern Microsurgical Nerve Repair. [Article]. Plastic & Reconstructive Surgery August 116:484-494.

Saalbach A, Arnhold J, Lessig J, Simon JC, Anderegg U (2008) Human Thy-1 induces secretion of matrix metalloproteinase-9 and CXCL8 from human neutrophils. European Journal of Immunology 38:1391-1403.

Sabatier MJ, Redmon N, Schwartz G, English AW (2008) Treadmill training promotes axon regeneration in injured peripheral nerves. Experimental Neurology 211:489-493.

Sahenk Z, Seharaseyon J, Mendell JR (1994) Cntf Potentiates Peripheral-Nerve Regeneration. Brain Research 655:246-250.

Said G, Hontebeyriejoskowicz M (1992) Nerve Lesions Induced By Macrophage Activation. Research in Immunology 143:589-599.

Scadding SR, Maden M (1986a) Comparison Of The Effects Of Vitamin-A On Limb Development And Regeneration In The Axolotl, Ambystoma-Mexicanum. Journal of Embryology and Experimental Morphology 91:19-34.

Scadding SR, Maden M (1986b) Comparison Of The Effects Of Vitamin-A On Limb Development And Regeneration In Xenopus-Laevis Tadpoles. Journal of Embryology and Experimental Morphology 91:35-53.

Scadding SR, Maden M (1986c) The Effects Of Local Application Of Retinoic Acid On Limb Development And Regeneration In Tadpoles Of Xenopus-Laevis. Journal of Embryology and Experimental Morphology 91:55-63.

Schlaepfer WW, Hasler MB (1979) Characterization Of The Calcium-Induced Disruption Of Neurofilaments In Rat Peripheral-Nerve. Brain Research 168:299-309.

Schlosshauer B, Dreesmann L, Schaller HE, Sinis N (2006) Synthetic nerve guide implants in humans: A comprehensive survey. Neurosurgery 59:740-747.

Schneiderschaulies J, Kirchhoff F, Archelos J, Schachner M (1991) Down-Regulation Of Myelin-Associated Glycoprotein On Schwann-Cells By Interferon-Gamma And Tumor-Necrosis-Factor-Alpha Affects Neurite Outgrowth. Neuron 7:995-1005.

Schnell E, Klinkhammer K, Balzer S, Brook G, Klee D, Dalton P, Mey J (2007) Guidance of glial cell. migration and axonal growth on electrospun nanofibers of poly-epsilon-caprolactone and a collagen/poly-epsilon-caprolactone blend. Biomaterials 28:3012-3025.

Schubert C, van Langeveld MC, Donoso LA (2014) Innovations in 3D printing: a 3D overview from optics to organs. British Journal of Ophthalmology 98:159-161.

Schulz C, Kunz U, Mauer UM (2012) Three years of neurosurgical experience in a multinational field hospital in northern Afghanistan. Acta Neurochirurgica 154:135-140.

Schumacher M, Guennoun R, Stein DG, De Nicola AF (2007) Progesterone: Therapeutic opportunities for neuroprotection and myelin repair. Pharmacology & Therapeutics 116:77-106.

Seddon HJ (1943) Three types of nerve injury. Brain 66:237-288.

Sendtner M, Gotz R, Holtmann B, Thoenen H (1997) Endogenous ciliary neurotrophic factor is a lesion factor for axotomized motoneurons in adult mice. Journal of Neuroscience 17:6999-7006.

Sendtner M, Kreutzberg GW, Thoenen H (1990) Ciliary Neurotrophic Factor Prevents The Degeneration Of Motor Neurons After Axotomy. Nature 345:440-441.

Senes FM, Campus R, Becchetti F, Catena N (2009) Upper Limb Nerve Injuries In Developmental Age. Microsurgery 29:529-535.

Serra T, Mateos-Timoneda MA, Planell JA, Navarro M (2013) 3D printed PLA-based scaffolds A versatile tool in regenerative medicine. Organogenesis 9:239-244.

Shah M, Foreman DM, Ferguson MWJ (1992) Control Of Scarring In Adult Wounds By Neutralizing Antibody To Transforming Growth-Factor-Beta. Lancet 339:213-214.

Shah M, Foreman DM, Ferguson MWJ (1994) Neutralizing Antibody To Tgf-Beta(1,2) Reduces Cutaneous Scarring In Adult Rodents. Journal of Cell Science 107:1137-1157.

Shah M, Foreman DM, Ferguson MWJ (1995) Neutralization Of Tgf-Beta(1) And Tgf-Beta(2) Or Exogenous Addition Of Tgf-Beta(3) To Cutaneous Rat Wounds Reduces Scarring. Journal of Cell Science 108:985-1002.

Shamash S, Reichert F, Rotshenker S (2002) The cytokine network of Wallerian degeneration: tumor necrosis factor-alpha, interleukin-1 alpha, and interleukin-1 beta. Journal of Neuroscience 22:3052-3060.

Sharma S, Mohanty S, Gupta D, Jassal M, Agrawal AK, Tandon R (2011) Cellular response of limbal epithelial cells on electrospun poly-epsilon-caprolactone nanofibrous scaffolds for ocular surface bioengineering: a preliminary in vitro study. Molecular Vision 17:2898-2910.

Shawe GDH (1955) On The Number Of Branches Formed By Regenerating Nerve-Fibres. British Journal of Surgery 42:474-488.

Shen ZL, Lassner F, Bader A, Becker M, Walter GF, Berger A (2000) Cellular activity of resident macrophages during Wallerian degeneration. Microsurgery 20:255-261.

Shimomura O, Johnson FH, Saiga Y (1962) Extraction, Purification And Properties Of Aequorin, A Bioluminescent Protein From Luminous Hydromedusan, Aequorea. Journal of Cellular and Comparative Physiology 59:223-&.

Shin DH, Lee E, Hyun JK, Lee SJ, Chang YP, Kim JW, Choi YS, Kwon BS (2003) Growth-associated protein-43 is elevated in the injured rat sciatic nerve after low power laser irradiation. Neuroscience Letters 344:71-74.

Siegel SG, Patton B, English AW (2000) Ciliary neurotrophic factor is required for motoneuron sprouting. Experimental Neurology 166:205-212.

Siemionow M, Brzezicki G (2009) Current Techniques And Concepts In Peripheral Nerve Repair. Essays on Peripheral Nerve Repair and Regeneration 87:141-172.

Singh B, Xu QG, Franz CK, Zhang RM, Dalton C, Gordon T, Verge VMK, Midha R, Zochodne DW (2012) Accelerated axon outgrowth, guidance, and target reinnervation across nerve transection gaps following a brief electrical stimulation paradigm. Journal of Neurosurgery 116:498-512.

Singh SP, He XP, McNamara JO, Danzer SC (2013) Morphological Changes among Hippocampal Dentate Granule Cells Exposed to Early Kindling-epileptogenesis. Hippocampus 23:1309-1320.

Sinis N, Schaller HE, Schulte-Eversum C, Schlosshauer B, Doser M, Dietz K, Rosner H, Muller HW, Haerle M (2005) Nerve regeneration across a 2-cm gap in the rat median nerve using a resorbable nerve conduit filled with Schwann cells. Journal of Neurosurgery 103:1067-1076.

Smith D, Tweed C, Fernyhough P, Glazner GW (2009) Nuclear Factor-kappa B Activation in Axons and Schwann Cells in Experimental Sciatic Nerve Injury and Its Role in Modulating Axon Regeneration: Studies With Etanercept. Journal of Neuropathology and Experimental Neurology 68:691-700.

Sorensen J, Fugleholm K, Moldovan M, Schmalbruch H, Krarup G (2001) Axonal elongation through long acellular nerve segments depends on recruitment of phagocytic cells from the near-nerve environment - Electrophysiological and morphological studies in the cat. Brain Research 903:185-197.

Sorrell MRJ, Waxman JS (2011) Restraint of Fgf8 signaling by retinoic acid signaling is required for proper heart and forelimb formation. Developmental Biology 358:44-55.

Stoll G, Griffin JW, Li CY, Trapp BD (1989) Wallerian Degeneration In The Peripheral Nervous-System - Participation Of Both Schwann-Cells And Macrophages In Myelin Degradation. Journal of Neurocytology 18:671-683.

Stratford T, Horton C, Maden M (1996) Retinoic acid is required for the initiation of outgrowth in the chick limb bud. Current Biology 6:1124-1133.

Sun HF, Mei L, Song CX, Cui XM, Wang PY (2006) The in vivo degradation, absorption and excretion of PCL-based implant. Biomaterials 27:1735-1740.

Sunderland S (1951) A classification of peripheral nerve injuries producing loss of function. Brain 74:491-516.

Sunderland S (1978) Nerves and Nerve Injury. New York: Churchill Livingstone.

Sunderland S (1991) Nerve Injuries and Their Repair: A Critical Appraisal. Edinburgh: Churchill Livingstone.

Suzuki M, Ogawa Y, Hasegawa T, Kawaguchi S, Yukawa K, Nishiyama N, Shimizu S (2010) Simultaneous, laser-sintered, three-dimensional modelling of bony structures and soft tissue for surgical navigation of extended cholesteatoma. Journal of Laryngology and Otology 124:564-568.

Suzuki T, Kunchala SR, Matsui M, Murayama A (1998) Molecular flexibility of retinoic acid under white fluorescent light. Journal of Nutritional Science and Vitaminology 44:729-736.

Swindle-Reilly KE, Papke JB, Kutosky HP, Throm A, Hammer JA, Harkins AB, Willits RK (2012) The impact of laminin on 3D neurite extension in collagen gels. Journal of Neural Engineering 9.

Taha MO, Rosseto M, Fraga MM, Mueller SF, Fagundes DJ, Novo NF, Caricati-Neto A (2004) Effect of retinoic acid on tibial nerve regeneration after anastomosis in rats: Histological and functional analyses. Transplantation Proceedings 36:404-408.

Thoms SD, Stocum DL (1984) Retinoic Acid-Induced Pattern Duplication In Regenerating Urodele Limbs. Developmental Biology 103:319-328.

Toft PB, Fugleholm K, Schmalbruch H (1988) Axonal Branching Following Crush Lesions Of Peripheral-Nerves Of Rat. Muscle & Nerve 11:880-889.

Tong XJ, Hirai KI, Shimada H, Mizutani Y, Izumi T, Toda N, Yu P (1994) Sciatic-Nerve Regeneration Navigated By Laminin-Fibronectin Double Coated Biodegradable Collagen Grafts In Rats. Brain Research 663:155-162.

Trachtenberg JT, Chen BE, Knott GW, Feng GP, Sanes JR, Welker E, Svoboda K (2002) Long-term in vivo imaging of experience-dependent synaptic plasticity in adult cortex. Nature 420:788-794.

Ueno T, Suita S, Zaizen Y (1993) Retinoic Acid Induces Insulin-Like Growth Factor-Ii Expression In A Neuroblastoma Cell-Line. Cancer Letters 71:177-182.

Unezaki S, Yoshii S, Mabuchi T, Saito A, Ito S (2009) Effects of neurotrophic factors on nerve regeneration monitored by in vivo imaging in thy1-YFP transgenic mice. Journal of Neuroscience Methods 178:308-315.

Vargas ME, Watanabe J, Singh SJ, Robinson WH, Barres BA (2010) Endogenous antibodies promote rapid myelin clearance and effective axon regeneration after nerve injury. Proceedings of the National Academy of Sciences of the United States of America 107:11993-11998.

Vaughan DW (1992) Effects Of Advancing Age On Peripheral-Nerve Regeneration. Journal of Comparative Neurology 323:219-237.

Verdu E, Ceballos D, Vilches JJ, Navarro X (2000) Influence of aging on peripheral nerve function and regeneration. Journal of the Peripheral Nervous System 5:191-208.

Vidal M, Morris R, Grosveld F, Spanopoulou E (1990) Tissue-Specific Control Elements Of The Thy-1 Gene. Embo Journal 9:833-840.

Vizoso AD (1950) The Relationship Between Internodal Length And Growth In Human Nerves. Journal of Anatomy 84:342-353.

Vizoso AD, Young JZ (1948) Internode Length And Fibre Diameter In Developing And Regenerating Nerves. Journal of Anatomy 82:110-&.

Volkenstein S, Kirkwood JE, Lai E, Dazert S, Fuller GG, Heller S (2012) Oriented collagen as a potential cochlear implant electrode surface coating to achieve directed neurite outgrowth. European Archives of Oto-Rhino-Laryngology 269:1111-1116.

Wade NJ (2004) Visual neuroscience before the neuron. Perception 33:869-889.

Wahl SM, Hunt DA, Wakefield LM, McCartneyfrancis N, Wahl LM, Roberts AB, Sporn MB (1987) Transforming Growth-Factor Type-Beta Induces Monocyte Chemotaxis And Growth-Factor Production. Proceedings of the National Academy of Sciences of the United States of America 84:5788-5792.

Waitayawinyu T, Parisi DM, Miller B, Luria S, Morton HJ, Chin SH, Trumble TE (2007) A comparison of polyglycolic acid versus type 1 collagen bioabsorbable nerve conduits in a rat model: An alternative to autografting. Journal of Hand Surgery-American Volume 32A:1521-1529.

Waller A (1850) Experiments on the Section of the Glossopharyngeal and Hypoglossal Nerves of the Frog, and Observations of the Alterations Produced Thereby in the Structure of Their Primitive Fibres. Philosophical Transactions of the Royal Society of London 140:423-429.

Wang C-Y, Zhang K-H, Fan C-Y, Mo X-M, Ruan H-J, Li F-F (2011) Aligned natural-synthetic polyblend nanofibers for peripheral nerve regeneration. Acta Biomaterialia 7:634-643.

Wang HB, Mullins ME, Cregg JM, Hurtado A, Oudega M, Trombley MT, Gilbert RJ (2009) Creation of highly aligned electrospun poly-L-lactic acid fibers for nerve regeneration applications. Journal of Neural Engineering 6.

Wang X, Allen C, Ballow M (2007) Retinoic acid enhances the production of IL-10 while reducing the synthesis of IL-12 and TNF-alpha from LPS-stimulated monocytes/macrophages. Journal of Clinical Immunology 27:193-200.

Wang X, Archibald ML, Stevens K, Baldridge WH, Chauhan BC (2010) Cyan fluorescent protein (CFP) expressing cells in the retina of Thy1-CFP transgenic mice before and after optic nerve injury. Neuroscience Letters 468:110-114.

Wang X, Halvorsen SW (1998) Retinoic acid up-regulates ciliary neurotrophic factor receptors in cultured chick neurons and cardiomyocytes. Neuroscience Letters 240:9-12.

Wang XD, Hu W, Cao Y, Yao J, Wu J, Gu XS (2005) Dog sciatic nerve regeneration across a 30-mm defect bridged by a chitosan/PGA artificial nerve graft. Brain 128:1897-1910.

Watson RA (2014) A Low-Cost Surgical Application of Additive Fabrication. Journal of Surgical Education 71:14-17.

Weber RA, Breidenbach WC, Brown RE, Jabaley ME, Mass DP (2000) A randomized prospective study of polyglycolic acid conduits for digital nerve reconstruction in humans. Plastic and Reconstructive Surgery 106:1036-1045.

Weber RA, Dellon AL (2004) Nerve Lacerations: Repair of Acute Injuries. In: Hand Injury (Berger, R. A. and Weiss, A.-P. C., eds), pp 819-845 Philadelphia, USA: Lippincott Williams & Wilkinson.

Weis J, Lie DC, Ragoss U, Zuchner SL, Schroder JM, Karpati G, Farruggella T, Stahl N, Yancopoulos GD, DiStefano PS (1998) Increased expression of CNTF receptor alpha in denervated human skeletal muscle. Journal of Neuropathology and Experimental Neurology 57:850-857.

Welch MB, Brummett CM, Welch TD, Tremper KK, Shanks AM, Guglani P, Mashour GA (2009) Perioperative Peripheral Nerve Injuries A Retrospective Study of 380,680 Cases during a 10-year Period at a Single Institution. Anesthesiology 111:490-497.

Whitby DJ, Ferguson MWJ (1991a) Immunohistochemical Localization Of Growth-Factors In Fetal Wound-Healing. Developmental Biology 147:207-215.

Whitby DJ, Ferguson MWJ (1991b) The Extracellular-Matrix Of Lip Wounds In Fetal, Neonatal And Adult Mice. Development 112:651-668.

Wilhelm JC, Xu M, Cucoranu D, Chmielewski S, Holmes T, Lau K, Bassell GJ, English AW (2012) Cooperative Roles of BDNF Expression in Neurons and Schwann Cells Are Modulated by Exercise to Facilitate Nerve Regeneration. Journal of Neuroscience 32.

Williams KR, Blayney AW (1987) Tissue-Response Of Several Polymeric Materials Implanted In The Rat Middle-Ear. Biomaterials 8:254-258.

Williams LR, Longo FM, Powell HC, Lundborg G, Varon S (1983) Spatial-Temporal Progress Of Peripheral-Nerve Regeneration Within A Silicone Chamber - Parameters For A Bioassay. Journal of Comparative Neurology 218:460-470.

Williams LR, Powell HC, Lundborg G, Varon S (1984) Competence Of Nerve-Tissue As Distal Insert Promoting Nerve Regeneration In A Silicone Chamber. Brain Research 293:201-211.

Williams LR, Varon S (1985) Modification Of Fibrin Matrix Formation Insitu Enhances Nerve Regeneration In Silicone Chambers. Journal of Comparative Neurology 231:209-220.

Wion D, Houlgatte R, Barbot N, Barrand P, Dicou E, Brachet P (1987) Retinoic Acid Increases The Expression Of Ngf Gene In Mouse-L Cells. Biochemical and Biophysical Research Communications 149:510-514.

Witzel C, Rohde C, Brushart TM (2005) Pathway sampling by regenerating peripheral axons. Journal of Comparative Neurology 485:183-190.

Wong AYC, Scott JJA (1991) Functional Recovery Following Direct Or Graft Repair Of Nerve Gaps In The Rat. Experimental Neurology 114:364-366.

Wong MG, Panchapakesan U, Qi W, Silva DG, Chen X-M, Pollock CA (2011) Cation-independent mannose 6-phosphate receptor inhibitor (PXS25) inhibits fibrosis in human proximal tubular cells by inhibiting conversion of latent to active TGF-beta(1). American Journal of Physiology-Renal Physiology 301:F84-F93.

Wood K, Wilhelm JC, Sabatier MJ, Liu K, Gu J, English AW (2012) Sex differences in the effectiveness of treadmill training in enhancing axon regeneration in injured peripheral nerves. Developmental Neurobiology 72:688-698.

Wu LMN, Williams A, Delaney A, Sherman DL, Brophy PJ (2012) Increasing Internodal Distance in Myelinated Nerves Accelerates Nerve Conduction to a Flat Maximum. Current Biology 22:1957-1961.

Xu J-j, Chen E-y, Lu C-l, He C (2009) Recombinant ciliary neurotrophic factor promotes nerve regeneration and induces gene expression in silicon tube-bridged transected sciatic nerves in adult rats. Journal of Clinical Neuroscience 16:812-817.

Xu QG, Midha R, Martinez JA, Glio G, Zochodne DW (2008) Facilitated sprouting in a peripheral nerve injury. Neuroscience 152:877-887.

Yamamoto T, Eckes B, Krieg T (2001) Effect of interleukin-10 on the gene expression of type I collagen, fibronectin, and decorin in human skin fibroblasts: Differential regulation by transforming growth factor-beta and monocyte chemoattractant protein-1. Biochemical and Biophysical Research Communications 281:200-205.

Yan Y, Sun HH, Mackinnon SE, Johnson PJ (2011) Evaluation of peripheral nerve regeneration via in vivo serial transcutaneous imaging using transgenic Thy1-YFP mice. Experimental Neurology 232:7-14.

Yao L, Billiar KL, Windebank AJ, Pandit A (2010a) Multichanneled Collagen Conduits for Peripheral Nerve Regeneration: Design, Fabrication, and Characterization. Tissue Engineering Part C-Methods 16:1585-1596.

Yao L, de Ruiter GCW, Wang H, Knight AM, Spinner RJ, Yaszemski MJ, Windebank AJ, Pandit A (2010b) Controlling dispersion of axonal regeneration using a multichannel collagen nerve conduit. Biomaterials 31:5789-5797.

Yee KK, Rawson NE (2000) Retinoic acid enhances the rate of olfactory recovery after olfactory nerve transection. Developmental Brain Research 124:129-132.

Yu WHA (1989) Survival Of Motoneurons Following Axotomy Is Enhanced By Lactation Or By Progesterone Treatment. Brain Research 491:379-382.

Zhang K, Wang H, Huang C, Su Y, Mo X, Ikada Y (2010) Fabrication of silk fibroin blended P(LLA-CL) nanofibrous scaffolds for tissue engineering. Journal of Biomedical Materials Research Part A 93A:984-993.

Zhao D, McCaffery P, Ivins KJ, Neve RL, Hogan P, Chin WW, Drager UC (1996) Molecular identification of a major retinoic-acid-synthesizing enzyme, a retinaldehyde-specific dehydrogenase. European Journal of Biochemistry 240:15-22.

Zhelyaznik N, Mey J (2006) Regulation of retinoic acid receptors alpha, beta and retinoid X receptor alpha after sciatic nerve injury. Neuroscience 141:1761-1774.

Zochodne DW (2008) Neurobiology of Peripheral Nerve Regeneration. Cambridge: Cambridge University Press.